



Analysis of *14-3-3 σ* methylation and associated changes in gene expression and function in colorectal carcinoma

Kirsty Anne Roberts

Thesis submitted for degree of Doctor
in Philosophy

The University of Edinburgh

2009

Declaration

I declare that this thesis was composed entirely by myself and that the research presented is my own unless otherwise stated.

Kirsty Anne Roberts

November 2009

Abstract

The aims of the work presented in this thesis were: to investigate the role of methylation of *14-3-3 σ* (a key regulator of p53-mediated G₂/M arrest and of translational control during mitosis) in colorectal cancer using colorectal cancer cell lines and fresh colorectal tumours; to investigate any relationship between *14-3-3 σ* methylation status and gene expression; to determine whether aberrant methylation is associated with cell cycle defects and other factors known to contribute to colorectal carcinogenesis.

PCR bisulphite sequencing showed that 78% (7/9) of colorectal cancer cell lines were unmethylated in the *14-3-3 σ* upstream promoter region (UPR). The unmethylated cell lines expressed high levels of *14-3-3 σ* , while methylated cell lines expressed negligible levels of *14-3-3 σ* protein or mRNA. Methylated colorectal cancer cell lines were treated with 5-aza-2'-deoxycytidine and demethylation was confirmed by MSP analysis. However, demethylation did not induce *14-3-3 σ* re-expression in the methylated cell lines, suggesting that CpG methylation may not be the only mechanism of transcriptional control. In contrast to colorectal cancer cell lines, 90% (89/99) of fresh colorectal tumours were methylated at CpG dinucleotides within the *14-3-3 σ* UPR. Bisulphite sequencing analysis of individual clones from *14-3-3 σ* methylated tumours (n =3) demonstrated that the clones displayed methylated CpG levels of approximately 41%. In agreement with previous PCR bisulphite sequencing analysis, there were a low percentage of methylated CpG dinucleotides (~ 15%) in clones from the *14-3-3 σ* unmethylated tumours (n =3). Unmethylated tumours expressed significantly higher levels of *14-3-3 σ* in comparison to methylated tumours (p =0.03), indicating that *14-3-3 σ* methylation may be associated with expression. PCR bisulphite sequencing analysis of matched normal mucosa tissues indicated that the *14-3-3 σ* UPR was methylated in all samples. Preliminary studies therefore suggest that there is tumour-specific loss of *14-3-3 σ* methylation in colorectal tumours within the *14-3-3 σ* UPR and CpG island. There were no apparent clinico-pathological correlations with *14-3-3 σ* methylation

status. Whilst *14-3-3 σ* methylation was associated with expression in fresh colorectal tumours, there was no significant difference in expression levels between unmethylated colorectal tumours and matched methylated normal tissue. Bisulphite sequencing analysis of individual clones from normal tissues (from patients free of cancer) revealed that the *14-3-3 σ* UPR and CpG island was methylated at the majority of CpG sites analysed in colonic tissue (422/495, ~85.2%) and approximately half (795/1557, 51.1%) of CpG sites in skin samples (n =3). Furthermore, higher levels of *14-3-3 σ* protein were observed in skin tissue samples compared to normal colonic tissue, suggesting that *14-3-3 σ* CpG island methylation may be associated with tissue-specific expression.

Experiments to assess the relationship between *14-3-3 σ* methylation and general methylation defects, suggest that methylation differences in *14-3-3 σ* were not simply a consequence of more general methylation phenomena well described in colorectal cancer. Nearest Neighbor analysis showed no evidence of generalised hypomethylation. Furthermore, MethyLight analysis of the CpG Island Methylator Phenotype (CIMP) showed no relationship between *14-3-3 σ* methylation status and CIMP; since, 1/5 (20%) tumours methylated at *14-3-3 σ* UPR and 1/5 (20%) tumours unmethylated at *14-3-3 σ* UPR were CIMP positive.

In vitro functional assays showed that overexpression of *14-3-3 σ* in SW480 cells (*14-3-3 σ* methylated) delayed the apoptotic response to UV-C, compared to control SW480 cells. This suggests that *14-3-3 σ* may protect colorectal cancer cells from apoptosis. MTT assays showed that overexpression of *14-3-3 σ* in SW480 cells resulted in a trend of increasing proliferation with a significant increase on day 4, compared to controls SW480 cells (p <0.01). Furthermore, FACS-sorted SW480 cells overexpressing *14-3-3 σ* , showed a significant shift to S-phase from G₁ compared to control SW480 cells (p <0.01). Western blot analysis and immunohistochemistry revealed no relationship between *p53* status and methylated *14-3-3 σ* in fresh tumours, while there was no relationship between published *p53*

status for colorectal cancer cell lines and *14-3-3 σ* methylation status defined experimentally.

I have presented data which shows that methylation status of *14-3-3 σ* varies between colorectal cancer tissue, colorectal cancer cell lines and normal colonic tissue. Overexpression of *14-3-3 σ* appears to contribute to colorectal cancer carcinogenesis, raising the hypothesis that *14-3-3 σ* expression and function may at least in part be dependent on CpG methylation.

Acknowledgements

Firstly, I wish to thank my supervisor Prof. Malcolm Dunlop, for his support and expert advice over the last four years. I would also like thank Dr Richard Meehan for his support, his guidance, and his excellent advice during my PhD. I am so very appreciative. A big thank-you must also go to Dr. Lesley Stark and Dr. Susan Farrington for their tips and guidance in the lab.

I'd also like to thank Dr Rob Elton and Dr Lilian Murray for their expert statistical tips and advice they have given me during my writing-up stages. A massive thank-you also to Dr Duncan Sproul and Sue Lawrenson for proofreading my thesis and to James Reddington and Nicole Gnadt for their help with the bisulphite sequencing. I'd also like to thank Marion Walker for her wonderful technical help over the last few years in the lab and for making me laugh and smile on a daily basis! I wish to also thank everyone else on the E4 floor past and present who made my time in the lab very enjoyable, encouraged me when things were not going well and provided endless entertainment!

This PhD also owes its success to my family and friends. A special thanks must go to my Mum and Dad and my brother Oliver. Your constant support has been unbelievable and words cannot describe how very grateful I am. Thank-you to all of my fantastic friends from Edinburgh and from afar; Kristy, Kate, Estelle, Anna, Susan, Jackie, David, Kelly and Chel. Thank-you for being good listeners, encouraging me and giving me hugs when times were hard, and for the excellent nights out over the years! You guys are amazing, I love you all!

Abbreviations

ADP	Adenosine diphosphate
AM	Laboratory sample identification
ANOVA	Analysis of variance
APC	Adenomatous polyposis coli
APS	Ammonium persulphate
ATCC	American/European type culture collections
ATP	Adenine tri phosphate
ChIP	Chromatin immunoprecipitation
CIMP	CpG island methylator phenotype
CIN	Chromosome Instability
CpG	Cytosine Guanine dinucleotide
CRA	Colorectal adenocarcinomas
CRC	Colorectal cancer
DAB	Diaminobenzidine tetrahydrochloride
dH ₂ O	Distilled water
DMRs	Differentially methylated regions
DMSO	Dimethyl sulfoxide
DNA	Deoxyribonucleotide acid
DNMT	DNA methyltransferase
dNTP	Deoxy nucleotide tri-phosphate
EDTA	Ethylenediaminetetra-acetic acid
EFP	Estrogen-induced zinc finger protein
ELISA	Enzyme-Linked ImmunoSorbent Assay

FACS	Fluorescent assisted cell sorting
FAP	Familial adenomatous polyposis coli
FAM	6-carboxyfluorescein
FCS	Fetal calf serum
FISH	Fluorescence <i>in situ</i> hybridisation
GFP	Green fluorescent protein
HAT	Histone acetyltransferase
HDAC	Histone deacetylase
HEM	Human epithelial marker
HEPES	N-2 hydroxyethylpiperazine-N'-2-ethanesulfonic acid
HMT	Histone methyltransferase
HNPCC	Hereditary non-polyposis colorectal cancer
HPV16	Human papillomavirus 16
ICF	Immunodeficiency, centromeric instability and facial anomalies
IRES	Internal ribosome entry site
Kb	Kilobase
KR	Laboratory sample identification
LCM	Laser capture microdissection
LINE	Long interspersed nucleotide elements
LOH	Loss of heterozygosity
MBD	Methylcytosine binding domain
MCA	Methylation CpG island amplification
MeDIP	Methylated DNA immunoprecipitation
MGB	Minor groove binder

MgCl	Magnesium chloride
MINT	Methylated in tumour
miRNA	MicroRNA
MMR	Mismatch repair
mRNA	Messenger RNA
MSI	Microsatellite instability
MSI-H	High-level microsatellite instability
MSI-L	Low-level microsatellite instability
MSP	Methylation specific PCR
MSS	Microsatellite stable
NaCl	Sodium chloride
NaOAc	Sodium acetate
Nt	Nucleotide
PAGE	Polyacrylamide gel electrophoresis
PBS	Phosphate buffer saline
PcG	Polycomb group
PCR	Polymerase chain reaction
PI	Propidium iodide
PMR	Percentage methylation ratio
qRT-PCR	Quantitative reverse transcription PCR amplification
rpm	Revolutions per minute
RLGS	Restriction landmark genome scanning
RNA	Ribonucleic acid
RNAi	RNA interference

SAGE	Serial analysis of gene expression
SAM	S-adenosyl methionine
SAP	Shrimp alkaline phosphatase
SDS	Sodium dodecyl sulphate
SFN	Stratifin
SNP	Single nucleotide polymorphism
SSC	Salt and sodium citrate buffer
SSCP	Single-strand conformation polymorphism
TAE	Tris Acetate EDTA buffer
TAP	Tandem affinity purification
T-DMRs	Tissue differentially methylated regions
TEMED	N, N, N', N' tetramethyl-1-2-diaminomethane
TLC	Thin layer chromatography
Tris	Tris(hydroxymethyl)aminomethane
TSA	Trichostatin A
TV	Trypsin versene
Ub	Ubiquitin
UPR	Upstream promoter region
X-gal	5-bromo-4-chloro-3-indolyl- β -D-galactosidase
XIC	X inactivation centre

Table of Contents

	Page
Declaration	i
Abstract	ii
Acknowledgements	v
Abbreviations	vi
Table of Contents	x
List of Figures and Tables	xv

CHAPTER 1

INTRODUCTION

1.1	BACKGROUND	1
1.2	DNA METHYLATION IN NORMAL CELLS	2
1.2.1	DNA Methylation in physiological circumstances	2
1.2.2	CpG Islands	8
1.2.3	DNA methyltransferases	11
1.3	DNA Methylation and mechanisms of gene silencing	14
1.3.1	Direct mechanism of gene silencing by DNA methylation	14
1.3.2	Indirect mechanisms of gene silencing by DNA methylation	15
1.4	ABERRANT METHYLATION AND CANCER	20
1.4.1	Global Hypomethylation	20
1.4.2	Hypomethylation of CpG Islands	23
1.4.3	Hypermethylation of CpG Islands	24
1.4.4	DNA methylation - Cause or consequence	28
1.4.5	DNA Methyltransferase activity in cancer	30
1.5	DNA METHYLATION AND COLORECTAL CANCER	32
1.5.1	Introduction	32
1.5.2	Age-related methylation in colorectal cancer	33
1.5.3	CpG Island Methylator Phenotype	35
1.6	METHODS UTILISED FOR DNA METHYLATION DETECTION IN TUMOURS	39
1.6.1	Fine mapping and quantitative analysis of DNA methylation	40
1.6.2	Global analysis of DNA methylation	42
1.7	14-3-3 σ	46
1.7.1	Introduction	46
1.7.2	Regulation and function of 14-3-3 σ	47
1.7.3	The role of 14-3-3 σ in cancer	54
1.7.4	Methylation of 14-3-3 σ in normal tissue	56
1.7.5	Aberrant methylation of 14-3-3 σ in cancer	57

1.8	HYPOTHESIS	62
1.9	RESEARCH AIM	63
CHAPTER 2		
MATERIAL AND METHODS		
2.1	BIOLOGICAL MATERIAL	65
2.1.1	Summary of cell lines	65
2.1.2	Maintenance of cell lines	66
2.1.3	Tissue sample collection	67
2.1.4	Colorectal tissue samples	67
2.1.5	Skin Samples	67
2.1.6	Tissue Lysate samples	68
2.1.7	Tumour sections	68
2.1	DNA AND RNA PURIFICATION PROTOCOLS	68
2.2.1	Purification of DNA from cell lines, skin, tumour and normal mucosa colorectal tissue	68
2.2.2	RNA Extraction	68
2.2.3	Estimation of DNA and RNA concentration	68
2.3	DNA SAMPLES	69
2.3.1	Colorectal tumour DNA	69
2.3.2	Colorectal cancer Cell line DNA	69
2.3.3	Control Tissue DNA from healthy individuals	69
2.4	TECHNIQUES FOR DETECTION OF DNA METHYLATION EMPLOYING SODIUM BISULPHITE MODIFICATION OF DNA	69
2.4.1	Large-scale bisulphite treatment: 96-well format	70
2.4.2	Small-scale bisulphite treatment	70
2.4.3	PCR reactions	70
2.4.4	Oligonucleotides for PCR reactions	71
2.4.5	Gel Electrophoresis	73
2.4.6	PCR product purification	73
2.4.7	DNA Sequencing	73
2.4.8	Precipitation of DNA from sequencing reactions	74
2.4.9	Characterisation of methylated CpG islands	74
2.5	CLONING AND BACTERIAL CULTURE	75
2.5.1	TA cloning and transformation	75
2.5.2	Colony selection and storage	75
2.6	EXPRESSION ANALYSIS	76
2.6.1	DNase I Treatment	76
2.6.2	cDNA synthesis	76
2.6.3	Quantitative RT-PCR: Taqman analysis	76
2.6.4	Protein expression analysis	77
2.6.4.1	Preparation of cytoplasmic cell extracts	79
2.6.4.2	Preparation of cytoplasmic extracts from tissue	79
2.6.4.3	Western Blot Analysis	80
2.7	CELL BIOLOGY	81
2.7.1	5-Aza-2'-deoxycytidine treatment	81
2.7.2	Transfection of cell lines	81

2.7.3	Annexin V Apoptosis Assay	82
2.7.4	Proliferation Assays	82
2.7.5	FACS analysis of GFP transfected cells	83
2.7.6	Flow Cytometry Cell Cycle Analysis	83
2.8	ANALYSIS OF GLOBAL METHYLATION STATUS	84
2.8.1	Methylight analysis	84
2.8.2	Nearest Neighbor Analysis	86
2.9	HISTOLOGY TECHNIQUES	87
2.9.1	Processing of colon tissue for paraffin wax sectioning	87
2.9.2	Immunohistochemistry	88
2.10	CALCULATIONS AND STATISTICS	89
2.10.1	Statistical Analysis	89

CHAPTER 3

METHYLATION ANALYSIS OF 14-3-3 σ IN COLORECTAL CANCER CELL LINES, COLON TUMOURS AND NORMAL MUCOSA

3.1	INTRODUCTION	90
3.2	METHODOLOGY	91
3.2.1	14-3-3 σ CpG island in silico analysis	91
3.2.2	Bisulphite sequencing analysis	94
3.2.3	MSP analysis of colorectal cancer cell lines	98
3.2.4	Statistical analysis	98
3.2.5	Colorectal cancer cell lines	98
3.2.6	Patient samples	98
3.3	RESULTS	99
3.3.1	14-3-3 σ methylation analysis of colorectal cancer cell lines	99
3.3.2	14-3-3 σ methylation analysis of colorectal tumour samples	103
3.3.3	Clinicopathological associations with Region A 14-3-3 σ methylation status	110
3.3.4	Lack of methylation in Region A is tumour-specific	112
3.3.5	14-3-3 σ Region A methylation analysis in normal tissues from non-cancer subjects	115
3.4	DISCUSSION	120

CHAPTER 4

ANALYSIS OF 14-3-3 σ EXPRESSION AND ITS ASSOCIATION WITH METHYLATION OF THE GENE PROMOTER IN VITRO AND IN VIVO

4.1	INTRODUCTION	128
4.2	METHODOLOGY	130
4.2.1	qRT-PCR analysis	130
4.2.2	Western blot analysis	131
4.2.3	5-Aza-2'-deoxycytidine treatment	131
4.2.4	Methylation-specific PCR (MSP)	131
4.2.5	Colorectal cancer cell lines	132

4.2.6	Patient samples	132
4.2.7	Statistical analysis	132
4.3	RESULTS	133
4.3.1	14-3-3 σ expression analysis in colorectal cancer cell lines	133
4.3.2	14-3-3 σ mRNA expression analysis in vivo	136
4.3.3	14-3-3 σ protein expression analysis in vivo	140
4.3.4	Demethylation of 14-3-3 σ in vitro by 5-Aza-2'-deoxycytidine	148
4.4	DISCUSSION	155

CHAPTER 5

SPECIFICITY OF 14-3-3 σ HYPOMETHYLATION IN COLORECTAL CANCER

5.1	INTRODUCTION	161
5.2	METHODOLOGY	162
5.2.1	Nearest Neighbor Analysis	162
5.2.2	MethyLight Analysis	163
5.2.3	Colorectal cancer cell lines	164
5.2.4	Patient samples	164
5.3	RESULTS	168
5.3.1	Global levels of 5-methylcytosine in colorectal cancer cell lines and tumours	168
5.3.2	CIMP analysis in colorectal tumours	173
5.4	DISCUSSION	180

CHAPTER 6

ANALYSIS OF THE FUNCTIONAL EFFECTS OF INCREASED 14-3-3 σ EXPRESSION

6.1	INTRODUCTION	185
6.2	METHODOLOGY	186
6.2.1	Transfection of colorectal cancer cell lines	186
6.2.2	Apoptosis assays	186
6.2.3	Proliferation assays	187
6.2.4	Western blot analysis	187
6.2.5	Immunohistochemistry	187
6.2.6	Statistical analysis	187
6.3	RESULTS	188
6.3.1	Analysis of UV-C induced apoptosis in 14-3-3 σ GFP-C1 overexpressing colorectal cancer cell lines	188
6.3.2	Analysis of proliferation in 14-3-3 σ GFP-C1 overexpressing SW480 cell line	192
6.3.3	Analysis of cell cycle in 14-3-3 σ GFP-C1 overexpressing SW480 cell line	194
6.3.4	Analysis of 14-3-3 σ methylation and p53 mutations	198
6.4	DISCUSSION	206

CHAPTER 7	
DISCUSSION	212
CHAPTER 8	
BIBLIOGRAPHY	219
APPENDIX A	
APPENDIX B	
APPENDIX C	
APPENDIX D	

List of Figures and Tables

Figure 1.1:	DNA methylation mechanism	3
Figure 1.2:	Mammalian development and epigenetic gene regulation	5
Figure 1.3:	Structure of human X-inactivation centre and associated epigenetic modifications involved in maintaining the inactive state	7
Figure 1.4:	Effect of DNA methylation within CpG island promoter regions on gene transcription	10
Figure 1.5:	Gene silencing by histone deacetylation may be mediated through CpG promoter methylation	17
Figure 1.6:	Aberrant DNA methylation and cancer	23
Figure 1.7:	The revised Knudson two-hit model hypothesis	26
Figure 1.8:	Vogelstein's proposed model for development of sporadic colorectal cancer	33
Figure 1.9:	14-3-3 σ causes stable G2/M cell cycle arrest mediated through p53 or BRCA1 after induction of DNA damage	49
Figure 1.10:	Regulation of 14-3-3 σ in normal and cancer cells	51
Figure 1.11:	14-3-3 σ plays a critical role in cap-dependent and Cap-independent mRNA translation during mitosis	53
Figure 3.1:	Bioinformatic analysis of 14-3-3 σ CpG island using various algorithms	93
Figure 3.2:	Region of 14-3-3 σ CpG island and upstream region analysed for methylation	97
Figure 3.3:	MSP analysis of 14-3-3 σ methylation in colorectal cancer cell lines	100
Figure 3.4:	14-3-3 σ methylation analysis of colorectal cancer cell lines	101
Figure 3.5:	Summary of bisulphite PCR sequencing data obtained from methylation analysis of 14-3-3 σ in colorectal cancer cell lines	102
Figure 3.6:	14-3-3 σ bisulphite PCR sequencing analysis of colorectal tumours	105
Figure 3.7:	Summary of bisulphite PCR sequencing data from methylation	

analysis of <i>14-3-3σ</i> in colorectal tumours	106
Figure 3.8: <i>14-3-3σ</i> methylation profile in colorectal tumours previously found to be unmethylated by direct sequencing of PCR products	108
Figure 3.9: <i>14-3-3σ</i> methylation profile in colorectal tumours previously found to be methylated by direct sequencing of PCR products	109
Figure 3.10: <i>14-3-3σ</i> methylation analysis in corresponding normal mucosal samples	113
Figure 3.11: Summary of direct PCR bisulphite sequencing data from methylation analysis of <i>14-3-3σ</i> in corresponding normal mucosa samples	114
Figure 3.12: <i>14-3-3σ</i> methylation profile in normal colonic mucosa from a non-colorectal cancer patient	116
Figure 3.13: <i>14-3-3σ</i> methylation profile in skin tissue sample A from a non-colorectal cancer patient	117
Figure 3.14: <i>14-3-3σ</i> methylation profile in skin tissue sample B from a non-colorectal cancer patient	118
Figure 3.15: <i>14-3-3σ</i> methylation profile in skin tissue sample C from a non-colorectal cancer patient	119
Figure 4.1: β -actin RT-PCR from colorectal cancer cell line cDNA samples	131
Figure 4.2: <i>14-3-3σ</i> qRT-PCR colorectal cancer cell lines	134
Figure 4.3: <i>14-3-3σ</i> Western blot analysis colorectal cancer cell lines	135
Figure 4.4: <i>14-3-3σ</i> qRT-PCR KR and AM colorectal tumours	138
Figure 4.5: <i>14-3-3σ</i> qRT-PCR colorectal tumours	139
Figure 4.6: <i>14-3-3σ</i> Western blot analysis normal mucosa samples and colorectal tumours	142
Figure 4.7: Densitometric analysis of <i>14-3-3σ</i> Western blot from Fig 4.6	143
Figure 4.8: <i>14-3-3σ</i> Western blot analysis colorectal tumours	144
Figure 4.9: Densitometric analysis of <i>14-3-3σ</i> Western blot from Fig 4.8	145
Figure 4.10: <i>14-3-3σ</i> Western blot analysis skin tissues and normal colon	146
Figure 4.11: Densitometric analysis of <i>14-3-3σ</i> Western blot from Fig 4.10	146
Figure 4.12: MSP analysis <i>14-3-3σ</i> of SW480 and Colo320DM 5-Aza-2'-deoxycytidine treated cells- dose response	150

Figure 4.13: MSP analysis <i>14-3-3σ</i> of SW480 and Colo320DM 5-Aza-2'-deoxycytidine treated cells- time course	152
Figure 4.14: <i>14-3-3σ</i> qRT-PCR 5-Aza-2'-deoxycytidine treated SW480 and Colo320DM cells	154
Figure 5.1: Nearest Neighbor analysis	165
Figure 5.2: Nearest Neighbor analysis validation experiment 1	166
Figure 5.3: Nearest Neighbor analysis validation experiment 2	167
Figure 5.4: Nearest Neighbor analysis autoradiograph of colorectal cancer cell lines	170
Figure 5.5: Nearest Neighbor analysis autoradiograph of colorectal tumours	171
Figure 5.6: Percentage CpG methylation in colorectal cancer cell lines and colorectal tumours	172
Figure 5.7: <i>MLH1</i> MethyLight analysis in colorectal tumours	175
Figure 5.8: <i>CDKN2A</i> MethyLight analysis in colorectal tumours	176
Figure 5.9: <i>MINT1</i> MethyLight analysis in colorectal tumours	177
Figure 5.10: <i>MINT2</i> MethyLight analysis in colorectal tumours	178
Figure 6.1: <i>14-3-3σ</i> Western blot analysis of transient transfections with <i>14-3-3σGFP-C1</i> and <i>GFP-C1</i>	190
Figure 6.2: Percentage apoptosis in SW480 and HCT116 cells transfected with <i>14-3-3σGFP-C1</i> and <i>GFP-C1</i>	191
Figure 6.3: Proliferation of SW480 cells transfected with <i>14-3-3σGFP-C1</i> and <i>GFP-C1</i>	193
Figure 6.4: Cell cycle analysis of FACS sorted SW480 cells transfected with <i>14-3-3σGFP-C1</i> and <i>GFP-C1</i>	196
Figure 6.5: p53 immunohistochemistry in colorectal tumours	201
Figure 6.6: p53 Western blot analysis in colorectal tumours	203

Table 1.1:	Summary of phenotypes of the DNMT knockout mice and methyltransferase activity for each DNMT enzyme	13
Table 1.2:	Tumour suppressor genes associated with CpG island hypermethylation in different cancer types	26
Table 1.3:	Frequency of CpG methylation of <i>14-3-3σ</i> in different types of epithelial tumours and techniques utilised for methylation detection	59
Table 2.1:	Summary of colorectal cell lines	66
Table 2.2:	Oligonucleotides used throughout this PhD	72
Table 2.3:	Primary antibodies used throughout this PhD	81
Table 2.4:	Probe and primer sequences used for MethyLight	85
Table 3.1:	Densitometric analysis of MSP products from colorectal cancer cell lines	100
Table 3.2:	Clinico-pathological associations with <i>14-3-3σ</i> hypomethylation 1	111
Table 3.3:	Clinico-pathological associations with <i>14-3-3σ</i> hypomethylation 2	111
Table 4.1:	<i>14-3-3σ</i> expression and relationship with <i>14-3-3σ</i> methylation status	147
Table 4.2:	Densitometric analysis of <i>14-3-3σ</i> MSP-dose response SW480 cells	151
Table 4.3:	Densitometric analysis of <i>14-3-3σ</i> MSP-dose response Colo320DM cells	151
Table 4.4:	Densitometric analysis of <i>14-3-3σ</i> MSP-time course SW480 cells	153
Table 4.5:	Densitometric analysis of <i>14-3-3σ</i> MSP-dose response Colo320DM	153
Table 5.1:	Phosphorimaging quantification of Nearest Neighbor analysis	172
Table 5.2:	<i>MLH1</i> MethyLight analysis	175
Table 5.3:	<i>CDKN2A</i> MethyLight analysis	176
Table 5.4:	<i>MINT1</i> MethyLight analysis	177
Table 5.5:	<i>MINT2</i> MethyLight analysis	178

Table 5.6:	MethyLight analysis of CIMP in colorectal tumours	179
Table 6.1:	Summary of cell cycle analysis of SW480 cells transfected with <i>14-3-3σGFP-C1</i> and <i>GFP-C1</i>	197
Table 6.2:	<i>p53</i> status and <i>14-3-3σ</i> methylation status in colorectal cancer cell lines	200
Table 6.3:	<i>p53</i> immunohistochemistry analysis in colorectal tumours	202
Table 6.4:	<i>p53</i> status and <i>14-3-3σ</i> methylation status in colorectal tumours from immunohistochemistry and Western blot analysis	204
Table 6.5:	Summary of relationship between <i>p53</i> status and <i>14-3-3σ</i> methylation status	205

Chapter 1

Introduction

1.1 Background

Cancer arises due to genetic alterations, which can be acquired somatically or inherited through the germline. Somatic mutations in critical genes such as in oncogenes or tumour suppressor genes can alter gene function and lead to a growth advantage in the host cell. Cancer development involves an additional accumulation of these somatic mutations. Within some tumours this can vary and it has been demonstrated that the actual rate of mutational accumulation is lower than was first expected (DePinho, 2000). Furthermore, it was hypothesised that the accumulation of somatic mutations in tissues accounts for the increased incidence of cancer with age, while, there has been little definitive evidence of an increase in mutation rate in ageing tissue (Bohr & Anson, 1995). This suggests that other molecular mechanisms are involved.

One definition of epigenetics is that it is the study of heritable changes in gene expression without the requirement for associated changes in DNA sequence. More specifically, epigenetics is the study of chemical modifications of DNA or chromatin-associated proteins (mainly histones), which can lead to alterations in gene expression between different tissues and in diseased states. DNA methylation is the main modification of vertebrate DNA and occurs when a methyl group (CH_3) is attached to the 5-carbon position of a cytosine base. DNA methylation only takes place when a guanine residue precedes the cytosine, therefore only the dinucleotide Cytosine/Guanine (CpG) is methylated. DNA methylation occurs on both strands and is stably transmitted during cell division, through the activity of DNA methyltransferase (DNMT) enzymes. In 1975, it was first proposed that DNA methylation regulates gene expression (Holliday & Pugh, 1975; Riggs, 1975). Subsequent research provided further evidence of a role for DNA methylation in transcriptional repression (Bird et al, 1985; Jones & Taylor, 1980) and the underlying

mechanistic pathways that were involved (Jones et al, 1998; Nan et al, 1998). Aberrant methylation at the promoter region of tumour suppressor genes is associated with changes in gene expression and loss of function in human cancers (Herman et al, 1996b; Kane et al, 1997). This phenomenon was first identified by Feinberg and Vogelstein, reporting that a substantial proportion of CpG dinucleotides were differently methylated in normal tissues compared to cancer cells (Feinberg & Vogelstein, 1983a). Building on this, it was shown that cancer cells often exhibit global loss of methylation, mainly occurring at repeat sequences, and gains of methylation at normally methylation-free promoters (Paz et al, 2003). A number of tumour suppressor genes found to be hypermethylated at their respective promoter regions include: *p16^{INK4A}* in colorectal cancer (Herman et al, 1995); the retinoblastoma 1 gene (*Rb1*) in retinoblastoma (Greger et al, 1989); and the von Hippel-Lindau gene (*VHL*) in renal cell cancers (Herman et al, 1994). There has been a recent surge in genome-wide methylation analysis in cancer and a number of different technologies have been developed to analyse DNA methylation patterns and screen for novel disease markers (epimarkers). Alterations in methylation patterns can be detected with a high degree of sensitivity and there is real prospect for its clinical use in prognostic and diagnostic applications. With greater understanding, there also lies the potential for therapeutic intervention to reverse aberrant DNA methylation, and this currently is the focus of intense research.

1.2 DNA Methylation in normal cells

1.2.1 DNA Methylation in physiological circumstances

Methylation is an enzymatically catalysed chemical reaction, which adds a methyl group to selected sites on proteins, DNA and RNA. A DNMT enzyme is required to methylate the cytosine of the CpG dinucleotide to form 5-methylcytosine; and S-Adenosyl-methionine (SAM) is used as a methyl donor (Figure 1.1). In mammalian cells, DNA methylation is the major modification of DNA. It has been proposed that the role of methylation is to control gene expression or act as a form of genomic protection by repressing the large number of the retro(transposon) families that are

present in vertebrate genomes (Bird, 1995). Transposable sequences are known to be heavily methylated and therefore this may contribute to active repression of transposition.

DNA methylation has also been viewed as a primary mechanism for the control of gene transcription (Jones et al, 1998; Nan et al, 1998). When present at promoters and regulatory sequences, it is associated with gene repression (Bird & Wolffe, 1999). DNA methylation may have evolved a role in reducing transcriptional noise through reducing background gene transcription that is unnecessary for the cell to function. From this perspective, DNA methylation could have enabled the increase in gene number and complexity that characterise vertebrates (Bird, 1995). Support for the idea that DNA methylation may be important in regulating gene expression during development comes from experiments in which the maintenance DNMT enzyme (DNMT1) is inactivated. This results in an embryonically lethal phenotype, although stem cells survive without the enzyme (Lei et al, 1996; Li et al, 1992). This suggests that DNA methylation or the DNMT enzyme itself is essential for development of complex organisms.

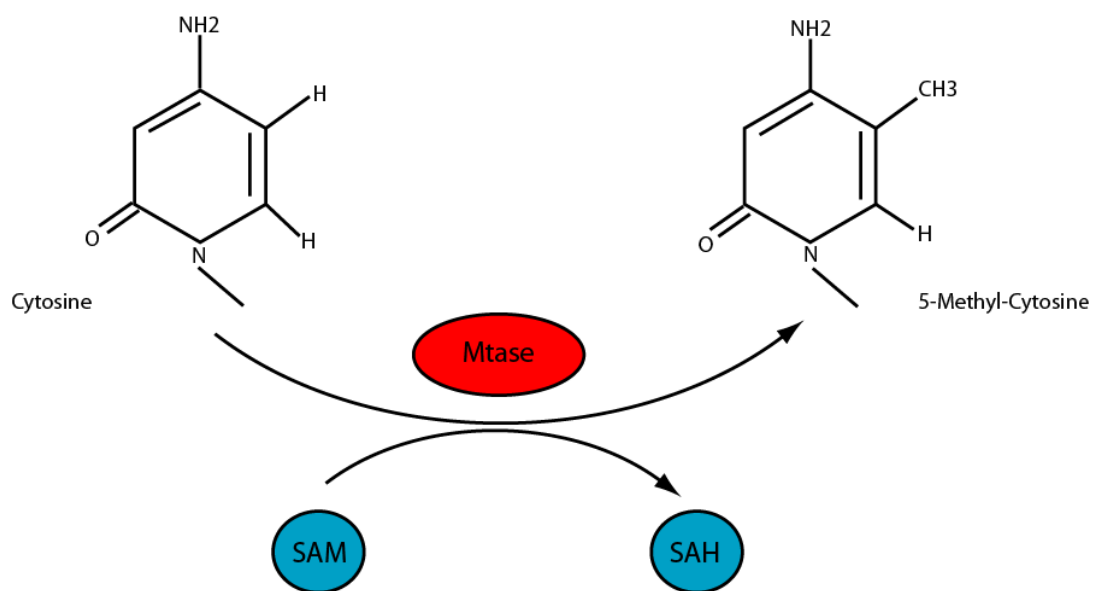


Figure 1.1: DNA methylation mechanism

Cytosine residue is methylated to form 5-methylcytosine by a DNA methyltransferase (Mtase) which catalyses the transfer of a methyl group (CH₃) from the methyl donor S-Adenosyl-methionine (SAM).

In the very early stages of mammalian development, cells are initially pluripotent with the potential to differentiate into many cells types. Cell and embryo specification is primarily governed by gene regulatory elements (GRN) during development; however, epigenetic regulation also has a role in initiating and maintaining developmental gene expression. Epigenetic regulation is mediated through the following modifications: changes in DNA methylation; histone modifications; and chromatin re-modelling (Figure 1.2). These epigenetic modifications will be discussed in more mechanistic detail in section 1.3. It has been reported that pluripotent stem cells express genes mainly encoding transcription factors and genes required later in development are flexibly suppressed by the polycomb group (PcG) proteins and histone methylation (Boyer et al, 2006). In contrast, in fully differentiated somatic cells, some pluripotency-associated genes (such as *Oct-3/4*), transposons, and imprinted genes are silenced long-term through DNA methylation and histone modifications inactivate repressed developmental genes (Feldman et al, 2006). In the germline, many of these epigenetic marks are erased. Development is geared so that silenced pluripotent-associated genes are re-expressed and imprinted genes are already epigenetically re-programmed in the next generation following fertilisation (Hajkova et al, 2002; Maatouk et al, 2006).

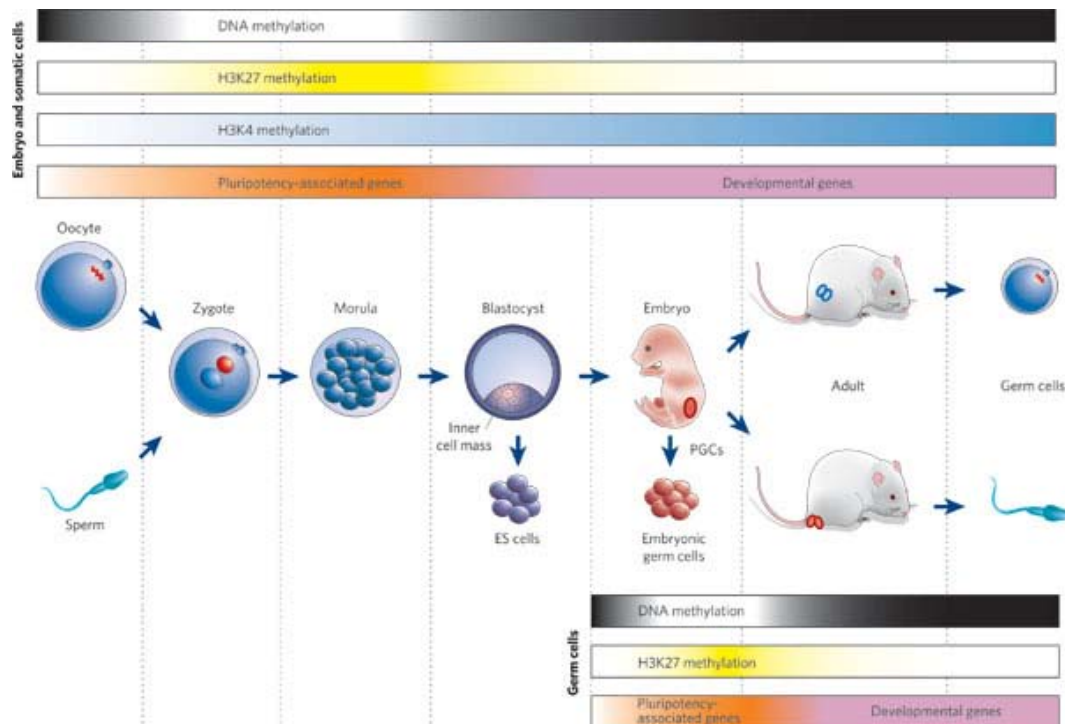


Figure 1.2: Mammalian development and epigenetic gene regulation

Both global epigenetic modifications and gene expression patterns are shown alongside key developmental events. DNA methylation is erased and pluripotent genes begin to be expressed very early in development. At the same time, developmental genes are repressed by both the PcG protein system and H3K27 methylation (respectively). When pluripotent cells (such as ES cells) differentiate, pluripotent-associated genes are potentially permanently repressed by DNA methylation. During this time, there is also an increase in H3K4 methylation, and developmental genes begin to be expressed. The early development of primordial germ cells (PGCs) involves the erasure of DNA methylation and repressive histone marks such as H3K9 methylation. As a result, pluripotent-associated genes are re-expressed and imprinted genes are re-programmed in the next generation. Developmental genes are expressed afterwards.

Source: Reik, 2007

Genetic imprinting is the process by which epigenetic changes in a specific parental chromosome (in the gamete or zygote) results in differential expression of two alleles of a gene in somatic cells of the offspring. A recent study identified over 150 imprinted genes in the human genome, using both a computational and experimental approach (Luedi et al, 2007). It should be noted however, that only two out of the 150 genes were verified experimentally to be imprinted, therefore further analysis is required to validate this study. The most widely recognised imprinted clusters are in a 1Mb region at 11p15 (encompassing the Beckwith Wiedemann region) (Brown et al, 1992) and a 2.3Mb region at 15q11-q13 (encompassing the Prader Willi and Angelman syndrome loci) (Driscoll et al, 1992). The silencing of imprinted genes occurs when differentially methylated regions (DMRs) that overlap a gene promoter region become heavily methylated (Birger et al, 1999). Methylation at a single DMR can also regulate expression of a whole cluster of imprinted genes (Sullivan et al, 1999). It is not fully understood how these regions are selected for *de novo* methylation following fertilisation. However, an exciting novel finding this year has suggested that transcription may play an important role in the methylation of germline DMRs (Chotalia et al, 2009). Using a mouse model, it was shown that disruption of a transcript upstream from the *Gnas* locus prevented the normal methylation of germline DMRs. Transcription across DMRs in germ cells could be essential for the re-modelling of histone modifications or to form chromatin domains which are required for *de novo* methylation (Chotalia et al, 2009).

X-chromosome inactivation is a stable silencing event, which is also associated with epigenetic modifications. X-inactivation involves the silencing of large areas of the X-chromosome instead of individual genes; and in humans is the random process by which one of the two copies of X-chromosome becomes inactivated in females. The X- inactivation centre (XIC) on the inactive X-chromosome encodes two RNA transcripts: Xist and Tsix, which are thought to initiate X-inactivation during embryonic development. Xist RNA coats the chromosome, spreading out from the XIC and subsequently causing gene silencing. Tsix also encodes RNA and is transcribed antisense to Xist; it overlaps the Xist RNA on the inactive X-chromosome (Brown et al, 1991; Lee et al, 1999) (Figure 1.3). The X-chromosome is

enriched 2-fold for Long Interspersed Element (LINE) repeat sequences compared to other human autosomes (Bailey et al, 2000), and it is thought that these repeat sequences have a functional role in the spreading of inactivation (the Lyon Repeat Hypothesis) (Lyon, 1998). It was initially believed that compared to the active X-chromosome, the inactive X-chromosome had higher levels of DNA methylation and histone marks in CpG islands. These epigenetic changes are thought to play a role in maintaining the inactive state as opposed to the initiation of X-inactivation (Bartlett et al, 1991; Heard et al, 2001; Kohlmaier et al, 2004; Sado et al, 2000). Unlike genomic imprinting, methylated CpG islands on the X-chromosome are not re-programmed during the normal life cycle. For example, the inactivated X-chromosome does not become methylated in the germline (Reik, 2007).

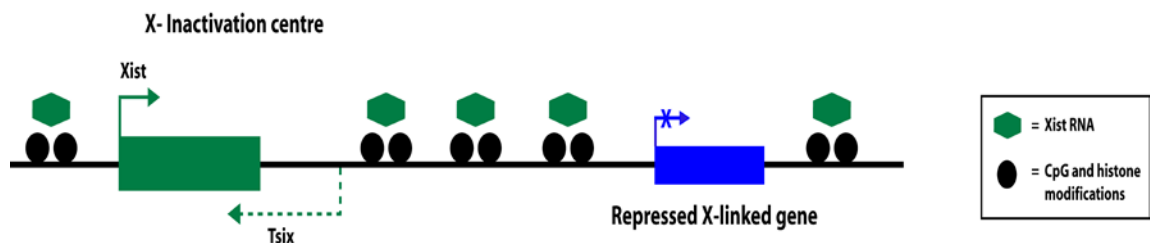


Figure 1.3: Structure of human X-inactivation centre (XIC) and associated epigenetic modifications involved in maintaining the inactive state

X-inactivation is initiated by the transcription of the *Xist* gene (green arrow) together with the overlapping antisense transcript *Tsix* (green dotted arrow). Transcription of *Xist* in cis coats the entire length of the X-chromosome resulting in its inactivation. Maintenance of the inactive state involves epigenetic modifications such as CpG methylation and histone marks.

Source: adapted from Heard et al., 2001

The overall global methylation state along the inactive X-chromosome was unknown until recently. Interestingly, the inactive X-chromosome has lower overall levels of methylation compared to the active X-chromosome (Hellman & Chess, 2007; Weber et al, 2005). Methylation on the active X-chromosome occurs mainly at transcribable, gene-rich regions (gene bodies), rather than at specific promoter regions. This suggests that on the active chromosome there is DNA hypomethylation at gene promoters and DNA hypermethylation at gene bodies and on the inactive X-

chromosome, there is DNA hypomethylation in gene bodies and hypermethylation at gene promoters (Hellman & Chess, 2007). The exact function of global hypermethylation at the gene bodies of active X-chromosomes is unclear. However, it may be involved in chromosome-wide epigenetic control.

It was initially hypothesised by Holliday and Pugh that specific modifying enzymes existed in eukaryotes which methylate and demethylate DNA and thereby control tissue-specific gene expression during mammalian development (Holliday & Pugh, 1975). Several investigators found no link between DNA methylation and tissue-specific expression during development (Hsiao et al, 1984; Walsh & Bestor, 1999), suggesting that methylation had no role in tissue-specific expression. Methylation was believed to only be involved in specialised biological functions, such as imprinting and X-inactivation. Although, recent studies have contradicted this belief, revealing a number of CpG islands which are methylated in normal tissues independent of imprinting and X-inactivation, many of which have been associated with tissue-specific methylation (Illingworth et al, 2008; Shen et al, 2007). Some of these non- X-linked novel promoter CpG islands were discovered to be densely methylated in normal somatic tissues and escape methylation in the germline cells. The CpG island hypermethylation occurring at these gene promoters appears to be an important mechanism for tissue-specific gene silencing (Shen et al, 2007). These studies identified approximately 4-8% of CpG islands with tissue-specific methylation. Similar to this, a separate report identified tissue-differential methylation regions (T-DMRs) with the majority of T-DMRs (76%) residing in regions located within 2kb of islands known as 'CpG island shores' rather than in CpG islands (6%) (Irizarry et al, 2009). The relationship between shore methylation and gene expression was confirmed using pharmaceutical inhibition of methylation and DNMT knock-out experiments. This suggests that the CpG island shores may play an important role in tissue-specific regulation (Irizarry et al, 2009).

1.2.2 CpG Islands

The likelihood of any dinucleotide pairing occurring in a DNA sequence is 1 in 16. However, the mammalian genome has disproportionately few CpG dinucleotides

(~1%, ~1 in 80 dinucleotides) a phenomenon known as CG suppression. This suppression was thought to have occurred over long periods of time as a result of DNA methylation deaminating CpG to Thymine/Guanine (TpG) (Coulondre et al, 1978). Even though the frequency of CpG dinucleotides is low in the mammalian genome, there are stretches of DNA that have CpG-rich regions and extend over hundreds of nucleotides. These regions are known as CpG islands (Bird et al, 1985; Cooper et al, 1983). Around half of the CpG islands in the human genome are associated with gene transcriptional start sites and half are associated with intra- or intergenic regions (Illingworth et al, 2008). Genes with widespread expression, such as housekeeping genes, often have CpG islands at the 5' end of genes, usually in the promoter region and surrounding transcriptional start site and rarely have downstream CpG islands (Illingworth et al, 2008). Downstream CpG islands occur in 49% of genes with limited expression (Larsen et al, 1992). Their function is unknown, but it is thought they may represent tissue or developmental specific promoters, or they may not act as functional promoters at all and have essential coding functions that have not been lost by mutation (Jones, 1999). The most widely accepted method of identifying a CpG island uses two sets of criteria: 'NCBI strict' and 'NCBI relaxed,' and these are described below (Takai & Jones, 2002). To introduce less bias, the algorithm (and cut-offs) to set these criteria were designed using the complete genomic sequences of human chromosomes 21 and 22 rather than using gene exon databases previously used to define a CpG island (Gardiner-Garden & Frommer, 1987). This new definition excludes many intragenic CpG-rich areas such as *Alu* sequences (Schmid, 1998), which are highly repetitive short interspersed elements and also excludes CpG dinucleotides not associated with the promoters of genes (Takai & Jones, 2002).

- **Relaxed**
 - 200 base pair (bp) min length
 - 50% or higher GC content
 - 0.60 or higher observed CpG/ expected CpG
- **Strict**
 - 500bp min length
 - 50% or higher GC content
 - 0.60 or higher observed CpG/ expected CpG

The vast majority of CpG islands are unmethylated. However, it has been shown that CpG island promoter methylation is physiologically variable and is associated with transcriptional silencing of genes (Figure 1.4), which can be passed between cellular generations (Bird, 1986).

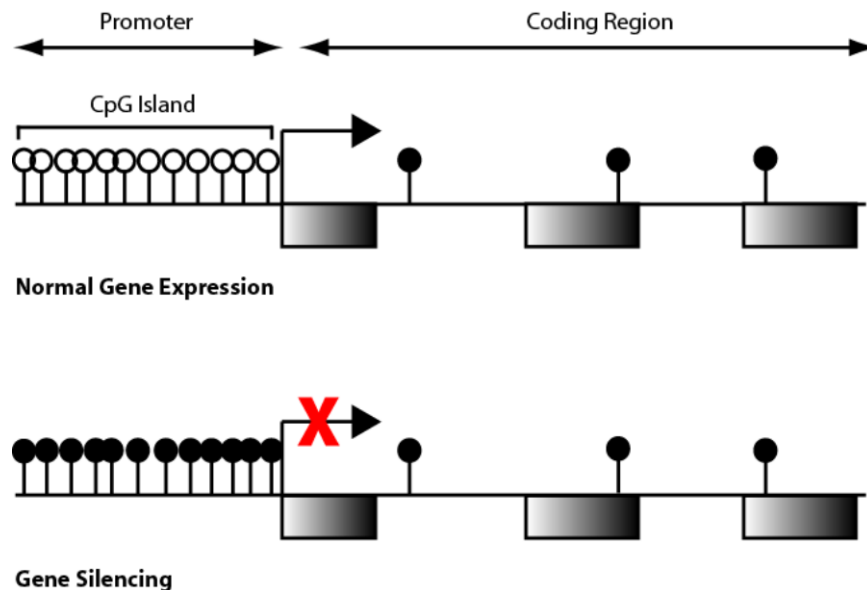


Figure 1.4: Effect of DNA methylation within CpG island promoter regions on gene transcription

Normal unmethylated CpG island at the promoter region (as depicted by unfilled lollipop sticks) where gene is transcribed. Methylated promoter region (as depicted by filled lollipop sticks) is associated with gene silencing.

1.2.3 DNA methyltransferases

CpG methylation is catalysed by a number of different DNMT enzymes. In eukaryotes there are three families of DNMTs (1, 2 & 3), which are likely to have diverged early in eukaryotic evolution. The enzymes are distantly related to each other and the genes are conserved between species in genomes that are methylated, such as in *Arabidopsis thaliana* and *Xenopus laevis* (Siedlecki & Zielenkiewicz, 2006). Studies have shown that these enzymes cooperate, some having distinct but also overlapping functions. DNMT1, DNMT3a and DNMT3b are the key players involved in establishing global methylation patterns in mammals, whereas DNMT2 and DNMT3L have not been shown to be directly involved (Brenner & Fuks, 2006).

DNMT1, the first mammalian DNMT to be cloned and purified, was initially described as having *de novo* methylation function (Bestor et al, 1988). However, it was later found that DNMT1 had a 5-30 fold preference for hemimethylated DNA (Yoder et al, 1997a) and therefore this enzyme was termed a 'maintenance methyltransferase'. This term refers to a system that reproduces parental DNA methylation on the daughter strand DNA, providing heritability, with genomic methylation patterns being copied during DNA replication and passed onto the next cell generation. DNMT1 is closely associated with the DNA replication machinery and has a preference for new unmethylated CpG sequences whose opposite strand has a methyl group attached (Leonhardt et al, 1992). Inactivation of *DNMT1* in mice results in embryonic lethality and widespread demethylation in all sequences analysed (Li et al, 1992). ES cells lacking *DNMT1* can no longer maintain differentiation (Damelin & Bestor, 2007; Lei et al, 1996; Panning & Jaenisch, 1996). However, they are viable and contain low but stable levels of *de novo* DNA methyltransferase activity (Lei et al, 1996; Li et al, 1992). This finding led to the hypothesis that an independent *de novo* methyltransferase may exist. *DNMT3a* and *DNMT3b* were subsequently cloned and characterised as *de novo* methyltransferase enzymes (Okano et al, 1998). Although both DNMT3 enzymes are regarded as *de novo* methyltransferases, they are also involved in maintaining methylation by restoring methylation sites missed by DNMT1 (Liang et al, 2002). Evidence has suggested that there is a cooperative function between the two DNMTs a model in

which: DNMT3a initiates *de novo* methylation by transferring methyl groups to one region of DNA; and then DNMT1 is recruited, which then methylates the entire region of the DNA (Fatemi et al, 2002). *DNMT3a* and *DNMT3b* are both highly expressed during development and are necessary for proper development in mammalian embryos. *DNMT3a*^{-/-} mice develop to term, however they die at approximately four weeks of age. *DNMT3b*^{-/-} mice are embryonically lethal (Okano et al, 1999). The DNMT3 enzymes are essential for establishing new methylation patterns and DNMT3b in particular is required for methylation of genome-specific regions, such as pericentromeric repetitive sequences and CpG islands on the inactive X-chromosome (Okano et al, 1999). Table 1.1 summarises the phenotypes of the *DNMT* knock-out mice and the DNA methyltransferase activity for each DNMT discussed in this section (DNMT1, DNMT3a & DNMT3b) and others not discussed (DNMT2 and DNMT3L).

Mutational events causing the deletion of DNMT3b function are associated with the disease Immunodeficiency, centromeric instability and facial anomalies (ICF) syndrome (Hansen et al, 1999; Xu et al, 1999). ICF patients display marked hypomethylation and decondensation of pericentromeric heterochromatin on certain chromosomes (Franceschini et al, 1995; Tuck-Muller et al, 2000) and is the only known genetic disorder that involves constitutive aberrations of genomic methylation.

DNMT Class	<i>Dnmt</i> knock-out in mice	DNA methyltransferase activity
DNMT1	<ul style="list-style-type: none"> - Embryonic Lethality (E8.5) - Global hypomethylation - Lack of imprinting 	<ul style="list-style-type: none"> - Yes - Maintenance DNMT <i>de novo</i> activity: possible but low
DNMT2	<ul style="list-style-type: none"> - Viable, fertile with only minor defects 	<ul style="list-style-type: none"> - Yes (low) - Preferences for centromeric structures - Methylates a tRNA*
DNMT3a	<ul style="list-style-type: none"> - Postnatal lethality (4 weeks) - Loss of <i>de novo</i> methylation - Severe intestinal defects - Impaired spermatogenesis 	<ul style="list-style-type: none"> - Yes - <i>de novo</i> activity; probably some maintenance activity
DNMT3b	<ul style="list-style-type: none"> - Embryonic lethality (E14.5-E18.5) - Loss of <i>de novo</i> methylation - Mild neural tube defects - Demethylation of centromeric repeat sequences 	<ul style="list-style-type: none"> - Yes - <i>de novo</i> activity; probably some maintenance activity - Preference for minor satellite repeats
DNMT3L	<ul style="list-style-type: none"> - Viable; males are sterile - Females have no viable progenitor - Loss of maternal and paternal imprinting in gametes 	<ul style="list-style-type: none"> - No - Cofactor of DNMT3a (enhances its <i>de novo</i> activity)

Table 1.1: Summary of phenotypes of the DNMT knock-out mice and methyltransferase activity for each DNMT enzyme

*function for DNMT2 published: (Goll et al, 2006).

Source: adapted from Brenner and Fuks, 2006

1.3 DNA Methylation and mechanisms of gene silencing

Mutational inactivation of tumour suppressor genes has long been known to be associated with tumour progression. However, cancer development is also associated with transcriptional silencing of tumour suppressor genes by DNA methylation (Herman et al, 1996b; Kane et al, 1997). It is currently unknown whether methylation of tumour suppressor genes directly causes the silencing of genes or if methylation occurs subsequent to gene silencing by another mechanism. There is an association between cancerous cells and aberrant methylation (Gama-Sosa et al, 1983; Herman et al, 1996b), however, there are likely to be other factors such as histone modifications and chromatin re-modelling events, in addition to DNA methylation, that contribute to gene silencing.

1.3.1 Direct mechanism of gene silencing by DNA methylation

DNA methylation may act independently from other epigenetic modifications and repress transcription by the direct interference of the methyl group in the binding of proteins, (such as transcription factors) to its DNA sequence (Jones & Wolffe, 1999). Most of the evidence for this is based on reports on c-Myc and the CCCTC-binding factor (CTCF). c-Myc is a transcription factor which is involved in regulating both differentiation and cell growth, and studies have demonstrated that a heavily methylated sequence inhibits c-Myc from binding to its consensus sequence (Prendergast et al, 1991). In addition, CTCF a transcriptional regulator protein best known for its role in the imprinting of the H19/Igf2 locus, is prevented from binding to a regulatory site on the paternal allele as it is methylated (Bell & Felsenfeld, 2000). In contrast, a recent study found that p53, a transcription factor involved in the response to carcinogenic stress, binds at similar affinities to methylated CpG sequences and unmethylated CpG sequences. Furthermore, for some sequences, methylation in the binding sites actually increases the binding of p53 four- to six-fold (Petrovich & Veprintsev, 2008). Very few other transcription factors, whose binding is affected by methylation, have been reported. In addition, it seems very improbable that in the entire genome, the function of DNA methylation is only restricted to recognition sites for individual transcription factors. Other indirect mechanisms

involving DNA methylation and chromatin re-modelling are more likely to have a prominent role in gene silencing.

1.3.2 Indirect mechanisms of gene silencing by DNA methylation

Chromatin undergoes varying degrees of organisation and comprises of subunits known as nucleosomes, where approximately 200bp of DNA sequence is organised, by an octamer of structural proteins called histones, into a bead-like structure. The core histones (H2A, H2B, H3 and H4) are susceptible to post-translational modifications, some of which include: acetylation, methylation, phosphorylation, ubiquitination and adenosine diphosphate (ADP) ribosylation (Spotswood & Turner, 2002; Strahl & Allis, 2000). These modifications function in the regulation of chromosome condensation, DNA repair, DNA synthesis and transcription (Kouzarides, 2007). Deacetylation and methylation of histone H3 at both lysine residue 9 (H3K9) and histone H3 lysine 27 (H3K27) for example, are the best characterised histone modifications associated with gene silencing (Margueron et al, 2005). It is generally considered that transcriptionally-active chromatin has an open, extended structure with unmethylated promoter regions and core histones are acetylated by histone acetyltransferases (HATs) (Tazi & Bird, 1990). Transcriptionally inactive chromatin has a highly condensed structure, high levels of methylation at promoter regions, and core histone proteins are deacetylated by histone deacetylases (HDACs). Studies have however shown a correlation between open chromatin structures and areas of high gene density, but not necessarily with high levels of gene expression due to the fact that inactive genes can be found in open chromatin and active genes can be found in regions of compact chromatin (Gilbert et al, 2004). From using mouse embryonic cells completely lacking both *DNMT3a* and *DNMT3b*, it was recently found that DNA methylation affects chromatin structure at the level of the nucleosome and at the level of nuclear organisation, but not at secondary levels of bulk chromatin and heterochromatin (Gilbert et al, 2007). This suggests that DNA methylation modifies both primary chromatin structure and nuclear organisation, and therefore adds more complexity to the role of DNA methylation in altering gene expression.

DNA methylation and histone deacetylation function can act together, using a common mechanistic pathway, to silence gene expression (Nan et al, 1998). A family of Methyl-CpG binding proteins, which have been cloned and fully characterised, mediates this. Some of these proteins have a homologous methylcytosine-binding domain (MBD). MBD1, MBD2, MBD4 and MeCP2 are known to be involved in transcriptional repression by binding 5-methylcytosine through their methyl-binding domain (Cross et al, 1997; Kondo et al, 2005; Nan et al, 1997; Ng et al, 1999). MeCP2 is a protein that specifically binds to methylated DNA and *in vitro* can invade chromatin and displace the histone H1 (Lewis et al, 1992; Nan et al, 1997; Nan et al, 1993). In 1998, MeCP2 was demonstrated to repress transcription by associating with HDAC proteins (Jones et al, 1998; Nan et al, 1998) (Figure 1.5). Both MeCP2 and the MBD proteins are thought to associate with HDACs, which deacetylate histones and in turn repress transcription (Ballestar & Esteller, 2002; Jones et al, 1998; Nan et al, 1998).

Kaiso is another methyl-CpG binding protein, which is involved in transcriptional repression. Kaiso is different to other MBD proteins, in that it binds methylated DNA through its zinc-finger motif (Prokhortchouk et al, 2001). The protein plays an essential role in maintaining transcriptional silencing during early *Xenopus laevis* development as the absence of *kaiso* results in early zygotic gene expression and subsequent developmental arrest and apoptosis (Ruzov et al, 2004). In comparison, *Kaiso*-null mice have no obvious phenotype but do show a resistance to intestinal tumours when bred onto an *Apc*^{Min/+} genetic background (Prokhortchouk et al, 2006). This suggests that Kaiso may be involved in epigenetic mechanisms which occur in tumorigenesis. Indeed, a recent report demonstrated that Kaiso represses the tumour suppressor gene *p16*^{INK4A} in a methylation dependent manner. Kaiso depletion resulted in induced expression of *p16*^{INK4A} without reversing aberrant hypermethylation, further reinforcing its epigenetic role in cancer (Lopes et al, 2008).

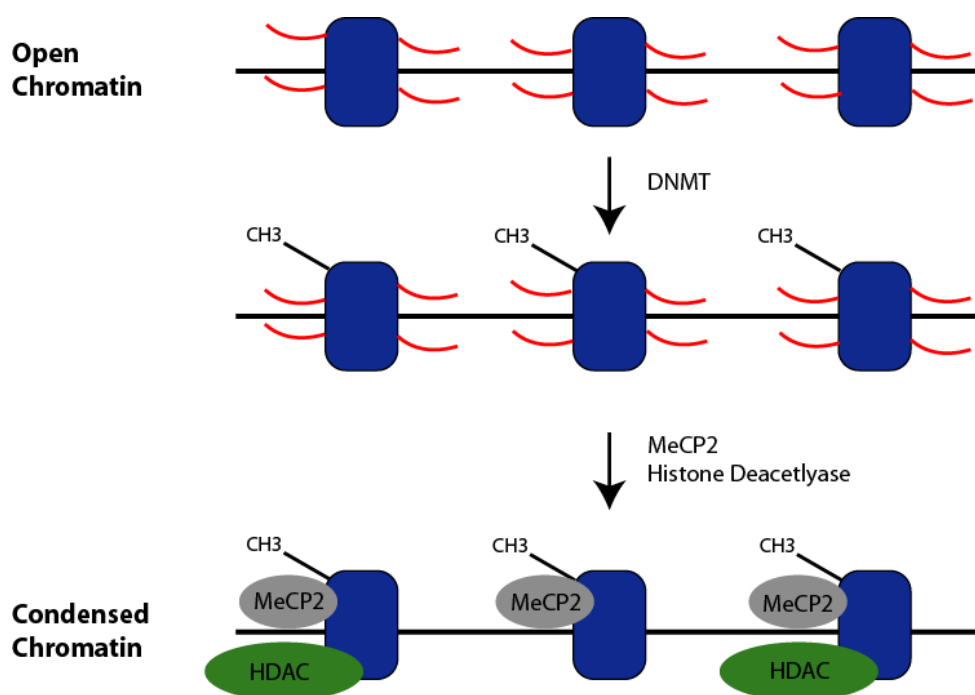


Figure 1.5: Gene silencing by histone deacetylation may be mediated through CpG promoter methylation

Nucleosome 'beads on a string' are shown (blue blocks) with DNA (thick black line), acetylated histone tails are protruding from the nucleosome (red lines) and methylated CpG dinucleotides are also indicated (CH_3). Transcriptional repressor MeCP2 recruits co-repressor complex consisting of transcription factor repressors (not shown) and histone deacetylases (HDACs).

In human neoplasia, MBD2 is selectively recruited at the hypermethylated promoter regions of *p14^{ARF}/p16^{INK4a}* but not at acetylated histones H3 and H4 (Magdinier & Wolffe, 2001). Recently, it was also shown that: MeCP2, MBD1 and MBD2 specifically bind to methylated *hMLH1* promoters in endometrial cancer; and hyperacetylated H3 and H4 histones were associated with unmethylated and actively transcribing *hMLH1* promoters (Xiong et al, 2006). This data suggests that DNA methylation and histone deacetylation work in synergy for gene silencing in cancer. It is unknown whether DNA hypermethylation has a dominant effect in the maintenance of gene silencing. Although, experiments have demonstrated that hypermethylated genes cannot be transcriptionally activated with treatment of a HDAC inhibitor alone (Trichostatin A -TSA) (Cameron et al, 1999).

It is unclear how histone deacetylation produces a transcriptionally inactive state, however, two models have been proposed. One theory is that acetylation/deacetylation modifications of the lysine residues directly alter electrostatic charges. This then subsequently changes the interaction between the histone tails and DNA and therefore decreases the accessibility to transcription factors (Lee et al, 1993). Another model proposes that histone acetylation/deacetylation combinations are interpreted as a 'histone code', which results in the interaction with *trans*-acting factors such as chromatin re-modelling factors (Strahl & Allis, 2000). Therefore, the action of the histone-modifying enzymes may be targeted by chromatin re-modelling events. Finally, it has been shown that DNMTs directly interact with HDACs. DNMT3a is known to be targeted to promoter regions through its association with a transcription factor, and then acts to repress transcription by recruiting HDAC activity (Fuks et al, 2001). This suggests that DNMT3a may have important functions other than *de novo* methylation, and further provides a link between DNA methylation and transcriptional activity.

In contrast to histone acetylation, histone methylation at lysine and arginine residues are thought to be relatively stable and represent 'marks' that are transmissible through cell divisions. Methylation of histones is catalysed by histone methyltransferases (HMTs), which use the methyl-donor SAM (Rice & Allis, 2001).

The monomethylations of H3K27, H3K9, H4K20, H3K79 and H2BK5 are related to gene activation, whereas trimethylations of H3K27, H3K9 and H3K79 are related to gene repression (Barski et al, 2007). It is unknown how histone methylation precisely affects gene transcription. Unlike histone acetylation, histone methylation does not alter the overall charge of the histone tails. Methylation does however increase the affinity of the histone tails for anionic molecules such as DNA (Baxter & Byvoet, 1975). Thus, it is believed that histone methylation may have an effect on the interaction of histone tails with DNA and/or chromatin re-modelling proteins (Rice & Allis, 2001). There is much speculation as to how DNA methylation affects histone methylation or vice versa. One model is that H3K9 methylation by a HMT leads to the recruitment of an adaptor molecule known as heterochromatin protein 1 (HP1) (Lachner et al, 2001). HP1 then recruits DNMT enzymes, which catalyse CpG methylation in the region of the methylated histone tails (Fuks et al, 2003). Methyl-CpG binding proteins could then bind methylated DNA, which subsequently leads to the recruitment of HDAC proteins. Therefore, it may be that DNA methylation, histone acetylation and H3K9 methylation cooperate to regulate gene transcription.

In the sections above, the role of DNA methylation in normal physiological processes has been described. In cancer, these processes can be disrupted due to aberrant methylation, which can subsequently affect the expression of single or even multiple genes.

1.4 Aberrant methylation and cancer

It is well established that neoplastic cells have a methylation imbalance and that this imbalance may fundamentally contribute to tumour progression (Esteller, 2008). Neoplastic cells can simultaneously display widespread genomic hypomethylation, regional areas of hypermethylation often involving the promoters of selected tumour suppressor genes, and increased total DNMT activity (Baylin et al, 1998). It is unknown whether global hypomethylation and region-specific hypermethylation are linked in tumorigenesis. However, it has been shown that these changes in methylation occur at specific but distinct sites, suggesting that they may have different effects within the neoplastic cell. Overall, the methylation status in cancer cells is complex and unravelling causality between general non-specific effects and specific methylation events requires extensive and painstaking research.

1.4.1 Global Hypomethylation

The first report of global loss of 5-methylcytosine in cancer cells was by Gama-Sosa et al (1983). Using high-performance liquid chromatography, loss of methylation was identified in both benign and malignant tumours and also in pre-malignant adenomas when compared with normal tissues, suggesting that demethylation of DNA may be involved in tumour progression (Gama-Sosa et al, 1983). Since then, various studies have shown that global hypomethylation occurs in a number of different tumour types and is highly specific with regard to tumour type and tumour stage. For example, hypomethylation is identified more commonly in solid tumour types such as hepatocellular cancer, cervical cancer and prostate tumours (Bedford & van Helden, 1987). Loss of genomic methylation in some tumours is a frequent and early event, relative to other epigenetic changes during tumorigenesis, and can correlate with disease severity and metastatic potential. For instance, extensive hypomethylation of chromosome 1 is a marker for poor prognosis in ovarian cancer and was found to be more informative than tumour grade or stage (Widschwendter et al, 2004). However, more recently it was demonstrated that global DNA hypomethylation occurs in later stages of prostate cancer progression, appearing to a significant extent only in metastatic disease stages (Yegnasubramanian et al, 2008).

Therefore, in prostate cancer, changes in DNA hypomethylation may occur following CpG island hypermethylation.

It is estimated that more than one third of DNA methylation is found at repetitive elements (Kochanek et al, 1993) and in tumour cells, DNA methylation at these regions is often lost (Yoder et al, 1997b) (Figure 1.6). In fact, one method for measuring global DNA methylation is based on measuring the methylation status of DNA repetitive elements, such as *Alu* elements and LINE sequences (Yang et al, 2004). Hypomethylation has also been observed at pericentromeric satellite sequences on chromosome 1 and chromosome 16 in a high percentage of Wilms tumours. Furthermore, there was a significant relationship between chromosomal rearrangements of 1q and 16q, and hypomethylation of satellite DNA in the pericentromeric regions of these chromosomes (Qu et al, 1999). Therefore, loss of methylation at pericentromeric satellite sequences in these cancers may predispose them to breakage or recombination. This is supported by *in vivo* studies, which have shown that mice with reduced levels of *DNMT1* develop T cell lymphomas with a high frequency of chromosome 15 trisomy (Gaudet et al, 2003). This implies that there may be an association between global hypomethylation, chromosome aberrations, and tumorigenesis. Another theory is that re-activation of transposon promoters following demethylation may contribute to aberrant gene regulation in tumorigenesis by transcriptional interference or the generation of antisense transcripts. Double-stranded RNA homologues (to the gene or its promoter) could be generated and the recruitment of the RNA interference (RNAi) machinery would then lead to the epigenetic marks, including DNA methylation (Robertson, 2005).

The underlying mechanism responsible for global DNA hypomethylation is not fully understood. One hypothesis is that hypomethylation is due to dysfunction of chromatin-remodelling proteins or maintenance DNMTs. Knock-out studies on *Lsh*, a SNF-2 family member, chromatin-remodelling protein, leads to a global defect in genomic methylation as well as chromosome instability (Fan et al, 2003). This is interesting, as *Lsh* is primarily known for its role in chromatin remodelling. *Lsh* may regulate methylation directly or indirectly. However, it has been shown to not affect

DNMT activity, which suggests that it may have a more direct role (Dennis et al, 2001). MBD proteins mediate histone deacetylase-dependent gene silencing at methylated CpG islands, and mouse studies have shown that deficiencies in methyl-CpG binding proteins such as MBD1, MBD2 and MeCP2 results in phenotypic changes, but there have been no reports of associated alterations in global methylation levels (Guy et al, 2001; Hendrich et al, 2001; Zhao et al, 2003). This is not surprising as these proteins are involved in machinery that binds and interprets methylation marks rather than actually producing them. Furthermore, they are not directly involved in chromatin re-modelling unlike *Lsh*.

DNMT proteins are more likely to have a role in DNA hypomethylation as they are directly involved, unlike the other proteins mentioned previously. *DNMT1* null mice are embryonically lethal (section 1.2.3). Although, mutations of *DNMT1* in homozygous murine embryonic stem cells results in a 3-fold decrease in global levels of methylated CpG compared to wild-type cells (Li et al, 1992). In addition, the splice variant of *DNMT3b* (*DNMT3b4*), which has been found in patients with liver cancer, is associated with hypomethylation of pericentromeric satellite sequences when transfected into human epithelial cells (Saito et al, 2002). The specific functions of the DNMT3b splice variants are not fully understood. Whilst *DNMT3b4* is a negative regulator of methylation, *DNMT3b3* is involved in methylating satellite repeat sequences but is dependent on other unknown factors that affect its activity (Weisenberger et al, 2004). Currently, no studies have identified a direct link between DNMT mutations and global levels of demethylation in tumours. Furthermore, whether the global epigenetic change manifests as hypomethylation is a cause or consequence of tumorigenesis is still under much debate, however, as mentioned previously, some studies propose that DNA hypomethylation plays a causal role by promoting chromosomal instability (Gaudet et al, 2003; Qu et al, 1999).

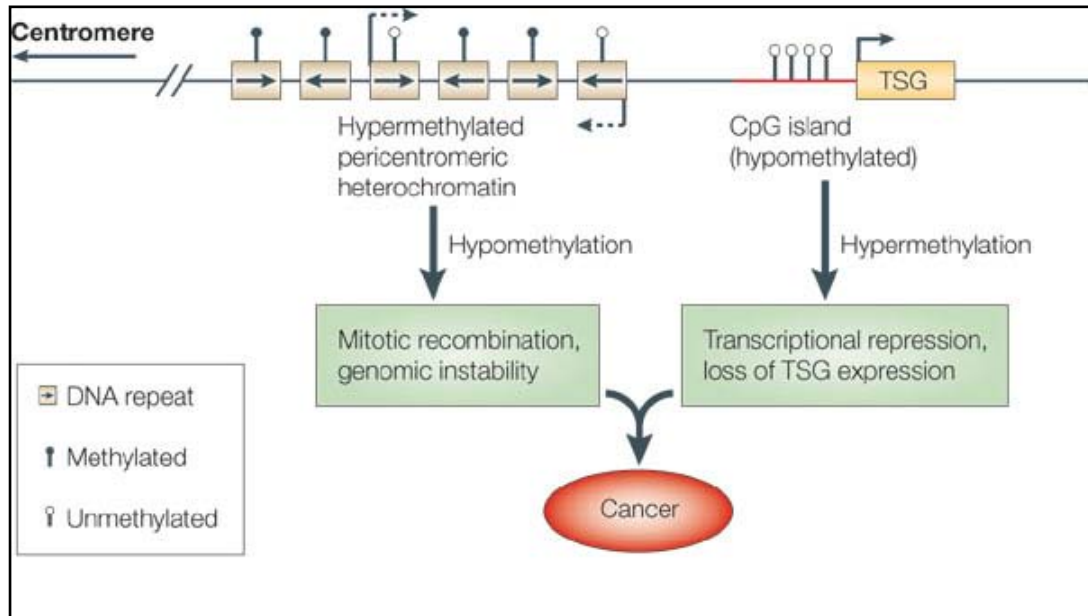


Figure 1.6: Aberrant DNA methylation and cancer.

The diagram shows a region of genomic DNA in a normal cell, consisting of a repeat-rich, hypermethylated pericentromeric heterochromatin and an actively transcribed tumour suppressor gene (TSG), hypomethylated at the CpG island (indicated in red). In tumour cells, the repeat-rich heterochromatin is hypomethylated and is associated with genomic instability, most likely through increased mitotic recombination. Hypermethylation of CpG islands can also occur in tumour cells, which results in transcriptional silencing.

Source: Robertson, 2005.

1.4.2 Hypomethylation of CpG Islands

Hypomethylation was the first epigenetic abnormality to be identified in cancer cells when a loss of DNA methylation at CpG dinucleotides in the *c-Ha-ras* and *c-Ki-ras* genes was observed in primary small cell lung carcinomas (Feinberg & Vogelstein, 1983b). Following on from this initial finding, the primary focus moved towards the search for hypermethylated genes, and studies involving hypomethylation of specific CpG islands were overlooked. High-throughput genomic methylation analysis in various different cancers has suggested that the number of hypomethylated sites in the human genome may be quite high (Adorjan et al, 2002; Iacobuzio-Donahue et al, 2003). In one study, using cDNA microarrays, 149 genes were found to be differentially expressed in pancreatic cancer tissues, compared to the normal pancreas. The majority of these genes tended to be overexpressed and one gene, *14-*

$3\text{-}3\sigma$ was associated with aberrant hypomethylation (Iacobuzio-Donahue et al, 2003). CpG-island-specific hypomethylation, followed by increased expression has been reported for many genes, including: the *S100* calcium-binding protein A4 gene (*S100A4*) in colorectal cancer (Nakamura & Takenaga, 1998); the normally silenced long control region (LCR) and *E6* genes of human papillomavirus 16 (HPV16) in cervical cancer (Badal et al, 2003; de Capoa et al, 2003); and the serpin peptidase inhibitor, clade B (ovalbumin) member 5 gene (*SERPINB5*) in gastric cancer (Akiyama et al, 2003). Little is known regarding the mechanisms responsible for gene-specific hypomethylation and as with global DNA hypomethylation, it is still unclear whether gene-specific hypomethylation is a cause or consequence of tumorigenesis.

1.4.3 Hypermethylation of CpG Islands

Abnormal methylation of promoter regions can result in transcriptional silencing and increased mutagenicity by the deamination of 5-methylcytosine to thymidine, both of which can contribute to carcinogenesis. Methylation is at least as common a mechanism as mutation for gene silencing in currently identified tumour suppressor genes (Jones & Baylin, 2002). Approximately half of genes mutated in the germline that cause familial forms of cancer are also known to undergo methylation-associated silencing in different sporadic cancers (Jones & Baylin, 2002). In addition, there are a growing number of tumour suppressor genes, which are inactivated by promoter hypermethylation, but not frequently mutated in different cancers. The first gene shown to have abnormal hypermethylation in its promoter region was *Calictonin* (Baylin et al, 1986). The functional significance of this epigenetic event was unclear, as *Calcitonin* is not ubiquitously expressed in adult tissues and does not function as a tumour suppressor gene. This finding did however lead on to the possibility that tumour suppressor genes may be inactivated in cancer as a result of promoter hypermethylation. A number of tumour-suppressor genes have been found to be methylated at their CpG islands in different cancer types (Table 1.2). Genes that are affected include those involved in cell cycle regulation, DNA repair, apoptosis, cell-to-cell interaction and angiogenesis, all of which have a role in cancer development (Esteller, 2008). Demethylation of some of these genes using the DNMT inhibitor 5-

Azacytidine is associated with re-expression at the mRNA and protein level. This suggests that methylation may play a role in silencing affected genes and thereby contribute to human carcinogenesis.

Type of Cancer	Hypermethylated genes	References
Colon cancer	<i>hMLH1</i> <i>p16^{INK4A}</i> <i>p14^{ARF}</i> <i>SFRP1</i> <i>WRN</i>	(Kane et al, 1997) (Herman et al, 1995; Merlo et al, 1995) (Robertson & Jones, 1998) (Caldwell et al, 2004) (Agrelo et al, 2006)
Breast cancer	<i>BRCA1</i> <i>E-cadherin</i> <i>TMS1</i>	(Dobrovic & Simpfendorfer, 1997) (Graff et al, 1995) (Conway et al, 2000)
Lung cancer	<i>p16^{INK4A}</i> <i>DAPK</i> <i>RASSF1A</i>	(Merlo et al, 1995) (Zochbauer-Muller et al, 2001) (Dammann et al, 2000)
Glioma	<i>MGMT</i> <i>EMP3</i> <i>THBS1</i>	(Costello et al, 1994) (Alaminos et al, 2005) (Alaminos et al, 2005)
Leukemia	<i>p15^{INK4b}</i> <i>EXT1</i> <i>ID4</i>	(Herman et al, 1996b) (Roperio et al, 2004) (Yu et al, 2005)
Lymphoma	<i>p16^{INK4A}</i> <i>p73</i> <i>MGMT</i>	(Herman et al, 1997) (Corn et al, 1999) (Esteller et al, 1999b)
Bladder cancer	<i>p16^{INK4A}</i> <i>TMEFF2/HPP1</i>	(Gonzalez-Zulueta et al, 1995) (Suzuki et al, 2005)
Kidney cancer	<i>VHL</i>	(Herman et al, 1994)
Prostate cancer	<i>GSTP1</i>	(Lee et al, 1994)
Esophageal cancer	<i>p16^{INK4A}</i> <i>p14^{ARF}</i>	(Maesawa et al, 1996) (Nie et al, 2002)
Stomach cancer	<i>hMLH1</i> <i>p14^{ARF}</i>	(Leung et al, 1999) (Iida et al, 2000)
Liver cancer	<i>SOCS1</i> <i>GSTP1</i>	(Yoshikawa et al, 2001) (Tchou et al, 2000)
Ovarian cancer	<i>BRCA1</i>	(Catteau et al, 1999)

Table 1.2: Tumour suppressor genes associated with CpG island hypermethylation in different cancer types.

BRCA1 (breast-cancer susceptibility gene 1), *DAPK* (death-associated protein kinase), *EMP3* (epithelial membrane protein 3), *EXT1* (exostosin 1), *GSTP1* (glutathione S-transferase 1), *hMLH1* (homologue of MutL *Escherichia coli*), *ID4* (inhibitor of DNA binding 4), *MGMT* (O6-methylguanine–DNA methyltransferase), *RASSF1A* (ras association domain family protein 1), *SFRP1* (secreted frizzled-related protein 1), *SOCS1* (suppressor of cytokine signaling 1), *THBS1* (thrombospondin 1), *TMEFF2/HPP1* (hyperplastic polyposis gene 1), *TMS1* (target of methylation-induced silencing), *VHL* (von Hippel–Lindau disease), and *WRN* (Werner's Syndrome). Note: this is not a definitive list.

Source: adapted from Esteller, 2008.

Aberrant methylation can be detected in the earliest precursor lesions in tumours with well-defined progression, such as in colon cancer. Aberrant crypt foci (34%) displayed hypermethylation of six genes frequently found to be methylated in established colorectal cancer (Chan et al, 2002). This suggests that methylation could directly contribute to transformation, and may not occur as a late event because of genetic alterations. Excluding haploinsufficiency, the phenotypic consequence of a loss of a tumour suppressor gene is usually only seen when both alleles of the gene are inactivated in a tumour ('two hit hypothesis') (Knudson, 2000). In addition to intragenic mutations and chromosomal loss (by loss of heterozygosity (LOH) or homozygous deletion), methylation of CpG islands within the promoter region of tumour suppressor genes represents a third pathway in which tumour suppressor genes are inactivated (Figure 1.7) (Jones & Laird, 1999). Promoter hypermethylation has been shown to play a significant role in the inactivation of tumour suppressor genes, either as a first or second hit in both sporadic and familial forms of different cancers (Esteller et al, 2001b).

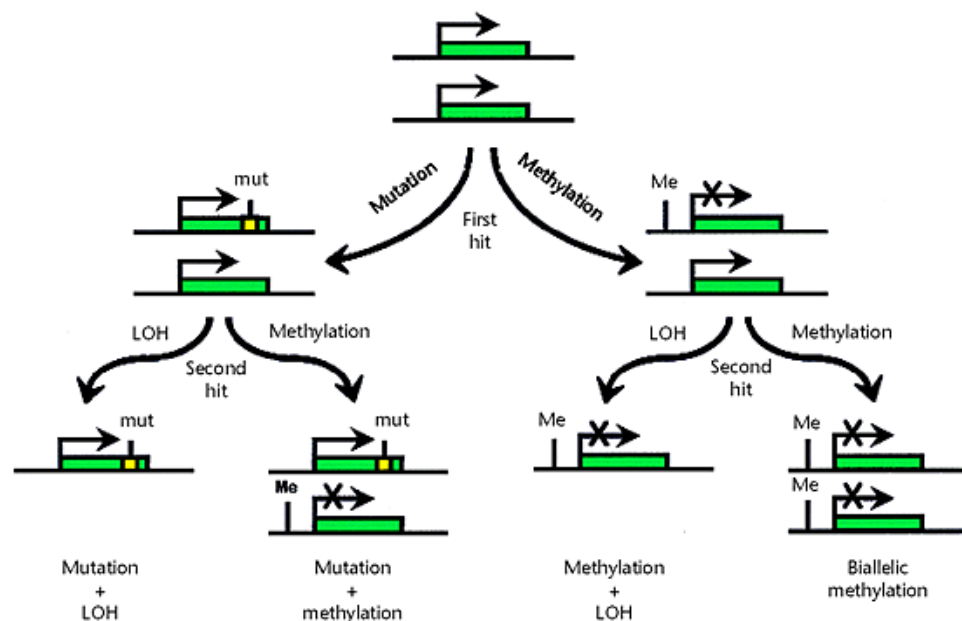


Figure 1.7: The revised Knudson two-hit model hypothesis.

Methylation of the promoter region can occur as a 'second hit' in addition to the 'first hit' of either intragenic mutations or deletions.

Source: Jones and Laird, 1999.

Following on from the initial studies carried out on CpG island hypermethylation in neoplastic cells, methylation analysis using a restriction enzyme approach found a small degree of methylation in the estrogen receptor 1 (*ESR1*) gene in normal colonic tissue adjacent to colorectal tumours. Furthermore, the degree of methylation positively correlated with the age of patient ($R^2 = 0.71$, $p < 0.000001$) (Issa et al, 1994). Subsequent studies in colorectal cancer and in other cancers revealed that there were many more genes methylated in normal tissues and that methylation increased with age (Ahuja et al, 1998; Issa et al, 1996; Kwabi-Addo et al, 2007). These will be discussed in more detail in section 1.5.2. It was observed however, that not all genes hypermethylated in cancer display age-related methylation and with these cases, hypermethylation may be a tumour-related event. It has therefore been suggested that there are in fact two types of methylation in cancer: age-related in which methylation precedes neoplasia; and cancer-related in which methylation occurs primarily and is a fundamental process in the formation of neoplasia. These two types of methylation were termed Type A (for Age-related) and Type C (for Cancer-related) (Toyota & Issa, 1999).

1.4.4 DNA methylation - Cause or consequence

There has been much debate as to whether methylation is the initial cause for gene silencing or methylation is a consequence of prior gene silencing. *De novo* methylation may be the result of loss of expression due to upstream mutational events in signal transduction cascades or transcription factor networks. It is also thought that aberrant histone modification may cause gene silencing in cancer cells, which consequently catalyses DNA methylation by recruiting DNMT enzymes. In one study, H3K9 deacetylation and H3K9 methylation preceded re-silencing and re-DNA methylation of *p16^{INK4A}* in cancer cells, which occurs after DNA demethylation (drug-induced) and re-expression (Bachman et al, 2003). Another hypothesis is that polycomb-induced H3K27 methylation, which is normally involved in gene silencing during development, brings about tumour-specific targeting of *de novo* methylation and is actually pre-programmed (Schlesinger et al, 2007).

The most generally held view is that DNA methylation results in repressive chromatin by recruiting chromatin modifying proteins, and this then leads to inactivation of genes early in carcinogenesis. However, if aberrant DNA hypermethylation is the initial event, it is still unclear what triggers it. The three main hypotheses are:

1. CpG island methylation occurs randomly and results from errors during DNA replication and these cells are then selected for because they lead to an enhanced growth phenotype (Herman et al, 1998).
2. Tumour-specific methylated genes belong to distinct functional categories, have common sequence motifs in their promoter regions, and are found in clusters on chromosomes, indicating that cancer-related *de novo* hypermethylation may be a pre-programmed event (Keshet et al, 2006).
3. CpG island hypermethylation arises from a defect in the methylation machinery that results in aberrant methylation.

It is speculated that a combination of the hypotheses above may be the actual answer to the aberrant CpG island hypermethylation phenomena and it is likely that age-related methylation has different etiological factors to that of cancer-related methylation. Type A methylation is so common and tissue-specific that it is more likely to be caused by a physiological process rather than a mutation in gene involved in the methylation machinery. Type C methylation, however, is less frequent and shows clustering in some tumours, suggesting that it may be a secondary event to an acquired defect in the CpG island methylation or demethylation processes (<http://mdanderson.org/departments/methylation>). There has only been one report of somatic mutations in a DNMT gene in colorectal cancer and this will be discussed further (in section 1.4.5). Therefore, there is currently a lack of genetic data to provide definitive support for a causative role of aberrant methylation in cancer.

1.4.5 DNA Methyltransferase activity in cancer

Many studies examining the expression of DNMTs at the RNA level in tumour tissue have reported variable levels of overexpression (el-Deiry et al, 1991; Lee et al, 1996; Robertson et al, 1999). Lee et al found a 1.8 - 2.5-fold increase in DNMT RNA levels in colonic carcinoma compared to matching normal mucosa, whereas el-Deiry et al found a 15-fold increase in DNMT1 overexpression in colonic carcinoma (el-Deiry et al, 1991; Lee et al, 1996). The extent to which DNMT1 overexpression contributes to cancer remains controversial, but it is likely that low level overexpression (2 - 4-fold) is relatively common (Robertson, 2001). Contradicting these studies, there are also reports of tumours which do not overexpress DNMTs (Eads et al, 1999; Ehrlich et al, 2006). Using MethyLight technology, Ehrlich et al concluded that there was no significant association between gene hypermethylation and altered DNMT RNA levels in ovarian cancer (Ehrlich et al, 2006). It has also been proposed that changes in DNMT activity in cancer may be due to improper DNMT expression during the cell cycle. *DNMT1*, *DNMT3a* and *DNMT3b* are all differentially expressed during the cell cycle (Robertson et al, 2000; Szyf et al, 1991; Tatematsu et al, 2000). DNMT levels are higher in G₀/G₁ in cancer cell lines compared to normal cell strains (Robertson et al, 2000). Thus, these studies demonstrate another level of control of the DNA machinery during the cell cycle, and disruption of this this may be another mechanism by which aberrant methylation is observed in tumour cells. Finally, microRNAs (miRNAs) may play a role in regulating DNMT levels in cancer cells. miRNAs are small non-coding RNAs that regulate the expression of different genes, and studies have shown the expression levels of miRNAs are downregulated in cancer compared to normal tissues (Volinia et al, 2006). The miRNA29 family has a complementary sequence to both DNMT3a and DNMT3b, and downregulated miRNA29 levels were inversely correlated to DNMT3a and DNMT3b RNA levels in lung cancer tissues. Furthermore, induced expression of miRNA29 in lung cancer cell lines restored normal patterns of DNA methylation, induced the re-expression of silenced tumour suppressor genes, and inhibited tumorigenicity *in vitro* and *in vivo* (Fabbri et al, 2007).

The disruption of DNA methyltransferase activity and subsequent genome-wide changes in DNA methylation may contribute to carcinogenesis, through promoting genomic instability. As mentioned previously, *DNMT1* and *DNMT3b* knock-out mice are embryonically lethal (Li et al, 1992) and *DNMT3a* knock-out mice are peri-lethal (Okano et al, 1999). Therefore, it is unlikely that a germline mutation of any of the *DNMT* genes contributes to carcinogenesis. However, there has been one report in which a loss-of-function mutation in a DNMT protein has been described (Kanai et al, 2003). This study identified mutations in the coding region of DNMT1 in 7% (2/29) of colorectal carcinomas. One of these mutations was a one-base deletion which consequently led to the deletion of the whole catalytic domain of DNMT1, and the other was a point mutation resulting in a single amino acid substitution. No stomach or hepatocellular carcinomas displayed mutations in the coding regions of DNMT1. Mutational screening was also carried out in the 5' region of DNMT1, although no mutations were detected in any of the colorectal carcinomas, stomach cancers or hepatocellular carcinomas (Kanai et al, 2003). This demonstrates that mutational inactivation of DNMT1 does occur in colorectal cancer, however, further studies are required to determine whether these mutations are associated with human carcinogenesis.

Interestingly, it was initially demonstrated that the disruption of *DNMT1* activity in HCT116 colorectal cancer cells does not result in a significant alteration in global DNA methylation levels or associated gene silencing (Rhee et al, 2000). It was believed that *DNMT1* functions in a cooperative manner with *DNMT3b*, since genetic disruption of both *DNMT1* and *DNMT3b* is required to significantly reduce genomic methylation levels and demethylate repeat sequences, imprinted genes and aberrantly silenced tumour suppressor genes (Rhee et al, 2002). However, recently it was reported that the 'double knock-out methyltransferase' (DKO) cells used in the earlier studies actually express an alternatively spliced variant, which bypasses the knock-out cassette and results in an active DNMT1 protein lacking a proliferating cell nuclear antigen (PCNA) binding domain (Spada et al, 2007). RNAi-mediated knock-down of the truncated DNMT1 in the DKO cells results in significantly reduced global genomic DNA methylation levels and cell death (Spada et al, 2007).

To lend further support to these results, another report also demonstrated that HCT116 cells which lack *DNMT1* methyltransferase activity undergo mitotic catastrophe and cell death (Chen et al, 2007). Thus, it appears from these studies that DNMT1 is required for maintaining DNA methylation levels in human cancer cells and plays a crucial role in their growth and survival.

1.5 DNA methylation and Colorectal Cancer

1.5.1 Introduction

Colorectal cancer accounts for 14.5% (males) and 11.3% (females) of all cancers in Scotland (Information Services Division Scotland, 2005). Colorectal cancer is associated with a relatively poor survival rate remaining around 40%, which resulted in 16,100 deaths in 2002 despite improved understanding of cellular and molecular events involved in the development of colorectal cancer and progresses in surgery, radiotherapy, and chemotherapy (CancerResearch UK, 2006). Hence, further understanding of initiation, progression, and metastasis of colorectal cancer at a mechanistic level will improve the development of new drugs and therapies to treat and potentially prevent colorectal cancer.

A series of morphological changes occur in the epithelium during colorectal cancer development. Vogelstein proposed a Darwinian model of adenoma to carcinoma progression in which an accumulation of genetic alterations can lead to the morphological changes seen in tumorigenesis (Fearon & Vogelstein, 1990; Vogelstein et al, 1988) (Figure 1.8). Recent studies have acquired a vast amount of molecular data on the ‘adenoma to carcinoma sequence’, which has been utilised to examine the genetic basis of human cancer as a whole (Quirke, 1997). The proposed model (Figure 1.8), illustrates the development of the histological stages in the majority of colorectal cancers, however, often the underlying genetic alterations are less predictable. As will be discussed in this section, the amalgamation of epigenetic and genetic research more than likely holds the key to providing a complete molecular understanding of colorectal cancer and this may be significant for the diagnosis, prognosis, and treatment of the disease.

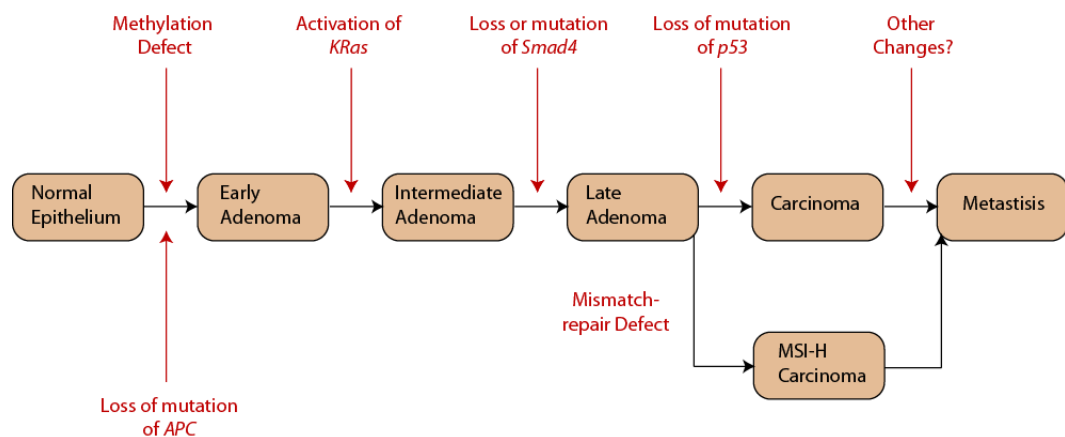


Figure 1.8: Vogelstein's proposed model for development of sporadic colorectal cancer.

The linear accumulation of epigenetic changes, gene mutations or chromosomal changes leading to tumour progression.

Source: Fearon & Vogelstein, 1990; adapted from Jubb et al 2001.

1.5.2 Age-related methylation in colorectal cancer

Aberrant CpG methylation is a frequent event resulting in gene silencing in neoplastic cells (Jones & Baylin, 2002). Research has suggested that the majority of aberrant methylation is associated with age-related changes in normal cells and tissues and is a generic effect that occurs over the lifetime of normal tissue. Neoplasia is then thought to occur through continuous selection (Ahuja et al, 1998). As mentioned previously, the first report of Age-related methylation (or Type A methylation) involving a promoter-associated CpG island was the *ESR1* gene in human colorectal tissue (Issa et al, 1994). The *ESR1* CpG island was methylated in all cell lines, adenomas, carcinomas, and in a small amount of normal colonic tissues adjacent to tumours. Experimental introduction of the *ESR1* gene into colorectal cancer cells resulted in growth inhibition, suggesting that *ESR1* functions to regulate cell growth, and its silencing through CpG hypermethylation leads to de-regulated growth of colonic cells (Issa et al, 1994). Other genes that have been found to be aberrantly methylated in the normal colon include the transcription factor myogenic differentiation gene (*MYOD*) and the tumour suppressor gene *N33*. Restriction

enzyme analysis showed that these genes displayed hypermethylation in the carcinoma, as well as low levels of methylation in normal colonic tissue, which increased with age (Ahuja et al, 1998). Another study looked at the methylation status of 19 tumour suppressor genes in normal colonic tissue and found that methylation of some genes was tightly correlated in adenomas, intermediate normal mucosa, and colorectal cancer (Takahashi et al, 2006). In addition, they confirmed that groups of genes are frequently methylated in normal appearing cells and tissues, and that methylation of these genes may contribute to increased cancer risk with the added factor of increased age (Takahashi et al, 2006). Normal colonic mucosa has also been reported to have higher levels of methylation in the distal (left side) compared to the proximal (right side) of the colon in both the *ESR1* and *MYOD* loci (Horii et al, 2008). As higher incidences of colorectal cancer have been reported in the distal colon than in the proximal colon (Cancer Research UK, 2008), this suggests that methylation changes in the normal mucosa may be at least partially responsible for these observed differences.

It has been proposed that Type A methylation is a gene-specific process and is modulated by tissue-specific factors such as environmental exposure or gene modifiers (Ahuja et al, 1998; Toyota & Issa, 1999). Initial studies have indicated that there is directionality *in-cis* to the process of age-related methylation with the spread of methylation emerging from methylation centres. Methylation centres have been described in many different systems and consist of highly repeated sequences such as *alu* repeat sequences. One example is the *MYOD* gene in which its methylation centre is in intron 1 and exon 2 of the gene and spreads progressively upstream with age (Ahuja et al, 1998). It has also been proposed that Type A methylation is responsible for the 'field defect' often observed in colorectal cancer (Issa et al, 1994). A field defect can be described as an area of abnormal tissue, which precedes and predisposes to carcinogenesis. One theory suggests that ageing is associated with gene-specific hypermethylation, which then alters the physiology of the aged cells, and the affects of aberrant hypermethylation are then further modulated through cell selection. For example, methylation of *ERS1* gene in the colon would promote the growth of these cells in the colon, and these cells would then progressively take the

place of normal cells, giving rise to an apparent increase in the process of age-related methylation (Issa, 1999). The multistep carcinogenesis process in the colon (as depicted in Figure 1.8) involves a series of pathways that may be activated or inhibited in a population of cells, which are then selected based on growth or survival advantages. In addition to the well-characterised pathways that are altered in colorectal tumours, aberrant methylation is believed to be another mechanism, which exists in aging cells and contributes to neoplastic transformation. Further research in this area is required to clarify its exact contribution to colorectal carcinogenesis and the etiology of age-related changes in methylation in normal-appearing cells.

It should be recognised that recently there has been some discrepancy to the above theories proposed by Jean Pierre Issa; specifically, as to whether Type A and Type C methylated genes represents two distinct groups. Several studies have found age-related increases in methylation for a number of Type C genes including *MLH1* and *p16^{INK4a}* (Belshaw et al, 2008; Kawakami et al, 2006). This suggests that the Type A and Type C classification first proposed by Toyota et al may not be as distinct as was first thought (Toyota & Issa, 1999). Nevertheless, recent quantitative methylation profiling has identified and classified field defects in colon cancer to a high degree of sensitivity and specificity (Belshaw et al, 2008). Thus, this type of analysis may assist in the early detection or determine the relative risk, of colorectal cancer.

1.5.3 CpG Island Methylator Phenotype

Although Type A methylation is frequent in colorectal cancer and precedes neoplasia in apparently normal cells, a number of genes are also thought to be specifically methylated in cancer tissues (Type C methylation, for Cancer-specific) (Toyota et al, 1999a). Various studies have shown clustering of hypermethylation events in a number of colorectal tumours, and these tumours are described as having the CpG Island Methylator Phenotype (CIMP) (Ahuja et al, 1997; Toyota et al, 1999a). CIMP is associated with promoter methylation of multiple tumour suppressor genes in colorectal cancers and the choice of promoters to describe CIMP in colorectal cancer has been under the focus of much discussion. The most popular list utilised to describe CIMP includes *p16^{INK4A}*; Calcium channel, voltage-dependent T type, alpha

1G subunit gene (*CACNA1G*); Insulin-like growth factor 2 (*IGF2*); suppressor of cytokine signalling 1 (*SOC1*); Runt-related transcription factor 3 (*RUNX3*); Neurogenin 1 (*NEUROG1*); cellular retinoic acid binding protein 1 (*CRABP1*); *MLH1* and the *MINT1*, *MINT2* and *MINT31* loci (Ahuja et al, 1997; Toyota et al, 1999a). Recently, a group validated the use of these markers by carrying out methylation analysis on a large independent dataset. They found all of these markers had high sensitivity and specificity (Ogino et al, 2007). CIMP-high tumours are generally diagnosed if 3 of the gene promoters from an analysed panel are methylated. If <3 of the gene promoters are methylated then they are classed as CIMP-low (Weisenberger et al, 2006). CIMP is thought to contribute to colorectal cancer formation and progression by inactivating genes involved in cell cycle regulation, apoptosis and angiogenesis (Toyota & Issa, 1999).

Microsatellite instability (MSI) in colorectal cancer tissue is a hallmark DNA mismatch repair deficiency. Thus, MSI is a characteristic feature of tumours arising in the familial colorectal cancer susceptibility syndrome hereditary non-polyposis colorectal cancer (HNPCC) or Lynch Syndrome (Liu et al, 1995a). Lynch Syndrome is due to germline mutations of *MLH1*, *MSH2*, *MSH6* and less frequently *PMS2* (Liu et al, 1996). MSI can also arise through somatic mutations and LOH (mainly *MLH1* and *MSH2* loci) (Liu et al, 1995b; Lothe et al, 1995). However, the most frequent mechanism is through epigenetic silencing of *MLH1* by promoter hypermethylation (Herman et al, 1998; Kane et al, 1997; Liu et al, 1996; Lothe et al, 1995). MSI is a result of defective mismatch-repair, leading to an increase frequency of insertional or deletional 'slippage' loops in microsatellite sequences during tumour cell DNA replication. This subsequently manifests in length variation mutations (MSI). Colorectal tumours with MSI are categorised into three groups, based on the number of markers showing instability. Markers include two mononucleotide repeat sequences Bat25 and Bat26 and three dinucleotide sequences D2S123, D5S346 and D17S250 (Bocker et al, 1997; Dietmaier et al, 1997). If more than 30 - 40% of markers display genomic instability then they are classed MSI-H(igh). MSI-L(ow) tumours display markers with less than 30 - 40% genomic instability. The third

group, MSS, are tumours where none of the markers tested exhibit instability (Boland et al, 1998).

MSI has been linked to CIMP since multiple-methylated CpG islands have been detected in MSI tumours. One frequently methylated promoter as part of the CIMP phenotype is that of *MLH1* (Ahuja et al, 1997). CIMP is also present in a proportion (approximately 45%) of colorectal adenomas in which MSI is rare. This provides circumstantial evidence that in mismatch-repair deficient tumours, CIMP precedes and may cause the mutator phenotype through silencing of *MLH1* (Issa, 2000). Population-based studies have suggested that CIMP tumours are pathologically and genetically distinct. For example, the behaviour of CIMP tumours can vary depending upon their MSI status; CIMP positive, MSS phenotype in tumours is associated with poor prognosis (Ward et al, 2003). In addition, CIMP tumours are similar to MSI tumours in that they usually occur in older individuals and in females; and are right-sided, high grade and mucinous, poorly differentiated type (Hawkins et al, 2002; Samowitz et al, 2005; van Rijnsoever et al, 2002). Genetically, CIMP tumours, MSS and MSI-L/MSI-H are often associated with *p53* mutations and a high rate of mutations in *KRAS* or *BRAF* (Kambara et al, 2004; Toyota et al, 2000). It is unknown why there is an association between *BRAF* and *KRAS* mutations and CIMP. However, it may be that these mutations are activating and are directly involved in causing CIMP. This was proposed by Ordway et al who found fibroblasts transformed by *fos* or *ras* had increased levels of DNMT expression and global hypermethylation (Ordway et al, 2004).

Not all researchers in the field accept CIMP as a distinct phenotype. There have been many discussions as to whether CIMP tumours represent a biologically distinct group of colorectal cancers, or are an arbitrarily selected group from a continuum of tumours displaying different methylation levels at particular loci (Yamashita et al, 2003). A feature of some of the papers that could not confirm the presence of CIMP was the use of unselected genes and/or non-quantitative, very sensitive methylation detection methods. All the papers that analysed the methylation profile of the originally described genes and methods confirmed CIMP (Issa et al, 2005). A recent

study attempted to resolve the controversy, utilising a robust new marker panel that classified CIMP positive tumours in colorectal cancer. A screen was performed using 195 markers to assess the methylation status of 100 different CpG islands on more than 100 different tissue samples. The conclusions of this study were that CIMP-positive tumours do indeed represent a distinct subset and sporadic cases of mismatch-repair deficient cancer occur almost exclusively as a consequence of CIMP-associated methylation of *MLH1* (Weisenberger et al, 2006).

1.6 Methods utilised for DNA methylation detection in tumours

In some cases, aberrant methylation has been described as an early occurring event in carcinogenesis (Esteller et al, 1999a; Umbricht et al, 2001). Thus, DNA methylation detection in clinical samples may be useful for the early detection of cancer screening. In addition to early cancer detection, different tumour types in the same organ as well as in different tissues have been found to have distinct methylation profiles (Costello et al, 2000; Esteller et al, 2001a). Therefore, analysis of DNA methylation profiles could be used to identify ‘original sites’ of cancer development. Furthermore, since many hypermethylated genes are tumour suppressor genes, drugs that reverse the effects of DNA methylation and restore gene expression of these genes could be utilised. Indeed, 5-aza-2’deoxycytidine (Decitabine) has been FDA approved for the treatment of patients with myelodysplastic syndrome. Thus, the main clinical application of DNA methylation research relies heavily on the discovery of novel and useful methylation markers. As a result, there has been a recent surge in research involving genome-wide approaches for methylation analysis, in both tumour material and in normal tissues and cell types. Global approaches are high-throughput with regard to the number of loci examined at one time and are developed for methylation profiling and screening novel disease markers. Some of the methods described include: microarray expression profiling before and after DNA methylation inhibition, either by pharmacological intervention or DNMT knock-down (Gius et al, 2004; Suzuki et al, 2002); restriction landmark genomic scanning (RLGS) (Hatada et al, 1991); and affinity purification or immunoprecipitation of methylated DNA combined with microarray analysis or high-throughput sequencing (Down et al, 2008; Keshet et al, 2006; Zhang et al, 2006). In contrast, fine mapping and quantitative analysis of DNA methylation in tumours is relatively high-throughput for samples, however, there is often a low throughput for individual gene analysis. Several methods are described, including: sodium bisulphite conversion and direct sequencing (Frommer et al, 1992); methylation-specific polymerase-chain reaction (PCR) (MSP) (Herman et al, 1996a); MethyLight, a fluorescence-based real-time PCR (Eads et al, 2000); and Pyrosequencing, a sequencing-by-synthesis technology (Uhlmann et al, 2002).

Each method, whether it is involving global methylation analysis or higher resolution mapping of individual CpG islands, has its advantages and disadvantages. Careful consideration of both the technical aspects of DNA methylation analysis and the biological material available for use need to be addressed before a study is carried out. Different types of materials and indeed the quality of the material may affect data interpretation. For example, methylation analysis of cancer cell lines, which represent a homogenous population of cells, will differ from the analysis of clinical samples, which can consist of a mixture different cell types. Tissue samples can contain a combination of tumour cells, normal cells, stroma, lymphocytes, leukocytes, and dead cells. Therefore, if the methylation status in the analysed region varies in any of these cell types compared to the tumour cells, or there are different admixtures of tumour cells in different samples, it may not be clear which methylation signal is actually being detected or quantified. A combination of microdissection, sufficient sample numbers, and a high level of accuracy and attention to detail can usually control for this variation.

1.6.1 Fine mapping and quantitative analysis of DNA methylation

Many of the high-resolution techniques utilised for DNA methylation detection and quantification usually involve the sodium bisulphite conversion of DNA prior to analysis. Sodium bisulphite is a mutagen that chemically modifies unmethylated cytosine residues to uracil residues. However, methylated cytosines cannot be modified in the same way and remain unchanged. Following the bisulphite conversion of DNA, methods such as MSP or direct sequencing can be carried out. For MSP analysis, PCR primers are designed to be complementary to unmethylated or methylated DNA sequences, therefore two PCRs are carried out on the same sample (Herman et al, 1996a). This method has a relatively high throughput with regard to samples but a low throughput for individual gene analysis. Therefore, MSP analysis of tumour samples is often used for the rapid analysis of a large number of samples for known markers. MSP analysis is limited by the fact that it is a qualitative method and false positive results are often obtained when PCR conditions are not optimal. Furthermore, the qualitative data obtained is based on the methylation status of only a few, or sometimes even one CpG dinucleotide. Direct sequencing of

bisulphite-modified DNA uses PCR primers that are specifically designed to amplify a region of interest and can include multiple CpG dinucleotides. All uracil and thymine residues are amplified as thymine and only 5-methylcytosine residues are amplified as cytosine. PCR products can then be sequenced directly, providing an average sequence for a population of molecules, or can be cloned and sequenced providing methylation maps of single DNA molecules. (Clark et al, 1994; Frommer et al, 1992). Bisulphite sequencing analysis provides a single base resolution and can be quantifiable, thus it is a highly informative method. The majority of reports involving methylation analysis of tumour DNA using bisulphite sequencing tend to be carried out on a small scale. There have however, been a few reports of large-scale bisulphite sequencing across large regions of the genome (Eckhardt et al, 2006; Rollins et al, 2006) but these methods are expensive and labour intensive. Similar to MSP, incomplete bisulphite conversion and PCR bias can prove to be problematic when interpreting sequencing data. Therefore, samples in which the methylation status is already known are often modified and sequenced alongside tumour samples to act as controls for these discrepancies.

Unlike MSP and bisulphite sequence analysis, MethyLight allows for the rapid quantitative methylation analysis of many samples at multiple gene loci (Eads et al, 2000; Eads et al, 1999). MethyLight involves the amplification of sodium bisulphite-converted DNA by fluorescence based, real-time quantitative PCR (Taqman), using gene-specific primers that flank an oligonucleotide probe with 5' fluorescence reported dye and a 3' quencher dye. Primers and probe sequences are both designed to overlap potential methylation sites. Therefore, there is sequence discrimination at the level of PCR amplification and the probe, which yields a high level of specificity. In addition, MethyLight is a highly quantitative method that determines the relative amounts of a particular methylation pattern compared to a control reaction, rather than detecting and measuring all methylated CpG dinucleotides in a heterogeneous DNA sample. Pyrosequencing is another technology that also involves real-time technology and has been combined with sodium bisulphite conversion of DNA to quantify methylation (Uhlmann et al, 2002). Pyrosequencing is a sequencing-by-synthesis technique that relies on luminometric detection of pyrophosphate release

upon nucleotide incorporation through a cascade of enzymatic reactions. The data that is produced from this technology are actual sequences rather than fluorescent data, which are obtained from other PCR-based techniques such as MethyLight. Pyrosequencing has recently been used to measure methylation levels across the entire CpG island region of the cyclin-dependent kinase inhibitor 2B gene (*CDKN2B*) (*p15^{INK4B}*) in myeloid malignancies (Brakensiek et al, 2007). Although only 15 CpG dinucleotides were measured at a time, 114 samples were analysed which meant 7762 individual methylation sites were analysed. This demonstrates that pyrosequencing is a high throughput method, which can be utilised for scanning large regions of CpG islands unlike MSP and bisulphite sequencing. Pyrosequencing is slowly superseding these conventional methods, although the technology does require specialist equipment, which is relatively expensive.

1.6.2 Global analysis of DNA methylation

Genome-wide mapping of DNA methylation is a less direct method of measuring and quantifying methylation in tumours, and at present, all methods are relatively expensive and labour-intensive. However, as mentioned previously, genome-wide mapping provides high-throughput analysis of individual loci and is extremely informative for discovering novel DNA methylation markers. RLGS was one of the first technologies developed for mapping global DNA methylation patterns (Hatada et al, 1991). RLGS uses a two-dimensional electrophoresis system and radiolabelled methylation sensitive restriction endonuclease sites to create ‘landmarks’ which can be observed on an autoradiograph. Highly reproducible profiles can display over 2000 radiolabelled restriction landmark sites in a single assay. Paired samples, which are ideally matched tumour and normal tissue profiles, are analysed alongside each other and methylation is detected from the absence or decrease in signal intensity (Rush & Plass, 2002). Distinguishing bands are then verified by subsequent cloning and sequencing in order to identify novel methylated sites. The main disadvantage of this method is the fact that novel methylation markers can only be detected at a small number of restriction sites, and therefore there is limited coverage. Moreover, not all restriction sites in the cloned libraries will be associated with gene loci, thus the relationship between methylation and expression needs to be examined separately.

Unlike RLGS, microarray-based methylation analysis can be used to analyse a set of specific candidate genes. Several reports have demonstrated that the methylation status of CpG islands in multiple and specific genes can be analysed simultaneously using microarray profiling (Adorjan et al, 2002). The microarray technology commonly utilises a pair of DNA oligonucleotides, one that reflects the methylated status of a CpG dinucleotide (CpG) and one reflecting the unmethylated status of a dinucleotide (TpG) following sodium bisulphite treatment. The oligonucleotides are spotted and immobilised onto an array and hybridised to labelled PCR fragments from a sample. This technique was utilised in the analysis of 232 CpG dinucleotides located in CpG rich regions of 56 different genes, randomly selected from a panel of genes associated with tumorigenesis. From the analysis of over 70 samples from four different human tumour types and matched controls, this method was shown to assist in predicting known tumour classes and discovering novel ones (Adorjan et al, 2002). In addition to combining sodium bisulphite pre-treatment with microarray analysis, restriction enzyme digestion (Schumacher et al, 2006) and affinity purification methods (Rauch et al, 2008) have also been coupled with microarray technology to detect global DNA methylation changes. The microarray-based profiling approach can also be used to detect novel methylation markers. One study screened over 10,000 genes for promoter hypermethylation in the RKO colorectal cancer cell line following treatment with the de-methylating agent 5-aza-2'-deoxycytidine and the HDAC inhibitor TSA, and subsequent cRNA hybridisation to a 12,599 oligonucleotide array (Suzuki et al, 2002). They identified a substantial number of genes which were upregulated following treatment, and subsequently confirmed a novel group of genes that were preferentially hypermethylated in colorectal cancer. One of the major disadvantages of using this approach is that 5-aza-2'-deoxycytidine is highly toxic to cells and affects the expression of many genes. Therefore, microarray expression profiling studies may not actually identify methylation as such; rather genes that respond to 5-aza-2'-deoxycytidine treatment. This can be demonstrated in reports that have shown that nearly half of the genes unregulated by 5-aza-2'-deoxycytidine treatment do not actually contain CpG islands (Shames et al, 2007; Suzuki et al, 2002). These genes may be regulated by long

range control through the methylation of 'CpG islands shores' mentioned previously (Irizarry et al, 2009). Alternatively, it has been shown recently that DNA methylation at some low CpG density promoters is inversely correlated with gene expression (Rakyan et al, 2008). Therefore, some of the genes upregulated following 5-aza-2'-deoxycytidine may include non-CpG island promoter genes.

Finally, recent high-throughput approaches have used protein affinity and immunoprecipitation to enrich methylated sequences prior to microarray or large-scale sequencing analysis. These methods are an improvement on the two methods discussed above as they provide a higher level of sensitivity and specificity. DNA which has been sonicated or digested is either immunoprecipitated using a monoclonal antibody to 5-methylcytosine (methylated DNA immunoprecipitation; MeDIP) (Weber et al, 2005) or purified using the DNA-binding domain of a methyl-CpG-binding protein (methyl-binding domain affinity purification; MAP) (Cross et al, 1994). When MeDIP is coupled with whole-genome microarray analysis (MeDIP-chip, or ChIP on chip), the reference sample is a sample of input DNA and the test sample is the immunoprecipitated DNA. Methylated sequences are identified by comparing the fluorescent signal from probes corresponding to known sequences in the test and reference samples (Keshet et al, 2006). MeDIP has also been combined with large-scale genome sequencing (MeDIP-seq) (Pomraning et al, 2009). Following MeDIP purification, DNA samples are processed to generate *in vitro* sequencing libraries. These libraries are then sequenced using Solexa/Illumina sequencing, which is currently able to produce approximately 1.5 Gb of sequence data in around three days (Pomraning et al, 2009). Genome-wide MeDIP-seq analysis has been used to map methylation patterns in a number of genomes (Down et al, 2008; Pomraning et al, 2009). However, as of yet, it has not been utilised for mapping DNA methylation patterns in tumours. The antibody used for the enrichment of methylated DNA sequences has been shown to recognise methylation in regions with a CpG density of only around 2-3% (Keshet et al, 2006). Therefore, whilst MeDIP may be very useful for detecting aberrantly methylated CpG islands, for example in tumours, this method may not be sensitive enough for mapping methylation in the majority of the genome where the CpG content is

considered to be less than 2% (Keshet et al, 2006). Moreover, as this is the case, MeDIP could introduce bias toward certain types of genomic sequences where the CpG density is higher in some regions than others. In an attempt to correct for this, an algorithm known as Bayesian tool for methylation analysis (Batman) was developed (Down et al, 2008). An alternative approach that was recently developed, enriches specifically for unmethylated DNA using CXXC affinity purification (CAP; X can represent any residue). The cysteine-rich CXXC3 domain was linked to a sepharose matrix and the DNA was fractionated over the CXXC column. Eluted DNA following CAP is believed to purify genomic DNA based on CpG density and methylation status. (Illingworth et al, 2008). As with MeDIP-seq, this method was utilised for scanning methylated CpG islands in human tissues and cell types and has not yet been used for screening aberrantly methylated CpG islands in tumours (see section 1.2.1 for more details on this study).

The recently developed genome-wide methods discussed above have revolutionised the analysis of methylated DNA. Although, as with all methylation analysis techniques, they have their limitations. Following all screening methods, the relationship between methylation and expression needs to be further explored. It cannot be assumed that tumour-specific methylation is associated with aberrant expression. Furthermore, when carrying out large-scale screening methods, there is always a risk of acquiring false positives. Therefore, researchers need to carefully consider how stringent the screen will be and apply the relevant statistics to test for the likelihood of attaining a false positive result. It is apparent that both global and locus-specific changes in methylation are involved in cellular transformation, and although there has been a recent increase in research carried out to investigate global epigenetic changes in cancer, studies involving a single candidate gene approach are still under investigation. The focus of the work presented in this thesis is on one such candidate gene; *14-3-3 σ* , for which there is evidence of aberrant methylation in cancer and which is a plausible gene involved in cancer biology.

1.7 14-3-3 σ

1.7.1 Introduction

There has been a great interest in the *14-3-3 σ* gene as it is a transcriptional target of p53, promoting stable cell cycle arrest upon its activation and is involved in regulating translational control during mitosis (Hermeking et al, 1997; Wilker et al, 2007). Furthermore, data has shown that it is frequently deregulated in primary human tumours suggesting that 14-3-3 σ may be an important mediator of p53's tumour suppressive function *in vivo*.

14-3-3 σ belongs to a large family of 14-3-3 encoded proteins which are highly conserved, acidic, small polypeptides ranging from 28-33 kDa, and are found in all eukaryotic species (Aitken et al, 1992; Ferl et al, 2002; Wang & Shakes, 1996). 14-3-3 proteins work as adaptor molecules and are able to move freely from the cytoplasm to the nucleus and vice-versa (Mhawech, 2005). The proteins can form heterodimers or homodimers and function by binding to phosphorylated protein ligands on serine/threonine residues in the consensus binding motif RSXpSXP (Muslin et al, 1996). A small number of proteins can also associate with 14-3-3 proteins independently of this motif such as the protein Bax (Pozuelo Rubio et al, 2004; Seimiya et al, 2000). 14-3-3 proteins regulate a number of different proteins by cytoplasmic sequestration, activation/repression of enzymatic activity, prevention of degradation, transactivation, promotion/inhibition of protein interactions, and assisting in protein modifications. As a result, 14-3-3 protein products have many diverse functions including key roles in cell cycle regulation and cellular signalling. In humans there are seven different expressed 14-3-3 isoforms: β , γ , ϵ , η , σ , τ (also called θ), and ζ (Hermeking, 2003). *14-3-3 σ* , also known as human epithelial marker-1 (*HEM-1*), or stratifin (*SFN*), was originally identified as a human mammary epithelial marker and interestingly, its expression was significantly reduced in human breast cancer cells (Prasad et al, 1992). *14-3-3 σ* is unique in that it has tissue-specific expression restricted to epithelial cells and keratinocytes, however, most other *14-3-3* isoforms are expressed ubiquitously (Hermeking, 2003). Phylogenetic analysis shows that 14-3-3 σ is the most divergent isoform and lacks

introns which is a unique feature of the gene (Wilker et al, 2005). In addition, and more importantly, 14-3-3 σ is structurally different compared to other 14-3-3 isoforms. 14-3-3 σ has a unique amino acid patch in its second ligand-binding site, which consists of amino acids Met202, Asp204, and His206. This site may be responsible for the binding of certain ligands that are not recognized by the other 14-3-3 proteins and may account for 14-3-3 σ -specific function (Benzinger et al, 2005; Wilker et al, 2005).

1.7.2 Regulation and function of 14-3-3 σ

It has been reported that 14-3-3 σ is regulated by different mechanisms, the major regulator being the tumour suppressor gene, *p53*. Upon DNA damage, *p53* is activated and this subsequently leads to cell cycle arrest or apoptosis in order to maintain genetic stability. Cell cycle arrest can occur at the G₁/S checkpoint, which is mediated by the interaction of the *p53*-inducible *p21^{WAF1/CIP1}* gene with the cyclin-dependent kinase 2 (cdk2)/cyclin E complex (el-Deiry et al, 1993; Xiong et al, 1993). Alternatively, cell cycle arrest in G₂ is induced by *p53*-activated 14-3-3 σ . The combination of both *p21^{WAF1/CIP1}* and 14-3-3 σ results in a coordinated arrest in which cells are blocked in either G₁ or G₂, prolonging the lifetime of the cell and thus mediating a significant part of the cell-cycle regulatory effects of *p53* because of DNA damage. 14-3-3 σ induction following DNA damage was first determined from a serial analysis of gene expression (SAGE) screen (Hermeking et al, 1997). SAGE is a method used for the comprehensive analysis of gene expression patterns. SAGE involves the sequencing and quantification of tags, which are representative of the RNA species present in a given sample. *p53*-mediated G₂ arrest was not fully understood, therefore SAGE was utilised to measure gene expression changes in the colorectal cancer cell line HCT116 (wild-type for *p53*) following irradiation. SAGE determined that a tag representing 14-3-3 σ was expressed at higher levels in the irradiated G₂ arrested cells compared to exponentially growing non-irradiated cells. To confirm the SAGE results and determine whether 14-3-3 σ is regulated by *p53*, Hermeking et al first investigated the induction of 14-3-3 σ following DNA damage in a series of colorectal cell lines using Northern blot analysis. *p53* wild type

colorectal cancer cell lines expressed high levels of *14-3-3 σ* upon DNA damage. However, colorectal cancer cell lines with mutated *p53* were unable to induce *14-3-3 σ* . Subsequent investigation found that *p53* can directly transactivate *14-3-3 σ* expression by binding to a *p53* responsive element 1.8kb upstream from the transcriptional site of *14-3-3 σ* . Mutated *p53* cannot bind the responsive element of *14-3-3 σ* and is therefore unable to induce *14-3-3 σ* expression. Thus, it was concluded *14-3-3 σ* expression is induced following DNA damage and induction of *14-3-3 σ* is mediated by *p53* (Hermeking et al, 1997).

DNA damage can also activate BRCA1 which acts synergistically with *p53* to activate *14-3-3 σ* expression (Aprelikova et al, 2001; Yarden et al, 2002). BRCA1 itself, is activated by upstream DNA damage response proteins such as ataxia telangiectasia and Rad 3-related (ATR)/ataxia telangiectasia mutated homolog (ATM) and cell cycle checkpoint kinase (Chk2) protein kinases (Yarden et al, 2002). Irradiation of BRCA1^{-/-} cells results in an unsustainable G₂/M growth arrest, which is similar to the phenotype observed in irradiated *14-3-3 σ* ^{-/-} cells (Chan et al, 1999). This further emphasises the functional affects of reduced *14-3-3 σ* expression in BRCA1 deficient cells following DNA damage (Aprelikova et al, 2001).

A positive feedback loop exists in the *14-3-3 σ* pathway since the protein has been shown to regulate *p53* (Yang et al, 2003). *In vitro* experiments demonstrated that *14-3-3 σ* stabilises *p53* by inhibiting Mdm2-mediated *p53* degradation. *14-3-3 σ* affects Mdm2 activity by inhibiting Mdm2 ubiquitin ligase function and interfering with nuclear export of Mdm2 (Yang et al, 2003). Furthermore, *14-3-3 σ* was shown to increase *p53* transcriptional activity and facilitate cooperative *p53* dimer-dimer formation, stabilising *p53* DNA binding and thus potentiating its transcriptional activity toward target genes (Yang et al, 2003). As mentioned previously, the downstream effect of *14-3-3 σ* transactivation by *p53* results in G₂/M arrest. *14-3-3 σ* protein causes G₂/M arrest by sequestering the cell division cycle 2 (CDC2)-cyclin B1 in the cytoplasm. This blocks the interaction of CDC2-cyclin B1 with substrates which have to be phosphorylated to achieve a G₂/M transition, thus providing time for

sufficient DNA repair (Chan et al, 1999; Hermeking et al, 1997; Peng et al, 1997). 14-3-3 σ also binds to G₁-specific Cdk2 and Cdk4. Therefore, 14-3-3 σ may additionally be involved in G₁ arrest in cells (Laronga et al, 2000). Figure 1.9 illustrates 14-3-3 σ function downstream and upstream of p53 upon DNA damage.

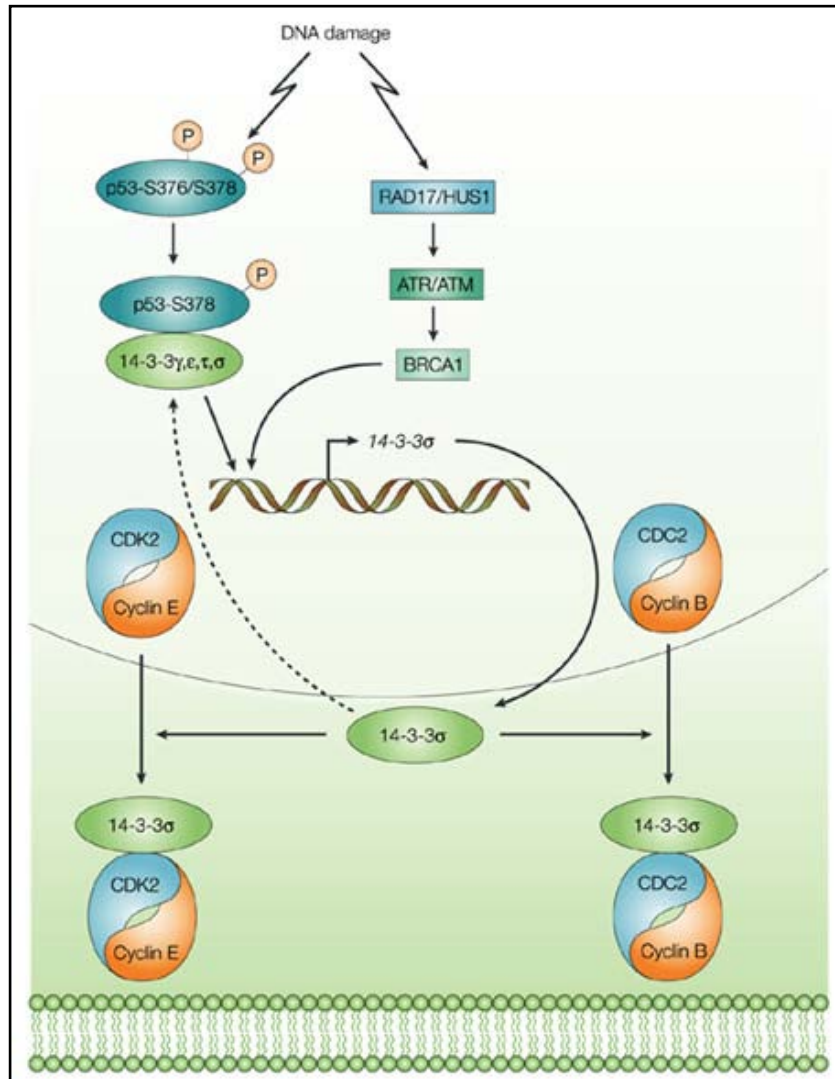


Figure 1.9: 14-3-3 σ causes stable G₂/M cell-cycle arrest mediated through p53 or BRCA1 after induction of DNA damage.

DNA damage leads to dephosphorylation of Ser376 producing a 14-3-3 binding site in p53. 14-3-3 σ is transactivated by p53 and induced 14-3-3 σ may contribute to further p53 activation in a positive feedback loop. 14-3-3 σ sequesters Cdk2 in the cytoplasm causing cell cycle arrest in G₁ (Cdk2). DNA damage activates BRCA1 which can also induce 14-3-3 σ expression.

Source: Hermeking et al, 2003.

In addition to the p53 and BRCA1 pathways, 14-3-3 σ is regulated by the p53 homologues p63 and p73, which have both been reported to be involved in controlling cell cycle and/or apoptosis (el-Deiry et al, 1993; Jost et al, 1997; Yang et al, 1998). The *p63* gene encodes two major isoforms; transcriptionally active p63 (TAp63) and the dominant negative p63 (Δ Np63) (Yang et al, 1998). 14-3-3 σ expression in keratinocytes within the epidermis of the skin varies depending upon the level of differentiation of the cell (Pellegrini et al, 2001). The suppression of 14-3-3 σ in the basal epidermal layer of skin is mediated by Δ Np63 binding to p53 responsive elements in the *14-3-3\sigma* promoter. 14-3-3 σ is highly expressed in terminal differentiated (stratifying) keratinocytes as Δ Np63 is absent and suppression of 14-3-3 σ is lifted (Ghahary et al, 2005). The other p53 homologue, p73, activates *14-3-3\sigma* suggesting that the G₂/M signalling pathway is conserved between p53 and p73 (Zhu et al, 1998). It has even been proposed that *14-3-3\sigma* may be the primary cellular target of p73 as activation of *14-3-3\sigma* by p73 is 3-6 times higher than by p53 (Zhu et al, 1998). 14-3-3 σ is also regulated post-transcriptionally by the estrogen-induced zinc finger protein (EFP) (Urano et al, 2002). EFP is a RING-finger-dependent ubiquitin ligase (E3) and targets the proteolysis of 14-3-3 σ . Moreover, overexpression of EFP *in vivo*, generates tumours thought to be due to the loss of 14-3-3 σ and the induction of genomic instability (Urano et al, 2002). Finally, in various cancers, aberrant expression and associated CpG methylation of *14-3-3\sigma* has been observed (Ferguson et al, 2000; Mhawech et al, 2005). Figure 1.10 shows the regulation of 14-3-3 σ in normal and cancer cells.

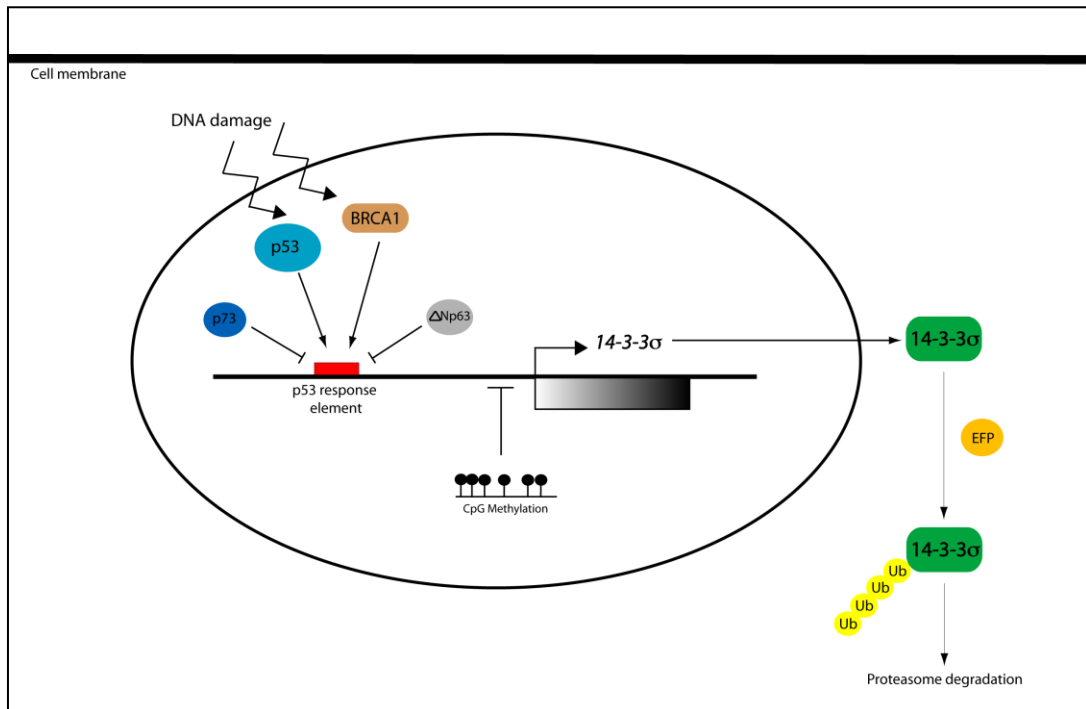


Figure 1.10: Regulation of 14-3-3 σ in normal and cancer cells.

DNA damage leads to increased expression of 14-3-3 σ mediated by p53 and BRCA1. p73 and Δ Np63 suppress 14-3-3 σ expression. In addition, CpG methylation at the promoter region has been shown in cancer cells to silence 14-3-3 σ expression. At the protein level, 14-3-3 σ levels are downregulated by proteolysis. This is regulated by an oestrogen dependent increase in expression of EFP, an E3 ubiquitin (Ub) ligase.

As well as its role in inducing cell cycle arrest following DNA damage, a recent report by Wilker et al demonstrated that 14-3-3 σ is involved in regulating translation during mitosis and is required for normal mitotic progression (Wilker et al, 2007). Throughout mitosis and directly afterwards, translation in mammals changes with a suppression of cap-dependent translation and a corresponding increase in cap-independent translation (Pyronnet et al, 2001). This is because mRNAs for cell cycle proteins, such as c-myc, contain an internal ribosome entry site (IRES) domain that allows for their rapid translation during mitosis (Pyronnet et al, 2000). The majority of ligands bound to 14-3-3 σ during mitosis and immediately following mitosis, are proteins involved in translation, including a number of initiation factors involved in mediating cap-dependent translation such as the eukaryotic initiation factor 4B (eIF4B) (Wilker et al, 2007). eIF4B is required for the translation of mRNAs with a 5' cap structure and recruits ribosomes to this site. Cells in which 14-3-3 σ is knocked down are unable to suppress cap-dependent translation or stimulate cap-independent translation throughout or immediately after mitosis (Figure 1.11). Thus suggesting that 14-3-3 σ is involved in the switch from cap-dependent to cap-independent translation, and consequentially plays an important role in regulating cell cycle progression (Wilker et al, 2007). More specifically, expression of a cell cycle protein cyclin-dependent kinase cdk11, which contains an IRES domain, is reduced in 14-3-3 σ depleted cells which results in impaired mitosis (Wilker et al, 2007). It is very likely that other cell cycle cap-independent mRNAs are also affected by the defective switch in 14-3-3 σ regulated translation, some of which may also contribute to the aberrant mitotic phenotype observed in 14-3-3 σ depleted cells. Wilker et al went on to investigate the cellular defects in the 14-3-3 σ knock-down cells and proposed how downregulation of 14-3-3 σ may contribute to cancer progression. This will be discussed in more detail in the following section.

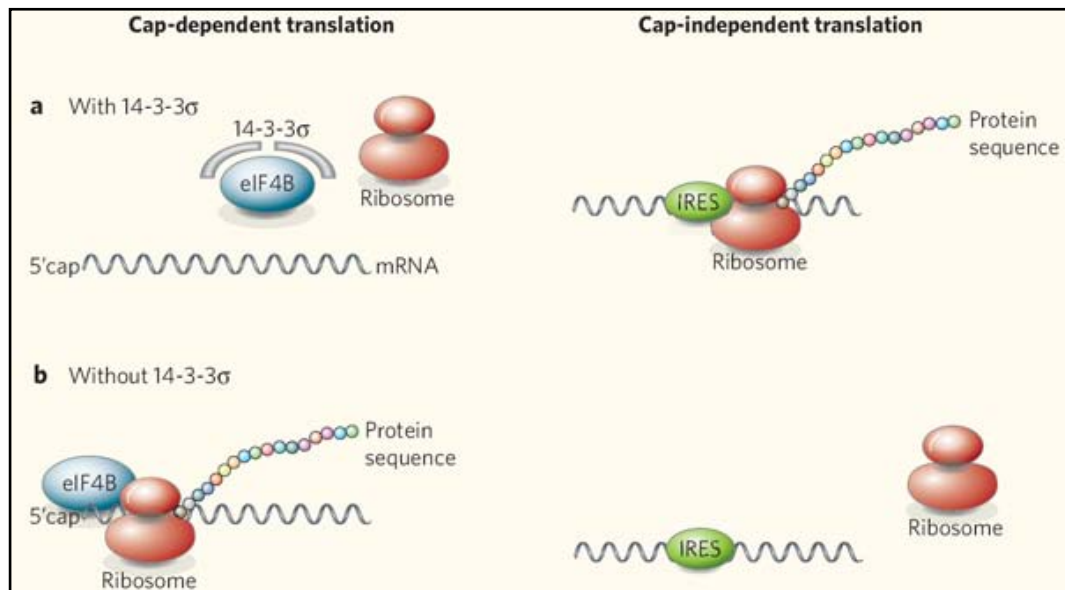


Figure 1.11: 14-3-3 σ plays a critical role in cap-dependent and cap-independent mRNA translation during mitosis.

(a) When 14-3-3 σ is bound to eIF4B, it cannot bind to the 5' cap. Therefore, cap-dependent translation is suppressed and only mRNA sequences containing an IRES domain undergo translation through a cap-independent mechanism. (b) When 14-3-3 σ is absent, eIF4B can bind the 5' cap initiating cap-dependent translation and cap-independent translation is not induced.

Source: (Wynshaw-Boris, 2007)

1.7.3 The role of 14-3-3 σ in cancer

The first study to examine 14-3-3 σ expression demonstrated that *14-3-3 σ* mRNA was downregulated in a number of breast cancer cell lines (Prasad et al, 1992). Similarly, complete loss of 14-3-3 σ protein expression was detected in 46% of keratinocytes that had undergone transformation to basal cell carcinomas (Lodygin et al, 2003). In contrast, 14-3-3 σ overexpression at both the mRNA and protein level has been detected in hematological malignancies (Motokura et al, 2007), and two studies have reported increased levels of 14-3-3 σ protein in colorectal cancer (Perathoner et al, 2005; Tanaka et al, 2004). The loss of 14-3-3 σ expression in cancer may be due to mutational inactivation of *14-3-3 σ* since the *14-3-3 σ* gene is localised on chromosome 1p35, a region frequently deleted in cancer. However, in a number of studies, mutational inactivation of *14-3-3 σ* has not been observed (Gasco et al, 2002a; Lodygin et al, 2003).

As mentioned in the previous section, 14-3-3 σ plays an important role in p53 mediated G₂/M arrest following DNA damage and in regulating protein synthesis during mitosis. In an experimental system using cancer cells, both *14-3-3 σ* alleles have been inactivated in the colorectal cancer cell line HCT116 (wild-type for p53) to generate somatic *14-3-3 σ* knock-outs. Irradiated HCT116 *14-3-3 σ ^{-/-}* cells initially arrest in the G₂ phase but are unable to maintain an arrested state. The CDC2-cyclinB1 complexes migrate to the nucleus, which results in mitotic catastrophe and cell death (Chan et al, 1999). Mitotic catastrophe is likely to occur due to the extent of DNA damage. Indeed, this theory is consistent with a study which showed that *14-3-3 σ ^{-/-}* cells have frequent loss of telomeric repeat sequences, increased frequency of chromosome end-end associations and terminal non-reciprocal translocations (Dhar et al, 2000). Therefore, even without radiation induced DNA damage, *14-3-3 σ ^{-/-}* cells have a greater frequency of chromosomal aberrations. A similar phenotype was observed in studies carried out by Wilker et al in which *14-3-3 σ* was stably knocked down in various cancer cell lines. Due to the defective switch in the mechanism of translation, the mitotic expression of a cap-independent cyclin-dependent kinase cdk11 was reduced, which resulted in impaired cytokinesis, loss of Polo-like kinase-

1 (Plk1) at the midbody, and an increase in the number of binucleated and fused cells (Wilker et al, 2007). Interestingly, the affects observed from *14-3-3 σ* knock-down could be reversed using the drug rapamycin, which suppresses cap-dependent translation and increases cap-independent translation during mitosis. Re-introduction of the cyclin-dependent kinase cdk11 into the knock-down cells however, only resulted in partial rescue of the defective mitosis phenotype (Wilker et al, 2007). This suggests that the expression of other cell cycle proteins via a cap-independent mechanism may also be affected by reduced *14-3-3 σ* levels, which subsequently contributes to the observed aberrant mitotic phenotype. The formation of binucleate cells as a result of impaired cytokinesis is associated with tumorigenesis and may underlie genomic instability (Fujiwara et al, 2005). Therefore, it is hypothesised that loss of *14-3-3 σ* contributes to tumorigenesis through aberrant mitotic translation and consequential impaired mitotic exit (Wilker et al, 2007). It should also be noted that primary keratinocytes from the normal human epidermis evade senescence because of *14-3-3 σ* downregulation. It is still unclear how loss of *14-3-3 σ* leads to this evasion, however, downregulation of *14-3-3 σ* is associated with the maintenance of telomerase activity and a strong reduction in *p16^{INK4A}* expression (Dellambra et al, 2000). These genetic alterations have been shown to contribute to the immortalisation of keratinocytes *in vitro* (Dickson et al, 2000; Kiyono et al, 1998). Thus, downregulation of *14-3-3 σ* in keratinocytes may promote immortalisation, a key feature that can lead to cell transformation.

Conversely, knock-in studies in cycling cancer cells using adenoviral infection have demonstrated that *14-3-3 σ* overexpression leads to an increase in cell size, with cells arresting at G₂/M. Further infection results in cells re-entering a synthetic phase with a number of cells displaying a DNA content of 4N and more. This suggests that the cells undergo an uncoordinated arrest in which cycles of synthesis occur without mitosis (Hermeking et al, 1997). In separate studies focusing purely on the tumour suppressive function of *14-3-3 σ* , it was shown that induced *14-3-3 σ* expression inhibited the tumorigenicity of *HER2* transformed NIH-3T3 cells. Moreover, *14-3-3 σ* expression reduced the tumorigenicity of these oncogene expressing cells in a

xenograft mouse model, further reinforcing its role in inhibiting tumour growth (Yang et al, 2003).

Adding even more complexity to the exact role 14-3-3 σ plays in tumorigenesis, one report has shown that 14-3-3 σ is also implicated in the protection of cancer cells from apoptosis (Samuel et al, 2001). 14-3-3 σ ^{-/-} colorectal cancer cell lines are sensitised to chemotherapy-induced apoptosis. Furthermore, it was shown that the reintroduction of 14-3-3 σ into these cells delays the apoptotic signal by sequestering the pro-apoptotic protein Bax into the cytoplasm. The authors proposed that p53-induced G₂/M arrest is accompanied by a separate mechanism that delays apoptosis (Samuel et al, 2001).

Collectively, aberrant 14-3-3 σ expression and function are common features of cancer (Prasad et al, 1992; Tanaka et al, 2004). Although, research involving 14-3-3 σ has created a paradox. 14-3-3 σ is silenced in a number of different cancers whilst overexpressed in others (Ferguson et al, 2000; Tanaka et al, 2004). In addition, 14-3-3 σ appears to act as a tumour suppressor as it is a negative regulator of the cell cycle and is involved in regulating translation during cell division (Hermeking et al, 1997; Wilker et al, 2007). The tumorigenicity experiments carried out by Yang et al further support this notion (Yang et al, 2003). However, 14-3-3 σ has also been implicated in protecting cancer cells from apoptosis and overexpression of 14-3-3 σ can also lead to an impaired cell cycle arrest and cycling of DNA synthesis occur without mitosis (Hermeking et al, 1997; Samuel et al, 2001). Therefore, it might be proposed that 14-3-3 σ expression has to be exquisitely controlled within the cell in order for it to function appropriately. Epigenetic changes at the promoter region of 14-3-3 σ could hold the key to this type of regulation.

1.7.4 Methylation of 14-3-3 σ in normal tissue

14-3-3 σ expression is restricted to different cell types, with the majority of epithelial cells expressing 14-3-3 σ (Nakajima et al, 2003). However, fibroblasts (Ghahary et al, 2005), lymphocytes (Bhatia et al, 2003), and brain tissues (Nakajima et al, 2003) do

not express *14-3-3 σ* . A recent report by Oshiro et al demonstrated that the normal cell type-specific expression of *14-3-3 σ* is regulated by epigenetic mechanisms (Oshiro et al, 2005). In normal *14-3-3 σ* positive cells, (these included epithelial cells from the airway, prostate, breast, skin and mouth) the *14-3-3 σ* promoter region was completely unmethylated; the associated histones hyperacetylated; unmethylated at histone H3K9; and an accessible chromatin structure was exhibited. In non-cancerous *14-3-3 σ* negative cells, (these included skin fibroblasts, lymphocytes, chondrocytes, bone marrow, heart and kidney) the *14-3-3 σ* promoter region was fully methylated; the associated H3 and H4 histones were hypoacetylated, methylated at histone H3K9; and an inaccessible chromatin structure was found (Oshiro et al, 2005). This study demonstrated that *14-3-3 σ* belongs to a large spectrum of cell type-specific genes that are regulated by epigenetic mechanisms. Given the important role of *14-3-3 σ* in regulating cell cycle arrest and protein translation during mitosis, it is surprising to find that the protein is not expressed in some cell types. It must however be considered that *14-3-3 σ* could be expressed at extremely low levels in these cell types and the sensitivity of current transcriptional assays may be limited.

1.7.5 Aberrant methylation of *14-3-3 σ* in cancer

As mentioned previously, an early study found that *14-3-3 σ* expression was dramatically reduced in a number of transformed breast cancer cell lines compared to non transformed human mammary epithelial cells (Prasad et al, 1992). Eight years later, the mechanism underlying the observed decrease of *14-3-3 σ* expression in breast cancers was deduced. LOH and intragenic mutations of *14-3-3 σ* were not found and instead epigenetic silencing was demonstrated to be the primary mechanism for reduced *14-3-3 σ* expression (Ferguson et al, 2000). Hypermethylation of *14-3-3 σ* was detected in 91% (75/82) of breast tumours and this was associated with very low levels of *14-3-3 σ* expression (Ferguson et al, 2000). Furthermore, an impaired G₂/M cell cycle checkpoint was identified in the *14-3-3 σ* silenced breast cancer cell lines, consistent with previous *14-3-3 σ* knock-out studies in colorectal cancer (Chan et al, 1999). Inactivation of *14-3-3 σ* by epigenetic

silencing has also been observed in other tumour types, some of which include prostate (Lodygin et al, 2004), gastric (Suzuki et al, 2000), hepatocellular (Iwata et al, 2000) and small-cell lung carcinomas (Osada et al, 2002) (Table 1.3 provides a more comprehensive list). In colorectal cancer, *14-3-3 σ* hypermethylation is a rare event (Ide et al, 2004; Suzuki et al, 2000). Suzuki et al showed *14-3-3 σ* hypermethylation in only one out of eight colorectal cancer cell lines. Ide et al demonstrated that all seven colorectal cancer cell lines studied were unmethylated and 70% (7/10) microdissected fresh tumour tissues were unmethylated.

Reversal of epigenetic effects by 5'-aza-2'-deoxycytidine treatment has demonstrated that *14-3-3 σ* can be re-expressed in breast (Ferguson et al, 2000) or gastric (Suzuki et al, 2000) cell-lines. This suggests that reduced *14-3-3 σ* expression is due to methylation of CpG sites within the *14-3-3 σ* gene. It is believed that *14-3-3 σ* hypermethylation is an early event during breast cancer formation and may be the case in the progression of other cancers (Umbricht et al, 2001). *14-3-3 σ* hypermethylation frequency increases during breast cancer progression and has been found in adjacent normal breast epithelial cells but not in individuals without evidence of breast cancer (Umbricht et al, 2001). *14-3-3 σ* hypermethylation and associated inactivation in mammary epithelial tissue can be classed as a field defect; occurring in pre-dysplastic tissue preceding carcinogenesis indicating that *14-3-3 σ* may have an important tumour suppressor function.

Type of cancer	Frequency of CpG hypermethylation	Methods used for detection	References
Breast cancer	86% (43/50) primary tumours 100% (32/32) microdissected carcinoma	Bisulphite sequencing	(Ferguson et al, 2000)
	83% (15/18) ductal carcinoma in situ 96% (24/25) invasive ductal carcinoma	Bisulphite sequencing and MSP	(Umbricht et al, 2001)
Gastric cancer	43% (26/60) primary gastric cancer	Bisulphite sequencing and bisulphite SSCP	(Suzuki et al, 2000)
Colorectal cancer	13% (1/8) CRC cell lines	Bisulphite sequencing and bisulphite SSCP	(Suzuki et al, 2000)
	0% (0/7) CRC cell lines 3/10 (30%) microdissected CRC	MSP and bisulphite sequencing	(Ide et al, 2004)
Liver cancer	89% (17/19) primary HCC	Bisulphite SSCP	(Iwata et al, 2000)
	60% (47/79) intrahepatic cholangiocarcinoma	Bisulphite sequencing and MSP	(Lee et al, 2002)
Lung	33% (8/24) microdissected primary SCLC 69% (9/13) SCLC cell lines 57% (4/7) large-cell NSCLC cell lines 6% (1/17) other NSCLC cell lines	Bisulphite sequencing and MSP	(Osada et al, 2002)
Skin	68% (28/41) microdissected primary basal cell carcinoma	MSP	(Lodygin et al, 2003)
Squamous cell carcinoma	35% (32/92) primary oral SSC 50% (3/6) oral dysplasia	Bisulphite sequencing and MSP	(Gasco et al, 2002a)
	56% (20/36) vulval SCC 47% (15/32) VIN		(Gasco et al, 2002b)
Ovarian cancer	79% (11/14) clear cell adenocarcinoma 26% (5/19) serous adenocarcinoma 36% (4/11) mucinous adenocarcinoma 20% (2/10) endometrioid adenocarcinoma	MSP	(Kaneuchi et al, 2004)
	58% (7/12) ovarian cancer cell lines 30% (3/10) IHC positive 80% (8/10) IHC negative microdissected adenocarcinoma	MSP	(Akahira et al, 2004)
Prostate cancer	100% (41/41) microdissected primary prostate adenocarcinomas	MSP	(Lodygin et al, 2004)
	33% (1/3) prostate carcinoma cell lines	MSP	(Urano et al, 2004)

Table 1.3: Frequency of 14-3-3 σ CpG methylation in different types of epithelial tumours and techniques utilised for methylation detection.

CRC = colorectal carcinoma; HCC = hepatocellular carcinoma; IHC = immunohistochemistry; NSCLC = non- small cell lung cancer; SCLC = small cell lung carcinoma; SSC = squamous cell carcinoma; VIN = vulval intraepithelial hyperplasia; MSP = Methylation-specific PCR; SSCP = Single-strand conformation polymorphism.

Source: adapted from Hermeking, 2003 and Lodygin & Hermeking, 2005.

Very few studies have investigated the relationship between *14-3-3 σ* methylation and p53 status in human cancers. Given that p53-induced *14-3-3 σ* expression is critical in maintaining G₂/M arrest following DNA damage (Chan et al, 1999; Hermeking et al, 1997), it might be hypothesised that inactivation of *14-3-3 σ* and p53 mutations are mutually exclusive occurring events. p53 plays a crucial role in preserving genomic stability and *14-3-3 σ* ^{-/-} cells are defective in maintaining G₂/M arrest following DNA damage, exhibiting chromosomal anomalies even in cancer cells with wild-type p53 (Chan et al, 1999). Therefore, it could be proposed that methylation and subsequent inactivation of *14-3-3 σ* may be determined by p53 status. Suzuki et al found that there was no difference in the frequency of p53 mutations between *14-3-3 σ* methylated and unmethylated cell lines. Although in gastric cancers, p53 mutations were at a lower frequency in *14-3-3 σ* methylated cases compared to unmethylated cases (p = 0.03, n = 16) (Suzuki et al, 2000). Similarly methylation of *14-3-3 σ* is detected more frequently in squamous cell carcinomas with wild-type p53 than cancers with mutant p53, although the difference just fails to reach significance (p = 0.074, n = 92) (Gasco et al, 2002a). These reports are inconclusive, however, they do suggest that there is no causal relationship between p53 status and *14-3-3 σ* methylation in cancer cells.

A number of reports suggest that *14-3-3 σ* functions as a tumour suppressor gene. Therefore, it would seem counter-intuitive that *14-3-3 σ* expression is elevated in a small number of human cancers compared to normal cells or tissues. As well as having increased expression in hematological malignances and colorectal cancer (Motokura et al, 2007; Perathoner et al, 2005; Tanaka et al, 2004), *14-3-3 σ* is overexpressed in pancreatic cancer. *14-3-3 σ* was identified as one of a 149 genes overexpressed in pancreatic cancer using cDNA microarray screening. This was subsequently confirmed by reverse transcription-polymerase chain reaction (RT-PCR) and immunohistochemistry. In the majority of pancreatic cancers, overexpression was associated with hypomethylation of CpG sites within *14-3-3 σ* (Iacobuzio-Donahue et al, 2003). Elevated levels of *14-3-3 σ* expression and associated hypomethylation have also been observed in high grade histological type

endometrial carcinomas (Nakayama et al, 2005). Furthermore, several studies have described overexpression of *14-3-3 σ* in lung cancer tissues (Qi et al, 2005) and head and neck cancer (Villaret et al, 2000). As with the reports of increased *14-3-3 σ* expression in hematological malignances and colorectal cancer, it is unknown whether the observed overexpression is associated with demethylation at CpG sites within *14-3-3 σ* as no methylation analysis was performed.

The exact role (if any) that *14-3-3 σ* plays in tumorigenesis appears to be complex. Firstly, in cancer, aberrant methylation at CpG sites within *14-3-3 σ* and associated changes in expression compared to normal tissue or cells varies in different tumour types. It is very likely that in cancer, other epigenetic modifications are involved in regulating *14-3-3 σ* expression as was shown in the study which examined *14-3-3 σ* in normal cell types (Oshiro et al, 2005). Secondly, the majority of published data supports the notion that *14-3-3 σ* functions as tumour suppressor gene (Hermeking et al, 1997; Wilker et al, 2007). However, one report has shown that *14-3-3 σ* may be tumour promoting as it delays apoptosis in cancer cells (Samuel et al, 2001). Furthermore, another study showed that not only loss of *14-3-3 σ* expression, but also overexpression of the gene can result in impaired cell cycle regulation (Hermeking et al, 1997). The common occurrence of *14-3-3 σ* methylation in cancer suggests that it may have diagnostic or prognostic benefits. It is likely that this may need to be tailored to individual cancer types due to the reason discussed above. It is believed that *14-3-3 σ* hypermethylation detection could in time assist in the diagnosis of cancer type. For example, one report demonstrated that inactivation of *14-3-3 σ* by methylation was restricted to a specific sub-type of lung cancer (Osada et al, 2002). *14-3-3 σ* hypermethylation could also be used as an early marker for detection of cancer in humans. *14-3-3 σ* methylation would be an attractive marker for breast cancer, since it is an early event in neoplastic transformation (Umbricht et al, 2001). Alternatively, *14-3-3 σ* could be a new target for anti-cancer therapy. As *14-3-3 σ* is overexpressed in some cancers, its activity could be inhibited and subsequent different pathways that are required for tumour growth could be disrupted.

1.8 Hypothesis

Taking all of the background literature reviewed above into consideration, it is hypothesised that *14-3-3 σ* is aberrantly methylated in colorectal cancer cell lines and in colorectal tumours. Despite the two previous studies on *14-3-3 σ* methylation analysis in colorectal cancer in which it was reported that *14-3-3 σ* methylation is a rare event in colorectal cancer, no corresponding normal colonic tissue was examined in either studies and hence the specificity of *14-3-3 σ* methylation in the colorectal tumours is still unknown (Ide et al, 2004; Suzuki et al, 2000). Therefore, from investigating the methylation status of *14-3-3 σ* in normal colonic mucosa tissue in addition to colorectal cancer cell lines and colorectal tumours it is proposed that aberrant *14-3-3 σ* methylation in colorectal cancer may be in contrast to what was previously thought. In addition, it is hypothesised that *14-3-3 σ* methylation in colorectal cancer will determine its expression as it has been previously shown to tightly associated in other cancers resulting in either overexpression or gene silencing of *14-3-3 σ* . Finally, it has been demonstrated that *14-3-3 σ* methylation occurs in a number of different cancers, in some cases at a high percentage and at different stages of tumorigenesis, and is associated with the tumour suppressor gene *p53*. Therefore, it is hypothesised that *14-3-3 σ* methylation and consequential aberrant expression in colorectal cancer will have a contributory effect on carcinogenesis or tumour progression.

1.9 Research Aim

The overall aim of the work presented in this thesis was to investigate the methylation status of the gene *14-3-3 σ* in colorectal carcinoma and to determine if methylation at the promoter region of *14-3-3 σ* determines expression and function of the gene in colorectal cancer and contributes to carcinogenesis or tumour progression.

Previously published data has demonstrated that *14-3-3 σ* hypermethylation and associated gene inactivation occurs at a high percentage in a number of different epithelial cancers (Ferguson et al, 2000; Lodygin et al, 2004). However, only a few studies have been carried out in colorectal cancer tissue and in these reports hypermethylation of *14-3-3 σ* was a rare event as it was detected in a low percentage of colorectal cancer cell lines and colorectal tumours (Ide et al, 2004; Suzuki et al, 2000). Interestingly, in both studies, methylation of *14-3-3 σ* in the normal colon tissue was not examined. Furthermore, several reports have shown *14-3-3 σ* overexpression in colorectal tumour tissue when compared against expression in adjacent normal mucosal tissue from the colon (Perathoner et al, 2005; Tanaka et al, 2004). I set out to investigate the methylation status of *14-3-3 σ* in more detail to resolve the previously conflicting data from various studies.

14-3-3 σ plays a pivotal role in arresting cells at G₂/M upon DNA damage and various knock-out studies further support its function as a tumour suppressor (Chan et al, 1999; Hermeking et al, 1997). In addition, certain findings have raised a *14-3-3 σ* paradox as the protein has been shown to suppress cell death by sequestering the pro-apoptotic Bax protein (Samuel et al, 2001). Therefore, I set out to examine the role of *14-3-3 σ* in colorectal cancer cells and determine if the protein can contribute to colorectal cancer carcinogenesis or tumour progression.

Specifically, the aims of this thesis were as follows:

1. Determine the methylation status in the upstream promoter region and CpG island of *14-3-3 σ* in colorectal cancer cell lines, colonic normal mucosa tissue and in colorectal tumours to determine any changes occurring in colorectal cancer carcinogenesis.
2. Measure expression of 14-3-3 σ at both the mRNA and protein level *in vitro* and *in vivo* to establish whether expression is related to methylation status.
3. Assess the specificity of methylation of *14-3-3 σ* by examining global levels of DNA methylation and CIMP phenotype in a small number of colorectal tumours.
4. Investigate whether altered 14-3-3 σ expression influences apoptosis, proliferation, and the cell cycle in an *in vitro* system.
5. Analyse the expression and status of *p53* in colorectal cancer cell lines and *in vivo* to examine whether there is a relationship between p53 status and *14-3-3 σ* methylation.

Chapter 2

Materials and Methods

The following chapter provides an overview of the methods used during the course of this thesis. Where appropriate, specific details are included in the relevant results chapters. Stock solutions and media marked with an asterisk (*) were prepared by the MRC Human Genetics Unit technical services department and sterilised by autoclaving. Standard operating procedures covered by risk assessments (including COSHH regulations) were adhered to throughout and in accordance with the MRC health and safety policies.

2.1 Biological Material

2.1.1 Summary of cell lines

A number of colorectal cancer cell lines examined throughout the duration of this PhD and are outlined in Table 2.1. Some colorectal cell lines were maintained as laboratory stocks and were originally purchased from the European Type Culture Collections (ECACC). For the interest of this PhD, information regarding *p53* status and chromosomal instability are listed for each cell line. *p53* status was obtained from the International Agency for Research on Cancer (IARC) TP53 mutation database (<http://www-p53.iarc.fr>) unless otherwise stated.

Cell line	p53 status	Chromosome Instability
SW480*	Mutated	Positive (Lengauer et al, 1997)
HT29*	Mutated	Positive (Lengauer et al, 1997)
HCT116*	Wild-type	Negative (Lengauer et al, 1997)
Colo320DM*	Mutated	Positive (Prof Ian Tomlinson, personal communication)
Caco 2	Mutated	Unknown
LoVo	Wild-type	Positive (Lengauer et al, 1997)
HRT-18	Mutated (Din et al, 2004)	Unknown
SW48	Unknown	Negative (Lengauer et al, 1997)
SW620	Mutated	Unknown

Table 2.1: Summary of colorectal cell lines.

*Colorectal cancer cell lines maintained as laboratory stocks. SW480 cell line was originally purchased from the ECACC in 2000; HT29: ECACC, 1998; HCT116: ECACC, 1998; and Colo320DM cells were a kind gift from Professor Ian Tomlinson (Wellcome Trust Centre for Human Genetics, University of Oxford) in 2007.

2.1.2 Maintenance of cell lines

The following methods were used to grow and maintain all cell lines for DNA, RNA and protein extraction, transfection, proliferation assays, apoptosis assays and fluorescence activated cell sorting (FACS) analysis:

Tissue Culture Medium

L-15 (SW480), RPMI (Colo320DM, HCT116) or DMEM (HT29) (Gibco BRL)

10% w/v Foetal calf serum*

1% w/v Penicillin and streptomycin*

Phosphate Buffered Saline (PBS)*

0.1M $\text{NaH}_2\text{PO}_4 \cdot \text{H}_2\text{O}$

0.1M $\text{Na}_2\text{HPO}_4 \cdot 7\text{H}_2\text{O}$

pH7.4

Freezing Media

8% w/v Dimethylsulfoxide (DMSO) in FCS*

Trypsin Versene (TV)

50% w/v Trypsin*

50% w/v Versin*

Maintenance of all cell-lines was carried out under sterile conditions in a category 1 containment hood. Cell lines were stored long-term in the liquid nitrogen storage facility at the MRC Human Genetics Unit. Cell lines were raised from liquid nitrogen rapidly by thawing in warm water then placed into the appropriate media as soon as possible, and washed twice with media, by centrifugation (1500rpm in an Eppendorf 5702 centrifuge). Cells were fed with media as required and split by a PBS wash, and incubating with TV (5 mins) for adherent cells, and then, as for all cell lines aliquoting 1/2 to 1/10 of cell suspension into fresh media. To maintain a renewable stock of the cell lines, at least 3×10^6 cells were split from the main culture, centrifuged at 1500rpm in an Eppendorf 5702 centrifuge and re-suspended in 1.5ml of freezing media. The cells were then subsequently frozen at -70°C before being transferred to liquid nitrogen (-140°C).

2.1.3 Tissue sample collection

Tissue collection was covered by ethical approval held by Prof M. Dunlop or covered by generic informed consent for anonymous samples.

2.1.4 Colorectal tissue samples

A panel of colorectal carcinomas and corresponding colonic normal mucosa tissue samples from patients with colorectal cancer treated in the Colorectal Surgery Unit, Western General Hospital, Edinburgh were collected. These samples were prefixed with KR and represent a selection of tissue samples analysed throughout this PhD. Colonic normal mucosa biopsies from individuals who were shown to be cancer and disease free during examination for a rectal bleed, were collected and used as control samples.

2.1.5 Skin Samples

Skin samples A, B & C were donated anonymously from healthy control individuals.

2.1.6 Tissue Lysate samples

Cytoplasmic protein extract from healthy human adult colonic mucosa tissue were supplied by Zyagen Laboratories, San Diego, California.

2.1.7 Tumour sections

Tumour samples from a Scottish cohort were available as laboratory stocks and were previously collected by Prof M. Dunlop and Dr S. Farrington (MRC Human Genetics Unit, Edinburgh). Paraffin embedding and sectioning of tumours was carried out by Aberdeen General Hospital, Pathology department.

2.2 DNA and RNA Purification protocols

2.2.1 Purification of DNA from cell lines, skin, tumour and normal mucosa colorectal tissue

Isolation of genomic DNA from cell cultures, skin samples, colorectal tumour and normal mucosa tissue was carried out using a QIAamp DNA mini kit (QIAGEN Ltd, Crawley, UK) according to the manufacturer's instructions.

2.2.2 RNA Extraction

Purification of RNA from cell cultures and human tissue was carried out using TRIzol reagent (Invitrogen, Paisley, UK) according to the manufacturer's instructions.

2.2.3 Estimation of DNA and RNA concentration

To estimate the concentration of DNA and RNA purified from the protocols listed above, optical densitometry on a GeneQuant Pro RNA/DNA calculator UV spectrophotometer (Amersham Pharmacia biotech, Cambridge, UK) was used. DNA samples were diluted 1 in 20 and the absorbency measured at 260nm and 280nm. A concentration in ng/μl was given.

2.3 DNA Samples

The following were acquired directly as DNA samples.

2.3.1 Colorectal tumour DNA

DNA samples from a Scottish cohort were available as laboratory stocks and were previously collected by Prof M. Dunlop and Dr S. Farrington (MRC Human Genetics Unit, Edinburgh). Prospective patients were recruited from the colorectal clinic at the Western General Hospital, Edinburgh, and following consent, a full family history was recorded from interviews with patients. Tumours were characterised as to AJCC stage, whether they were located proximal to the splenic flexure or distal, mucin content and degree of differentiation from pathology reports. Screening for germline mutations in *MLH1*, *MSH2*, *MSH6* & *PMS2* were performed and MSI status determined by comparison of matched normal and tumour DNA using a panel of 8 recommended microsatellite markers (Rodriguez-Bigas *et al.*, 1997; Boland *et al.*, 1998).

2.3.2 Colorectal cancer Cell line DNA

A number of genomic DNA samples from colorectal cancer cell lines were available as laboratory stocks. These included DNA samples from the following colorectal cancer cell lines; Caco-2, LoVo, HRT18, SW48 & SW620.

2.3.3 Control Tissue DNA from healthy individuals

Genomic DNA from colonic mucosa tissue was obtained from Zyagen Laboratories, San Diego, California.

2.4 Techniques for detection of DNA Methylation employing sodium bisulphite modification of DNA

Two methods were utilised throughout this PhD for detecting DNA methylation, bisulphite sequencing and methylation-specific PCR (MSP) (Herman *et al.*, 1996a).

Bisulphite conversion kits have recently been developed which combine the denaturation and bisulphite treatment of DNA, subsequent desulphonation and then clean-up of the converted DNA for methylation analysis. During this PhD, two kits were used depending on the number of DNA samples that were to be treated at one time. These are listed below.

2.4.1 Large-scale bisulphite treatment: 96-well format

The 96-well format EZ-96 DNA Methylation-Gold Kit (Zymo Research, CA, US) was used to bisulphite treat the majority of DNA samples according to the manufacturer's instructions. Approximately 500ng of DNA was bisulphite converted if sufficient material was available otherwise the maximum volume allowable by the kit (20µl) was converted. A universal methylated DNA standard and control primers (Zymo Research) were utilised in conjunction with the EZ-96 DNA methylation kit to assess the efficiency of bisulphite conversion of DNA.

2.4.2 Small-scale bisulphite treatment

For the bisulphite conversion of a small number of DNA samples, the EpiTect Bisulfite Kit (Qiagen Ltd) was carried out according to the manufacturer's instructions. Approximately 500ng of DNA was bisulphite converted using the standard protocol. DNA samples with low concentrations of DNA were bisulphite converted using a protocol modified for low concentrations of DNA, which employs a larger volume of DNA for processing and the addition of carrier RNA to enhance binding of DNA to the EpiTect spin column membrane. In the first instances, the universal methylated DNA standard and control primers (Zymo Research) were used to test the efficiency of bisulphite conversion. For subsequent conversions, DNA from the *14-3-3σ* methylated colorectal cancer cell-line SW480 and the *14-3-3σ* unmethylated colorectal cancer cell line HCT116, were used alongside other DNA samples to assess the efficiency of bisulphite modification.

2.4.3 PCR reactions

PCR amplification was carried out on bisulphite converted DNA and amplified products were sequenced directly from PCR products or from clones (see section 2.5)

to identify methylated cytosine residues (bisulphite sequencing). Nested PCR primers were required to sufficiently amplify DNA due to the low concentration of DNA following bisulphite treatment. MSP uses PCR primers which are designed to distinguish unconverted (methylated) cytosines from converted (unmethylated) cytosines using bisulphite treated DNA as a template. Hence, two PCR reactions are performed and methylated sequences or unmethylated sequences are amplified depending on the methylation status of the sample. Densitometric analysis of captured image was performed following MSP reactions using a BioRad Chemi Doc system, QuantityOne (version 4.4.1) software (BioRad Laboratories, Hercules, CA, US).

All PCR reactions were performed in a final volume of 30µl using the Platinum Taq Polymerase kit (Invitrogen). Final reaction concentrations for the Platinum Taq system were 1 X PCR buffer, 3mM MgCl₂, 0.1 units of Platinum Taq, 300µM dNTPs, 0.5µM of each oligonucleotide and 21µl dH₂O. A Peltier PCT225 thermal cycler (MJ Research, Waltham, US) was used for PCR amplification under the following conditions, unless otherwise stated: 94°C – 5min, (95°C – 30secs, 60°C – 30secs, 72°C – 30secs) x 30, final extension 72°C – 5min.

2.4.4 Oligonucleotides for PCR reactions

Primers were supplied from Sigma-Aldrich (Dorset, UK) as precipitates and were re-suspended in dH₂O to a stock concentration of 100µM. The primers were further diluted with dH₂O to a working concentration of 20µM. Bisulphite sequencing primers were designed by eye or using the MethPrimer program (Li & Dahiya, 2002) at <http://www.urogene.org/methprimer/index.html> unless otherwise referenced. Table 2.2 lists all oligonucleotides utilised throughout this PhD. Bisulphite sequencing primers (BS) and MSP primers are specified. ‘Nest’ refers to nested (inner) primers used in bisulphite sequencing PCR reactions. M and U refer to methylated and unmethylated MSP primers respectively.

Oligonucleotide	Sequence 5'-3'	PCR conditions	References
BS 14-3-3sRegA5' 14-3-3sRegA3' 14-3-3sRegA5'nest BS_hSFN_F1 BS_hSFN_R1 BS_hSFN_F2 BS_hSFN_R2	TGATGTGGGTAGTTATGTGAT CCTTTCATAAAAACTACCATATCCTC TGGAAAGGTGTTAGTGTAGGTG TGATGTTAGTTTYGAATAAGAGG TTTCTACTCAATACTAAACAACAC GTTTGGAAAGGTGTTAGTGTAG ACCACRTTCTTATAAACTACTAAAAAC	Standard Designed by James Reddington, MRC Human Genetics Unit	Novel
BS 14-3-3sRegB5' 14-3-3sRegB3' 14-3-3sRegB5'nest	AGAAGGTTAAGTTGGTAGAGTAGG AATCACCCCTTCATCTTCAAATAAAA TCCTTAATAAAATAACTATCCAAC	Standard	14-33sRegB5' is from Suzuki <i>et al</i> 2000. All others are novel
BS 14-3-3sRegA3'2	TACTCAATACTAAACAACACCCTCC	Standard	Novel
BS 14-3-3sRegC5' 14-3-3sRegC3' 14-3-3sRegC5'nest 14-3-3sRegC3'nest	GAGGATATGGTAGTTTTTATGAAAGG AAAAATTCAAACCAAACCCAA GGAGGGTGTTGTTTAGTATTGAGTAG AATCACCCCTTCATCTTCAAATAAAA	62°C annealing temp, 35 cycles	Novel
MSP 14-3-3sM5' 14-3-3sM3' 14-3-3sU5' 14-3-3sU3'	TGGTAGTTTTTATGAAAGGCGTC CCTCTAACCGCCCACCACG ATGGTAGTTTTTATGAAAGGTGTT CCCTCTAACCACCCACCACA	58°C annealing temp, 35 cycles	(Ferguson et al, 2000)
ACTIN 5' ACTIN 3'	CTGTGCTATCCCTGTACGCCTC CATGATGGAGTTGAAGGTAGTTTCGT	58°C annealing temp, 35 cycles	(Eis et al, 2005)
BS 14-3-3sMm5' 14-3-3sMm3' 14-3-3sMm5'nest	GGAAAGTTTTTTAAGGTTTAGGG AATAACAACCTTATCTAAATAAAACC GTAGGGAGTTGGGTTGAGTAGTTTA	55°C	Novel
M13F M13R	GTAAAACGACGGCCAG CAGGAAACAGCTATGAC	Standard	

Table 2.2: Oligonucleotides used throughout this PhD. R denotes any purine nucleotide and Y denotes any pyrimidine nucleotide.

2.4.5 Gel Electrophoresis

Solutions:

10 X Tris-Acetate EDTA (TAE)*

2M Tris

5.7% w/v Glacial acetic acid

50nM Na₂EDTA (pH 8.0)

To resolve PCR products ranging in size from 100 – 1000 base pairs, 2% agarose gels were prepared using routine grade agarose (Biogene, Kimbolton, UK) and 1 X TAE solution. Ethidium bromide (BDH, Electran, Poole, England) was added at a final concentration of 0.3 mg/ml to the dissolved gel prior to pouring. 10µl of PCR product was loaded into the gel with 2µl 1 X loading buffer (Promega). A 100bp ladder (Promega) was additionally loaded into the gel to determine the size of PCR products. DNA was electrophoresed at 40-60V for approximately 40min. The BioRad Chemi Doc system using QuantityOne (version 4.4.1) software was used to visualise PCR products.

2.4.6 PCR product purification

For sequencing analysis, PCR products were purified using exonuclease I (USB, Ohio, US) and shrimp alkaline phosphatase (SAP; USB). 5µl of PCR product was added to a combination of 1µl exonuclease I (10U/µl) and 2µl SAP (1U/µl). The mixture was incubated for 15min at 37°C in a Peltier PCT225 thermal cycler (MJ Research) and then heated to 80°C to inactivate the exonuclease and phosphatase.

2.4.7 DNA Sequencing

All DNA sequencing reactions were carried out using ABI PRISM Ready Big Dye Terminator cycle sequencing kit with Amplitaq DNA polymerase FS (Applied Biosystems, Cheshire, UK).

Sequencing of PCR products was performed in 10µl reactions using approximately 10ng of purified DNA, 3µM primer (forward and reverse separate reactions) and 2µl

Big Dye Version 3.1 (Applied Biosystems). Amplification was carried out using the following reaction conditions (96°C – 30secs, 50°C – 15secs, 60°C – 4min) 25 cycles in a Peltier PCT225 thermal cycler (MJ Research).

2.4.8 Precipitation of DNA from sequencing reactions

Sequenced DNA was precipitated by adding 55µl of 95% ethanol and 2µl of NaOAC (pH4.0) to the sequencing reaction mix and incubated at room temperature for 30min. Samples were then spun at 1500rpm in a Micromax IEC centrifuge for 30min, the DNA pellet washed with 70% ethanol, and then allowed to completely evaporate at room temperature before storing the DNA pellet at -20°C for analysis.

The same procedure above was carried out for DNA in a 96-well format, except a Sorvell Multifuge 3 S-R Heraeus centrifuge was used to spin plates at 2000rpm for 30min and the supernatant removed by flicking the plates and then pulse spinning them upturned on paper towels at 800rpm. Pellets were washed with 70% ethanol and rapidly removed by flicking the plate and further pulse spinning.

Precipitated DNA from the reaction products were re-suspended in Hi-Di™ (Applied Biosystems) and heated to 90°C for 2min by Agnes Gallacher (MRC, Human Genetics Unit, Edinburgh). Samples were resolved on an ABI PRISM® 3100 or a 3700 genetic analyser machine according to the manufacturer's instructions.

2.4.9 Characterisation of methylated CpG islands

Sequence data was analysed using Sequencing analysis software Version 3.7 or 5.2 (for 3100 and 3730 respectively) (Applied Biosystems). Multiple sequences of the same fragment were aligned using the Consed program by importing all sequence data. Sequencing traces were viewed and aligned using the Phred/Phrap/Consed packages (www.phrap.org/phredphrapconsed.html). Methylated CpG dinucleotides were identified by the presence of cytosine residues at CpG sites.

2.5 Cloning and Bacterial Culture

Media:

Luria Broth (L-Broth)*

0.1% w/v Tryptone (Difco)

0.05% w/v Yeast extract (Difco)

171mM NaCl

Luria Agar (L-agar)*

0.1% w/v Tryptone

0.05% w/v Yeast Extract

171mM NaCl

0.15% w/v Agar (Oxoid Ltd)

Additives:

Ampicillin Stock solution

20mg/ml ampicillin (Sigma-Aldrich)

5-Bromo-4-Chloro-3-Indolyl- β -D-galactosidase (X-Gal)

40mg/ml X-Gal (Sigma-Aldrich) in Dimethylformamide (DMF)

2.5.1 TA cloning and transformation

Individual alleles were cloned using a Dual Promoter TA Cloning Kit (Invitrogen). Bisulphite treated DNA was PCR amplified as described in section 2.4.3 and products were cloned into pCR[®] II vector (Invitrogen) according to the manufacturer's instructions. Clones were then transformed into One Shot[®] TOP10 Chemically Competent E. coli (Invitrogen) according to the manufacturer's instructions. 30 - 80 μ l of each transformant was spread onto selective L-agar plates containing ampicillin (50 μ g/ml) and X-gal (40 μ g/ml). Plates were incubated overnight at 37°C, upside down.

2.5.2 Colony selection and storage

White bacterial colonies, indicative of positive transformants, were picked and PCR amplified directly from colonies using M13 specific primers. Approximately 288 white colonies were picked to carry out PCR reactions in 3 X 96-well plates as

described in section 2.4.3. Positive transformants containing the correct size insert were identified using gel electrophoresis as described in section 2.4.5 and clones with the correct length insert were then sequenced directly from the PCR reaction as described in section 2.4.7. For long-term storage, selected white colonies were cultured in 96-well plates containing 1.2ml/well L-Broth with 100µg/ml ampicillin overnight at 37°C, shaking at 160rpm. 25µl of glycerol was added to each well the next day and plates were stored at -70°C.

2.6 Expression Analysis

2.6.1 DNase I Treatment

Prior to quantitative RT-PCR (qRT-PCR) analysis, RNA was treated with DNase I RNase-Free (Ambion, Cambridgeshire, UK) according to the manufacturer's instructions.

2.6.2 cDNA synthesis

For cDNA synthesis, 1µg of total RNA was transcribed using the 1st Strand cDNA Synthesis kit for RT-PCR (AMV) (Roche Diagnostics, Mannheim, Germany) according to the manufacturer's instructions. Negative reverse transcribed reactions (AMV Reverse Transcriptase omitted) were amplified by PCR using actin primers listed in Table 2.2 and carried out as described in section 2.5 to test all gDNA contamination had been removed from the RNA sample. This was carried out in addition to testing cDNA contamination by analysing negative reverse transcriptase reactions using Taqman analysis.

2.6.3 Quantitative RT-PCR: Taqman analysis

qRT-PCR was performed to quantify relative levels of *14-3-3σ* mRNA expression using a Taqman[®] Gene Expression Assay (Applied Biosystems) on an ABI PRISM[®] HT7900 Sequence Detection System thermal cycler. The assay chosen from a list of available TaqMan[®] Gene Expression Assays was Hs00602835_s1. As *14-3-3σ* only contains one exon, the primers and probe were designed within the exon. Expression of beta actin (Human ACTB endogenous control probe, Applied Biosystems) was used as endogenous reference control. The *14-3-3σ* probe was labelled with the

reporter dye FAM and the beta actin probe labelled with the reporter dye VIC at the 5' end of the oligonucleotide. A quencher dye (TAMRA) was used to label the 3' ends of both probes.

For each cDNA sample, triplicate amplifications were carried out in 384 well PCR plates (ABgene, Surrey, UK) and sealed using Absolute QPCR optically clear adhesive sheets (ABgene). Negative reverse transcriptase reactions and non-template controls were run on each plate. PCR reactions were performed in a final volume of 5µl using 0.5µl of cDNA, 1.75µl of sterile H₂O, 2.5µl Taqman[®] Universal Master Mix No AmpErase[®] UNG (2 X; PE Biosystems, New Jersey, USA) and 0.25µl probe mix (20 X). PCR conditions were as follows: 50°C – 2min, 95°C – 10min, (95°C – 15secs, 60°C – 1min) x 40.

Data analysis was carried out using SDS Version 2.1 program (Applied Biosystems). The standard curve method was used to quantify relative levels of *14-3-3σ* mRNA. Standard curves for *14-3-3σ* and *β-actin* amplifications were constructed by plotting threshold cycle values (C_t) against logged quantity of a calibrator, which was serially diluted cDNA prepared from the HT29 colorectal cancer cell line. Only standard curves with an R² value close to 1 were subsequently used to calculate relative expression values. For each sample, the relative expression was calculated using linear regression analysis from the corresponding standard curves. To obtain a *14-3-3σ* expression value normalised for initial cDNA quantity variations, *14-3-3σ* values were divided by *β-actin* values.

2.6.4 Protein expression analysis

Solutions:

Buffer A

50mM NaCl

10mM N-2 hydroxyethylpiperazine- N'-2-ethanesulfonic acid (HEPES) (pH8)

500mM Sucrose

1mM EDTA

0.5mM Spermidine

0.15mM Spermine
0.2% w/v Triton X-100
6 x Sample Buffer
20% w/v Glycerol
2% w/v SDS
0.25% w/v Bromophenol blue
1 x Stacking buffer
5% w/v β -mercaptoethanol
4 x Resolving Buffer
1.5M Tris
0.4% w/v SDS
pH 8.8
4 x Stacking Buffer
500mM Tris
0.4% w/v SDS
pH 6.8
10 x Running Buffer
250mM Tris
2M Glycine
1% w/v SDS
Semi-Dry Transfer Buffer
47mM Tris
40mM Glycine
0.037% w/v SDS
100mM Methanol
10% Resolving Gel
1 x Resolving buffer
10% w/v Acrylamide
0.15% w/v Ammonium persulphate (APS)
0.01% w/v N, N, N', N', tetramethyl-1-2-diaminomethane (TEMED)
5% Stacking Gel
1 x Stacking buffer

5% w/v acrylamide

0.15% w/v APS

0.01% TEMED

2.6.4.1 Preparation of cytoplasmic cell extracts

Cells were scraped in PBS* from confluent T25 flasks. Cells were pulsed at 6000rpm in an Eppendorf 5415R centrifuge to pellet the cells and re-suspended in 3 x volumes (~ 300µl) of Buffer A containing Complete™ protease inhibitor cocktail at 1:1250 dilution (Roche Diagnostics), 1mM pepstatin A (Sigma), 100mM PEFA block (Roche Diagnostics) and 1mM Dithiothreitol (DTT). Nuclei were then pelleted by centrifugation (Eppendorf 5415R centrifuge) at 6000rpm for 20 minutes at 4°C. The supernatant containing the cytoplasmic fraction was collected and immediately frozen on dry ice.

2.6.4.2 Preparation of cytoplasmic extracts from tissue

Approximately 20mg of tissue was dissected from frozen 'stock' tissue, transferred into an eppendorf tube and re-frozen by placing on dry-ice. Samples were then thawed on a Dri Block® DB-2A hot block (Techne, New Jersey, USA). 3 x volumes of Buffer A (~300µl) containing Complete™ protease inhibitor cocktail at 1:1250 dilution (Roche Diagnostics), 1mM pepstatin A (Sigma), 100mM PEFA block (Roche Diagnostics) and 1mM Dithiothreitol (DTT) was added to the tissue and ground using a pestle. The freeze-thawing with subsequent grinding of the tissue was repeated a further 3 times and samples were then centrifuged in an Eppendorf 5415R centrifuge at 1000rpm for 2 minutes to remove tissue debris. Nuclei were then pelleted by centrifugation (Eppendorf 5415R centrifuge) at 6000rpm for 20 minutes at 4°C. The supernatant containing the cytoplasmic fraction was collected and immediately frozen on dry ice.

Total concentrations of protein was verified by Bradford assays (Biorad, Hercules, USA), read on a Multiskan MS plate reader (Labsystems), and extracts adjusted for Western Blot analysis by adding PBS*.

2.6.4.3 Western Blot Analysis

Approximately 30µg of protein extract was added to a 1:6 dilution of sample buffer, boiled on a hot block for 5 minutes and then placed on ice. Samples were resolved by denaturing SDS-PAGE on a 10% polyacrylamide gel in 1 x running buffer at 160 volts for approximately 1 hour. Kaleidoscope prestained molecular weight markers (BioRad) were run on each gel. Gels were pre-soaked in semi-dry transfer buffer prior to transfer and the nitrocellulose membrane (Amersham Biosciences) prepared by soaking first in 100% methanol and then also in semi-dry transfer buffer. Proteins were transferred to the nitrocellulose buffer using a mini Trans-blot semi-dry transfer cell (BioRad) for 30 minutes at 10 volts.

Nitrocellulose membranes were blocked overnight at 4°C in 5% milk (Marvel) dissolved in PBS* 0.05% Tween-20 (Sigma). The membranes were incubated with primary monoclonal antibodies (see table 2.3) for 1 hour, washed in 0.05% Tween (Sigma) in PBS* for 3 x 15 minutes and then incubated for 1 hour with horseradish peroxidase conjugated sheep antimouse IgG secondary antibody 1 in 1000 (for both primary antibodies) (GE Healthcare Ltd, Buckinghamshire UK), and washed as described before. β -actin was employed as a loading control on each membrane. A goat anti-mouse IgM horseradish peroxidase secondary antibody (Calbiochem, San Diego USA), 1 in 4000 dilution was used for actin detection.

ECL western blotting protocol (Santa Cruz Biotechnology, Buckinghamshire, UK) was used to detect protein bands and carried out according to the manufacturers instructions. Densitometric analysis of protein bands was performed using the BioRad Chemi Doc system, QuantityOne (version 4.4.1) software.

Antibody	Manufacturer	Dilution Used
14-3-3 sigma Ab-1 (Clone 1433S01) Mouse mAb	Strattech Scientific Ltd, Cambridge, UK	1:200
p53 Ab-6 Pantropic Mouse mAb (DO-1)	Merck, Calbiochem, San Diego, USA	1:1000
β - actin Ab-1 Mouse mAb	Merk, Calbiochem, San Diego, USA	1:400
GFP (FL) Rabbit Polyclonal GFP (B-2) Mouse mAb	Santa Cruz Biotechnology, Buckinghamshire, UK Santa Cruz Biotechnology	1:1000 1:500

Table 2.3: Primary antibodies utilised in Western Blot analysis in this thesis, details of manufacturer and dilutions. mAb refers to monoclonal antibodies.

2.7 Cell Biology

2.7.1 5-Aza-2'-deoxycytidine treatment

Cell lines were treated with 0.5 μ M to 10 μ M of 5-aza-2'-deoxycytidine (Sigma) dissolved in 50% acetic acid for the desired time points (1-4 days). Fresh 5-aza-2'-deoxycytidine was added every 24hrs following PBS* wash and addition of fresh media. Control cells were untreated with and without vehicle, 50% acetic acid, for 4 days.

2.7.2 Transfection of cell lines

Cell lines were transfected with the overexpressing 14-3-3 σ GFP-C1 construct (kindly donated by Tomoshige Kino, National Institute of Child Health and Human Development, MD USA) or the empty vector control pEGFP-C1 (BD Biosciences Clontech, MD USA) using LipofectamineTM 2000 or LipofectinTM (both Invitrogen) in

6-well plates according to the manufacturer's instructions. Lipofectamine[™] 2000 was used for transfections preceding apoptosis assays and FACS cell cycle analysis. Lipofectin[™] was used preceding proliferation assays. In both cases, approximately 4µg of vector DNA was employed for transfections. Transfection efficiencies were calculated using fluorescence light microscopy.

2.7.3 Annexin V Apoptosis Assay

The Annexin V-Biotin kit (Calbiochem) was used according to the manufacturer's instructions to determine the total percentage of apoptotic cells in the transfected cell lines.

Briefly, triplicate wells of cell lines were transfected with both 14-3-3σGFP-C1 construct and empty vector control pEGFP-C1 and then either UV-C treated (UV-C exposed) or not UV-C treated (UV-C unexposed) using a UV Stratalinker 1800 (Stratagene, Texas USA) at 50J/M² to induce apoptosis. Apoptosis levels were determined 24 hours following UV-C treatment. Cell concentrations were adjusted to 1 x 10⁶ cells/ml, 0.5ml cell suspension was removed to an eppendorf, pelleted by centrifugation using an Eppendorf 5415R centrifuge, and re-suspended in 0.5ml of cold 1 x binding buffer (Calbiochem). 2.5µl of Annexin V-biotin (Calbiochem) was added to the appropriate tubes and incubated for 30 minutes in the dark at room temperature. Cells were pelleted using an Eppendorf 5415R centrifuge, re-suspended in 0.5ml of 1 x cold binding buffer (Calbiochem), and 15µl of fluorescent streptavidin texas-red conjugate (Calbiochem) added to each tube. Each sample was then stored at 4°C overnight to allow cells to settle to the bottom of the tubes. 20µl of cells were placed on SUPERFROST PLUS[®] slides and apoptotic cells were counted using fluorescent light microscopy. 200 GFP transfected cells were counted for each sample and the number of apoptotic cells calculated as a percentage from these cells.

2.7.4 Proliferation Assays

Cell growth in overexpressing 14-3-3σGFP-C1 SW480 cells and empty vector control GFP-C1 SW480 cells was measured. Cell proliferation assays were performed over a period of 4 days of growth in 96-well plates, in triplicate, using the

CellTiter 96 One Solution Cell Proliferation Assay (Promega). 5000 cells were seeded per well prior to transfection; this number was decided by performing a cell titration assay to ensure the signal measured at the end of the assay did not exceed the linear range. Absorbance at 490 nm was recorded using a Multiskan Spectrum Plate Reader (Thermo electron corporation, Waltham, MA USA) 24 hours post transfection and then every 24 hours for 4 days total following 2 hours of incubation of the cells with CellTiter 96 One Solution reagent. Absorbance readings were corrected for transfection efficiency, which was measured separately for each experiment.

2.7.5 FACS analysis of GFP transfected cells

Assistance with FACS analysis was given by Shonna Johnston (QMRI, Edinburgh New Royal Infirmary) using a FACS Vantage SE with DIVA option (BD Biosciences). GFP cells were sorted using a 100µm nozzle and a 4 way 0240 precision sort, with an efficiency of 70%, and approximately 4000 events sorted per second.

1×10^7 cells/ml of each GFP cell sample were harvested using TV*, centrifuged at 1500rpm in an Eppendorf 5702 centrifuge and re-suspended in 1ml of the appropriate media with 2% FCS*. Approximately 3×10^6 GFP cells for each sample were collected following sorting and placed in the appropriate media with 10% FCS*.

GFP cells were spun down at 1500rpm in an Eppendorf 5702 centrifuge for 5 minutes and fixed by adding ice-cold 70% ethanol in a drop-wise manner whilst vortexing. Fixed GFP cells were stored at -20°C until day of cell cycle analysis.

2.7.6 Flow Cytometry Cell Cycle Analysis

Fixed GFP cells were spun down at 1500rpm for 5 minutes in a Micromax IEC centrifuge and washed twice in PBS*. GFP cells were then re-suspended in 500µl of Propidium Iodide (PI) solution containing 500µl PBS* with 0.1% Triton X-100, 10µg PI (Sigma) and 100µg RNase A (Sigma) and incubated at room temperature for 30 minutes in the dark until analysis.

Assistance with Flow Cytometry was given by Shonna Johnston (QMRI, Edinburgh New Royal Infirmary) using a FACSCaliber cytometer with CellQuest software (BD Biosciences). The PI signal was quantified at emission spectra/bandpass 585/42nm. Output data obtained for 5000 cells in each GFP sample group and data analysed using Flowjo Version 7.0 (Tree Star, OR USA).

2.8 Analysis of Global Methylation status

2.8.1 MethyLight analysis

The presence of the CIMP phenotype in colorectal carcinomas was determined using MethyLight analysis (Eads et al, 2000). A four marker panel comprising of *hMLH1*, *CDKN2A*, *MINT1* & *MINT2* was measured for methylation.

Bisulphite treated tumour DNA samples were subjected to real time PCR reaction on an ABI PRISM® HT7900 Sequence Detection System thermal cycler. Two types of MethyLight reactions were set-up: 1) A MethyLight reaction using bisulphite converted DNA, with forward and reverse primers and probes specific for methylated DNA and bisulphite converted DNA. 2) A bisulphite specific control reaction using β -ACTIN specific primers and probes to measure the loading of bisulphite converted DNA. The β -ACTIN reactions are not methylation specific but are specific for bisulphite converted DNA. Primer and probe sequences for the 4 marker panel and β -ACTIN are listed in Table 2.4. The four marker probes were labelled with the reporter dye FAM and the beta actin probe labelled with the reporter dye VIC at the 5' end of the oligonucleotide. A quencher dye (TAMRA) was used to label the 3' ends of all probes.

Primers and Probes	Sequences	References
hMLH1	6FAM- CCCGCTACCTAAAAAATATACGCTTACGCG 5' AGGAAGAGCGGATAGCGATTT 3' TCTTCGTCCCTCCCTAAAACG	(Weisenberger et al, 2006)
CDKN2A	6FAM- ACCCGACCCCGAACCGCG 5' TGGAGTTTTTCGGTTGATTGGTT 3' AACACGCCCCGCACCTCCT	(Weisenberger et al, 2006)
MINT1	6FAM-CTACTTCGCCTAACCTAACGCACAACAAACG 5' GGGTTGAGGTTTTTTTGTAGCG 3' CCCCTCTAAACTTCACAACCTCG	(Weisenberger et al, 2006)
MINT2	6FAM-CTTACGCCACCGCCTCCGA 5' TTGAGTGGCGCGTTTCGT 3' TCCCCGCCTAAACCAACC	(Weisenberger et al, 2006)
β-ACTIN	VIC- ACCACCACCCAACACACAATAACAAACACA 5' TGGTGATGGAGGAGGTTTAGTAAGT 3' AACCAATAAAACCTACTCCTCCCTTAA	(Eads et al, 2000)

Table 2.4: Probe and primer sequences used for MethyLight analysis

Duplicate PCR amplifications were carried out in 96 well optical MicroAmp™ reaction plates (Applied Biosystems) and sealed using Absolute QPCR optically clear adhesive sheets (ABgene). PCR reactions were performed in a final volume of 25µl using 5µl of bisulphite treated DNA sample, 4.5µl of sterile H₂O, 12.5µl Taqman® Universal Master Mix No AmpErase® UNG (2 X; PE Biosystems, New Jersey, USA) 200nM probe (Applied Biosystems) and 600nM of each primer (Applied Biosystems). PCR conditions were as follows: 50°C – 2min, (95°C – 10min, 95°C – 15secs, 60°C – 1min) x 40.

Data analysis was carried out using SDS Version 2.1 program (Applied Biosystems). Ct values were used to create relative values for each sample by generating standard curves. These were created by plotting the threshold cycle (Ct) against logged quantity of a calibrator, which was serially diluted bisulphite-treated, fully

methyated CpGenomeTM Universal Methylated DNA (Chemicon International Inc, Dundee Scotland). The coefficient of linear regression (r) was calculated for each standard curve and curves with values close to 1 were further utilised. Samples were normalised for initial bisulphite treated DNA quantity variations by dividing relative values by β -actin values. Percentage methylation ratio (PMR) values were calculated by dividing normalised values with fully methylated CpGenome DNA relative values and multiplying by 100.

2.8.2 Nearest Neighbor Analysis

Nearest Neighbor analysis (Ramsahoye, 2002) is a modification of a technique first published by Gruenbaum et al, 1981 (Gruenbaum et al, 1981). Assistance with Nearest Neighbor analysis was given by Dr Bernard Ramsahoye (Cancer Research UK, University of Edinburgh).

Approximately 1 μ g of DNA was RNaseA (Sigma-Aldrich) treated according to the manufacturer's instructions and then ethanol precipitated. DNA was digested with 10U of *MboI* (New England Biolabs, MA US) overnight at 37°C and heat inactivated at 70°C for 20 minutes. The digested DNA was again precipitated in ethanol and resuspended in 10 μ l H₂O. 3 μ l of [α -32p]dGTP at 30 μ Ci (Amersham Pharmacia Biotech), 1.5 μ l 10X labelling buffer and 0.5 μ l Klenow (Amersham Pharmacia Biotech) was then added to the DNA and incubated at 15°C for 15 minutes. 2 μ l of 0.2M EDTA (Sigma-Aldrich) was added to terminate the reaction before transferring the labelling mixture to Sephadex G50 spin columns (Roche). The spin columns were spun at 1100g for 4 minutes in a Micromax IEC centrifuge and the flow through collected. The labelled DNA was dried down using a Savant DN120 DNA speed vac (ThermoFisher Scientific, Surrey UK) and digested in a volume of 7 μ l, (5 μ l micrococcal nuclease digestion buffer: 15mM CaCl₂, 100mM Tris-HCL, 0.2U micrococcal nuclease and 2 μ g of spleen phosphodiesterase (Worthington Biochemical Corporation, NJ, US) for 4 hours at 37°C.

0.3µl of digest was spotted onto a 20 x 20 cm glass-backed cellulose TLC plate (Sigma-Aldrich) 1.5cm from the bottom right corner. 44ml of solution A (66 volumes isobutyric acid: 18 volumes H₂O: 3 volumes 30 ammonia solution) was poured into a TLC developing tank and the TLC plate placed into the tank at an angle. The plate was left for approximately 12 hours to develop and then removed from the tank and dried thoroughly for 4 hours. The dried plate was turned 90° and the sample subjected to the second dimension of chromatography using solution B (80 volumes saturated ammonium sulphate: 18 volumes 1M acetic acid: 2 volumes isopropanol). After approximately 12 hours of developing, the plate was dried thoroughly for 4 hours and then analysed using a FLA5100 phosphorimager (Fuji, Bedfordshire, UK) 635 nm laser and a 665 nm bandpass filter.

2.9 Histology techniques

2.9.1 Processing of colon tissue for paraffin wax sectioning

Tumour KR tissue samples were embedded using the Tissue Tek VIP[®] processing machine (Miles Scientific, Glasgow, UK) with the assistance of Allyson Ross and Naila Haq. The following program was run and left overnight:

Stage 1: 3 hours PBS, 38°C

Stage 2: 6 hours 70% ethanol, 38°C

Stage 3: 3 hours 100% ethanol 38°C

Stage 4: 3 hours xylene 38°C

Stage 5: 4 hours wax 58°C.

A *Leica* microtome and ACCU-Edge[®] low profile blades were used to cut 3µm sections of paraffin wax embedded tissue material. Sections were floated onto a waterbath set at 42°C. The sections were immediately attached to SUPERFROST PLUS[®] slides.

2.9.2 Immunohistochemistry

Assistance with immunohistochemistry was given by Naila Haq (University of Edinburgh, MRC Human Genetics Unit). Tumour sections were deparaffinised and re-hydrated by immersing three times for 5 minutes in xylene, two times for 5 minutes in 100% ethanol, two times for 5 minutes in 95% ethanol, and once for 5 minutes in 80% ethanol. Sections were boiled in 10mM citrate buffer (pH 6.0) two times for 5 minutes each in a microwave and then cooled for 1 hour at room temperature. Sections were rinsed in deionised water two times for 5 minutes and endogenous peroxidase activity was blocked with 3% hydrogen peroxide in water for 20 minutes followed by washing for 5 minutes with PBS* 0.1% Tween. The tissue sections were blocked with 2.5% swine serum (Dako Cytomation, Dako Denmark) for 30 minutes and then washed in PBS* 0.1% Tween before incubating with the primary antibody p53 D-01 (Merk Calbiochem) diluted 1 in 200 at room temperature for 1 hour. Sections were washed twice for 5 minutes in PBS* 0.1% Tween and incubated for 30 minutes at room temperature in ImmPRESS Peroxidase UNIVERSAL anti mouse/rabbit Ig reagent, 100µl (Vector, California USA). Sections were rinsed twice in PBS* 0.1% Tween, developed with diaminobenzidine tetrahydrochloride (DAB) tablet, 10mg (Sigma) for 2 minutes and lightly counterstained with Harris haematoxylin. The slides were then rinsed in deionised water and immersed in saturated lithium bicarbonate diluted 1 in 5. The slides were rinsed three times for 5 minutes in deionised water and dehydrated by carrying out the reverse immersions as described before for re-hydration. Slides were mounted using non-aqueous Histomount mounting media (National Diagnostics, Georgia USA) and analysed using light microscopy. p53 staining was scored 1-3 according to intensity of staining and 100-300 according to coverage of staining.

2.10 Calculations and Statistics

2.10.1 Statistical Analysis

Fishers exact tests, non-parametric Mann Whitney tests and paired Wilcoxon signed rank test, unpaired T-tests, Two-way ANOVA tests and Chi-Squared analysis were performed using GraphPad Prism 4 (GraphPad software, CA, USA). Associations between two variables were deemed significant when $p < 0.05$.

Chapter 3

Methylation analysis of *14-3-3 σ* in colorectal cancer cell lines, colorectal tumours and normal mucosa

3.1 Introduction

Gene silencing of *14-3-3 σ* by hypermethylation has been reported in several tumour types but data on colorectal cancer are limited, despite aberrant gene methylation being well recognised in colorectal carcinogenesis. My main aim in this chapter was to establish the methylation status of *14-3-3 σ* in the region encompassing the 5' region of the CpG island and upstream promoter region in colorectal cancer cell lines, colorectal tumours and normal mucosa samples. The *14-3-3 σ* CpG island was delineated using a number of algorithms available as online tools. In order to effectively analyse the methylation status of *14-3-3 σ* , bisulphite sequencing of the upstream promoter region and 5' region of the CpG island was divided into separate regions and sequenced accordingly. Methylation-specific PCR was also used alongside bisulphite sequencing to determine the methylation status of *14-3-3 σ* in colorectal cancer cell lines. A total of 9 colorectal cancer cell lines, 99 colorectal tumours and 10 matched normal mucosa samples were examined for *14-3-3 σ* methylation by bisulphite sequencing. The relationship between *14-3-3 σ* methylation status in tumour DNA and clinicopathological variables was also subsequently examined. The colorectal tumour material and corresponding normal mucosa samples from patients have been extensively screened for mismatch-repair defects and none have been found (Prof Dunlop and Dr Susan Farrington, personal communication). Mismatch-repair defects were excluded by screening for mutations in *MLH1*, *MSH2* and *MSH6* in germline DNA and tumour microsatellite instability testing.

The majority of the sequencing analysis was carried out directly on PCR products to provide the average level of *14-3-3 σ* methylation in a given sample. However, in

conjunction with this, bisulphite sequencing of individual clones was performed on 6 colorectal tumour samples and normal tissue samples from individuals free from cancer; including one colonic mucosa tissue sample and three skin tissue samples, in order to further verify the bisulphite PCR sequencing and the tumour-specificity of *14-3-3 σ* methylation in colorectal cancer. Keratinocytes, a cell-type which is present in the skin, are known to be unmethylated for *14-3-3 σ* and express high levels of the gene (Leffers et al, 1993; Oshiro et al, 2005). Therefore, *14-3-3 σ* methylation analysis in skin tissue was performed alongside methylation analysis in normal colonic mucosa for comparison.

My overall aim of this chapter was thus to investigate the qualitative and quantitative status of *14-3-3 σ* methylation and determine whether there are any relationships to suggest differential methylation plays a role in colorectal carcinogenesis.

3.2 Methodology

3.2.1 *14-3-3 σ* CpG island *in silico* analysis

In order to determine the exact region of the *14-3-3 σ* CpG island, bioinformatics analysis using algorithms previously tested; NCBI “relaxed” (<http://www.ncbi.nlm.nih.gov/mapview/static/humansearch.html#cpg>) (% GC \geq 50, obs/exp \geq 0.6, > 200bp in length) (Gardiner-Garden & Frommer, 1987) and the newer, more stringent algorithm NCBI “strict” (<http://www.ncbi.nlm.nih.gov/mapview/static/humansearch.html#cpg>) (% GC \geq 50, obs/exp \geq 0.6, > 500bp in length) (Takai & Jones, 2002) was carried out. An online program called ‘The CpG island searcher’ (<http://www.cpgislands.com>), based on the study carried out by Takai and Jones, 2002 was employed to determine the *14-3-3 σ* CpG island using the different algorithms (Figure 3.1 (A) & (B)). MethPrimer, (<http://www.urogene.org/methprimer/index1.html>) another online program was used alongside CpG Island searcher for comparison and to assist in designing bisulphite sequencing primers (Figure 3.1 (C)). The *14-3-3 σ* transcript sequence was based on the Ensembl (release 49) gene ENSG00000175793. To define the position of the *14-*

$3\text{-}3\sigma$ CpG island, the complete *14-3-3* σ transcript sequence, including 300 base pair upstream sequence was analysed.

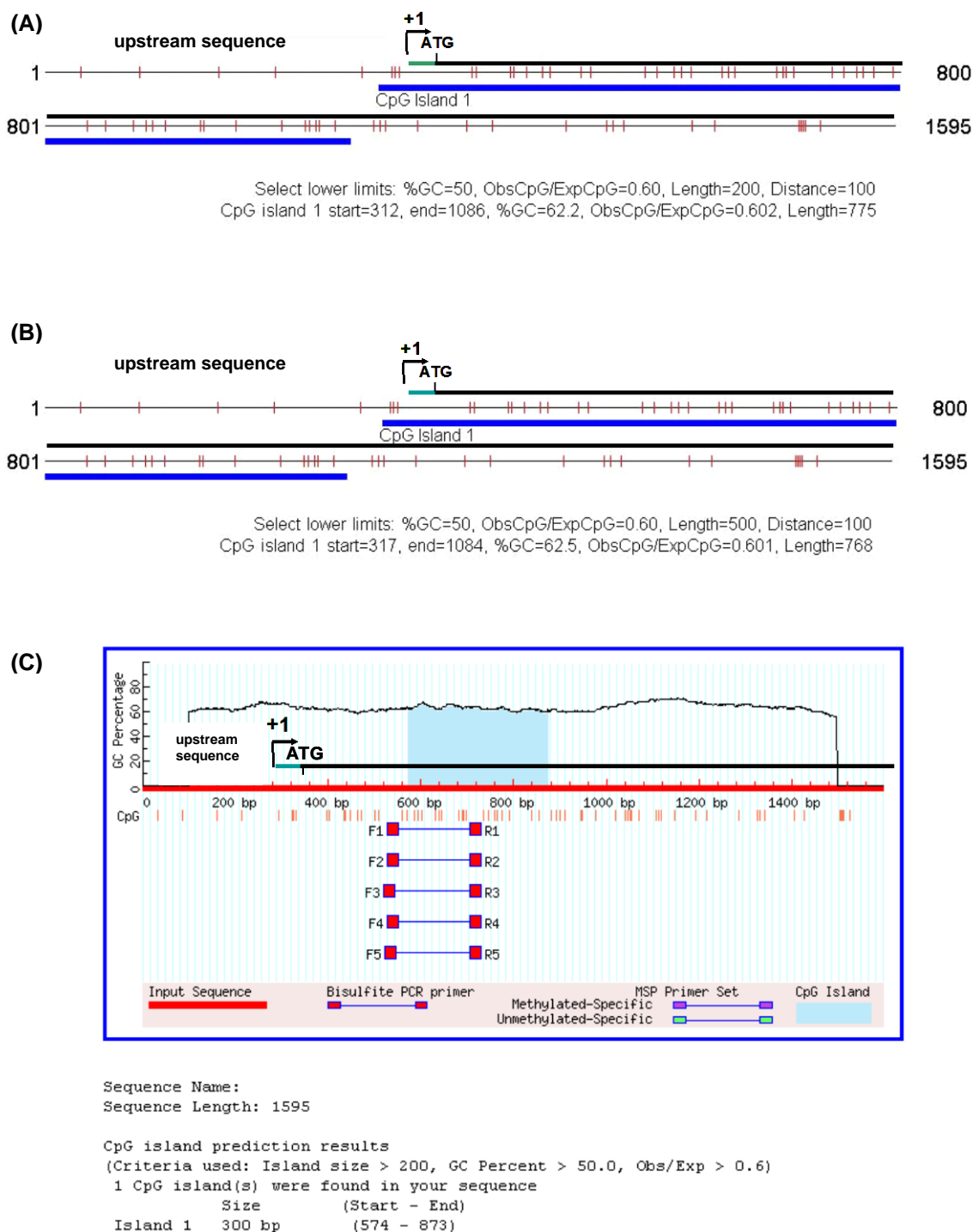


Figure 3.1: Bioinformatic analysis of 14-3-3 σ CpG island using various algorithms.

Complete 14-3-3 σ transcript was analysed and an additional 300 base pairs of upstream sequence. Exon 1 of 14-3-3 σ is depicted as a thick horizontal black line with untranslated region (UTR) shown as a thick horizontal green line. Transcriptional start site is indicated by an arrow and start codon also indicated (ATG). CpG island (thick horizontal blue line) with individual CpG dinucleotides (fine vertical red lines) are additionally shown. The CpG island was defined according to (A) The CpG island searcher (Takai & Jones, 2002) using NCBI “relaxed” criteria. (B) The CpG island searcher using NCBI “strict” criteria (<http://www.ncbi.nlm.nih.gov/mapview/static/humansearch.html#cpg>) and (C) MethPrimer (<http://www.urogene.org/methprimer/index1.html>) (Li & Dahiya, 2002) using NCBI “relaxed” criteria.

3.2.2 Bisulphite sequencing analysis

CpG island *in silico* analysis of the *14-3-3 σ* gene locus indicated a distinct CpG island in which the transcriptional start site is at the 5' end of the island with the majority of the CpG dinucleotides residing in the coding region of the gene. This is interesting as CpG islands frequently co-localise with the upstream sequence and transcriptional start site of genes (Illingworth et al, 2008; Larsen et al, 1992). This finding and the possible implications will be discussed in more detail towards the end of this chapter. The CpG island delineated by CpG island searcher with NCBI "strict" and "relaxed" criteria spans approximately 800 base pairs. The *14-3-3 σ* CpG island defined by the "relaxed" and "strict" criteria were very similar as there was only a 7 base pair difference. According to MethPrimer, the CpG island spans approximately 300 base pairs. A study reported by Suzuki et al, analysed two regions of *14-3-3 σ* for aberrant methylation (Suzuki et al, 2000). Region 1, a region upstream of the *14-3-3 σ* CpG island, corresponding to nucleotide (nt) -220 to nt 116 and region 2 corresponding to nt 93 to nt 350 (assuming transcriptional start site = +1). Taking into consideration the previously published data by Suzuki et al and results from the *in silico* analysis, it was decided to analyse a region which spanned both the upstream promoter region and the 5' region of the *14-3-3 σ* CpG island, which contains the highest frequency of CpG dinucleotides. Furthermore, it was considered important to examine a region encompassing the transcriptional start site and promoter sequence, accepting that the online tools determined that the majority of this region resided outside of the *14-3-3 σ* CpG island, since aberrant methylation in this region could have the most direct effect on gene expression. Three sets of bisulphite sequencing primers were designed to analyse the methylation status of *14-3-3 σ* in an area spanning approximately 700 base pairs (nt -242 to nt 431). Bisulphite PCR sequencing of this area *in vivo*, suggested that there were three regions which may be differently methylated (see 3.3.2 for more details). Figure 3.2 illustrates the three regions in relation to the transcriptional start site and CpG island of *14-3-3 σ* as determined by bioinformatic analysis. These three regions were denoted Region A, Region B and Region C respectively. Nested and hemi-nested primers were designed using MethPrimer (Table 2.2 and Appendix A). Inner primer positions are shown in Figure 3.2. 14-3-3sRegA5', 14-3-3RegA3', 14-3-3RegA3'2 and 14-3-3RegA5'nest

primers were used in a hemi-nested PCR to amplify a 376 and a 493 base pair region from nt -242 to nt 134 and nt -242 to nt 251 respectively, this allowed analysis of methylation in the upstream region of *14-3-3 σ* (similar to region 1 in Suzuki et al study) (2.4.4). Primers 14-3-3sRegB5', 14-3-3RegB3' and 14-3-3RegB3'nest (2.4.4) were also utilised in a hemi-nested PCR to amplify a 307 base pair region from nt 74 to nt 381 further downstream in the CpG rich coding region of *14-3-3 σ* . 14-3-3sRegC5', 14-3-3sRegC3', 14-3-3sRegC5'nest and 14-3-3sRegC3'nest (2.4.4) primers were used in a nested PCR to amplify a 204 base pair region from nt 227 to nt 431 to analyse methylation further downstream from Region B. Primer sets were designed to overlap to ensure that the methylation status of each individual CpG dinucleotide could be determined.

For colorectal cancer cell line, colorectal tumour and normal mucosa DNAs, ~500ng was bisulphite treated as described in 2.4.1 and then used for amplification with the Platinum Taq PCR kit (2.4.3). Direct sequencing of the PCR products was carried out as described in 2.4.7 and the sequence data analysed for methylated CpG dinucleotides as described in 2.4.9. Each sequencing chromatogram was assessed for background noise and full conversion of the DNA following bisulphite treatment by analysing relevant controls and verifying the conversion of non-CpG associated cytosine residues to thymine residues in each sequence. Bisulphite sequencing was also performed in triplicate for some samples in order to unambiguously determine the methylation status of individual CpG dinucleotides. The numbers of colorectal cancer cell lines, tumours and corresponding normal mucosa samples that were investigated for each of the defined regions are outlined in subsequent sections of this chapter for clarity.

Six colorectal tumours, and one colonic normal mucosa sample and three skin tissue samples from non-colorectal cancer individuals were analysed for *14-3-3 σ* methylation in Regions A and B by bisulphite sequencing individual clones. PCR products were cloned into TA vectors as described in 2.5.1. Using the M13F and M13R primers each bacterial colony was directly amplified as described (2.4.3). PCR products from clones with the correct size inserts were subsequently sequenced

and analysed for methylated CpG dinucleotides as described in 2.4.9 and as above. Data analysis consisted of plotting CpG dinucleotides for each clone and calculating the total percentage which were methylated for each sample.

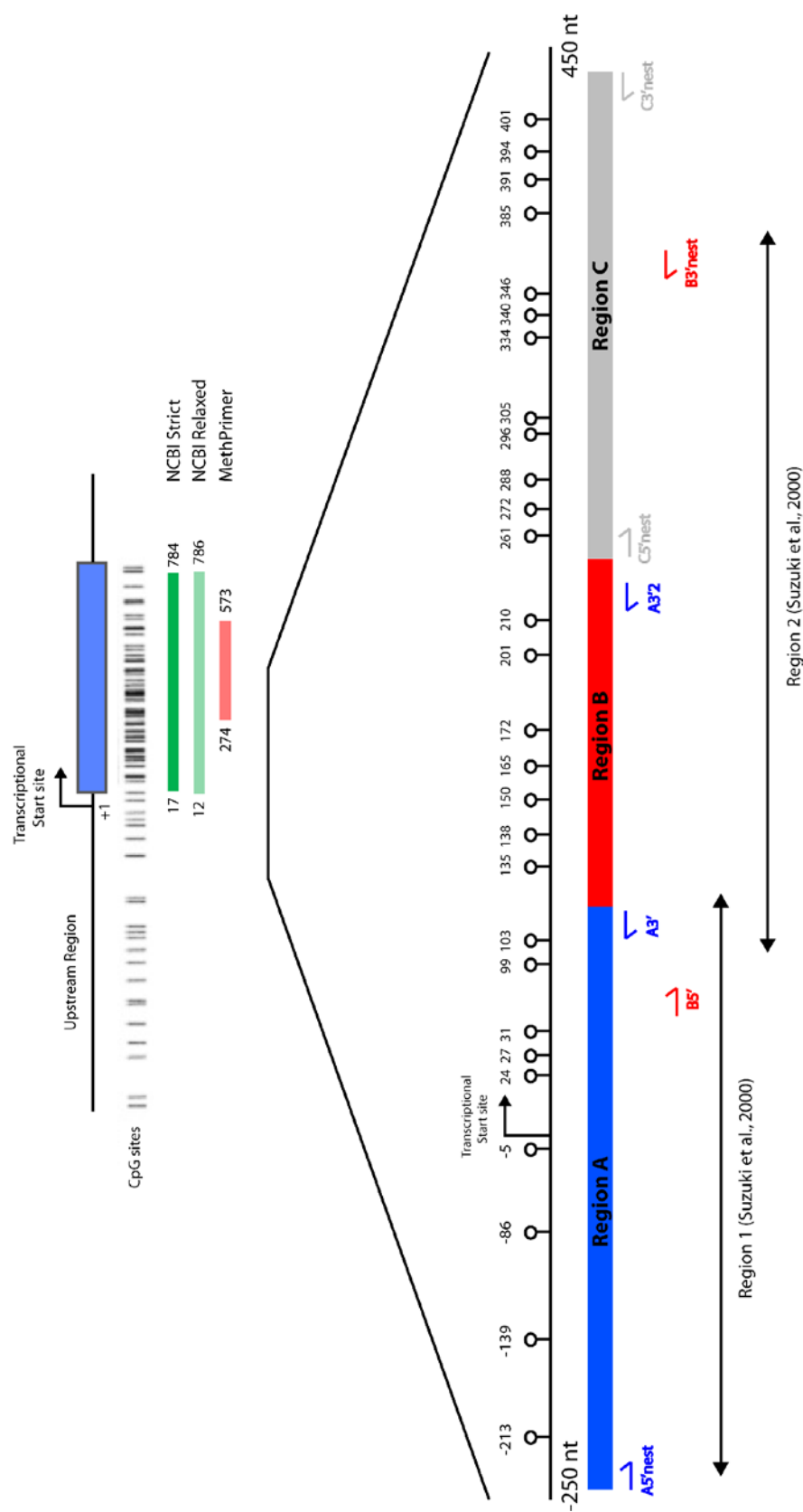


Figure 3.2: Region of 14-3-3 σ CpG island and upstream region analysed for methylation. Exon 1 of 14-3-3 σ is indicated by a solid blue box. Transcriptional start site and the positions of CpG islands as determined by bioinformatic algorithms are shown. Individual CpG dinucleotides are represented by vertical black lines in the top diagram and as "lollipops" in the diagram below. The three regions defined from *in vivo* methylation analysis are indicated below. Annotated 14-3-3 σ Reg bisulphite sequencing inner primers utilised to analyse methylation status of 14-3-3 σ are shown. Regions analysed by Suzuki et al (Region 1 & Region 2) are also shown (diagram not to scale).

3.2.3 MSP analysis of colorectal cancer cell lines

500ng colorectal cancer cell line DNA was bisulphite treated as described (2.4.2) and analysed by MSP using primers that covered CpG sites 135, 138, 201 and 210 in the 5' region of the *14-3-3 σ* CpG island (Figure 3.2). MSP reactions were carried out as described (2.4.3) to generate 105 base pair and a 107 base pair unmethylated and methylated products respectively, which were separated by gel electrophoresis to differentiate methylated from unmethylated *14-3-3 σ* 5' regions (2.4.5). Densitometric analysis was performed as described (2.4.3).

3.2.4 Statistical analysis

Significant difference in the percentage of methylated CpG dinucleotides between *14-3-3 σ* methylated and unmethylated colorectal tumours (previously determined by bisulphite PCR sequencing), were examined using non-parametric Mann Whitney tests as described in 2.10.1. The cut-off for significance was taken at 5% ($p < 0.05$).

The relationship between *14-3-3 σ* Region A methylation status in colorectal tumours and patient clinicopathological variables (gender, age, site of tumour, AJCC stage and presence of synchronous cancer) was assessed to determine any associations. Fishers exact test, unpaired t-test and Chi-squared tests were used as appropriate. The null hypothesis was rejected at the 5% level ($p < 0.05$). Correction for multiple testing was not appropriate, as none of the variables were statistically significantly associated with *14-3-3 σ* Region A methylation.

3.2.5 Colorectal cancer cell lines

DNA was purified from the following cell lines: HCT116, HT29, SW480 & Colo320DM as described in 2.2.1. Other colorectal cancer cell line DNA samples (HRT18, SW48, Caco-2, LoVo & SW620) were available directly from laboratory stocks.

3.2.6 Patient samples

Colonic normal mucosa tissue (NM) and tumour (T) samples from colorectal cancer patients, and skin tissues (skin A, skin B and skin C) from non-colorectal cancer

patients, were used for analysis and presented in this chapter. DNA was purified from fresh samples as described in 2.2.1. Other DNA samples were available directly from laboratory stocks, or directly from an external source (normal colonic mucosa from a cancer free patient, (Zyagen)).

3.3 Results

3.3.1 *14-3-3 σ* methylation analysis of colorectal cancer cell lines

Methylation-specific PCR (MSP) was first carried out on 9 colorectal cancer cell lines: SW480, Colo320DM, HT29, HCT116, Caco-2, LoVo, HRT18, SW48 and SW620 to determine the methylation status of *14-3-3 σ* . The MSP primers anneal to CpG dinucleotides 135 & 138 and 201 & 210 residing in Region B. MSP analysis showed that 78% (7/9) cell lines were unmethylated in this region (Figure 3.3). This was observed by the presence of amplified products in unmethylated-specific PCR reactions and little or no amplification in the methylated-specific PCR reactions. In addition, densitometric analysis showed higher intensity levels for unmethylated-specific PCR reactions compared to methylated-specific PCR reactions (Table 3.1). Conversely, amplification of PCR products in methylated-specific PCR reactions (high densitometric intensity) and little or no amplification in the unmethylated-specific PCR reactions (low densitometric intensity) are shown for two methylated colorectal cancer cell lines SW480 and Colo320DM.

14-3-3 σ methylation in the colorectal cancer cell lines was investigated further by bisulphite PCR sequencing. Bisulphite sequencing demonstrated that 7 of 9 cell lines were unmethylated in the upstream promoter region (Region A) of the *14-3-3 σ* CpG island. Figure 3.4 (A) shows sequencing chromatograms for two Region A unmethylated cell lines (HCT116 and HT29) and two Region A methylated cell lines (Colo320DM and SW480). HCT116 and HT29 cell lines were also completely unmethylated further downstream in the 5' region of the *14-3-3 σ* CpG island (Regions B & C) (Figure 3.4 (B) & (C)) and cell lines Colo320DM and SW480 were fully methylated further downstream (Figure 3.4 (B) & (C)). A summary of the methylation profile of the three regions in *14-3-3 σ* for each colorectal cancer cell line is illustrated in Figure 3.5.

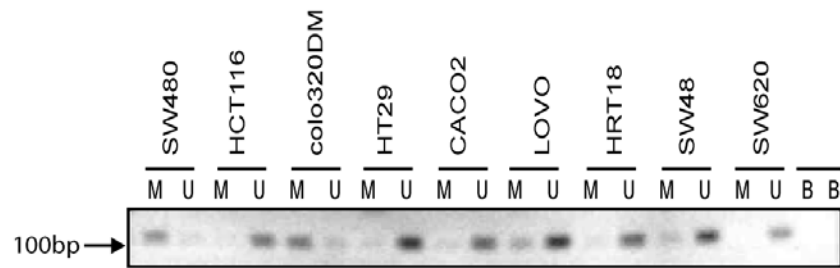


Figure 3.3: MSP analysis of 14-3-3 σ methylation in colorectal cancer cell lines. 2/9 cell lines (SW480 and Colo320DM) were methylated. M = methylated specific reactions, U = unmethylated specific reactions, B = blank PCR reactions.

Cell line	M Intensity	U Intensity
SW480	86.17	27.58
HCT116	11.55	108.34
Colo320DM	84.81	13.61
HT29	16.61	147.22
CACO2	18.60	132.04
LOVO	79.64	190.96
HRT18	23.70	108.20
SW48	27.45	143.48
SW620	11.29	80.68

Table 3.1: Densitometric analysis of MSP products from colorectal cancer cell lines. 2/9 cell lines (SW480 and Colo320DM) were methylated. M = methylated specific reactions, U = unmethylated specific reactions.

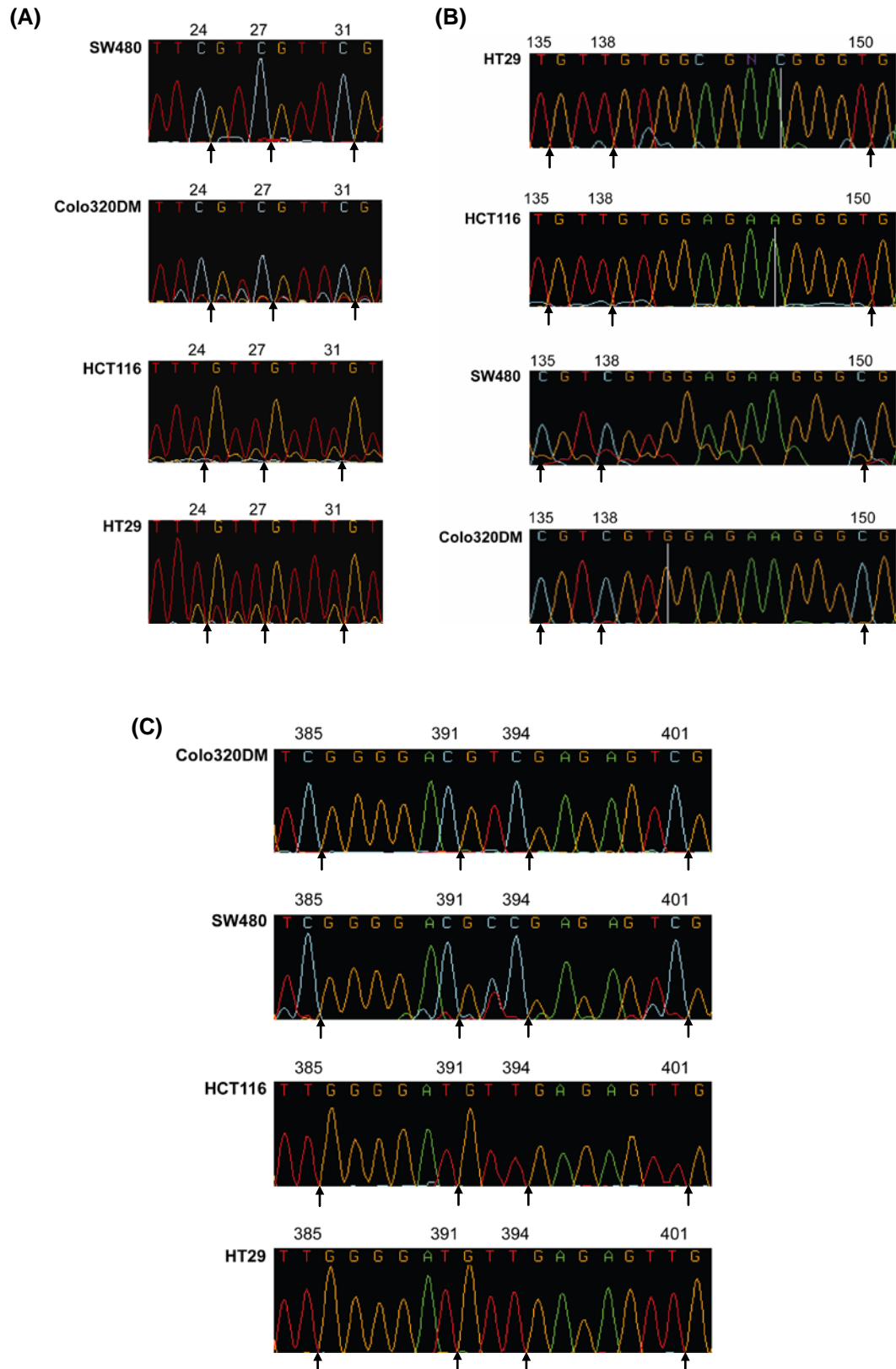


Figure 3.4: 14-3-3 σ methylation analysis of colorectal cancer cell lines in (A) upstream promoter region (Region A) (nts 24, 27, & 31) (B) 5' CpG island (Region B) (nts 135, 138 & 150) and (C) further downstream in 5' CpG island (Region C) (385, 391, 394 & 401) using bisulphite sequencing directly from PCR products. Chromatograms show universal methylation status across the three regions: SW480 and Colo320DM 14-3-3 σ methylated cell lines, HT29 and HCT116 unmethylated cell lines. Arrows indicate CpG dinucleotides.

Colorectal Cancer Cell Line methylation status at individual CpG sites

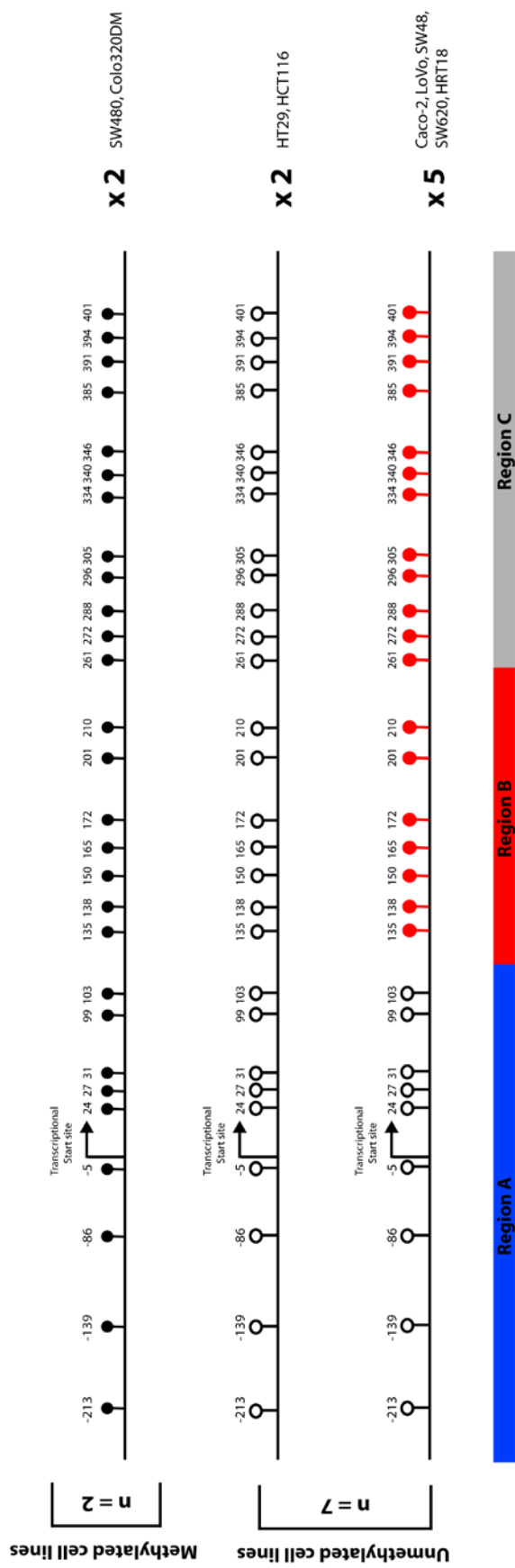


Figure 3.5: Summary of bisulphite PCR sequencing data obtained from methylation analysis of 14-3-3 σ in colorectal cancer cell lines. Transcriptional start site and differently methylated regions A, B & C are indicated. CpG dinucleotides are represented by "lollipops".

3.3.2 *14-3-3 σ* methylation analysis of colorectal tumour samples

The upstream region of *14-3-3 σ* (Region A; nt -242 to nt 134) was first analysed for methylation in a small number of colorectal tumour samples (n =12). Contrary to expectation, bisulphite PCR sequencing analysis revealed that 83% (10/12) of tumour samples were methylated in the upstream promoter region of *14-3-3 σ* . In some tumour samples, both cytosine and thymine peaks were present at the CpG sites. However, cytosine peaks were always higher in the chromatograms compared to the corresponding thymine peak suggesting that the region is methylated. Figure 3.6 (A) shows bisulphite sequencing chromatograms from tumour sample (KR2T), which is unmethylated in the upstream region of *14-3-3 σ* and tumour sample (KR6T), which is methylated in the upstream region. In the unmethylated *14-3-3 σ* upstream region tumours, cytosine peaks were minimal in height or completely absent at CpG sites. In the methylated tumour sample KR6T there appears to be some background noise in the sequencing chromatogram, however this is negligible compared to the peak heights of the methylated cytosine residues at the individual CpG sites. Methylation analysis of a selection of these tumour samples further downstream, in the 5' region of the *14-3-3 σ* CpG island (Region B; nt 74 to nt 381), demonstrated that all tumour samples exhibited both cytosine and thymine peaks of equal heights at the majority of CpG dinucleotides (n =6). This is shown in the bisulphite sequencing chromatograms for tumour samples KR2T and KR6T (Figure 3.6 (B)). The occurrence of cytosine and thymine peaks of equal heights at individual CpG sites may be due to heterogeneity within the tumour sample. This will be discussed in more detail in later sections of the chapter. Bisulphite sequence analysis further downstream at a region corresponding to nt 227 to nt 431 (Region C) in a number of tumour samples demonstrated that all of the tumour samples (n =10) were methylated at CpG sites. Bisulphite sequencing chromatograms from tumour samples KR2T and KR4T are shown in Figure 3.6 (C). In this region, a mixture of cytosine and thymine peaks at CpG sites are often observed, however the cytosine peaks at the CpG sites were always of full height and higher than the corresponding thymine peak suggesting that this region of *14-3-3 σ* is methylated in the tumours examined. Overall, these results show that the upstream promoter region of *14-3-3 σ* is differentially methylated in individual tumour samples and regions further

downstream in the 5' region of the CpG island are universally methylated or contain a mixture of both methylated and unmethylated CpG sites (hemi-methylated). As only the upstream promoter region of *14-3-3 σ* was found to be differentially methylated between individual tumours, it was decided to examine the *14-3-3 σ* methylation status in this region in a larger set of tumour samples. A total of 99 colorectal tumours were examined by bisulphite sequencing and 90% (89/99) were methylated. A summary of the methylation data for each region and each tumour sample analysed by bisulphite sequencing is illustrated in Figure 3.7.

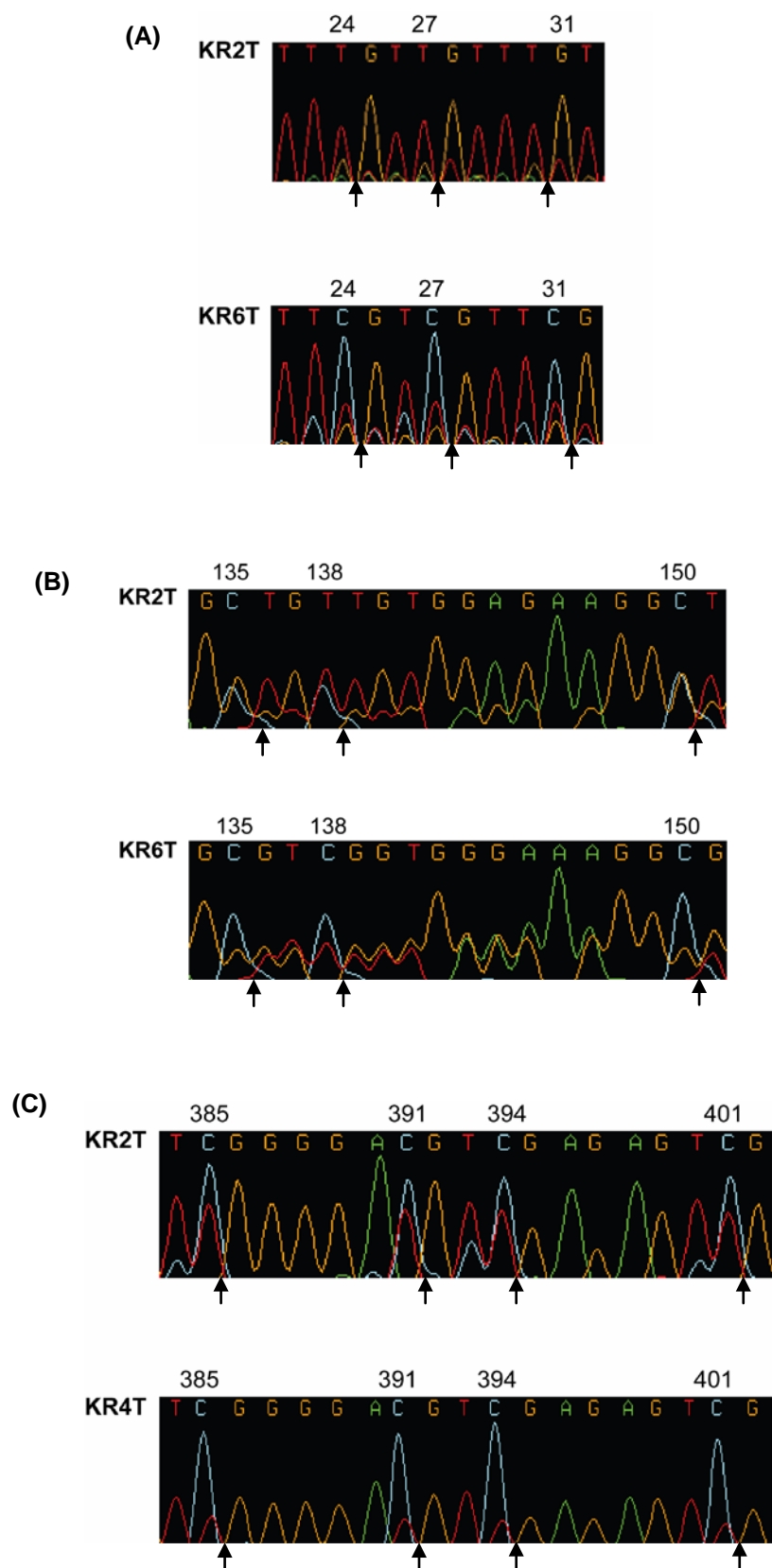


Figure 3.6: 14-3-3 σ direct PCR bisulphite sequencing analysis of colorectal tumours in (A) upstream region: Region A (nt -242 to nt 134) (CpG sites 24, 27, & 31) (B) 5' region of CpG island: Region B (nt 74 to nt 381) (CpG sites 135, 138 & 150) and (C) Region further downstream: Region C (nt 227 to nt 431) (CpG sites 385, 391, 394 & 401). Differential methylation is shown in the upstream region with KR2T unmethylated and KR6T methylated. The two regions further downstream were universally methylated or hemi-methylated. Arrows indicate CpG dinucleotides.

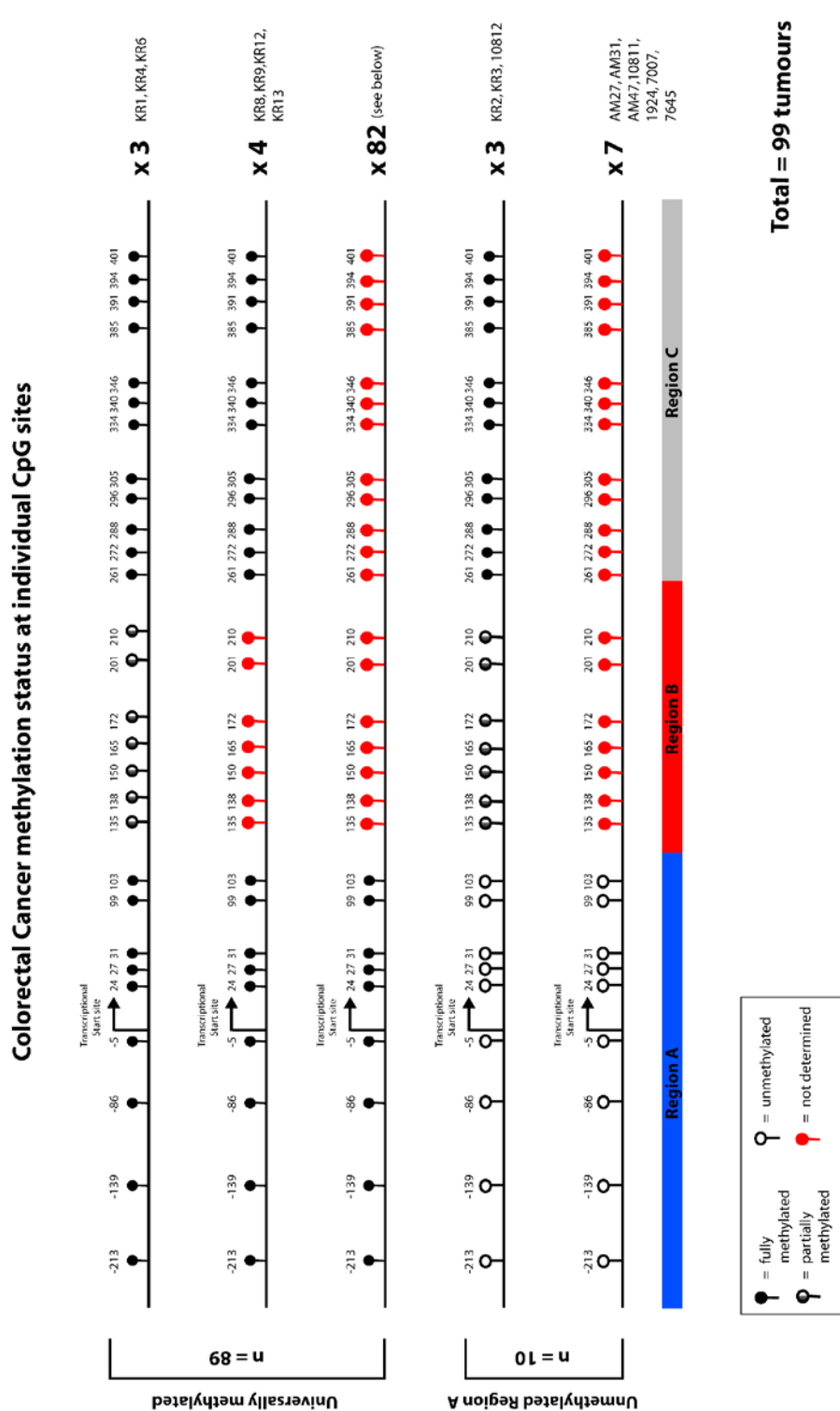


Figure 3.7: Summary of direct bisulphite PCR sequencing data obtained from methylation analysis of 14-3-3 σ in colorectal tumours. Transcriptional start site and regions A, B & C, each analysed separately by PCR bisulphite sequencing are indicated. CpG dinucleotides are represented by "lollipops". 82 colorectal tumours analysed and methylated in Region A include: KR7T, KR10T, KR11T, 2867, 5123, 7329, 7867, 8117, 7716, 6470, 5731, 7862, 7903, 3841, 10512, 3691, 10818, 7962, 1736, 2109, 1745, 2213, 3486, 4123, 1950, 1951, 3264, 5372, 7226, 7988, 3814, 6843, 5741, 7478, 7643, 10202, 7324, 4134, 6766, 5383, 7515, 3752, 6314, 7514, 10107, 2902, 5469, 7219, AM1, AM3, AM4, AM5, AM6, AM7, AM8, AM10, AM11, AM13, AM14, AM15, AM16, AM17, AM18, AM20, AM22, AM23, AM24, AM28, AM29, AM30, AM32, AM33, AM36, AM38, AM39, AM41, AM42, AM43, AM45, AM46, AM52 & 2533.

Methylation analysis from the direct sequencing of PCR products demonstrated that 90% of colorectal tumours were methylated in the upstream promoter region (Region A) of *14-3-3σ*. Bisulphite sequencing analysis carried out directly from PCR amplified products is useful in that the average level of methylation in the sample can be assessed and is good for screening purposes. However, bisulphite sequencing from clones provides methylation maps of single DNA strands from individual DNA molecules, and thus can be utilised for more detailed methylation analysis. Methylation in the upstream promoter region and 5' region of the *14-3-3σ* CpG island (CpG sites -5 to 172; encompassing CpG sites in both Regions A and B) was re-analysed in 3 colorectal tumours previously found to be unmethylated in Region A (KR2T, KR3T & 7645) and 3 colorectal tumours previously found to be methylated in Region A (KR4T, KR11T & KR12T). 288 colonies from each tumour sample were picked and inserts checked for size using M13 primers. All colonies containing the correct size insert (~700bp) were subsequently PCR amplified and sequenced directly. Bisulphite sequencing analysis demonstrated that there were a lower percentage of methylated CpG dinucleotides in the *14-3-3σ* unmethylated tumours KR2T, KR3T and 7645 (3.6%, 17.4% & 24.1% respectively) (Figure 3.8) compared to the previously found methylated tumours KR4T, KR11T and KR12T (29.8%, 45.9% & 46.9% respectively) (Figure 3.9) ($p = 0.05$, Mann Whitney test). Tumour samples 7645 and KR12T had similar methylation profiles (7645: 24.1% and KR12T: 29.8% methylated CpG sites), despite previous direct bisulphite sequencing analysis demonstrating that 7645 was unmethylated and KR12T was methylated in the *14-3-3σ* upstream promoter region (Region A). Thus, further bisulphite sequencing analysis from sequencing individual clones is needed to confirm these initial findings. However, overall, the sequencing analysis showed that the *14-3-3σ* methylated tumours have a clonal pattern of methylation where approximately half of the clones were methylated and half were unmethylated at CpG sites within the upstream region and 5' region of the *14-3-3σ* CpG island. In contrast, the majority of the clones sequenced from the *14-3-3σ* unmethylated tumours were unmethylated, which agrees with the previous methylation analysis obtained by direct sequencing.

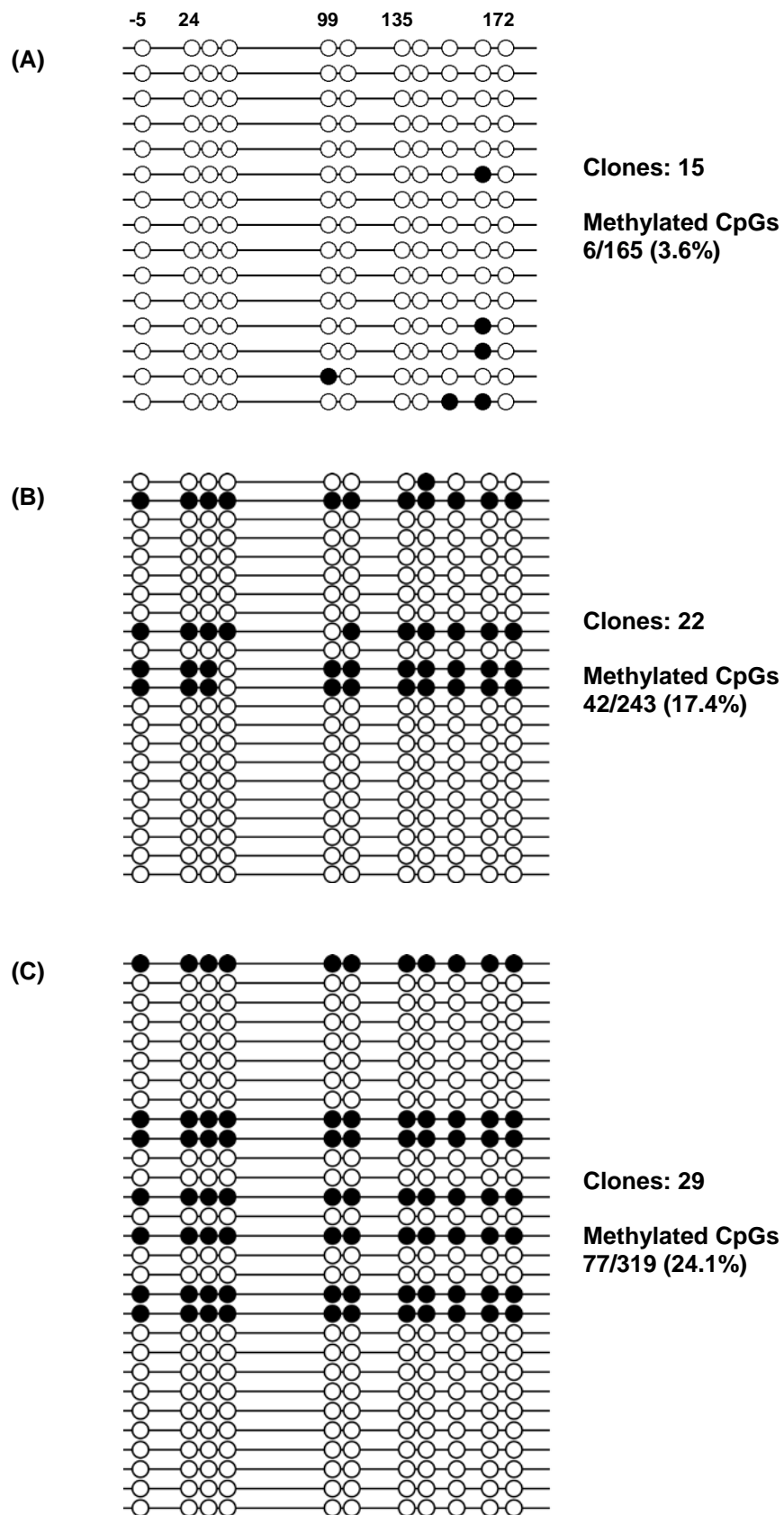


Figure 3.8: 14-3-3 σ methylation profile (CpG sites -5 to 172, encompassing CpG sites in both Regions A & B) in colorectal tumours (A) KR2T (B) KR3T & (C) 7645 previously found to be unmethylated by direct sequencing of PCR products. The number of clones analysed for each tumour sample are shown vertically and CpG dinucleotides (-5 to 172, 11 total, shown in profile (A) only) across Regions A & B of 14-3-3 σ are shown horizontally. Filled circles represent methylated CpG dinucleotides. Unfilled circles represent unmethylated CpG dinucleotides. Number of clones sequenced and total percentage of methylated CpG dinucleotides is indicated alongside each tumour sample.

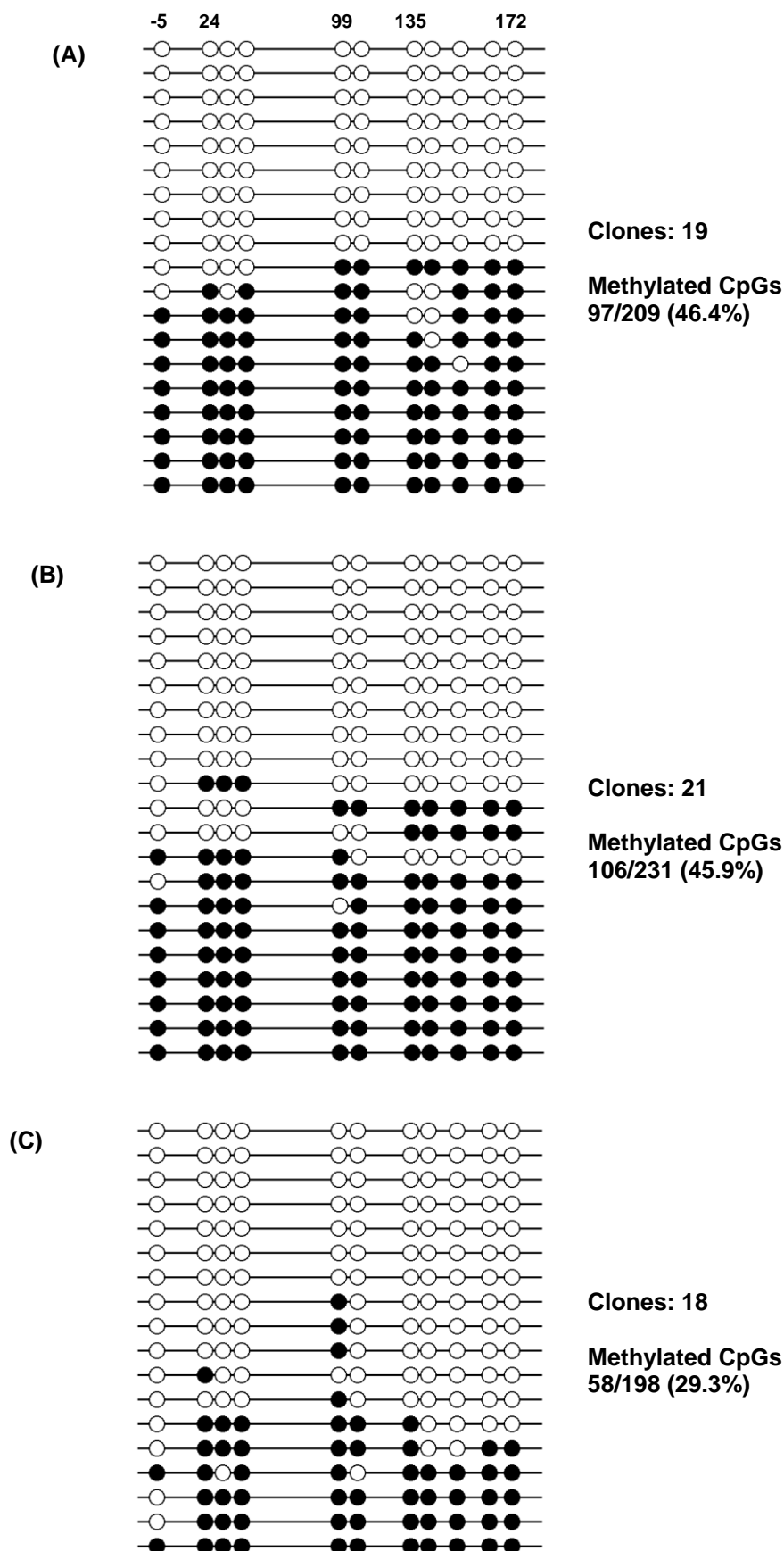


Figure 3.9: 14-3-3 σ methylation profile (CpG sites -5 to 172, encompassing CpG sites in both Regions A & B) in colorectal tumours (A) KR4T (B) KR11T & (C) KR12T previously found to be methylated by direct sequencing of PCR products. The number of clones analysed for each tumour sample are shown vertically and CpG dinucleotides (-5 to 172, 11 total, shown in profile (A) only) across Regions A & B of 14-3-3 σ are shown horizontally. Filled circles represent methylated CpG dinucleotides. Unfilled circles represent unmethylated CpG dinucleotides. Number of clones sequenced and total percentage of methylated CpG dinucleotides is indicated alongside each tumour sample.

3.3.3 Clinicopathological associations with Region A *14-3-3 σ* methylation status

Since the upstream promoter region (Region A) was differentially methylated in the 99 colorectal tumour samples analysed for methylation, associations between *14-3-3 σ* methylation status in this region and clinicopathological data was investigated using various statistical tests. There was no significant association between gender and Region A *14-3-3 σ* methylation status (Table 3.2, $p = 0.11$, Fishers Exact test). There was no significant difference in age and Region A *14-3-3 σ* methylation status (*14-3-3 σ* methylated Region A mean age = 63.9, *14-3-3 σ* unmethylated Region A mean age = 59.8, $p = 0.51$, unpaired T-test). There was no significant association between the site of tumour and Region A *14-3-3 σ* methylation status (Table 3.2, $p = 0.67$, Fishers Exact test). There was also no significant association with Region A *14-3-3 σ* methylation status and the presence of a synchronous cancer (Table 3.2, $p = 1$, Fishers Exact test). Finally, there was no significant association between *14-3-3 σ* Region A methylation status and the AJCC stage of cancer (Table 3.3, $p = 0.23$, Chi squared analysis). Overall, these results indicate that there is no significant association between Region A *14-3-3 σ* methylation status and clinicopathological data examined in this thesis. However, it must be emphasised that only relatively small number of tumours were examined. Hence, the power to detect associations may be limited.

	Methylated <i>14-3-3σ</i>	Unmethylated <i>14-3-3σ</i>	Total
Gender			
Male	53	3	56
Female	36	7	43
Site of tumour			
Left	40	6	46
Right	15	1	16
Synchronous cancers			
Yes	6	0	6
No	49	7	56

Table 3.2: There was no significant association between Region A *14-3-3 σ* methylation status and gender, location or cancer multiplicity.

AJCC	Methylated <i>14-3-3σ</i>	Unmethylated <i>14-3-3σ</i>	Total
1	8	2	10
2	15	4	19
3	26	1	27
4	3	0	3

Table 3.3: There was no significant association between Region A *14-3-3 σ* methylation status and AJCC stage of the tumour.

3.3.4 Lack of methylation in Region A is tumour-specific

To determine the specificity of *14-3-3 σ* methylation, bisulphite PCR sequencing analysis of all three regions was undertaken in corresponding fresh colonic normal mucosa samples. CpG dinucleotides were fully methylated in Region A (CpG sites -213 to 103) in 100% (10/10) normal mucosa samples analysed by bisulphite sequencing (Figure 3.10 (A)). Further downstream in Region B (CpG sites 135 to 210), the chromatograms showed both thymine and cytosine peaks of equal height at each CpG dinucleotide suggesting that Region B in normal mucosa is hemi-methylated (n =3) (Figure 3.10 (B)). Bisulphite sequencing analysis of *14-3-3 σ* further downstream again in Region C (CpG sites 261 to 401) in 10 normal mucosa samples demonstrated that all samples were fully methylated (Figure 3.10 (C)). In contrast to the minority of tumours (10%) in which there was complete loss of methylation at CpG sites -213 to 103 (Region A), tumours that were unmethylated in Region A (KR2T and KR3T), both corresponding normal mucosa samples were fully methylated in this region. Thus, the observed effect appears tumour-specific. A summary of the methylation profile for each normal mucosa sample in the three different regions is illustrated in Figure 3.11.

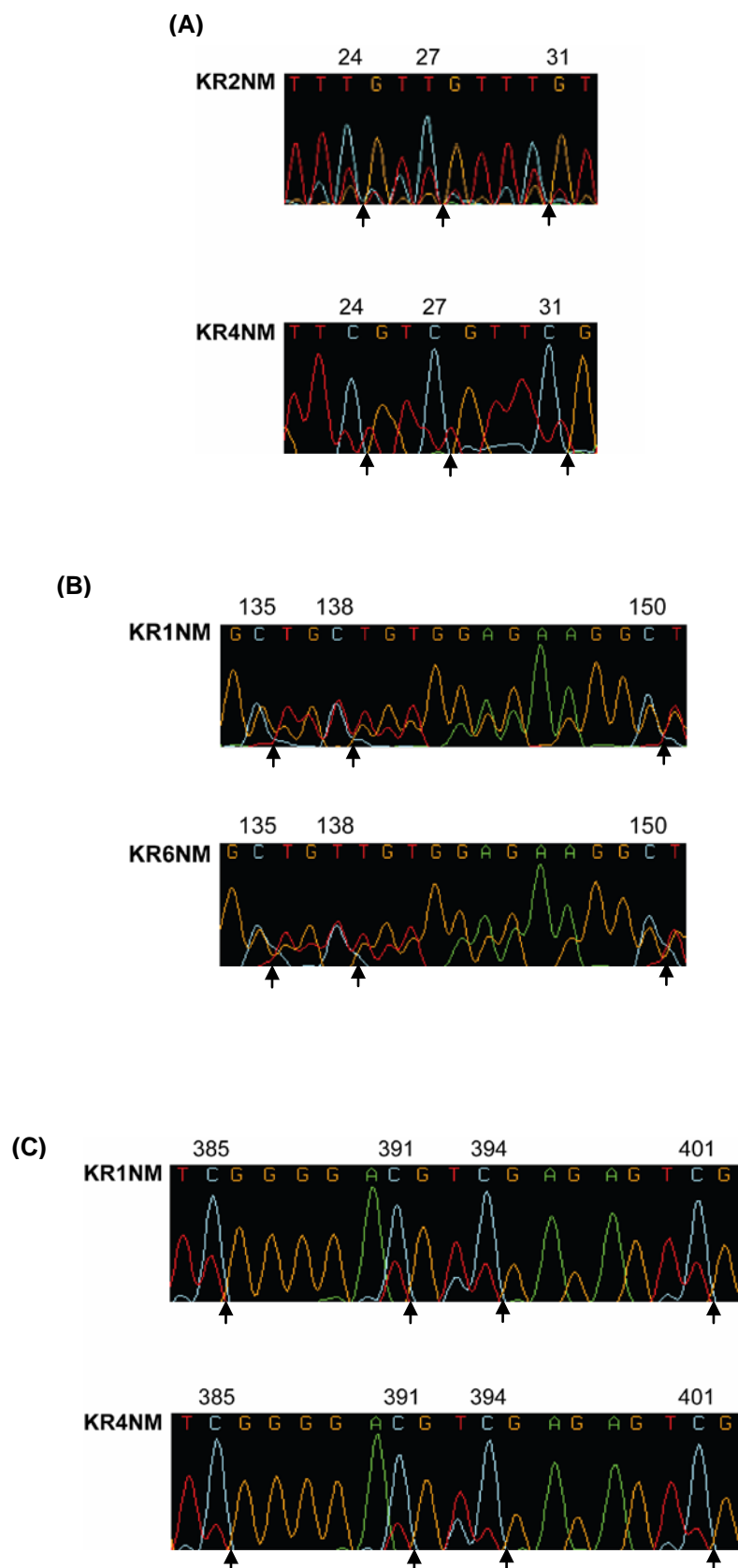


Figure 3.10: 14-3-3 σ methylation analysis of (A) Region A (nts 24, 27, & 31) which was methylated (B) Region B (nts 135, 138, 150) which was hemi-methylated and (C) Region C (385, 391, 394 & 401) which was methylated in normal mucosal samples using direct PCR bisulphite sequencing. Arrows indicate CpG dinucleotides.

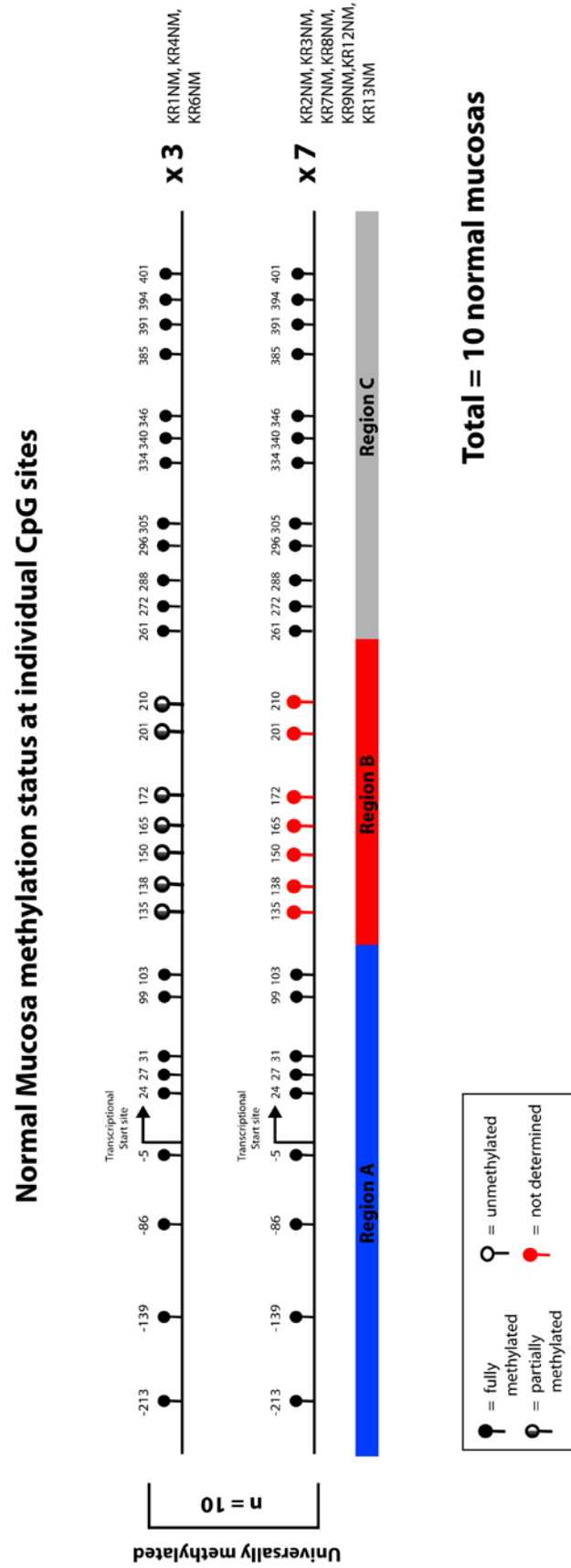


Figure 3.11: Summary of bisulphite PCR sequencing data obtained from methylation analysis of 14-3-3 σ in corresponding normal mucosa samples. Transcriptional start site and differently methylated regions A, B & C are indicated. CpG dinucleotides are represented by "lollipops".

3.3.5 14-3-3 σ Region A methylation analysis in normal tissues from non-cancer subjects

14-3-3 σ methylation analysis in corresponding normal mucosa tissue showed that all CpG dinucleotides within the upstream promoter region (Region A: CpG sites -213 to 103) were methylated. Bisulphite sequencing analysis was carried out directly from PCR amplified products, thus it was decided to analyse the methylation status of Region A 14-3-3 σ methylation status further by bisulphite sequencing individual clones. Normal colonic tissue from a non-colorectal cancer patient was analysed, and for comparison three skin tissues were also analysed for Region A 14-3-3 σ methylation.

288 colonies from normal colon tissue and 288 for each of the three skin samples were picked and inserts checked for size using M13 primers and PCR amplification. All colonies containing the correct size insert (~700bp) were sequenced directly. Figure 3.12 shows the degree of methylation in normal colon across Region A (nt -213 to nt 103) at individual CpG dinucleotide sites. Figure 3.12 demonstrates that in the normal colonic tissue, clones were methylated at most CpG dinucleotides within the analysed region (85.2%). In comparison, there were a lower number of methylated CpG dinucleotides in the skin tissue samples A, B and C (48.4%, 55.6% & 45.9% respectively) (Figure 3.13, 3.14 & 3.15 respectively). These results indicate that Region A of 14-3-3 σ is methylated in the normal colon, confirming the previous bisulphite sequencing analysis (3.3.4), and there were lower levels of methylation in the skin tissue compared to normal colonic mucosa, as approximately half of the CpG dinucleotides were methylated and half were unmethylated in all three skin tissues that were analysed.

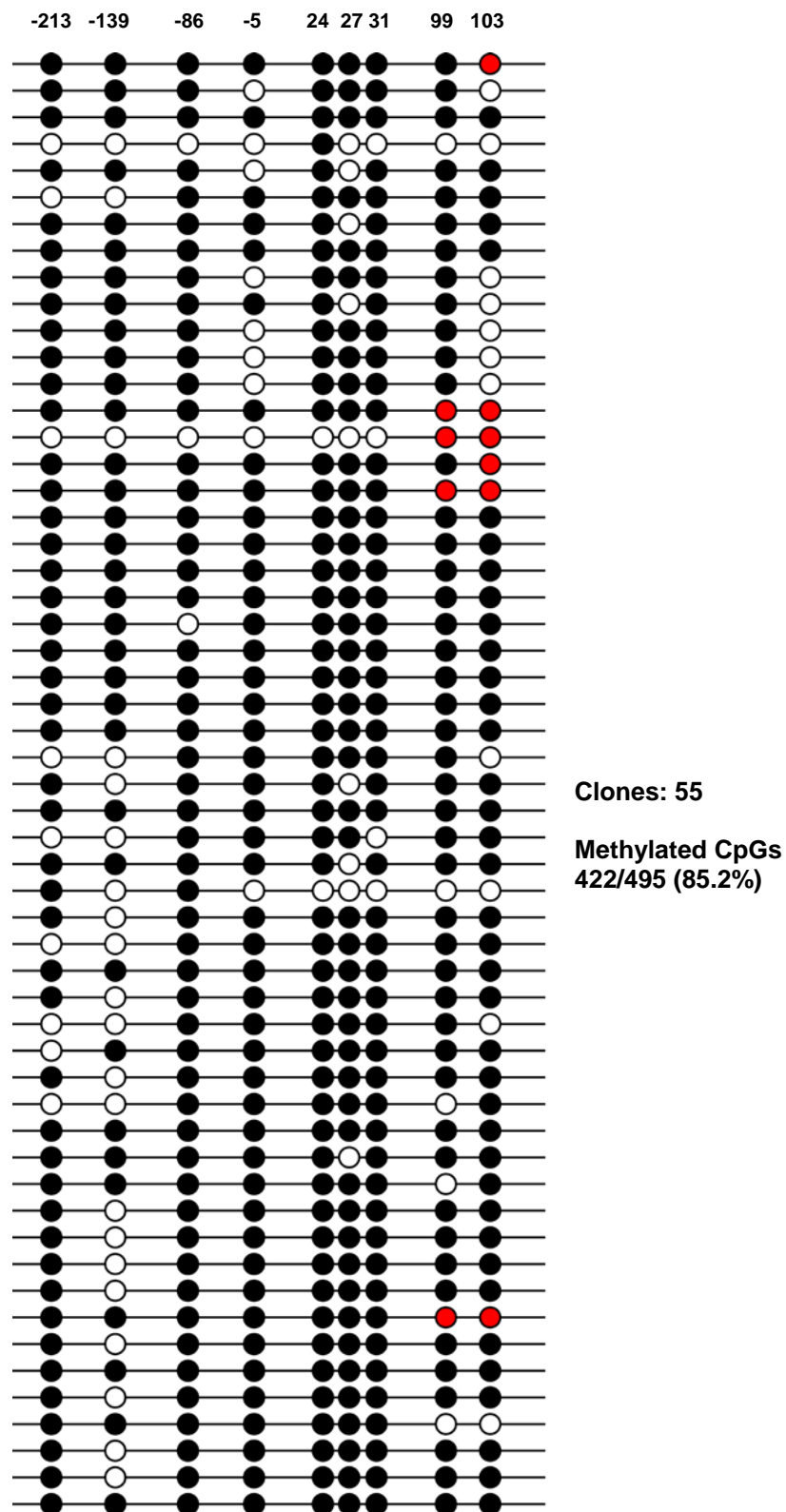


Figure 3.12: 14-3-3 σ methylation profile in normal colonic mucosa from a non-colorectal cancer patient. The number of clones analysed is shown vertically and CpG dinucleotides (Region A; nt -213 to 103, 9 total) are shown horizontally. Filled circles represent methylated CpG dinucleotides. Unfilled circles represent unmethylated CpG dinucleotides. Red circles represent undetermined methylation status due to the end of the run of sequencing. The number of clones sequenced and total percentage of methylated CpG dinucleotides is indicated alongside the methylation profile.

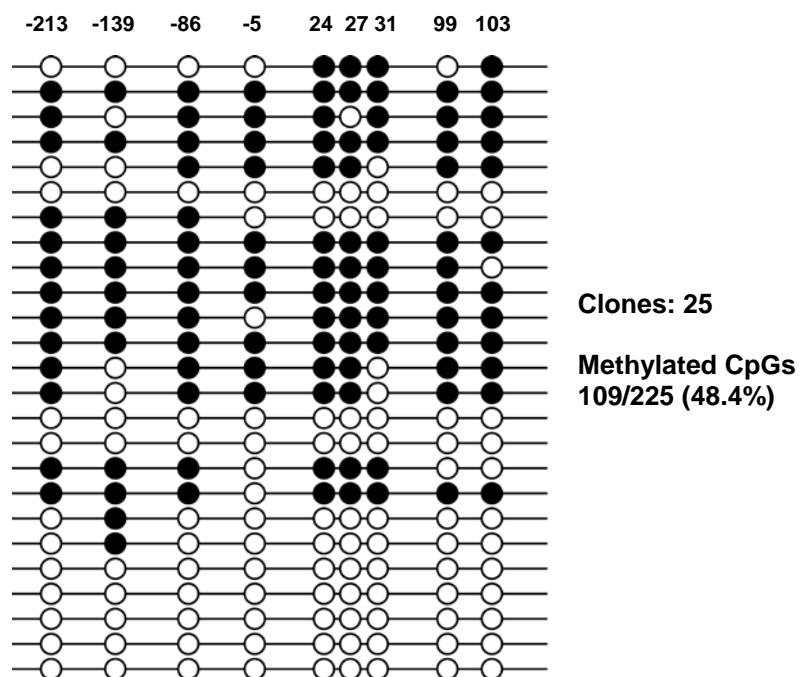


Figure 3.13: $14\text{-}3\text{-}3\sigma$ methylation profile in skin tissue sample A from a non-colorectal cancer patient. The number of clones analysed is shown vertically and CpG dinucleotides (Region A; nt -213 to 103, 9 total) are shown horizontally. Filled circles represent methylated CpG dinucleotides. Unfilled circles represent unmethylated CpG dinucleotides. Number of clones sequenced and total percentage of methylated CpG dinucleotides is indicated alongside the methylation profile.

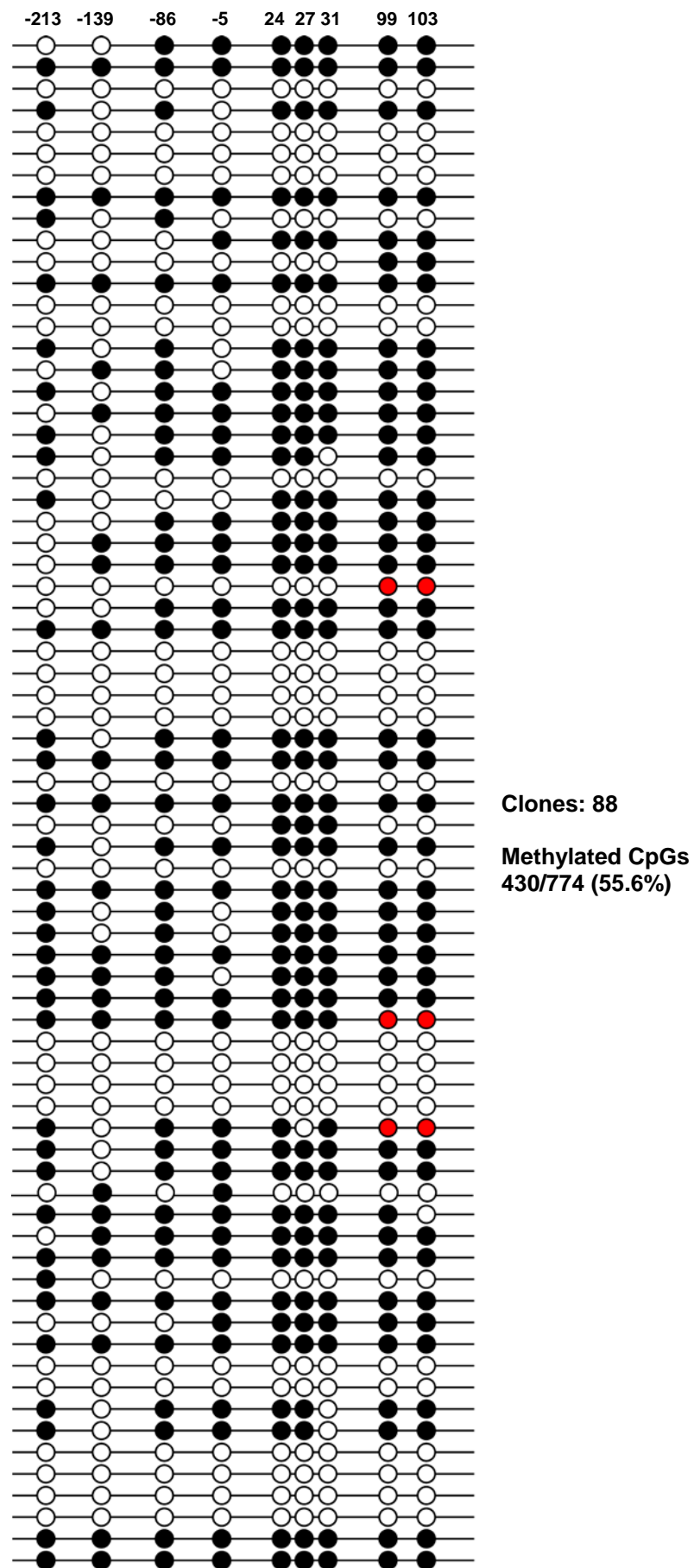


Figure 3.14: 14-3-3 σ methylation profile in skin tissue sample B from a non-colorectal cancer patient. The number of clones analysed is shown vertically and CpG dinucleotides (Region A; nt -213 to 103, 9 total) are shown horizontally. Filled circles represent methylated CpG dinucleotides. Unfilled circles represent unmethylated CpG dinucleotides. Number of clones sequenced and total percentage of methylated CpG dinucleotides is indicated alongside the methylation profile.

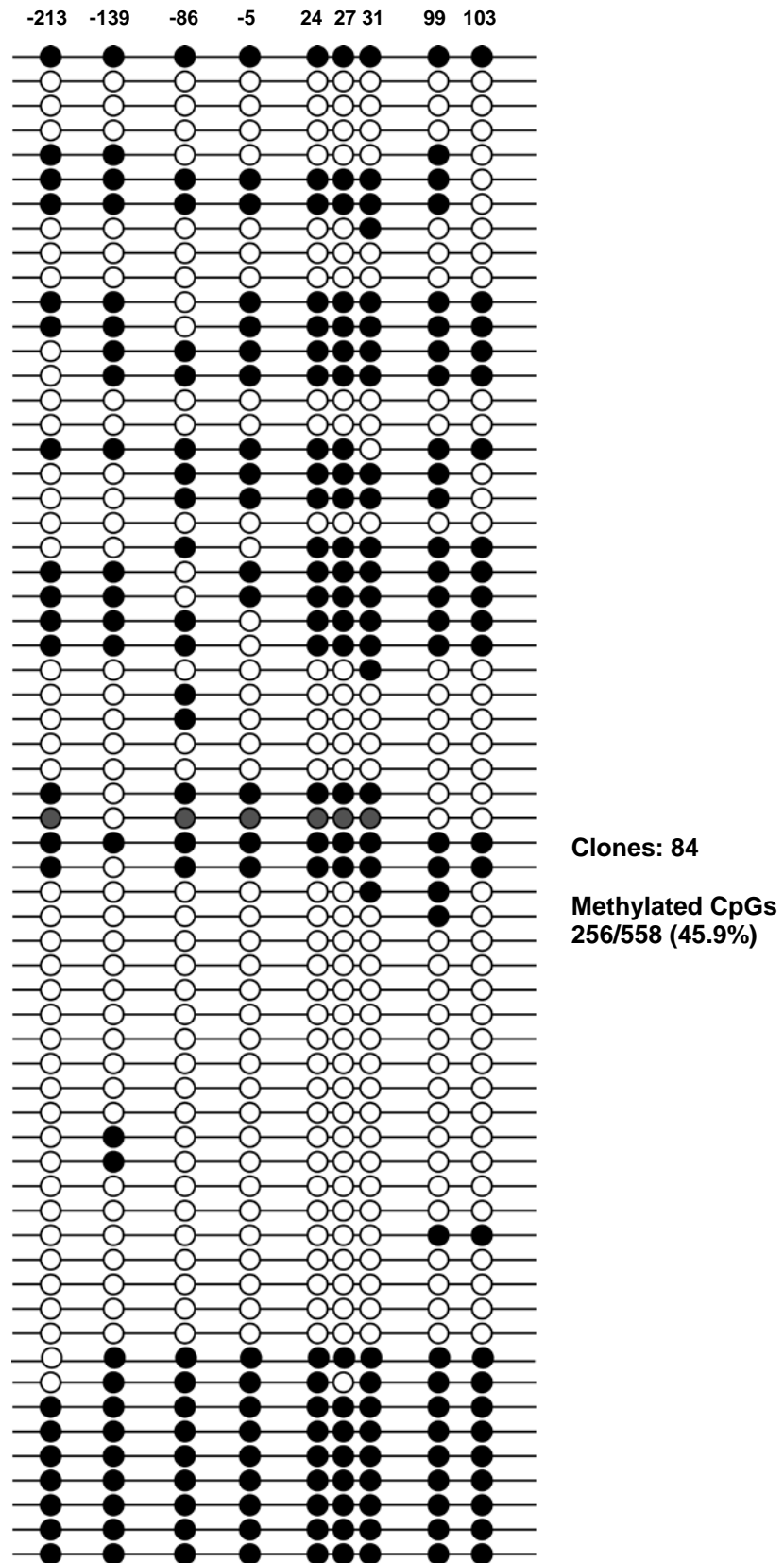


Figure 3.15: 14-3-3 σ methylation profile in skin tissue sample C from a non-colorectal cancer patient. The number of clones analysed is shown vertically and CpG dinucleotides (Region A; nt -213 to 103, 9 total) are shown horizontally. Filled circles represent methylated CpG dinucleotides. Unfilled circles represent unmethylated CpG dinucleotides. Number of clones sequenced and total percentage of methylated CpG dinucleotides is indicated alongside the methylation profile.

3.4 Discussion

Research investigating the role of *14-3-3 σ* methylation in colorectal cancer has been limited and in the few studies carried out, tumour-specificity of aberrant *14-3-3 σ* methylation in colorectal cancer was not fully investigated. Therefore, my aims for this chapter were to analyse *14-3-3 σ* methylation status in a series of colorectal cancer cell lines, colorectal tumours and corresponding colonic normal mucosa tissues. From using online tools and taking into account previous published results, I decided to analyse a region spanning approximately 800 base pairs, which encompassed the upstream promoter region of the gene and the 5' region of the *14-3-3 σ* CpG island. This region was mainly analysed by bisulphite sequencing to examine region-specific methylation and investigate whether differential methylation of *14-3-3 σ* plays a role in colorectal carcinogenesis. To further examine the specificity of *14-3-3 σ* methylation in colorectal cancer, I also examined methylation in the upstream promoter region of the gene and in the 5' region of the CpG island in colonic mucosa tissue and skin tissues from individuals free of cancer.

As discussed in section 3.2.2, the *14-3-3 σ* CpG island is unusual as almost all of the CpG island resides in the exon rather than localised to the upstream promoter region of the gene. However, a recent study found that a large proportion of CpG islands are either inter- or intragenic and that these particular CpG islands were preferentially susceptible to methylation (Illingworth et al, 2008). This is interesting as the *14-3-3 σ* CpG island is methylated in some cell types and tissues (Oshiro et al, 2005). Therefore, it may be that the *14-3-3 σ* CpG island belongs to this subset of methylated intragenic CpG islands.

In contrast to colorectal tumour tissue, analysis of colorectal cancer cell lines revealed that 78% (7/9) were unmethylated in the upstream promoter region (Region A) of *14-3-3 σ* . Analysis of Regions B and C in colorectal cancer cell lines unmethylated in Region A also indicated that CpG dinucleotides are unmethylated further downstream in the CpG island. Bisulphite PCR sequencing of *14-3-3 σ* in SW480 and Colo320DM colorectal cancer cell lines showed that all CpG sites were

fully methylated in all three regions examined. These results demonstrate that the methylation status of *14-3-3σ* in the majority of colorectal cancer cell lines is very different to the methylation status of the majority of colorectal tumours and normal mucosa samples. There is also a difference in the distribution of methylated or unmethylated CpG dinucleotides across the upstream region and the 5' region of the *14-3-3σ* CpG island. The methylation profile of *14-3-3σ* in the cell lines is uniform across the upstream promoter region and the 5' CpG island, unlike in fresh colorectal tumours in which the peak heights of methylated CpG sites varied across the regions. The differences observed may be due to the heterogeneity of cells in the tumour samples compared to the population of cells in the cell lines. The tumour samples will consist of an admixture of cell types whereas the cell lines will consist of a homogenous cell population. The heterogeneity of the tissues examined in this thesis and its implications on the data that I have presented will be discussed in more detail throughout this section. It must also be considered that the cell lines may not be closely related to their primary tumours from which they originated from. For example, the epigenetic changes in the colorectal cancer cell lines may be induced by cell culture. Methylation profiling in cancer cell lines has however shown that they generally have higher levels of CpG island hypermethylation than primary tumours (Paz et al, 2003; Suter et al, 2003). This suggests that in the colorectal cancer cell lines, *14-3-3σ* may have escaped this “induction”.

Methylation analysis of *14-3-3σ* in colorectal tumours by bisulphite PCR sequencing demonstrated that there may be three distinct regions of methylation. It is recognised however, that each of these regions were sequenced separately and so they cannot be directly linked. Region A (CpG sites -213 to 103) had variable methylation status between individual tumour samples. 90% (89/99) of colorectal tumours were methylated and 10% were unmethylated in the upstream region. All tumours examined for methylation in the two regions further downstream were either hemi-methylated (Region B, CpG sites 135 to 210) or fully methylated (Region C, CpG sites 261 to 401). As mentioned above, the occurrence of both cytosine and thymine peaks at CpG sites in Region B may be due to tumour heterogeneity. However, it must also be considered that the observed ‘hemi-methylation’ could be a

result of differences in the efficiencies of the PCR or sequencing reactions. This is discussed in more detail below.

Following the initial analysis of *14-3-3 σ* methylation in a small number of tumours, I decided it was important to concentrate primarily on the upstream promoter region of *14-3-3 σ* , as this was the only region in which the bisulphite PCR sequencing data suggested that there could be differential methylation between individual tumour samples. However, *14-3-3 σ* methylation analysis further downstream in the 5' CpG island region (Regions B & C) also in a larger dataset is required in order to fully determine the methylation profile across the CpG island and confirm the preliminary sequencing data that was carried out. Furthermore, the algorithms calculated that the *14-3-3 σ* CpG island is 800 base pairs, therefore it would be interesting to analyse the methylation status of CpG sites downstream from Region C, across the entire CpG island. The majority of *14-3-3 σ* methylation analysis was performed by bisulphite sequencing directly from PCR products. Direct sequencing is advantageous in that it can assess the average level of methylation in a given sequence as a pool of PCR products are sequenced rather than single DNA strands. As well as providing the overall level of methylation, direct sequencing can introduce less bias compared to sequencing individual clones and is a useful method for rapid screening. Conversely, bisulphite sequencing of single clones is utilised for more detailed analysis and to determine methylation maps of CpG islands. This was carried out for a subset of colorectal tumours for the analysis of methylation in the upstream promoter region of *14-3-3 σ* and the 5' region of the CpG island, encompassing CpG sites in both Regions A and B. The analysis partly confirmed the previous bisulphite sequencing data as it revealed that the majority of clones were unmethylated at CpG sites in the *14-3-3 σ* unmethylated tumours and had a low percentage of overall CpG methylation. Sequencing analysis of the *14-3-3 σ* methylated tumours demonstrated that they had a clonal pattern of methylation with approximately half of the clones displaying mainly methylated CpG sites and half displaying mainly unmethylated CpG sites. Therefore, this suggests that in the majority of colorectal tumours, the upstream promoter region and the 5' region of the *14-3-3 σ* CpG island is both methylated and unmethylated. In comparison with the previous bisulphite PCR

sequencing, there was no change in methylation across Regions A and B. This may be because there is no actual change in the methylation status across the *14-3-3 σ* island, and as mentioned above, the observed ‘hemi-methylation’ is actually due to tumour heterogeneity, which is discussed in more detail below. As only six tumours were analysed by bisulphite sequencing individual clones, and because the percentage of methylated CpG dinucleotides between one of the previously found methylated tumours (KR12T) and one of the unmethylated tumours (7645) were fairly similar, further analysis is required to confirm these initial findings. Nevertheless, the bisulphite sequencing analysis carried out indicated that the *14-3-3 σ* unmethylated tumours had a lower percentage of methylated CpG sites compared to the methylated tumours, therefore suggesting that their methylation profiles are different. The ‘mixed’ clonal methylation pattern observed in the majority of colorectal tumours may be a result of intra-tumour heterogeneity, with *14-3-3 σ* methylation status varying between individual tumour cells. Interestingly, in a recent report, *MLH1* was found to have a heterogeneous pattern of promoter methylation within endometrial tumours (Varley et al, 2009). It could also be possible that the different alleles of the *14-3-3 σ* upstream region and CpG island display different methylation patterns. To investigate this further, the heterozygosity of a Single Nucleotide Polymorphism (SNP) within or in close proximity to the promoter region or the CpG island of the gene would need to be analysed. Alternatively, it should also be considered that *14-3-3 σ* may actually be unmethylated in the majority of colorectal tumours, in agreement with what was found in the report by Ide et al (Ide et al, 2004), and the methylation detected in the tumour samples is due to other factors. It may be that there has been incomplete conversion of the tumour DNA following bisulphite treatment. Although, this is probably not the case since the conversion of each sample is verified by the relevant bisulphite controls and the sequence is assessed by eye for complete conversion. The methylation detected could also be a result of a combination of PCR bias and the amplification of methylated *14-3-3 σ* in other cell types within the tumour sample. All tumour samples are biopsied from the proliferative edge of the tumour and assessed by immunohistochemistry (prior to use) to ensure that more than 85% of cells are tumour derived. Therefore, despite the fact that the majority of cells will be tumour derived, the samples still

consist of a heterogeneous cell population. *14-3-3 σ* methylation has been shown previously in peripheral blood lymphocytes (Bhatia et al, 2003; Umbricht et al, 2001) and in stroma surrounding epithelium tissue (Lodygin et al, 2003; Umbricht et al, 2001). Thus, the methylation observed in the colorectal tumours may be from these cell types and the higher levels are simply a result of more stromal cells being present in the tumour sample for example. In order to control for tissue heterogeneity, the tumours could be microdissected. Laser Capture Microdissection (LCM) is a technique routinely used to isolate a pure population of cancer cells from frozen or embedded tumour sections leaving behind remaining stromal and inflammatory cells. The study by Ide et al examined *14-3-3 σ* methylation in ten microdissected colorectal tumours and found that the majority of tumours were unmethylated (Ide et al, 2004). The differences observed between this study and the results presented in this chapter may be a result of the different sample preparations that were used. In hindsight, LCM of the tumour samples prior to *14-3-3 σ* methylation analysis would have provided the purest sample for methylation analysis and control for tissue heterogeneity. However, LCM was not available during my PhD and there were also insufficient amounts of tumour material available for me to use this technique prior to methylation analysis.

Bisulphite PCR sequencing of *14-3-3 σ* in corresponding normal mucosa samples indicated that the upstream promoter region (Region A) was fully methylated in all samples. Bisulphite sequencing analysis of *14-3-3 σ* further downstream in Region B revealed that methylation status in this region was similar to the methylation status initially found in the colorectal tumours, as it was hemi-methylated in all of the normal mucosa samples analysed. *14-3-3 σ* Region C methylation status in the normal mucosa was similar to the tumour samples and was methylated. Again, as with the bisulphite PCR sequencing of the colorectal tumours, the observed 'hemi-methylation' in region B could be a result of tissue heterogeneity or PCR/sequencing bias. Region A of *14-3-3 σ* was however found to be methylated in all normal mucosa samples, including KR2NM and KR3NM in which Region A was unmethylated in the corresponding tumours. Therefore, this suggests that the absence of methylation in the upstream promoter region of *14-3-3 σ* is a tumour-specific event. Tumour-

specific loss of methylation in the upstream region was not associated with any clinicopathological variable, perhaps due to the small number of Region A *14-3-3 σ* unmethylated colorectal tumours analysed (n =10). In order to examine this further, a larger dataset of colorectal tumour samples would need to be analysed for Region A *14-3-3 σ* methylation.

Similar to the adjacent normal mucosa tissue, Region A of *14-3-3 σ* was shown to be methylated at the majority of CpG sites in nearly all of the clones amplified from normal mucosa from an individual free from cancer. In comparison, approximately half of the CpG sites were shown to be methylated in skin tissues, indicating that skin and colonic epithelium may have different methylation profiles. The mixture of methylated and unmethylated CpG sites of *14-3-3 σ* in the skin tissue could be due to tissue heterogeneity or unequal methylation of the two *14-3-3 σ* alleles (as discussed previously with regard to the colorectal tumours). It should be noted however, that the methylation profiles from the three skin samples do not display a clonal pattern of methylation unlike the colorectal tumours. Instead, the heterogeneity exists at each CpG dinucleotide, suggesting that the observed methylation pattern may be the result of a separate process in comparison to the colorectal tumours.

From the detailed bisulphite sequencing analysis of *14-3-3 σ* in both colorectal tumours and normal colonic epithelium from a non-colorectal cancer patient, the preliminary data suggests that there may be a tumour-specific loss of methylation in Region A of *14-3-3 σ* in all tumours with 10% showing an almost complete loss. *14-3-3 σ* methylation analysis in corresponding adjacent normal mucosa samples by bisulphite sequencing individual clones, as well as sequencing more tumour samples, would support this notion. Furthermore, only one normal colonic mucosa tissue sample from a cancer free individual has been sequenced, therefore this also needs to be taken into consideration. Follow-up *14-3-3 σ* methylation analysis in more normal colonic tissue samples from cancer free individuals is also needed to support these preliminary findings. As with the tumour material, it should also be considered that the normal mucosa tissue consists of a heterogeneous cell population. The collection and assessment (by immunohistochemistry) of corresponding normal mucosa tissue

in the laboratory is well established and it is believed that the majority of cells will be epithelial in origin (Prof Malcolm Dunlop & Dr Susan Farrington, personal communication). Despite this, a small proportion of lymphocyte cells and stromal cells will be present in the tissue samples, therefore these cells may also contribute to the methylation of *14-3-3 σ* observed in the normal mucosa samples. In order to test this, LCM could be used to isolate a pure population of epithelial cells from the normal mucosa tissues examined in this chapter and subsequently analysed for *14-3-3 σ* methylation by bisulphite sequencing. In addition to the heterogeneity of the normal tissue, the possibility that contaminating tumour cells are present in the normal tissues must also be addressed. All normal mucosa tissue samples are biopsied from areas on the opposite side of the colon to the tumour site, so it is unlikely that there will be any contaminating tumour cells within the samples. However, “tumour-like” cells may be present in the normal mucosa samples as a result of field cancerisation. A recent study found that the O⁶-methylguanine-DNA methyltransferase gene (*MGMT*) was methylated in 50% of normal colon tissues with *MGMT* promoter methylation in adjacent tumours and in 12% of normal colon tissues from patients with no evidence of cancer (Shen et al, 2005). Thus, the *14-3-3 σ* Region A methylation observed in both the adjacent normal mucosa tissues and the normal mucosa tissue from a non-colorectal cancer patient may be a result of a field defect. To investigate this further, a larger study would need to be conducted in which *14-3-3 σ* methylation is analysed in colorectal tumours, corresponding adjacent normal mucosa tissues and normal mucosa tissues from patients free of cancer. Examining normal mucosa tissues from the opposite side of the colon to the tumour site may be advantageous with regards to lowering the possibility of analysing contaminating tumour cells, however it must also be considered that the methylation status of *14-3-3 σ* may vary in different areas of the colon. As discussed in the introduction section, a significantly higher proportion of CIMP tumours are right-sided (Hawkins et al, 2002). Therefore, it may be that the observed difference in *14-3-3 σ* methylation status in the normal colonic tissue is a result of biopsies taken from the opposite side of colon to the tumour site. In order to test this, *14-3-3 σ* methylation analysis would need to be carried out on two normal colonic tissue

biopsies, one on the opposite side of the tumour site and one on the same side as the tumour site.

In summary, I have demonstrated that the majority of colorectal cancer cell lines are unmethylated in the upstream promoter region and 5' region of the *14-3-3 σ* CpG island. In the majority of colorectal tumours, bisulphite sequencing analysis of individual clones suggested that the upstream promoter region and 5' region of the *14-3-3 σ* CpG island is both methylated and unmethylated in colorectal tumours with a small percentage of tumours being almost completely unmethylated. *14-3-3 σ* methylation was observed in all the corresponding normal mucosa tissues examined and in normal mucosa tissue from a non-colorectal cancer patient, therefore suggesting that there may be a tumour-specific loss or *hypomethylation* of *14-3-3 σ* in colorectal tumours. However, as discussed, to fully understand the role of *14-3-3 σ* methylation in colorectal cancer, further investigations, including the methylation analysis of larger datasets, the investigation of the effects of tissue heterogeneity, and field cancerisation are required.

With the aim to support the preliminary data presented thus far, and the notion that *14-3-3 σ* hypomethylation in colorectal cancer may contribute to further downstream effects, the relationship between *14-3-3 σ* expression and methylation status is examined in the following chapter.

Chapter 4

Analysis of 14-3-3 σ expression and its association with methylation of the gene promoter in vitro and in vivo

4.1 Introduction

Preliminary findings in chapter 3 demonstrated that 14-3-3 σ is unmethylated in the upstream promoter region (UPR) and 5' region of the CpG island in the majority of colorectal cancer cell lines. *In vivo*, analysis in the same regions showed that 14-3-3 σ was differentially methylated in tumour samples, with the majority of tumours displaying a clonal pattern of methylation and a small proportion showing low to negligible levels of methylation. Analysis of 14-3-3 σ methylation in both corresponding colonic normal mucosas and colonic normal mucosa tissue from an individual free from cancer revealed that the gene was methylated in all samples examined, suggesting that there may be a tumour-specific loss of 14-3-3 σ methylation in colorectal tumours. Furthermore, in comparison to methylated normal colon tissue, 14-3-3 σ was shown to be both methylated and unmethylated at individual CpG sites in skin tissue, which is known to positively express 14-3-3 σ (Leffers et al, 1993; Oshiro et al, 2005).

Previous reports have shown that in a number of different cancers, aberrant methylation of 14-3-3 σ is associated with changes in gene expression (Ferguson et al, 2000; Mhawech et al, 2005; Suzuki et al, 2000). With this in mind, including the preliminary data presented in chapter 3, the hypothesis I wish to test is that 14-3-3 σ expression levels will be associated with 14-3-3 σ methylation status in colorectal cancer cell lines, colorectal tumours and in normal colonic tissue. Henceforth in this chapter, methylated and unmethylated 14-3-3 σ refers to the methylation status in the UPR of 14-3-3 σ of a given sample determined from the earlier bisulphite PCR sequencing data. The association between 14-3-3 σ expression and UPR methylation status in normal tissues from individuals free from cancer will be investigated based

on the bisulphite sequencing analysis from individual clones. The aim of this chapter is thus to establish whether the UPR methylation status of *14-3-3 σ* is associated with gene expression in colorectal cancer cell lines, colorectal tumours, matched normal mucosa samples and also in colonic mucosa and skin tissues from individuals free from cancer. Expression analysis of *14-3-3 σ* in colorectal cancer cell lines, colorectal tumours and in matched normal colonic mucosa was carried out at both the mRNA and protein level using a qRT-PCR and Western Blot approach respectively. Comparison of *14-3-3 σ* protein expression in normal colonic mucosa and skin tissues was examined by Western blot analysis only. Demethylation of *14-3-3 σ* in two methylated colorectal cancer cell lines by 5-Aza-2'-deoxycytidine treatment was optimised and subsequently examined by MSP analysis. Relative levels of *14-3-3 σ* mRNA expression were examined in the colorectal cancer cell lines following 5-Aza-2'-deoxycytidine treatment to determine whether *14-3-3 σ* can be re-expressed as a result of demethylation.

4.2 Methodology

4.2.1 qRT-PCR analysis

RNA from colorectal cancer cell lines (including 5-Aza-2'-deoxycytidine treated cell lines), normal mucosa tissues and colorectal tumours were DNase treated to remove contaminating genomic DNA (gDNA) as described in section 2.6.1. This was required as the *14-3-3 σ* primers and probe were designed within the exon of the gene and not on the exon junction (*14-3-3 σ* has only one exon). Therefore, qRT-PCR amplification would not distinguish between gDNA and cDNA amplification. Following DNase treatment, cDNA synthesis was carried out as described in section 2.6.2 and the removal of gDNA contamination was verified by amplifying the control gene template, β -actin, from cDNA and corresponding negative reverse transcriptase reactions as described in section 2.4.3. The β -actin primers were designed to amplify a region within a single exon and therefore could detect any contaminating gDNA in the negative reverse transcriptase reactions. Each RNA sample extracted was tested in this way and cDNA samples with contaminating gDNA were discarded. Figure 4.1 shows a β -actin RT-PCR reaction from colorectal cancer cell lines. Amplified β -actin products are visible from the positive cDNA samples however, they are not present in the negative reverse transcriptase reactions. Thus, confirming that the DNase treatment was successful in removing all contaminating gDNA from the RNA sample. β -actin RT-PCR reactions from all other cDNA samples are illustrated in Appendix B. Negative reverse transcriptase reactions were also tested for gDNA contamination alongside cDNA samples during qRT-PCR analysis.

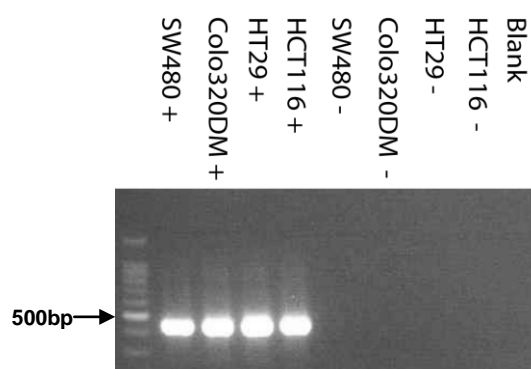


Figure 4.1: β -Actin RT-PCR from colorectal cancer cell line cDNA samples (+) and corresponding negative reverse transcriptase reactions (-) confirming removal of gDNA contamination.

Following the verification of gDNA removal, cDNA samples were subjected to qRT-PCR Taqman analysis as described in section 2.6.3. Relative quantification of *14-3-3 σ* mRNA levels was performed using the standard curve method and the target *14-3-3 σ* mRNA levels normalised by the endogenous control (β -Actin). All raw data and subsequent calculations, including standard curves for each analysis are listed in Appendix B.

4.2.2 Western blot analysis

Cytoplasmic cell extracts from colorectal cancer cell lines, normal mucosa tissues, colorectal tumours and skin tissues were examined for *14-3-3 σ* expression by Western blot analysis as described in section 2.6.5.3. Protein loading was assessed by probing for β -actin levels and densitometric analysis carried out as described in 2.6.5.3.

4.2.3 5-Aza-2'-deoxycytidine treatment

SW480 and Colo320DM colorectal cancer cell lines (*14-3-3 σ* methylated) were treated with 5-Aza-2'-deoxycytidine as described in section 2.7.1. Both cell lines were treated with 0.1 μ M to 10 μ M 5-Aza-2'-deoxycytidine over a 4 day period in order to test optimal conditions. Control experiments comprised of cells completely untreated or treated with vehicle (50% acetic acid). DNA was extracted from treated and control cells, bisulphite treated (2.4.2) and examined by MSP analysis to determine *14-3-3 σ* demethylation.

4.2.4 Methylation-specific PCR (MSP)

14-3-3 σ MSP was performed on bisulphite treated DNA extracted from 5-Aza-2'-deoxycytidine treated colorectal cancer cell lines as described in section 2.4.3 and 2.4.4 to verify the demethylation of *14-3-3 σ* following treatment. Products were analysed for methylation by gel electrophoresis (2.4.5) and densitometric analysis carried out as described in 2.4.3.

4.2.5 Colorectal cancer cell lines

RNA and cytoplasmic cell extracts were purified from the following cell lines: HCT116, HT29, SW480 & Colo320DM as described in 2.2.3 and 2.6.5.1 respectively. DNA was extracted from the 5-Aza-2'-deoxycytidine treated cell lines SW480 and Colo320DM as described in 2.2.1.

4.2.6 Patient samples

Matched normal mucosa tissue (NM) and tumour samples (T) from colorectal cancer patients were used in this chapter. Three skin tissue samples (Skin A, Skin B and Skin C) from individuals free from cancer were also used. Fresh normal colonic mucosa from an individual free from disease and cancer (NC) was used for qRT-PCR analysis, whereas cytoplasmic extract from normal colonic mucosa from an individual free from cancer (NC) was used directly from an external source (Zyagen). RNA and cytoplasmic extracts were purified from fresh samples as described in 2.2.3 and 2.6.5.2 respectively.

4.2.7 Statistical analysis

Significant differences were examined by performing paired Wilcoxon signed rank tests and unpaired non-parametric Mann Whitney tests as described in 2.10.1. The cut-off for significant p-values was taken at 5%.

4.3 Results

4.3.1 14-3-3 σ expression analysis in colorectal cancer cell lines

The work presented in chapter 3 investigated the methylation status of 14-3-3 σ in nine colorectal cancer cell lines and found that the majority were unmethylated. Only two cell lines were methylated: SW480 and Colo320DM. To investigate whether there are any associations between 14-3-3 σ methylation status and expression, mRNA expression and protein levels in the two methylated cell lines SW480 and Colo320DM and two unmethylated cell lines HT29 and HCT116 were examined. Firstly, qRT-PCR analysis demonstrated that there were high 14-3-3 σ mRNA levels in the unmethylated cell lines HT29 and HCT116 and only a negligible level of 14-3-3 σ mRNA in the methylated cell lines SW480 and Colo320DM (Figure 4.2). 14-3-3 σ mRNA levels in the unmethylated cell lines was approximately 400-fold higher than in the methylated cell lines. Further analysis was carried using Western blot analysis to investigate the expression of the 14-3-3 σ protein in methylated and unmethylated cell lines. Western blot analysis demonstrated that there were high levels of 14-3-3 σ protein in the two unmethylated colorectal cancer cell lines HT29 and HCT116 and again only negligible levels of 14-3-3 σ protein in the two methylated colorectal cancer cell lines SW480 and Colo320DM (Figure 4.3). As only two methylated and two unmethylated colorectal cell lines were examined for 14-3-3 σ expression, the sample numbers are too small to test for differences in expression levels between the colorectal cancer cell lines. The data does however demonstrate that there are lower levels of 14-3-3 σ expression in the methylated cell lines compared to the unmethylated cell lines.

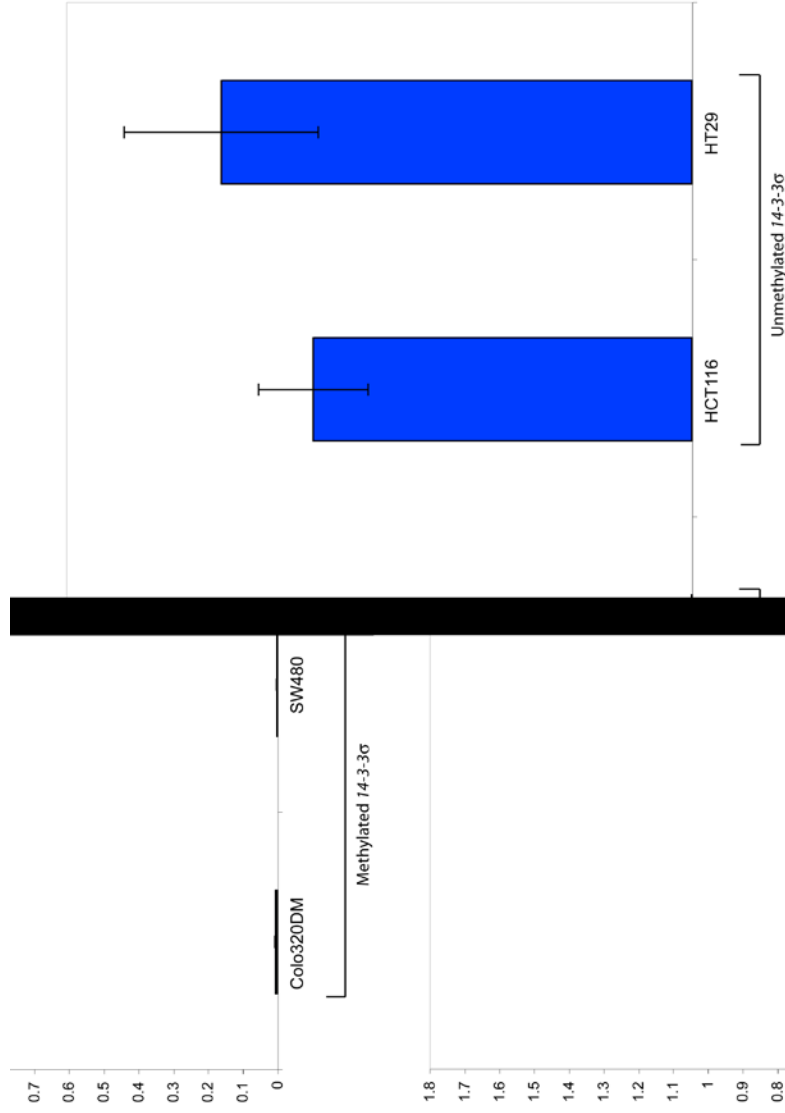


Figure 4.2: qRT-PCR analysis measuring relative levels of 14-3-3 σ mRNA in colorectal cancer cell lines: Colo320DM, HCT116, HT29 and SW480. 14-3-3 σ expression levels are expressed relative to β actin endogenous control levels. The results are the means of triplicate results \pm standard errors. There was approximately a 400-fold difference in 14-3-3 σ mRNA expression between the unmethylated and methylated cell lines.

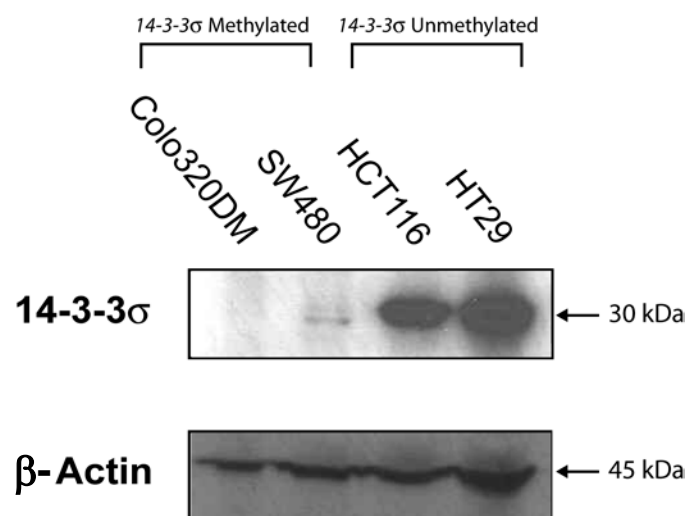


Figure 4.3: Detection of cytoplasmic 14-3-3 σ protein by Western blot in colorectal cancer cell lines: Colo320DM and SW480 (14-3-3 σ methylated) and HCT116 and HT29 (14-3-3 σ unmethylated). β -actin levels were analysed to assess protein loading. Film was exposed for 3 minutes for the detection of 14-3-3 σ protein and 10 seconds for the detection of β -actin.

4.3.2 14-3-3 σ mRNA expression analysis *in vivo*

Expression studies *in vitro* demonstrated that there were lower levels of 14-3-3 σ expression in the methylated colorectal cancer cell lines compared to the unmethylated colorectal cell lines which expressed high levels of 14-3-3 σ . Following on from this initial finding, the expression levels of 14-3-3 σ at the mRNA level was first examined in a set of colorectal tumours and corresponding normal mucosa samples. A total of 5 colorectal tumours and matched normal mucosa tissues were examined: 3 of the tumours were unmethylated (KR2, KR3 and AM27) and 2 tumours were methylated (KR10 and KR11). In addition, normal colonic mucosa from an individual free from cancer was analysed for comparison. qRT-PCR analysis demonstrated higher levels of 14-3-3 σ mRNA in two of the 14-3-3 σ unmethylated tumours (KR2 and KR3) compared to 14-3-3 σ mRNA levels in the corresponding normal tissues (Figure 4.4). Interestingly, unlike other 14-3-3 σ unmethylated tumour samples, AM27 displayed low 14-3-3 σ mRNA levels and 14-3-3 σ mRNA could not be detected in the matched normal mucosa tissue. The normal mucosa sample did express the endogenous control β -actin, indicating that the lack of 14-3-3 σ mRNA was not due to low concentration of cDNA in this sample. It is not clear why this result was obtained but complete lack of 14-3-3 σ in normal tissue suggests that another mechanism may be involved in silencing 14-3-3 σ expression. When combining expression data from all three unmethylated tumours and matched normal tissues, it was found that there was no significant difference in 14-3-3 σ mRNA levels between the unmethylated tumours and matched normal mucosa tissues ($p = 0.25$, paired Wilcoxon signed rank test). These initial findings also demonstrated that 14-3-3 σ mRNA levels in the unmethylated KR2 and KR3 tumours were relatively higher compared to methylated tumours KR10 and KR11. In order to test whether there is a significant difference in expression between methylated and unmethylated tumours, a separate set of tumour samples were examined for 14-3-3 σ mRNA expression (Figure 4.5). There was an average 3-fold difference in expression between the methylated and unmethylated tumours with higher mRNA expression in the 14-3-3 σ unmethylated tumours ($p = 0.03$, Mann Whitney test). Therefore,

preliminary data suggests that there may be an association *in vivo* between *14-3-3 σ* methylation status and mRNA expression in the colorectal tumours examined.

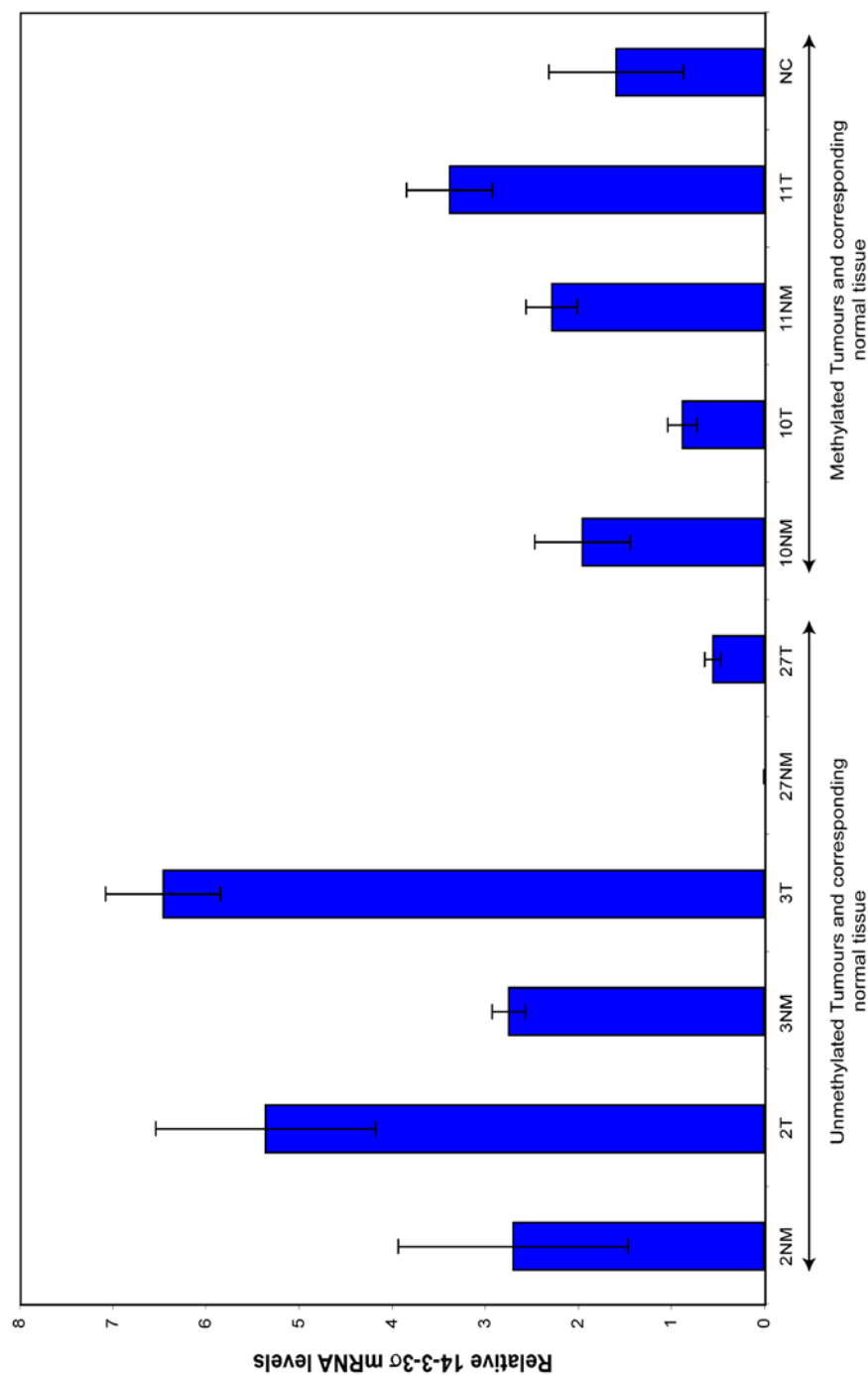


Figure 4.4: qRT-PCR analysis measuring relative expression of 14-3-3 σ in KR and AM colorectal tumours and corresponding matched normal mucosa tissues. 14-3-3 σ expression levels are expressed relative to β actin endogenous control levels. The results are the means of triplicate results \pm standard errors. NM = normal mucosa tissue, T = tumour, NC = normal mucosa tissue from an individual free from cancer and disease.

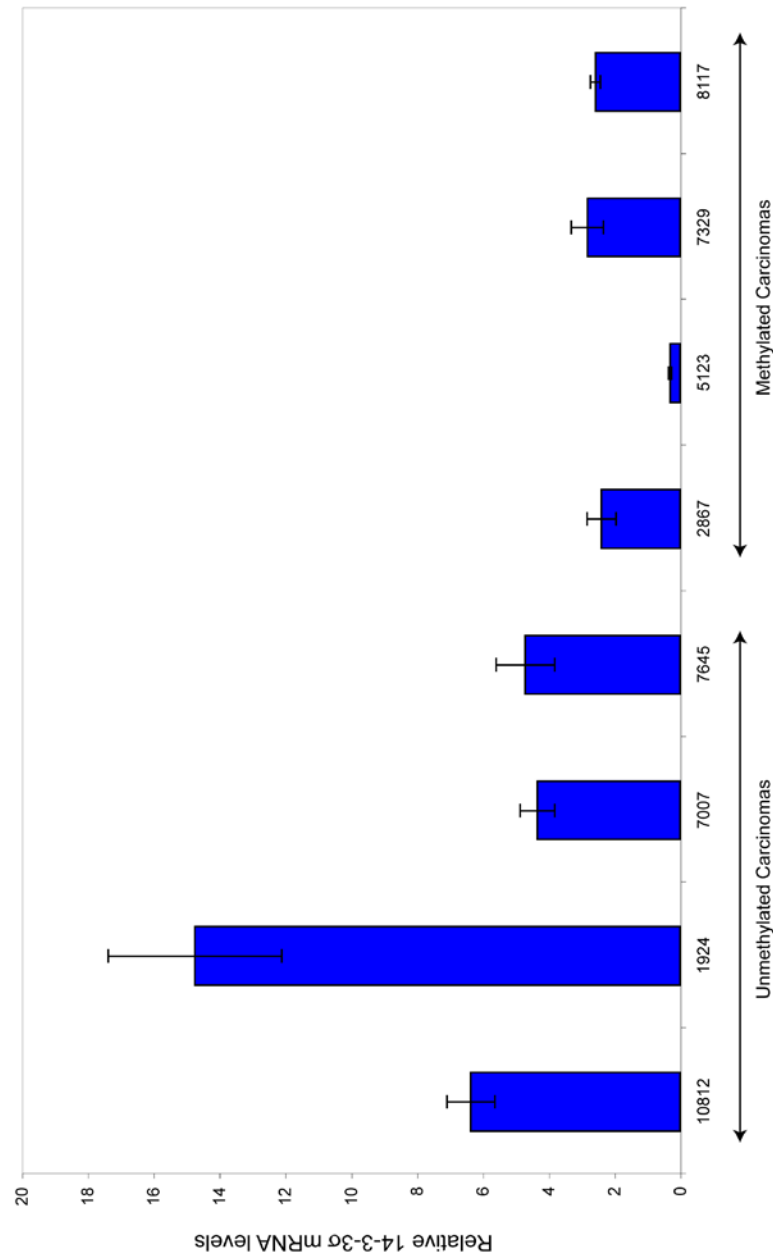


Figure 4.5: qRT-PCR analysis measuring relative expression of 14-3-3 σ in colorectal tumours. 14-3-3 σ expression levels are expressed relative to β actin endogenous control levels. The results are the means of triplicate results \pm standard errors.

4.3.3 14-3-3 σ protein expression analysis *in vivo*

Section 4.3.2 demonstrated that there were significantly higher levels of 14-3-3 σ mRNA in unmethylated colorectal tumours compared to methylated tumours. This initial finding and previous analysis carried out *in vitro* suggests that 14-3-3 σ protein expression may also be associated with methylation status in colorectal tumours and matched normal tissues. To examine this, 14-3-3 σ protein levels were first examined in 4 colorectal tumours and matched normal tissue samples: 2 unmethylated tumours (KR2 and KR3) and 2 methylated tumours (KR1 and KR4) by Western blot analysis. Figure 4.6 shows Western blot analysis of 14-3-3 σ detection in the tumours and matched normal tissues. 14-3-3 σ protein is detected at higher levels in the unmethylated tumours KR2 and KR3 compared to the matched normal tissue. It should however be taken into account that there is unequal protein loading in some of these samples and therefore the differences observed may not be so considerable. In the methylated tumours there is a decrease in 14-3-3 σ protein levels in the tumour KR1 compared to matched normal tissue and a small increase in protein levels in the tumour KR4 compared to matched normal tissue. Interestingly, when grouping all corresponding normal mucosa tissues and tumour samples analysed by Western blot, densitometric analysis demonstrated an overall higher level of 14-3-3 σ protein in the tumour samples compared to the matched normal tissue (Figure 4.7). Secondly, to further investigate the relationship between 14-3-3 σ methylation status and protein expression in colorectal tumours, 14-3-3 σ protein levels were examined in 9 additional colorectal tumour samples: 5 14-3-3 σ unmethylated tumours (10811, 10812, 7007, 7645 and 1924) and 4 14-3-3 σ methylated (2109, KR8, KR9 and KR10) and one normal mucosa tissue sample from a non-colorectal cancer patient (Figure 4.8). Western blot and subsequent densitometric analysis (Figure 4.9), demonstrated that 14-3-3 σ protein levels were higher in unmethylated tumours compared to the majority of methylated tumours and the normal mucosa tissue from a non-colorectal cancer patient. However, tumour sample KR8, which is methylated in the upstream promoter region of 14-3-3 σ has a higher level of 14-3-3 σ protein expression compared to the other methylated tumours. This anomalous finding may

be the result of another mechanism such as gene amplification and is discussed in further detail in the discussion section of this chapter.

To further examine the relationship between *14-3-3* σ UPR methylation status and expression, Western blot analysis was utilised for the analysis of *14-3-3* σ protein levels in skin tissue compared to normal colonic tissue from colorectal cancer patients (Figure 4.10). Western blot and subsequent densitometry analysis (Figure 4.11) demonstrates that *14-3-3* σ protein levels are higher in the three skin tissues compared to the normal colonic mucosa tissue. Overall, these initial findings suggest that at the protein level, there may be an association between *14-3-3* σ methylation status and expression in both colorectal tumours, matched normal colonic tissues and in skin tissue. A list of the *in vitro* and *in vivo* expression data and corresponding methylation status of each individual cell line or tissue sample is listed in Table 4.1.

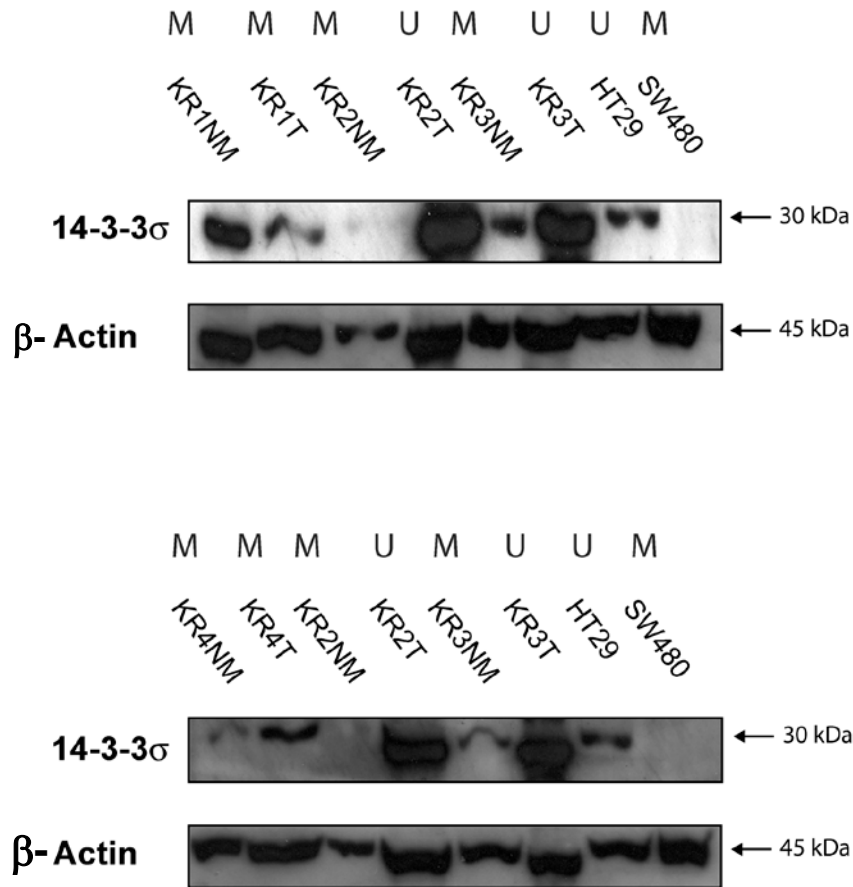
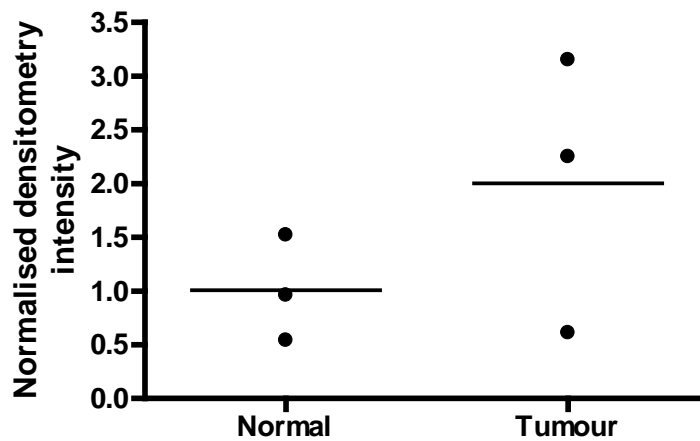


Figure 4.6: 14-3-3 σ protein detection by Western blot analysis in unmethylated colorectal tumours (KR2 and KR3) and paired normal tissues (methylated) from same patient; in methylated colorectal tumours (KR1 and KR4) and paired normal tissues (methylated) from same patient. HT29 serves as a positive control for 14-3-3 σ expression and SW480 as a negative control for 14-3-3 σ expression. 14-3-3 σ methylation status is indicated from analysis presented in chapter 3: M = methylated U = unmethylated. β actin levels were analysed to assess protein loading.

(A) UPPER BLOT



(B) LOWER BLOT

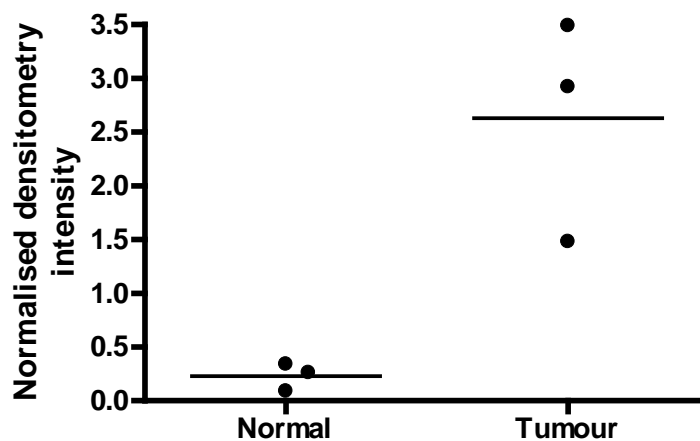


Figure 4.7: Densitometric analysis of 14-3-3 σ Western blot (A) upper and (B) lower blot from Figure 4.6, in colorectal tumours and matched normal tissues. Densitometric intensities of 14-3-3 σ bands were normalised by β -actin densitometric intensities. Horizontal lines represent mean densitometric value.

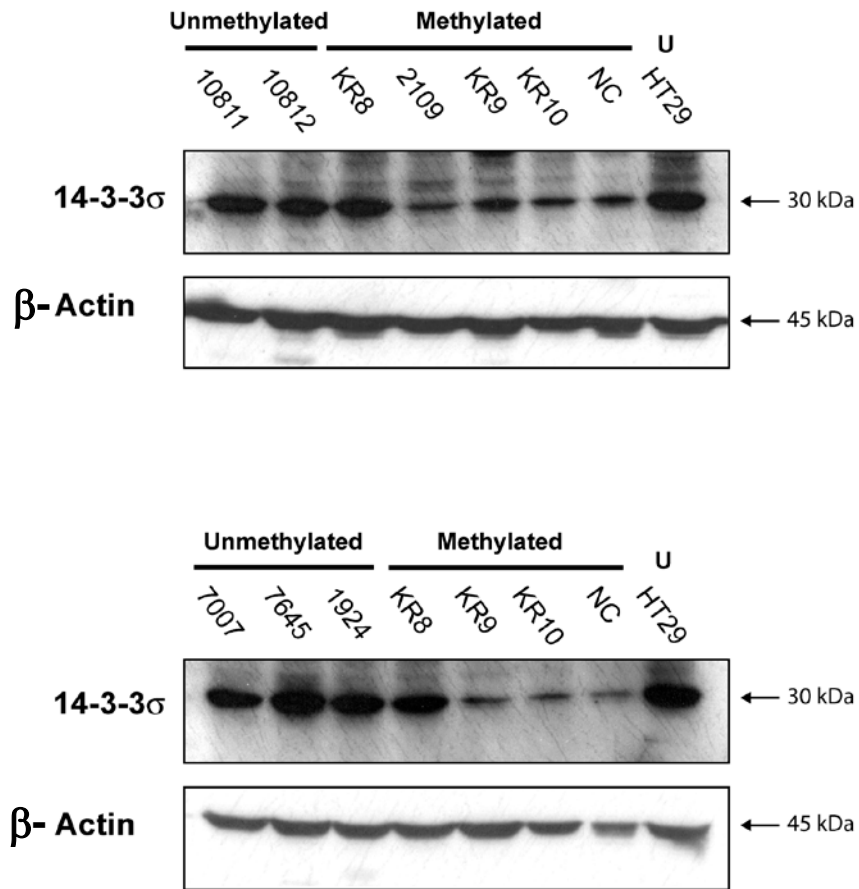
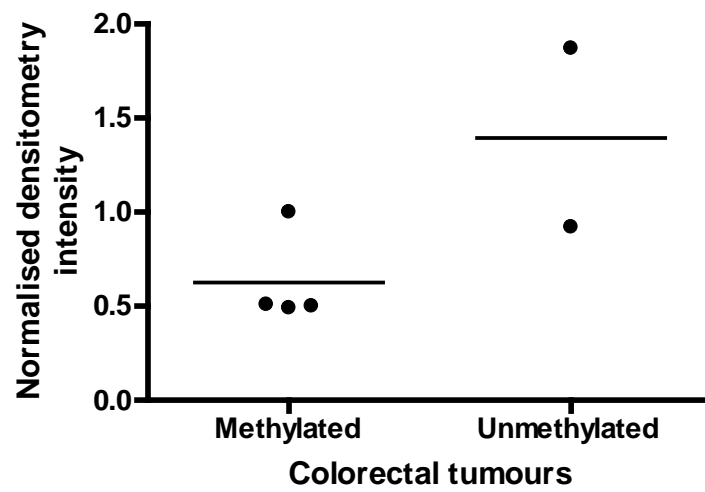


Figure 4.8: 14-3-3 σ protein detection by Western blot analysis in colorectal tumours. 14-3-3 σ methylated or unmethylated tumours are indicated. NC corresponds to normal mucosa tissue from a cancer-free individual. High levels of 14-3-3 σ protein in methylated KR8 explained in text. HT29 (U = unmethylated 14-3-3 σ) serves as a positive control for 14-3-3 σ expression. β actin levels were analysed to assess protein loading.

(A) UPPER BLOT



(B) LOWER BLOT

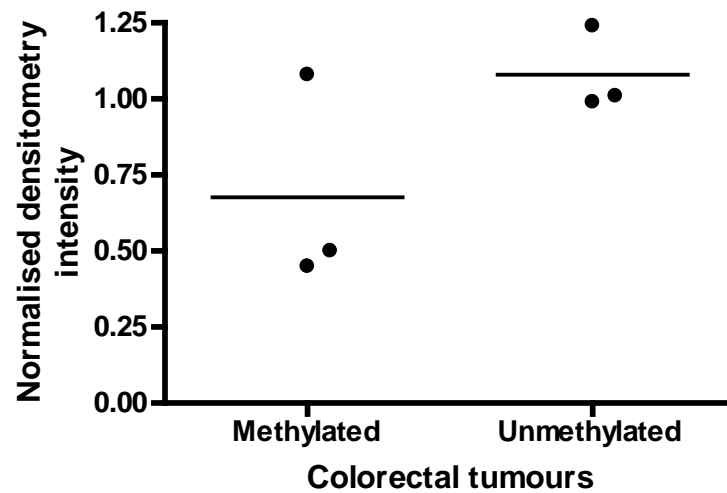


Figure 4.9: Densitometric analysis of 14-3-3 σ Western blot (A) upper and (B) lower blot from Figure 4.8, in 14-3-3 σ methylated and unmethylated colorectal tumours. Densitometric intensities of 14-3-3 σ bands were normalised by β -actin densitometric intensities. Horizontal lines represent mean densitometric value.

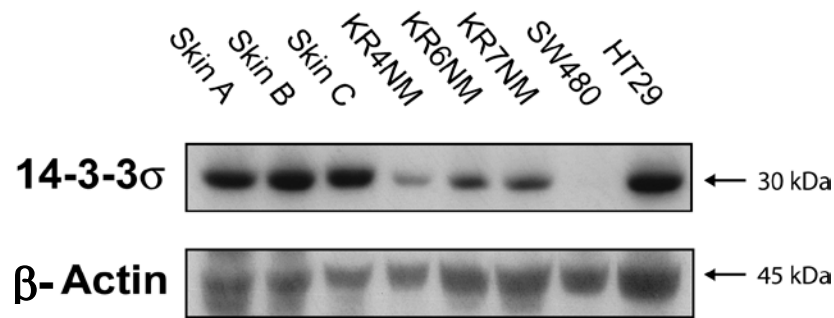


Figure 4.10: 14-3-3 σ protein detection by Western blot analysis in skin tissue compared to normal colon from colorectal cancer patients (NM). SW480 (methylated 14-3-3 σ) serves as negative control for 14-3-3 σ expression. HT29 (unmethylated 14-3-3 σ) serves as a positive control for 14-3-3 σ expression. β actin levels were analysed to assess protein loading.

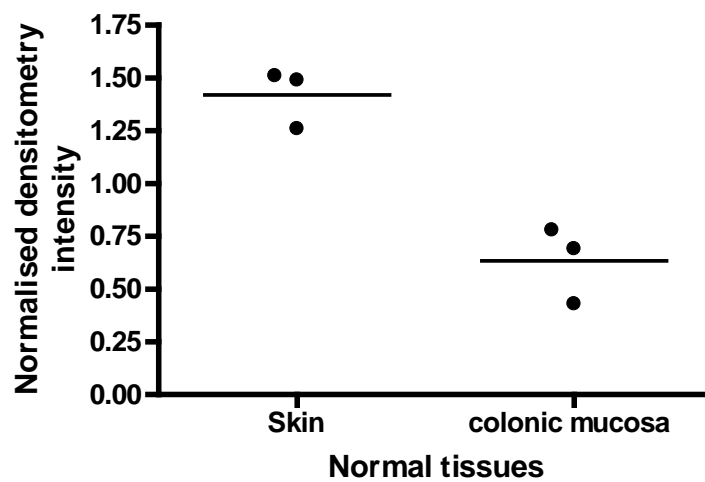


Figure 4.11: Densitometric analysis of 14-3-3 σ Western blot from Figure 4.10 in normal skin tissues and normal colonic mucosa from colorectal cancer patients. Densitometric intensities of 14-3-3 σ bands were normalised by β -actin densitometric intensities. Horizontal lines represent mean densitometric value.

	Methylation Status	mRNA expression	Protein expression
<u>Colorectal cancer cell lines</u>			
HT29	U	+++	+++
HCT116	U	+++	+++
SW480	M	+	-
Colo320DM	M	+	-
<u>Normal Mucosa Tissues</u>			
1N	M	ND	++
2N	M	++	+
3N	M	++	+
4N	M	ND	+
10N	M	++	ND
11N	M	++	ND
AM27N	M	-	ND
NC	M	++	+
<u>Skin Tissues</u>			
Skin A	P	ND	+++
Skin B	P	ND	+++
Skin C	P	ND	+++
<u>Colorectal Tumours</u>			
1T	M	ND	+
4T	M	ND	+
8T	M	ND	+++
9T	M	ND	+
10T	M	+	+
2109	M	ND	+
2867	M	+	ND
5123	M	+	ND
7329	M	+	ND
8117	M	+	ND
2T	U	+++	+++
3T	U	+++	+++
10811	U	ND	+++
10812	U	ND	+++
7007	U	+++	+++
7645	U	+++	+++
1924	U	+++	+++
AM27T	U	+	ND

Table 4.1: 14-3-3 σ expression data and relationship with 14-3-3 σ methylation status.
M = methylated, U = unmethylated, P = partially methylated, methylated and unmethylated CpG sites (+) = expression level, (-) = no expression, NC = normal colon from non-colorectal cancer patient, ND = not determined.

4.3.4 Demethylation of *14-3-3 σ* *in vitro* by 5-Aza-2'-deoxycytidine

Initial studies carried out so far suggest that *14-3-3 σ* UPR methylation may be associated with expression in colorectal tumours. More detailed analysis in a larger sample set is required to verify this initial finding and determine whether loss of methylation in the UPR of *14-3-3 σ* may be responsible for overexpression of *14-3-3 σ* in colorectal cancer. Experiments demonstrating the re-expression of *14-3-3 σ* in the methylated colorectal cancer cell lines SW480 and Colo320DM following demethylation treatment may provide further evidence to support this notion.

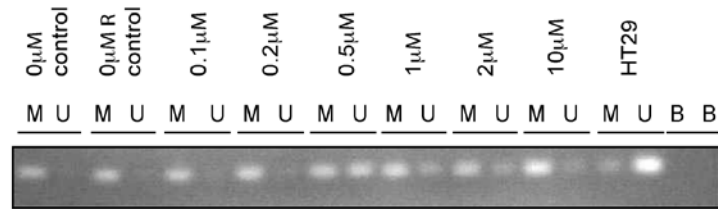
In order to establish the optimal concentration of 5-Aza-2'-deoxycytidine for *14-3-3 σ* demethylation, dose response experiments (0.1 μ M to 10 μ M) for 4 days in both cell lines were performed. MSP, which analyses the 5' region of the *14-3-3 σ* CpG island, and subsequent densitometric analysis, showed that a concentration of 0.5 μ M was optimal for demethylation of *14-3-3 σ* in SW480 cells over 4 days (Figure 4.12 (A)) (Table 4.2). Similarly, in the Colo320DM cells, a strong PCR signal and densitometric intensity for the *14-3-3 σ* unmethylated product was observed at 0.5 μ M and 1 μ M of 5-Aza-2'-deoxycytidine (Figure 4.12(B)) (Table 4.3). Hence, a concentration of 0.5 μ M was used for all subsequent experiments in SW480 and Colo320DM cells. Interestingly, in Colo320DM cells treated with 5 μ M of 5-Aza-2'-deoxycytidine there appears to be re-methylation of *14-3-3 σ* . It is not understood why this occurs. However, higher concentrations of 5-Aza-2'-deoxycytidine (5 μ M and 10 μ M) were often toxic as SW480 and Colo320DM cells sometimes died after 4 days of treatment. Therefore, the lower concentration of 5-Aza-2'-deoxycytidine was considered optimal for cell viability as well as for demethylation of *14-3-3 σ* and expression studies in these cell lines.

Following dose response optimisation, the length of treatment to demethylate *14-3-3 σ* was investigated in both cell lines by carrying out time course experiments. SW480 and Colo320DM cells were treated at 0.5 μ M for 4 consecutive days and each day the media was replaced with fresh media including fresh 5-Aza-2'-deoxycytidine. MSP analysis showed that in both SW480 and Colo320DM cells, *14-*

3-3 σ was demethylated at day 1, evidenced by the presence of a stronger PCR signal and higher densitometric intensity for the unmethylated product in cells treated for 1 day compared to the signal and densitometric intensity for the unmethylated product in control cells (Figure 4.13) (Table 4.4 & 4.5). The signal for the 14-3-3 σ unmethylated product (in both cell lines) increases with further treatment to day 4 with a progressively stronger signal and increase in densitometric intensity for the unmethylated product. This suggests that 4 days treatment with 0.5 μ M 5-Aza-2'-deoxycytidine is optimal in both colorectal cancer cell lines to demethylate 14-3-3 σ . At longer time points, cells were dying likely due to the toxicity of 5-Aza-2'-deoxycytidine or high confluency of the flask.

In order to examine whether the demethylation of 14-3-3 σ results in re-expression of 14-3-3 σ , 14-3-3 σ mRNA levels were measured in SW480 and Colo320DM cells following 5-Aza-2'-deoxycytidine treatment by qRT-PCR analysis. The cell lines were treated with 0.5 μ M of 5-Aza-2'-deoxycytidine for 4 consecutive days and relative 14-3-3 σ mRNA levels were determined for day 4 and compared with untreated control day 4 cells. As shown in Figure 4.14 (A), there is no change in relative 14-3-3 σ mRNA levels in 5-Aza-2'-deoxycytidine treated SW480 cells on day 4 compared to untreated control cells. A similar result is observed in 5-Aza-2'-deoxycytidine treated Colo320DM cells. At day 4 there is also no change in 14-3-3 σ mRNA levels in 5-Aza-2'-deoxycytidine treated cells compared to untreated control cells (Figure 4.14 (B)). Collectively these results demonstrate that even though demethylation was achieved in both cell lines on day 4 of 5-aza-2'-deoxycytidine treatment, 14-3-3 σ was not re-expressed. The explanations for this are examined in the discussion.

(A) SW480



(B) Colo320DM

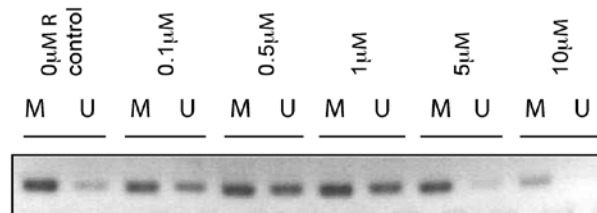


Figure 4.12: MSP analysis. SW480 (A) and Colo320DM (B) cells were treated for 4 days with 5-Aza-2'-deoxycytidine (0.1 μ M to 10 μ M) Control cells were either completely untreated (0 μ M control) or untreated with vehicle 50% acetic acid (0 μ M R control). HT29 is shown for unmethylated control and B = blank PCR reaction, shown in (A) only. M, methylated PCR product and U, unmethylated PCR product.

SW480

Dose (uM)	M Intensity	U Intensity
0 Control	164.61	8.96
0 Control Vehicle	168.95	10.01
0.1	184.82	18.70
0.2	164.62	10.18
0.5	202.39	183.24
1	199.84	83.25
2	205.70	65.77
10	331.21	65.01
HT29	77.93	619.92

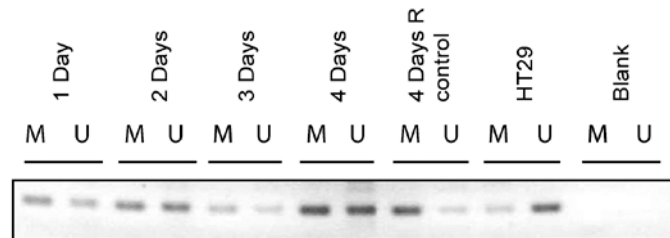
Table 4.2: Densitometric analysis of MSP reactions from SW480 cells treated for 4 days with 5-Aza-2'-deoxycytidine (0.1µM to 10µM) Control cells were either completely untreated (0 Control) or untreated with vehicle 50% acetic acid (0 Control Vehicle). HT29 analysis was carried out for unmethylated control. M, methylated PCR product and U, unmethylated PCR product.

Colo320DM

Dose (uM)	M Intensity	U Intensity
0 Control Vehicle	713.18	136.57
0.1	528.47	270.45
0.5	546.35	505.85
1	722.08	535.59
5	529.32	75.45
10	256.43	16.42

Table 4.3: Densitometric analysis of MSP reactions from Colo320DM cells treated for 4 days with 5-Aza-2'-deoxycytidine (0.1µM to 10µM) Control cells were untreated with vehicle 50% acetic acid (0 Control Vehicle). M, methylated PCR product and U, unmethylated PCR product.

(A) SW480



(B) Colo320DM

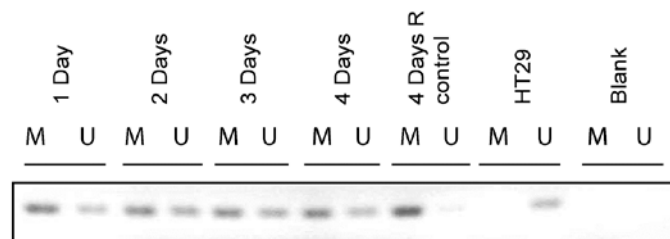


Figure 4.13: MSP analysis. SW480 (A) and Colo320DM (B) cells were treated with 5-Aza-2'-deoxycytidine (0.5 μ M) for 4 days. Control cells were untreated for 4 days with vehicle 50% acetic acid (R control). HT29 is shown for unmethylated control and B = blank PCR reaction. M, methylated PCR product and U, unmethylated PCR product.

SW480

Days Treatment	M Intensity	U Intensity
1	385.36	206.94
2	406.24	507.81
3	227.85	145.14
4	669.36	596.76
4 Control Vehicle	639.40	78.66
HT29	156.88	609.72

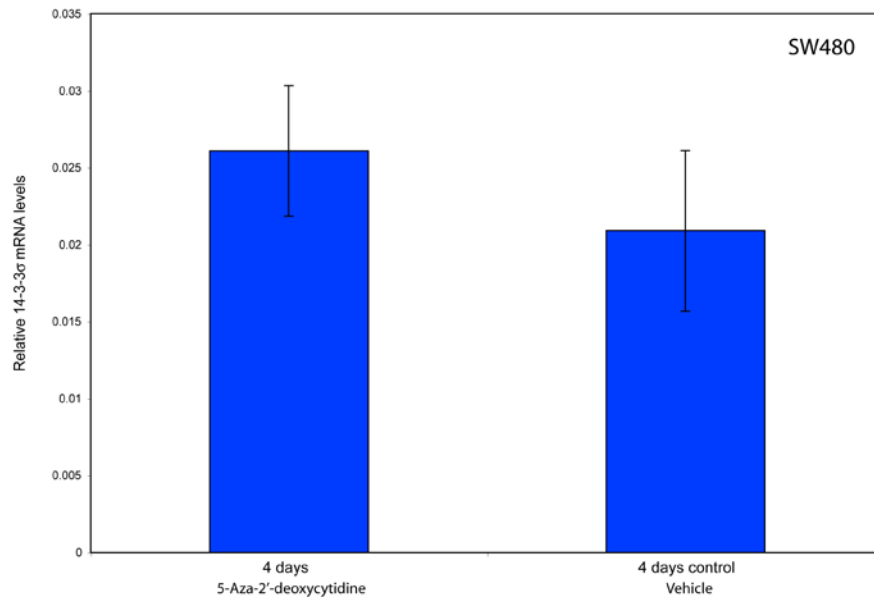
Table 4.4: Densitometric analysis of MSP reactions from SW480 cells treated with 5-Aza-2'-deoxycytidine (0.5 μ M) for 4 days. Control cells were untreated for 4 days with vehicle 50% acetic acid (Control Vehicle). HT29 analysis was carried out as a unmethylated control. M, methylated PCR product and U, unmethylated PCR product.

Colo320DM

Days Treatment	M Intensity	U Intensity
1	361.23	196.09
2	310.62	128.83
3	265.01	169.11
4	297.33	156.68
4 Control Vehicle	415.47	17.85
HT29	0	147.47

Table 4.5: Densitometric analysis of MSP reactions from Colo320DM cells treated with 5-Aza-2'-deoxycytidine (0.5 μ M) for 4 days. Control cells were untreated for 4 days with vehicle 50% acetic acid (Control Vehicle). HT29 analysis was carried out as a unmethylated control. M, methylated PCR product and U, unmethylated PCR product.

(A)



(B)

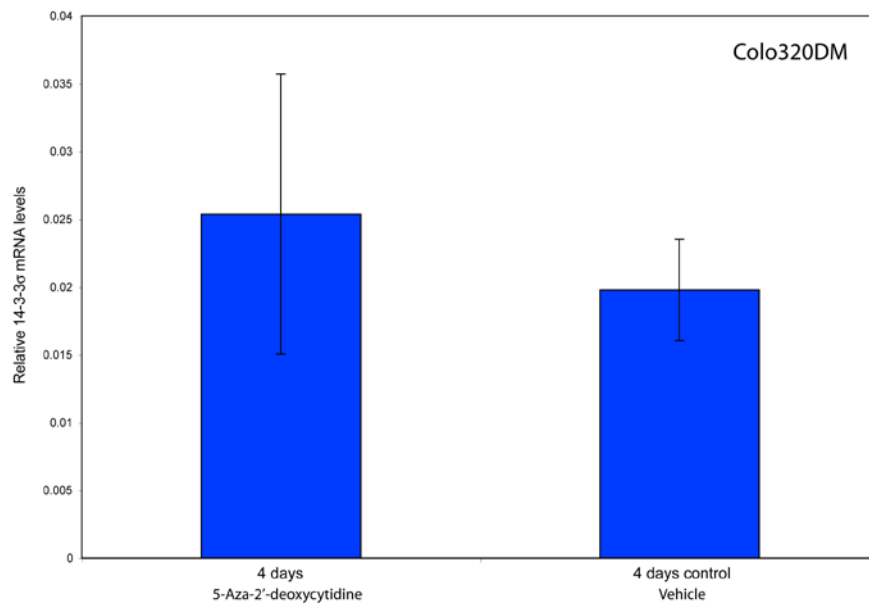


Figure 4.14: Relative 14-3-3 σ mRNA levels in SW480 (A) and Colo320DM (B) cells upon treatment with 5-Aza-2'-deoxycytidine (0.5 μ M) for 4 days determined by qRT-PCR. Relative levels were normalized to β -actin endogenous control gene mRNA levels. The results are the means of triplicate results \pm standard errors.

4.4 Discussion

My aim for this chapter was to establish whether *14-3-3 σ* methylation status is associated with expression in colorectal cancer. I analysed comparative expression at the mRNA and protein level in a small number of *14-3-3 σ* methylated and unmethylated colorectal cancer cell lines, tumours and corresponding normal tissues. I also decided to examine *14-3-3 σ* protein levels in three separate skin tissues in which *14-3-3 σ* is both methylated and unmethylated at individual CpG sites and normal colonic tissue, which has higher levels of methylation with the majority of CpG sites methylated. Finally, I analysed the demethylation of *14-3-3 σ* *in vitro* by 5-Aza-2'-deoxycytidine treatment and subsequent *14-3-3 σ* expression analysis to deduce whether demethylation of the gene can result in its re-expression.

14-3-3 σ expression analysis in colorectal cancer cell lines by qRT-PCR and Western blot analysis demonstrated that there were higher levels of *14-3-3 σ* expression at both the mRNA and protein level in the unmethylated cell lines HT29 and HCT116 compared to the methylated cell lines SW480 and Colo320DM. More specifically, the data showed that the unmethylated cell lines expressed approximately 400-fold higher mRNA levels than the methylated cell lines. Therefore, this suggests that there could be an association between *14-3-3 σ* methylation status and expression *in vitro*. However, analysis in a larger sample set of *14-3-3 σ* methylated and unmethylated colorectal cell lines is needed to confirm this.

In human tissues, the majority of *14-3-3 σ* unmethylated tumours had higher levels of expression compared to matched normal mucosa tissues. At the mRNA level, the higher levels however, were not significantly different from the expression levels in normal tissue possibly due to the small number of samples analysed and the anomalous finding in one of the samples. It is therefore unclear whether loss of *14-3-3 σ* methylation is associated with higher expression levels in the colorectal tumours compared to the matched normal tissues examined. Analysis of a larger number of colorectal tumours and matched normal mucosa samples is required in order to fully determine whether there is any associated change in *14-3-3 σ* expression levels.

When comparing the expression of *14-3-3 σ* mRNA in unmethylated tumours with methylated tumours, there were significantly higher levels of expression in the unmethylated tumours compared to the methylated tumours and western blot analysis also showed that there were higher levels of 14-3-3 σ protein in the majority of unmethylated tumours compared to the methylated tumours. Furthermore, there may be an association between the degree of *14-3-3 σ* methylation and expression in the subset of colorectal tumours examined by bisulphite sequencing individual clones. Tumours KR2 and KR3 (3.6% and 17.4% methylated CpGs respectively) expressed higher levels of 14-3-3 σ in comparison to tumours KR4 and KR11 (46.9% and 45.9% methylated CpGs respectively). Therefore, overall, these preliminary results suggest that *14-3-3 σ* methylation status is associated with 14-3-3 σ expression in colorectal tumours. Conversely, the tumour sample AM27, which was determined as unmethylated in the UPR of *14-3-3 σ* , did not express higher levels of 14-3-3 σ compared to other methylated tumours. As discussed previously, this result is difficult to explain, but may be due to other mechanisms involved in gene silencing, such as a rare control region SNP or other variants. Tumour sample KR8 displayed an opposite affect; methylation analysis in chapter 3 deduced that *14-3-3 σ* was methylated in the UPR. However, Western blot analysis showed that the tumour had higher levels of 14-3-3 σ protein similar to the unmethylated tumours. This anomalous finding may be a result of other genetic aberrations in the tumour such as Chromosome instability (CIN). Alternatively, these anomalous findings may be due to other mechanisms involved in regulating *14-3-3 σ* expression. These are discussed in more detail below.

Comparison of 14-3-3 σ protein levels in skin tissue and normal colon tissue using Western blot analysis determined that there were higher levels in skin tissue compared to normal colon tissue from colorectal patients. Chapter 3 demonstrated that the *14-3-3 σ* UPR was methylated in matched normal mucosa samples and normal mucosa from a cancer free individual had a higher percentage methylation level compared to the three skin tissues which were examined. Therefore, this suggests that in addition to colorectal tumours, *14-3-3 σ* methylation status and expression may also be associated in normal tissues. Indeed, this has been

demonstrated in a previous report in which cell type-specific expression of *14-3-3σ* was found to be regulated by epigenetic mechanisms including *14-3-3σ* CpG island methylation (Oshiro et al, 2005). In this published study, *14-3-3σ* expression analysis was examined in skin keratinocytes rather than whole skin tissue. However, *14-3-3σ* was shown to be expressed in the skin keratinocytes and was associated with low levels of percentage CpG methylation in the *14-3-3σ* CpG island. In addition to skin keratinocytes; oral keratinocytes and airway, prostate and mammary epithelium positively express *14-3-3σ* and are associated with low levels of CpG island methylation. In contrast, *14-3-3σ* expression is absent in non-epithelial tissues such as chondrocytes, fibroblasts and lymphocytes and is associated with high levels of *14-3-3σ* CpG island methylation (Oshiro et al, 2005). Further details of this study are discussed below.

An important observation from the expression analysis in clinical samples is that *14-3-3σ* is maintained at low levels in normal colonic mucosa tissues and in some tumours despite being methylated in the UPR. In addition to the effect of small sample numbers, this finding contributed to the overall the analysis of differences in expression between methylated and unmethylated samples *in vivo*. It would be expected that normal tissues and tumours which are methylated in the UPR of *14-3-3σ* would express negligible levels of *14-3-3σ* or indeed none at all. This lack of tight association *in vivo* may be due to tissue heterogeneity (as discussed in chapter 3). Cell type heterogeneity in both the tumours and normal tissues could be resolved by re-analysing *14-3-3σ* expression in microdissected samples. Alternatively, *14-3-3σ* expression could be analysed by immunohistochemistry. Expression analysis in both tumour and matched normal sections would determine which cell types express *14-3-3σ*. During the course of this PhD, I attempted to examine *14-3-3σ* expression on a number of tumours and matched normal colorectal tissue sections by immunohistochemistry. However, due to problems with antibody specificity the technique was not fully optimised. One previous study which analysed the expression of *14-3-3σ* in colorectal tumour sections by immunohistochemistry found diffuse immunoreactivity in the cytoplasm of normal epithelial crypts (Ide et al,

2004). No staining was observed in surrounding stromal cells. Interestingly, the majority of tumours displayed positive expression for 14-3-3 σ however, stronger staining was observed in the invasion front and to a lesser extent in other areas of the tumour (Ide et al, 2004). This study firstly indicates that normal colonic epithelial cells in the tissue are probably responsible for the observed 14-3-3 σ expression and not from other cell types. Secondly, the study also demonstrated that 14-3-3 σ was expressed in the majority of colorectal tumours examined. The authors believed that there was no association between 14-3-3 σ methylation status and expression as low levels of 14-3-3 σ methylation was observed even in microdissected immunohistochemically negative areas of the tumour. This is not in complete agreement with the preliminary findings presented in this chapter, however it should be recognised that this is in comparison to only one other study and therefore further analysis is required. It should also be considered that the expression observed in the corresponding normal tissues may be due to contaminating tumour cells or field cancerisation effects. However, the analysis of 14-3-3 σ expression in normal colonic mucosa from a patient free from cancer carried out in this chapter suggests that this may not be the case since the expression levels in the normal colonic tissues from colon cancer patients and the non-colon cancer patient were very similar. Two separate studies which examined the level of 14-3-3 σ expression in colorectal cancer and corresponding normal mucosa tissue (but not 14-3-3 σ methylation status) found that 14-3-3 σ at both the mRNA and protein level was expressed at higher levels in colorectal cancer compared to normal tissue (Perathoner et al, 2005; Tanaka et al, 2004). As with the study by Ide et al, positive staining was observed in the majority of colorectal tumours, however immunohistochemical analysis of staining intensity and percentage of positively stained tumour cells showed that high levels of 14-3-3 σ expression occurred in 38.8% of cases (n =121). Furthermore, there was a significant correlation of 14-3-3 σ expression with tumour differentiation (p =0.001) and tumour stage (p =0.003), suggesting that 14-3-3 σ may be involved in tumour progression (Perathoner et al, 2005). These expression studies are somewhat in agreement with the findings in this chapter. The low level of 14-3-3 σ expression in the normal mucosa and in the majority of colorectal tumours may be the base-line level of expression despite 14-3-3 σ being methylated in the UPR. An increase in expression

from the base-line level is then observed in a small proportion of colorectal tumours, and this may be associated with lower levels of methylation at the UPR. Similar 14-3-3 σ expression analysis in a larger dataset of methylated and unmethylated colon tumours and corresponding normal tissues would provide further insight.

Since 14-3-3 σ expression is observed in methylated normal tissues and colorectal tumours, this suggests that mechanisms in addition to, or indeed instead of CpG methylation, may be involved in regulating 14-3-3 σ expression. A generally held view is that methylation in the promoter region of genes is not the only epigenetic level of gene expression regulation, as discussed in the introduction of this thesis. MBD protein recruitment to the methylated promoter region and subsequent histone modifications may also be involved (Jones et al, 1998; Nan et al, 1998). It would be interesting to investigate MBD occupancy and the acetylation state of histones H3 and H4, which are associated with the 14-3-3 σ CpG island using Chromatin immunoprecipitation (ChIP) assays. Furthermore, H3K9 methylation, chromatin structure and downstream effects on transcription factor accessibility at the 14-3-3 σ promoter region could also be examined. The report by Oshiro et al strongly suggests that in cancer, deregulation at the 14-3-3 σ promoter may also be a result of aberrant changes in other levels of epigenetic control as well as CpG island methylation (Oshiro et al, 2005). The study demonstrated that cell type-specific expression of 14-3-3 σ is associated with DNA methylation, histone modifications and changes in chromatin structure at the CpG island region (Oshiro et al, 2005). Indeed, the 5-Aza-2'-deoxycytidine studies carried out in this chapter support the notion that other mechanisms may be involved in regulating 14-3-3 σ expression since the demethylation of the 14-3-3 σ gene following 5-Aza-2'-deoxycytidine treatment did not result in re-expression of the gene in either of the methylated cell lines. In addition to demethylation, the effects of histone acetylation could be investigated further by treating colorectal cancer cell lines with a combination of 5-Aza-2'-deoxycytidine and the deacetylating agent TSA. Similar experiments in methylated prostate cancer cell lines have however shown that 5-Aza-2'-deoxycytidine treatment alone, can induce 14-3-3 σ mRNA expression, with one cell line displaying an approximate 10-fold increase compared to control cells (Mhawech et al, 2005). This,

as well as the fact that the experiments conducted here were only carried out once, suggests that further optimisation of the technique may be required before exploring the effects of the combined treatment mentioned above. In hindsight, it would have also been beneficial to have analysed alongside the *14-3-3 σ* gene, another gene which is known to be re-expressed in cell lines following 5-Aza-2'-deoxycytidine treatment. This could have acted as a positive control for the experiment, testing the specificity of *14-3-3 σ* re-expression following treatment, and perhaps providing further evidence to suggest whether the optimal conditions were established. It should also be noted that 5-Aza-2'-deoxycytidine is very toxic to mammalian cells (Juttermann et al, 1994) and is non-specific, demethylating many genes which could counter the expected effect on *14-3-3 σ* in the colorectal cancer cells.

Whilst these preliminary results indicate that there is a significant difference in *14-3-3 σ* expression in unmethylated tumours and methylated tumours, further expression analysis *in vivo* is required to conclusively determine whether *14-3-3 σ* methylation is associated with expression in colorectal cancer. Furthermore, the findings in this chapter and previous studies suggest that other epigenetic mechanisms, including CpG methylation may be involved in regulating *14-3-3 σ* expression, such as histone modifications and chromatin re-modelling. Additional studies investigating these mechanisms at the *14-3-3 σ* promoter in colorectal cancer would perhaps provide further insight.

The mechanism leading to aberrant methylation of gene promoters in cancer is under intensive investigation. It is possible that difference in *14-3-3 σ* methylation status observed in colorectal tumours is not a *14-3-3 σ* specific effect but in fact related to other generalised aberrant methylation phenotypes, such as genome-wide demethylation or CIMP. Hence, the specificity of *14-3-3 σ* hypomethylation in colorectal cancer is investigated in chapter 5.

Chapter 5

Specificity of 14-3-3 σ hypomethylation in colorectal cancer

5.1 Introduction

The results of experimental work that I presented in chapter 3 suggest that there may be a tumour-specific loss of 14-3-3 σ UPR methylation in approximately 10% of colorectal tumours. Furthermore, I have shown that the loss of methylation or indeed *hypomethylation* of 14-3-3 σ in some colorectal tumours was associated with higher levels of 14-3-3 σ mRNA expression and increased protein levels compared to the methylated tumours. The hypothesis I wish to test in this chapter is that the demethylation of 14-3-3 σ in colorectal cancer is specific to the 14-3-3 σ gene and not a result of more general methylation phenomenon. Thus, the aim of this chapter is to determine whether loss of methylation in the 14-3-3 σ UPR is associated with global hypomethylation or the CIMP phenotype (Toyota et al, 1999a). The degree of 5-methylcytosine content has been quantified by a technique known as Nearest Neighbor analysis (Ramsahoye, 2002) in colorectal cancer cell lines and colorectal tumours. 14-3-3 σ UPR methylated and 14-3-3 σ UPR unmethylated cell lines and tumours were investigated to determine whether 14-3-3 σ hypomethylation is a result of genome-wide demethylation or is specific to the gene 14-3-3 σ . CIMP analysis in a small number of colorectal tumours has also been carried out using MethyLight, a Taqman-based methylation technique (Eads et al, 2000). CIMP phenotype for 14-3-3 σ UPR methylated and unmethylated tumours were determined by examining the methylation status of 4 CIMP markers (Toyota et al, 1999a), and from this any associations between 14-3-3 σ methylation status and CIMP were deduced.

5.2 Methodology

5.2.1 Nearest Neighbor Analysis

DNA from HT29 and SW480 cell lines and DNA from tumours KR2, KR3, KR10 & KR12 were subjected to Nearest Neighbor analysis as described in 2.8.2. The technique was carried out with assistance from Dr Bernard Ramsahoye (Cancer Research UK, University of Edinburgh) who developed the procedure. Figure 5.1 illustrates the outline of the procedure in more detail. Briefly, the restriction endonuclease *MboI*(GATC) was used to cut DNA and [α - 32 P] dGTP was used to end label the DNA using Klenow. Following the digestion of labelled DNA to deoxyribonucleotide 3'-monophosphates (dNps), the radio-labelled 5' α -phosphate of the [α - 32 P] appears as the 3' phosphate of the nucleotide (X) that was immediately 5' to it in the DNA – its nearest neighbor. Therefore, as labelling is template dependent, the frequencies of labelled dNps (dCp, dTp, dGp, dAp and 5mdCp) reflect the relative amounts of dinucleotides (XpG): dCpG, dTpG, dGpG, dApG and 5mdCpG at the *MboI* restriction sites. Radio-labelled dNps were separated, visualised and quantified following two-dimensional TLC and subsequent phosphorimaging (Ramsahoye, 2002). This technique has been previously used in a number of different reports to measure the level of methylated CpG (5mdCpG) compared to unmethylated CpG (dCpG) across an entire genome (Meissner et al, 2005; Ramsahoye et al, 2000; Tollefsbol & Hutchison, 1998). In order to verify the efficiency and specificity of the Nearest Neighbor technique, control experiments were performed during the optimisation of the technique (Dr Bernie Ramsahoye, personal correspondence). Firstly, to test that a global change in CpG methylation can be detected using Nearest Neighbor analysis, *DNMT3a*^{-/-} /*DNMT3b*^{-/-} early passage ES cells prior to and following the expression of a short-hairpin RNAi molecule specific for *DNMT1*, were applied to the technique (Figure 5.2). Wild-type, early passage ES cells display CpG methylation levels of approximately 65% (Jackson et al, 2004). In comparison, *DNMT3a*^{-/-} /*DNMT3b*^{-/-} early passage ES cells display overall levels of approximately 35% CpG methylation (Figure 5.2 (A)) and following the expression of the *DNMT1* short-hairpin RNAi (shRNAi) any residual CpG methylation is removed to 2% (Figure 5.2 (B)). Secondly, to further confirm the

specificity of the technique, a PCR product, which is known to be unmethylated (as only dCTP and not 5mdCTP was included in the dNTP mix) was applied. Figure 5.3 (A) shows that there is no labelling of the 5mdCp spot, as no 5mdCp is present. The same PCR product was also spiked with transfer RNA (tRNA) to ensure that the 5mdCp spot was not due to the presence of a ribonucleotide (Figure 5.3 (B)). Overall, these experiments confirm that Nearest Neighbor analysis can be used to specifically and efficiently determine global methylation changes in a given DNA sample.

5.2.2 MethyLight Analysis

Four CIMP markers; *hMLH1*, *CDKN2A (p16)*, *MINT1* and *MINT2* were analysed for methylation in tumours 1924, 10811, 10812, KR10, 8117, KR3, KR8, 7867, 7329 & 7007 using MethyLight analysis as described in section 2.8.1. At present there is no consensus definition for the CIMP panel, therefore it was decided to use four of the five classical CIMP markers (*hMLH1*, *CDKN2A (p16)*, *MINT1*, *MINT2* and *MINT31*) defined by Issa (Issa, 2004). The choice of these markers to study CIMP in the tumours listed above are discussed in the final section of this chapter. MethyLight utilises fluorescence-based real time PCR (TaqMan[®]) technology and is a high-throughput methylation assay, which has a high degree of sensitivity (Eads et al, 2000). The assay is semi-quantitative and determines the relative frequency of a particular pattern of DNA methylation rather than quantifying all methylation occurrences of CpG dinucleotides in a genomic DNA sample. The primers and fluorescent probes designed for this study overlap potential sites of DNA methylation at CpG sites following bisulphite treatment of the DNA. Hence, sequence discrimination of the CIMP markers occurs at both the level of PCR amplification and at the level of probe hybridisation. For the control reaction (β -actin), neither the primers or probe overlies any CpG sites, therefore the PCR reaction is unbiased and acts as a control for the amount of bisulphite treated DNA input. The semi-quantification for each individual CIMP marker was determined relative to the β -actin control reaction. The percentage methylated reference (PMR – the degree of methylation) was calculated by dividing this relative value by the methylation level of the CIMP marker in fully methylated CpGenome DNA (which is presumably

100% methylated), and multiplied by 100. PMR values for each CIMP marker were calculated in each individual tumour. Verification of methylated tumours for each CIMP marker and determination of whether the tumour is CIMP positive or negative was based on the report by Weisenberger et al (Weisenberger et al, 2006). PMR values above 10 for a given sample and locus were considered positive for methylation. A sample, which was CIMP positive, was defined if it has ≥ 3 of the 4 CIMP markers with positive methylation (PMR >10). If the samples has ≤ 2 of the 4 CIMP markers with positive methylation (PMR >10) then it was considered to be CIMP negative.

5.2.3 Colorectal cancer cell lines

DNA was purified from the colorectal cancer cell lines SW480 and HT29 as described in 2.2.1.

5.2.4 Patient samples

DNA was purified from fresh KR colorectal tumour samples as described in 2.2.1. Other DNA samples were obtained directly from laboratory stocks. For MethyLight analysis purified tumour DNA was subsequently subjected to bisulphite treatment as described in 2.4.2 before analysis.

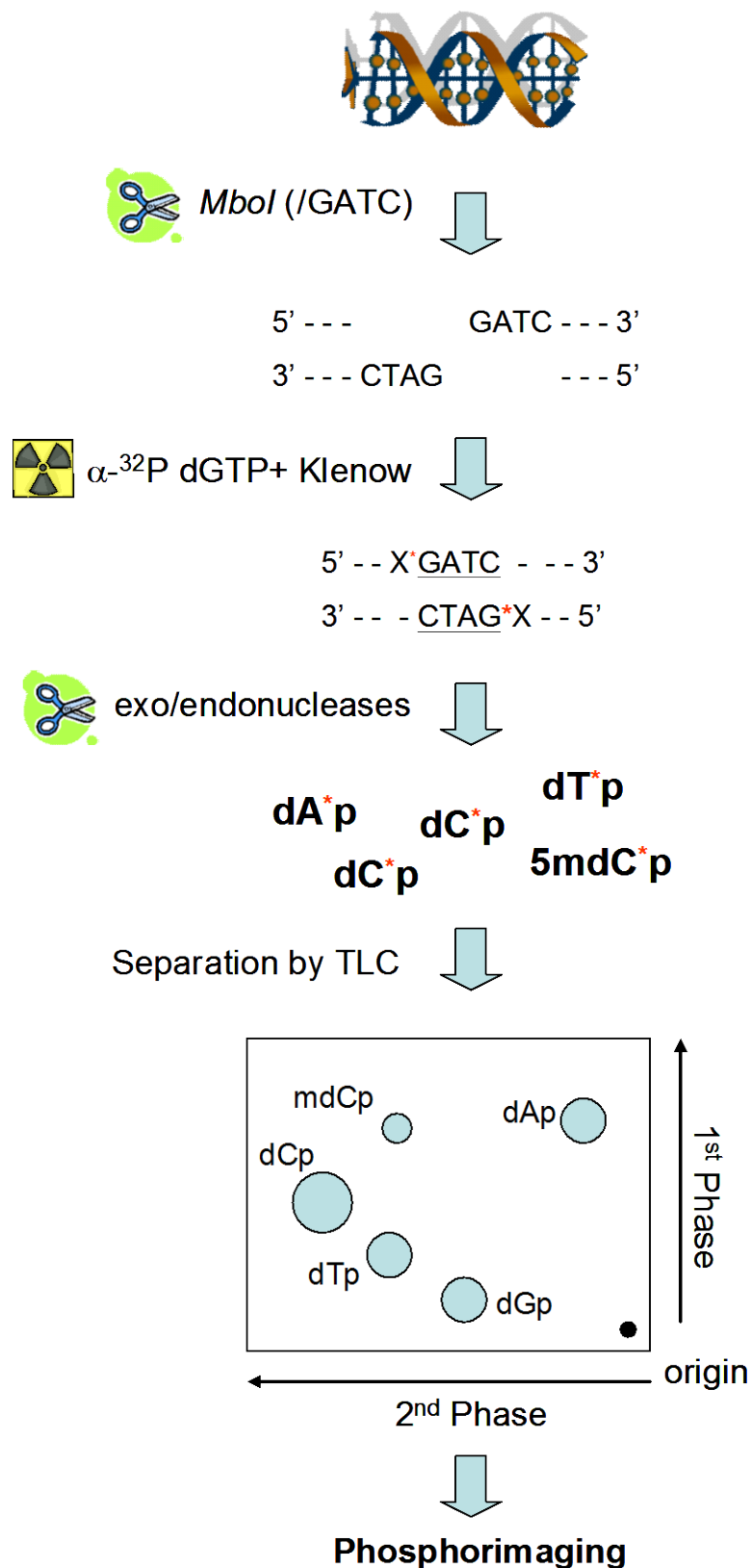
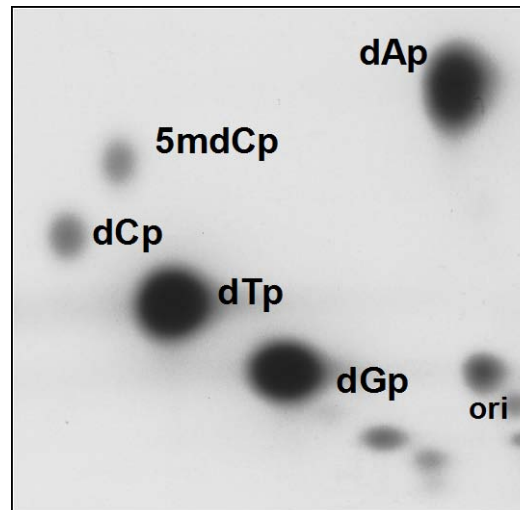


Figure 5.1: Nearest Neighbor analysis *Mbol* is used to cut DNA and [α -³²P] dGTP was used to end label the DNA at the restriction cut sites using Klenow. Labelled nucleotides (X) are marked * and filled in nucleotides are underlined. Radio-labelled 5' α -phosphate of the [α -³²P] dGTP appears as the 3' phosphate of the nucleotide (X) that was immediately 5' to it in the DNA – its 'nearest neighbor'. Labelled double-stranded DNA was digested to dNps by a mixture of exo/endonucleases. Frequencies of labelled dNps (dCp, dTp, dGp, dAp and 5mdCp) reflect the relative amounts of dinucleotides (XpG): dCpG, dTpG, dGpG, dApG and 5mdCpG at the *Mbol* restriction sites. Radio-labelled dNps were separated, visualised and quantified following two-dimensional thin-layer chromatography (TLC) and subsequent phosphorimaging (Ramsahoye, 2002).

(A) *DNMT3a*^{-/-}/*DNMT3b*^{-/-} ES cells



(B) *DNMT3a*^{-/-}/*DNMT3b*^{-/-} ES cells + *DNMT1* shRNAi

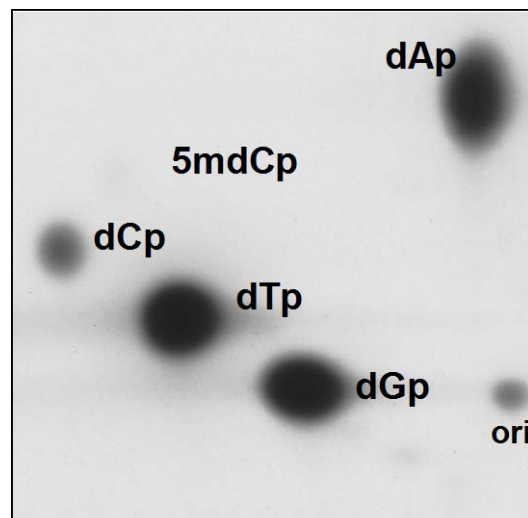
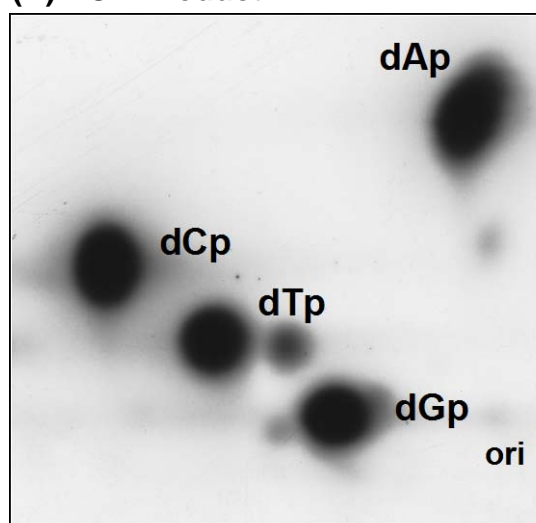


Figure 5.2: Control experiment for testing the efficiency of Nearest Neighbor analysis: Nearest Neighbor analysis of DNA from *DNMT3a*^{-/-}/*DNMT3b*^{-/-} early passage ES cells (A) and following expression of a short-hairpin (sh) RNAi molecule specific for *DNMT1*, (also early passage ES cells) (B). Autoradiographs indicate a removal of most residual methylation following *DNMT1* shRNAi expression. *Mbol* was used to cut the DNA and [α -³²P] dGTP and klenow were used to end label the DNA. Labelled DNA was digested to dNPs by a mixture of exo/endonucleases and separated by TLC. Phosphorimaging was subsequently used to visualise and quantify the labelled dNPs. (dNPs are indicated, origin of application for two-dimensional chromatography (ori). Other spots may be indicative of diphosphates or deoxyribose phosphates).

(A) PCR Product



(B) PCR Product + tRNA

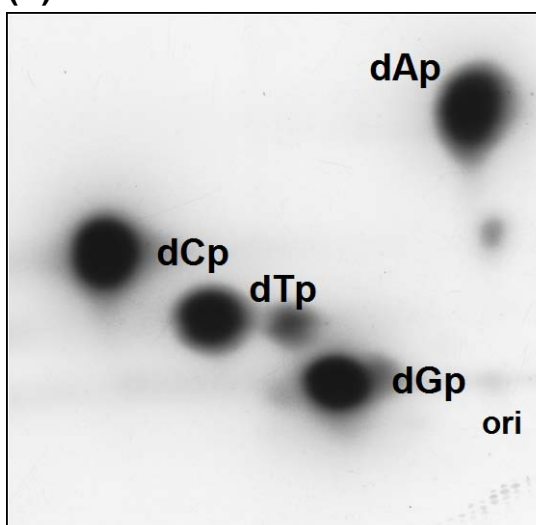


Figure 5.3: Control experiment for testing the specificity of Nearest Neighbor analysis: Nearest Neighbor analysis of a PCR product (A) and the same PCR product spiked with tRNA (B) indicates absence of 5mdCp spot in both samples. (dNps are indicated, origin of application for two-dimensional chromatography (ori). Other spots may be indicative of diphosphates, deoxyribose phosphates or impurities from the dNTP mix).

5.3 Results

5.3.1 Global levels of 5-methylcytosine in colorectal cancer cell lines and tumours

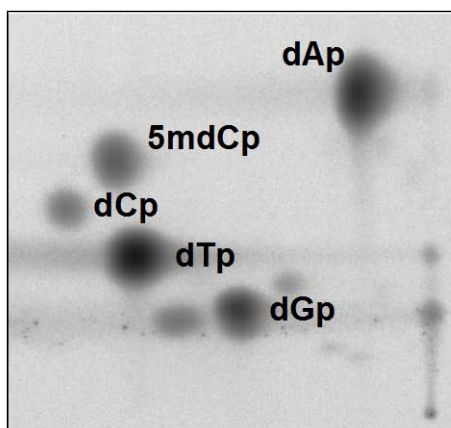
Levels of CpG methylation were first quantified in the two colorectal cancer cell lines HT29 and SW480 using Nearest Neighbor analysis. Figure 5.4 shows autoradiographs from the two cell lines of labelled dNps following separation by two-dimensional TLC. The relative intensities of the spots indicates the frequencies of dinucleotide XpG at *Mbo*I cut sites. The intensities of the spots were quantified by first subtracting the background intensities from dCp and 5mdCp. Percentage 5mdCp was calculated from the following equation:

$$\% \text{ 5mdCp} = \frac{\text{5mdCp}}{\text{5mdCp} + \text{dCp}}$$

Analysis of the nearest neighbors of 5-methylcytosine at *Mbo*I cut sites in the *14-3-3 σ* unmethylated cell line HT29 and the *14-3-3 σ* methylated SW480 colorectal cancer cell line demonstrates that 70.8% of CpG sites were methylated in the HT29 cell line compared to 79.4% of CpG sites in the SW480 cell line (Table 5.1). A recent report has estimated a 70 to 80% CpG methylation content in non-malignant somatic cells (Yegnasubramanian et al, 2008). Therefore, this suggests that neither of the cell lines examined are globally demethylated. Nearest Neighbor analysis was then carried out in colorectal tumours KR2 and KR3 (*14-3-3 σ* UPR unmethylated) and KR10 and KR12 (*14-3-3 σ* UPR methylated). Autoradiographs of labelled dNps following separation by two-dimensional TLC from the four colorectal tumours are shown in Figure 5.5. Nearest neighbors of 5-methylcytosine at *Mbo*I cut sites were quantified as described previously. 80.4% and 63% of CpG sites were methylated in the *14-3-3 σ* unmethylated tumours KR2 and KR3 respectively (Table 5.1). 71.2% and 68% of CpG sites were methylated in the *14-3-3 σ* methylated tumours KR10 and KR12 respectively (Table 5.1). As a reduction in global levels of CpG methylation was detected in both the *14-3-3 σ* methylated and unmethylated tumours, this suggests that a reduction in global levels of methylation may be independent of *14-3-3 σ* demethylation in the tumours examined. Percentage levels of 5-methylcytosine

for the individual colorectal cancer cell lines and tumours are illustrated in Figure 5.6. Overall, these studies suggest that in the samples examined, there is no relationship between global methylation levels and the specific methylation status of *14-3-3 σ* itself.

SW480



HT29

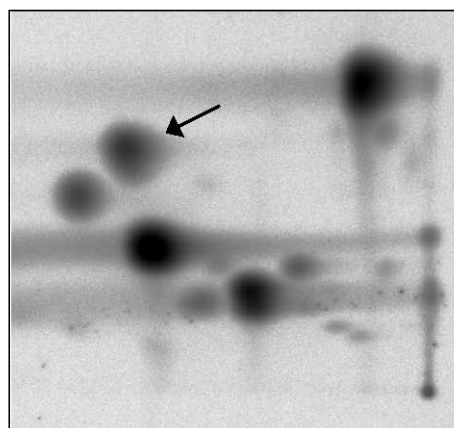
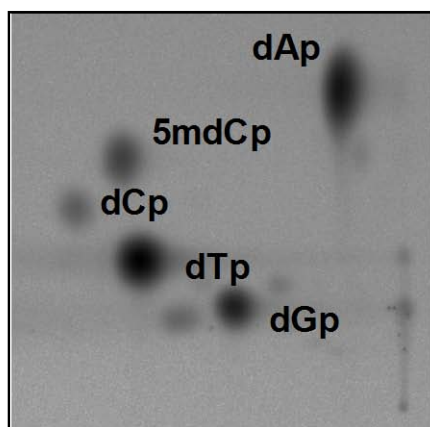
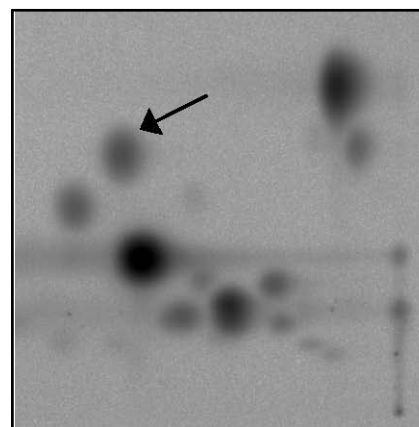


Figure 5.4: Autoradiographs of labeled dNPs after separation by two-dimensional TLC from colorectal cancer cell lines SW480 (*14-3-3 σ* UPR methylated) and HT29 (*14-3-3 σ* UPR unmethylated). dNPs are indicated in one autoradiograph. An arrow in the second autoradiograph indicates position of 5mdCp.

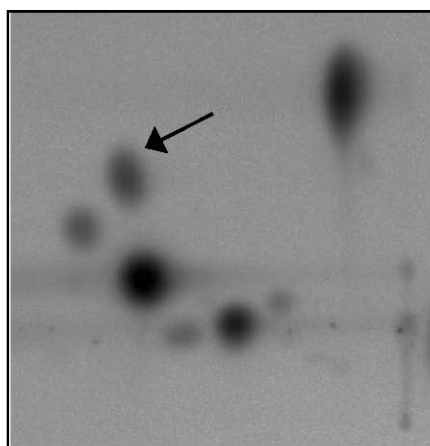
KR2



KR3



KR10



KR12

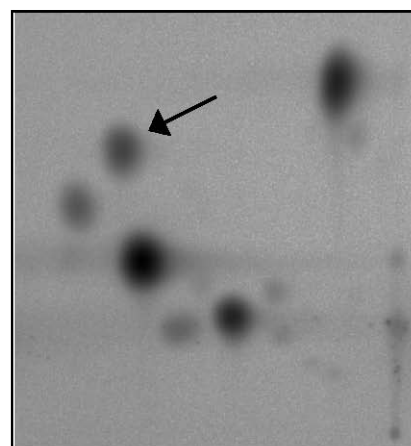


Figure 5.5: Autoradiographs of labeled dNps after separation by two-dimensional TLC from colorectal tumours. KR2 and KR3 (*14-3-3 σ* UPR unmethylated), KR10 and KR12 (*14-3-3 σ* UPR methylated). dNps are indicated in one autoradiograph, an arrows indicates position of 5mdCp in subsequent autoradiographs.

	HT29	SW480	2T	3T	10T	12T
Background	1615.5	676.1	13722.1	7397.3	14860.1	10484.3
dCp	81670.6	7830.6	37149.7	45232.6	60154.2	46860.9
5mdCp	195703	28248	109834.9	71748.2	126725.3	90037.3
dCp - Background	80055.1	7154.5	23427.6	37835.3	45294.1	36376.6
5mdCp - Background	194087.5	27571.9	96112.8	64350.9	111865.2	79553
total C	274142.6	34726.4	119540.4	102186.2	157159.3	115929.6
% 5mdCp	70.8	79.4	80.4	63.0	71.2	68.6

Table 5.1: Phosphorimaging quantification of intensities of spots (dNps) and subsequent calculation of percentage 5mdCp, which reflects the percentage of 5mdCpG in colorectal cancer cell lines and colorectal tumours.

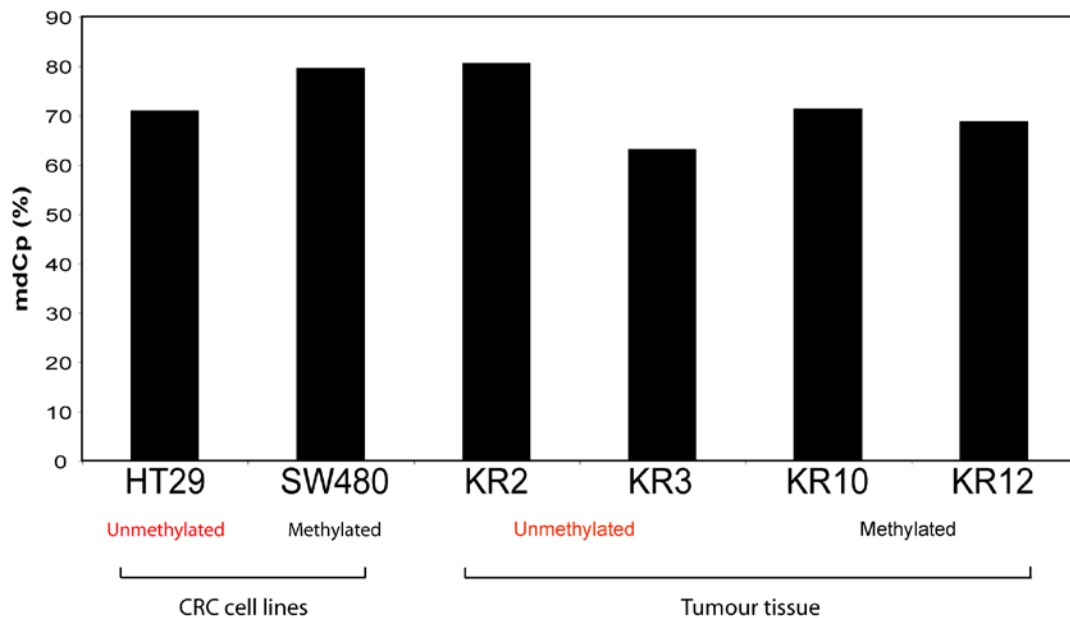


Figure 5.6: Percentage CpG methylation in colorectal cancer cell lines and colorectal tumours. Methylation status of 14-3-3σ UPR is indicated for each sample.

5.3.2 CIMP analysis in colorectal tumours

MethyLight, a Taqman[®] based real time PCR assay was used to assay for the presence of CIMP in 5 $14\text{-}3\text{-}3\sigma$ UPR unmethylated colorectal tumours and 5 $14\text{-}3\text{-}3\sigma$ UPR methylated tumours. The CIMP marker panel consisted of *MLH1*, *CDKN2A*, *MINT1*, and *MINT2*. MethyLight analysis of *MLH1* methylation status in the 10 tumours showed that only one tumour sample (KR3) was positive for methylation of *MLH1* with a PMR value >10 (Table 5.2) (Figure 5.7). The PMR value was markedly above the PMR cut-off value and therefore is a strong positive result for methylation. Furthermore, previous bisulphite sequencing analysis of *MLH1* methylation (data not shown), has demonstrated that the tumour sample KR3 is fully methylated in the promoter region and the majority of other tumour samples (including KR8, which was examined in this chapter for *MLH1* methylation) is unmethylated, thus supporting the validity of the MethyLight assay. Interestingly, the PMR value for tumour sample KR3 was higher than the CpGenome DNA sample, which is presumably fully methylated. KR3 and KR10 also displayed higher PMR values than the CpGenome DNA sample for the CIMP markers *CDKN2A* and *MINT1*. This has previously been described in a number of reports (Friedrich et al, 2004; Siegmund & Laird, 2002), and is thought to be a result of fluctuations in the real time PCR measurements or due to incomplete methylation of the DNA reference sample (CpGenome DNA). Alternatively, this finding may also be a result of a high copy number variation of the gene locus of interest. MethyLight analysis of tumours for *CDKN2A* methylation demonstrated that two tumours KR3 and KR10 were positive for methylation with PMR values above the cut-off value therefore indicating positive methylation (Table 5.3) (Figure 5.8). Analysis of methylation of the *MINT1* locus in the tumours showed that 4/10 were positive for methylation (Table 5.4) (Figure 5.9). KR3 and KR10 demonstrated high PMR values. It should be noted however, that there were high levels of variability for tumour KR10 thus the PMR value may not be as high as is illustrated in Figure 5.9. Variability of the MethyLight assay has been previously reported and it is thought that this may be a result of stochastic PCR amplification which can occur at low template concentration (Eads et al, 2000). Tumours KR8 and 7329 displayed lower PMR values respectively, with tumour sample 7329 only just being above the PMR cut-off value

of 10. Finally, MethyLight analysis of the *MINT2* locus for methylation in the tumours demonstrated that 5/10 tumours were positive for methylation with a PMR >10. Table 5.5 and Figure 5.10 show that the tumour samples KR3, KR10, 1924, 10811 and 7007 were positive for *MINT2* methylation with high PMR values.

Following the analysis of the four individual CIMP markers for methylation in the colorectal tumours, the CIMP phenotype was determined for each sample. Table 5.6 summarises the results from the MethyLight analysis and the CIMP status for each tumour. 2/10 tumours were CIMP positive: KR3 and KR10. KR3 displayed positive methylation for all four of the CIMP markers. KR10 displayed positive methylation for *CDKN2A*, *MINT1* and *MINT2* CIMP markers. All other tumours analysed were CIMP negative with either one or no CIMP markers positive for methylation. For the two CIMP positive tumours, KR3 is a *14-3-3 σ* UPR unmethylated tumour and KR10 is a *14-3-3 σ* UPR methylated tumour. Therefore, this study suggests there is no relationship between *14-3-3 σ* UPR methylation status and CIMP in the colorectal tumour sample set examined.

Sample	PMR
CpG (100%)	100
1924	0
10811	0
10812	0
KR10	4.13
8117	0
KR3	429.27
KR8	0
7867	0.06
7329	0
7007	0

Table 5.2: MethyLight analysis of *MLH1* methylation status in colorectal tumours. Tumours with positive *MLH1* methylation (PMR > 10) are highlighted. CpG (100%) = fully methylated CpGenome DNA.

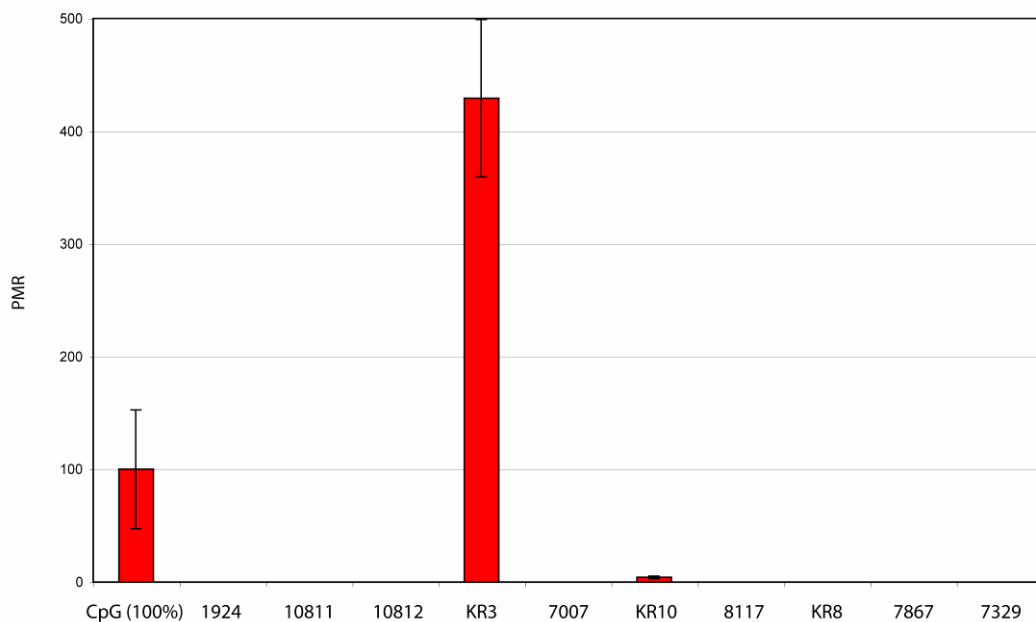


Figure 5.7: MethyLight analysis of *MLH1* methylation status in colorectal tumours. The results are the means of duplicate results \pm standard errors. CpG (100%) = fully methylated CpGenome DNA.

Sample	PMR
CpG (100%)	100
1924	0.14
10811	0
10812	0.02
KR3	52.13
7007	0.37
KR10	353.92
8117	0.10
KR8	0.50
7867	0.01
7329	0.35

Table 5.3: MethyLight analysis of *CDKN2A* methylation status in colorectal tumours. Tumours with positive *CDKN2A* methylation (PMR > 10) are highlighted. CpG (100%) = fully methylated CpGenome DNA.

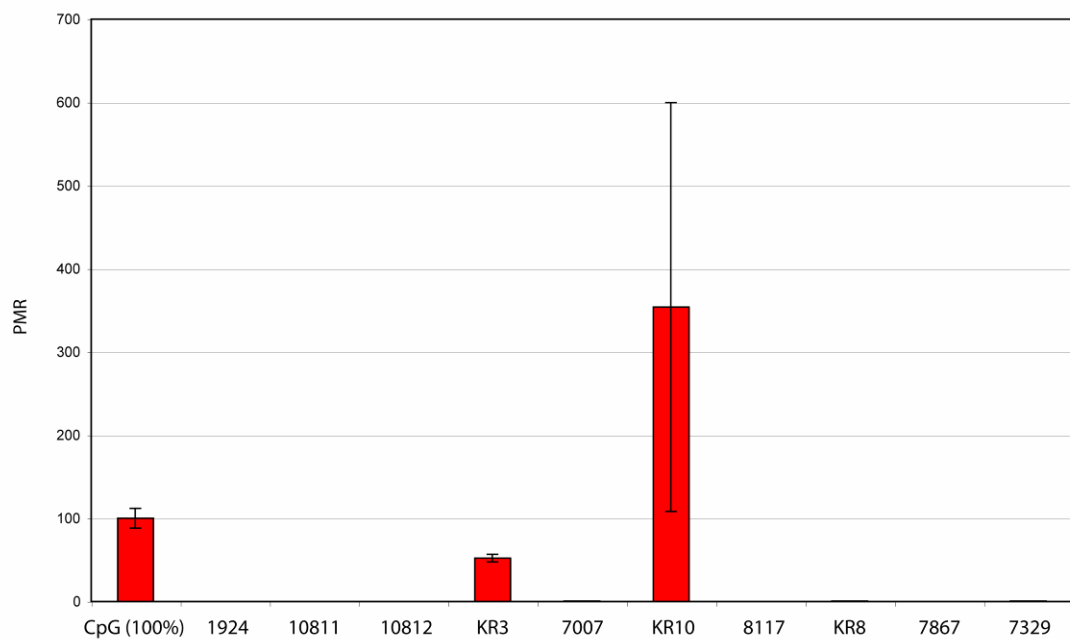


Figure 5.8: MethyLight analysis of *CDKN2A* methylation status in colorectal tumours. The results are the means of duplicate results \pm standard errors. CpG (100%) = fully methylated CpGenome DNA.

Sample	PMR
CpG (100%)	100
1924	6.58
10811	0
10812	0
KR3	500.26
7007	0
KR10	192.73
8117	1.88
KR8	16.59
7867	6.00
7329	11.18

Table 5.4: MethyLight analysis of *MINT1* methylation status in colorectal tumours. Tumours with positive *MINT1* methylation (PMR > 10) are highlighted. CpG (100%) = fully methylated CpGenome DNA.

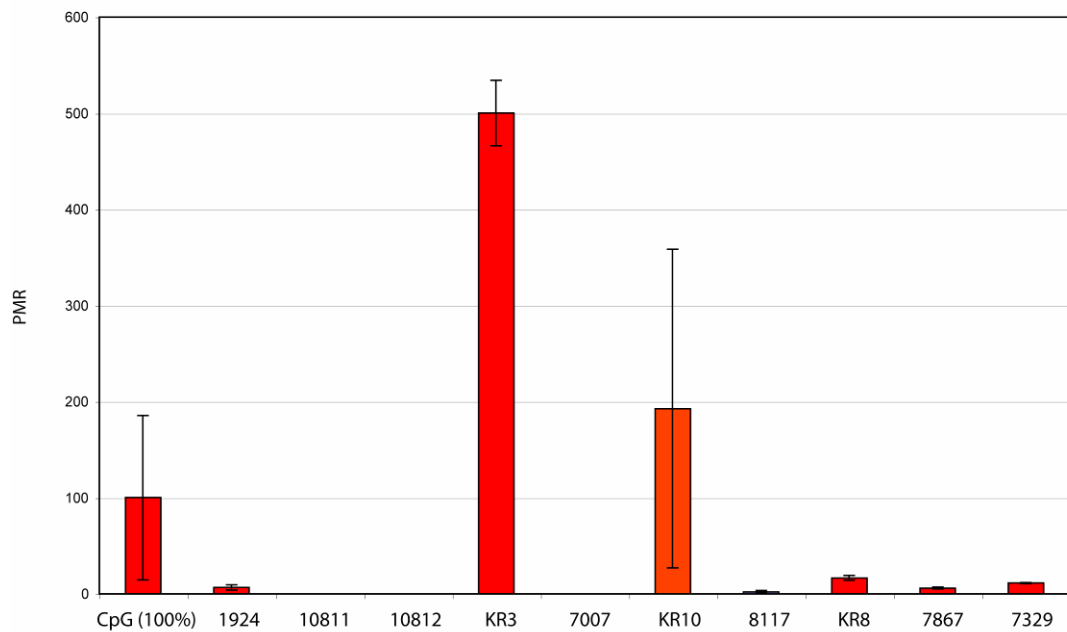


Figure 5.9: MethyLight analysis of *MINT1* methylation status in colorectal tumours. The results are the means of duplicate results \pm standard errors. CpG (100%) = fully methylated CpGenome DNA.

Sample	PMR
CpG (100%)	100
1924	38.83
10811	25.87
10812	5.81
KR3	47.93
7007	16.24
KR10	26.21
8117	0.42
KR8	5.54
7867	5.12
7329	3.07

Table 5.5: MethyLight analysis of *MINT2* methylation status in colorectal tumours. Tumours with positive *MINT2* methylation (PMR > 10) are highlighted. CpG (100%) = fully methylated CpGenome DNA.

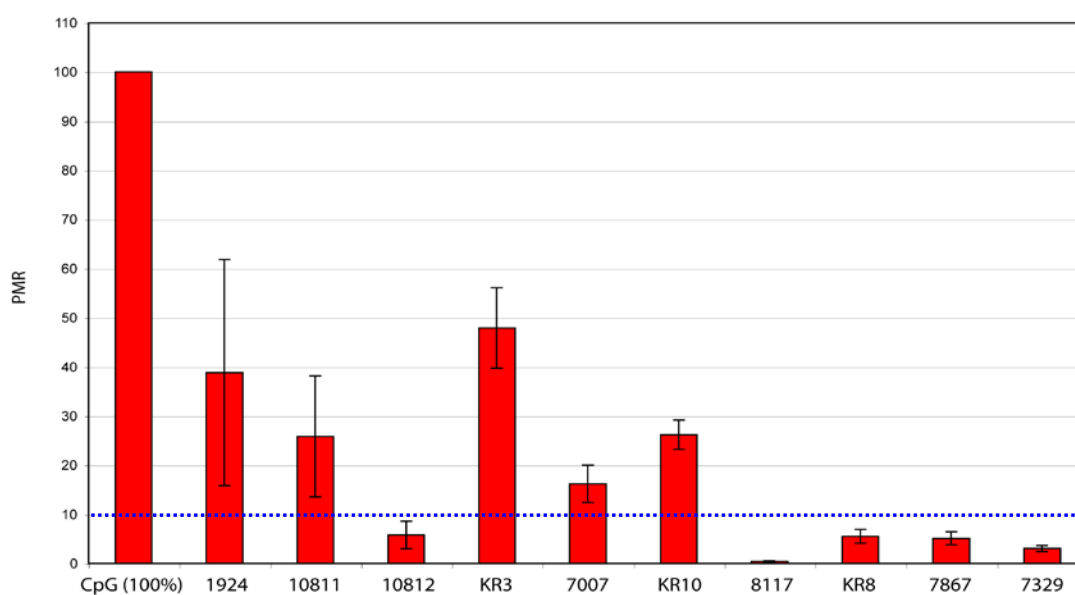


Figure 5.10: MethyLight analysis of *MINT2* methylation status in colorectal tumours. The results are the means of duplicate results \pm standard errors. CpG (100%) = fully methylated CpGenome DNA. Blue dashed line indicates PMR cut-off value.

Sample	14-3-3 σ Methylation Status	MLH1	CDKN2A	MINT1	MINT2	CIMP Phenotype
1924	Unmethylated					NEGATIVE
10811	Unmethylated					NEGATIVE
10812	Unmethylated					NEGATIVE
KR3	Unmethylated					POSITIVE
7007	Unmethylated					NEGATIVE
KR10	Methylated					POSITIVE
8117	Methylated					NEGATIVE
KR8	Methylated					NEGATIVE
7867	Methylated					NEGATIVE
7329	Methylated					NEGATIVE

Table 5.6: MethyLight analysis of four CIMP markers *MLH1*, *CDKN2A*, *MINT1* and *MINT2* determines CIMP phenotype in colorectal tumours. 14-3-3 σ UPR methylation status is indicated for each tumour. Positive methylation of CIMP markers is indicated by filled red box. CIMP positive tumours = ≥ 3 markers methylated. CIMP negative tumours = ≤ 2 markers methylated.

5.4 Discussion

My aim for this chapter was to investigate the specificity of *14-3-3 σ* UPR hypomethylation in colorectal cancer. The percentage of methylated CpG levels were determined in *14-3-3 σ* UPR methylated and unmethylated colorectal cancer cell lines and tumours to examine whether there is relationship between *14-3-3 σ* hypomethylation and global levels of DNA methylation in colorectal cancer. The CIMP phenotype (Toyota et al, 1999a) was also investigated in a number of *14-3-3 σ* UPR methylated and unmethylated colorectal tumours to deduce any associations between CIMP and *14-3-3 σ* methylation status.

Nearest Neighbor analysis (Ramsahoye, 2002) suggested that there was no relationship between *14-3-3 σ* UPR methylation status and global levels of CpG methylation in the colorectal cancer cell lines or tumours studied. Further studies are however required to confirm these initial findings due to the small sample numbers. A previous study estimated that 70-80% of CpGs are methylated in non-malignant mammalian cells (Yegnasubramanian et al, 2008), thus suggesting that two of the four tumour samples examined by the Nearest Neighbor technique were globally hypomethylated (KR3T: 63%, KR12T: 68.6%). It should be noted that the technique utilised to measure methylated CpG content in the Yegnasubramanian et al study was different to the technique carried out in this thesis, therefore direct comparisons cannot be made. However, the data presented in this chapter shows that one potentially globally hypomethylated tumour was unmethylated in the UPR of *14-3-3 σ* (KR3T) and the other globally hypomethylated tumour was methylated (KR12T). Therefore, these preliminary findings suggest that *14-3-3 σ* hypomethylation in colorectal cancer may be a specific event and not due to the explanation that it is part of global methylation status as an epiphenomenon.

MethyLight analysis (Eads et al, 2000) was undertaken to determine the methylation status of CIMP markers MLH1, CDKN2A, MINT1 and MINT2 (Toyota et al, 1999b) in a number of colorectal tumours which I had defined with respect to *14-3-3 σ* methylation status. 2/10 (20%) colorectal tumours were determined as CIMP

positive, a similar frequency to previous reports (Weisenberger et al, 2006). One of the CIMP positive tumours was unmethylated at the *14-3-3 σ* UPR and the other tumour was methylated at the *14-3-3 σ* UPR. This suggested that there may be no relationship between *14-3-3 σ* methylation status and CIMP. However, CIMP analysis in a larger dataset is required in order to draw any firm conclusions and determine whether *14-3-3 σ* hypomethylation is independent of the CIMP phenotype in colorectal carcinomas.

The observations made here in colorectal cancer are in line with the results of Sato *et al* who proposed that *14-3-3 σ* hypomethylation and its associated overexpression in pancreatic cancer is gene-specific rather than a random result of genome-wide hypomethylation (Sato et al, 2003). Genome-wide effects have however been shown to activate the Melanoma Antigen 1 (*MAGE-1*) gene, indicating that genome-wide hypomethylation may be responsible for the activation of genes specifically involved in cancer (De Smet et al, 1996). This study used a similar approach to measure global levels of methylation, although only one tumour cell line was examined and no fresh tumour material was investigated. As previously discussed, colorectal cancer cell lines are highly selected for and therefore may not be wholly representative of the epigenetic architecture of colorectal tumours. Indeed, several studies have found that cancer cell lines generally have higher levels of CpG island hypermethylation and lower levels of 5-methylcytosine DNA content compared to primary tissue (Paz et al, 2003; Suter et al, 2003). The proportion of CpG dinucleotides that were methylated in colorectal cancer cell lines examined in this chapter were higher (HT29 70.8%, SW480 79.4%) relative to some of the tumour samples and compared to a previous report, which determined genome-wide hypomethylation levels in colorectal cancer cell lines by measuring LINE-1 methylation (Estecio et al, 2007). An average proportion of 46% CpG methylation (n = 10) was observed compared to the mean proportion of 75.1% presented in this chapter. The dissimilarities observed are probably due to the different techniques that were used and the difference in sample sizes. LINE-1 methylation is often measured to estimate the genome-wide demethylation level as it has been shown to correlate with global DNA methylation levels (Weisenberger et al, 2005; Yang et al, 2004). Nearest Neighbor analysis

utilised in this chapter on the other hand, measures the level of methylation of a specifically methylated CpG dinucleotide in a given DNA sample. Therefore, the levels of methylation in a DNA sample can be quantified directly.

As mentioned previously, there are some discrepancies associated with CIMP analysis (Ogino et al, 2007; Toyota et al, 1999a; Yamashita et al, 2003). Firstly, whether it is actually a distinct phenotype and secondly if CIMP is a distinct phenotype, which methylated genes should be used to define it. Currently, there is no consensus definition for the CIMP panel in colorectal cancer. As this is the case, it was decided to investigate CIMP in a number of $14\text{-}3\text{-}3\sigma$ methylated and unmethylated colorectal tumours using a select number of markers first described by Jean-Pierre Issa (Issa, 2004). These markers have been previously shown to correlate with CIMP (Goel et al, 2007; Samowitz et al, 2005; Toyota et al, 1999b). A recent large-scale study however, showed that the MINT1, MINT2 and MINT31 loci were non-specific for BRAF mutated CIMP tumours, and therefore it was concluded that these markers may not be useful for CIMP analysis (Weisenberger et al, 2006). The authors of this study proposed a 'robust new marker panel' consisting of RUNX3, CACNA1G, IGF2, NEUROG1, and SOCS1 (Weisenberger et al, 2006). Another study tested the validity of these new proposed markers and that the found levels of specificity of each individual marker varied slightly compared to the report by Weisenberger et al. This study suggested that RUNX3 followed by CACNA1G, IGF2, MLH1, NEUROG1, CRABP1, SOCS1 and CDKN2A were the best individual markers to evaluate CIMP status (Ogino et al, 2007). MINT1, MINT2 and MINT31 were not examined in this study, however this was not because they were deemed inappropriate for the assessment of CIMP. MLH1 and CDKN2A were found to have 98% and 80% specificity respectively in this study (Ogino et al, 2007). The specificity of these two CIMP markers may also be reflected in the data presented in this chapter since fewer colorectal tumours were positively methylated for MLH1 and CDKN2A compared to the other CIMP markers MINT1 and MINT2. Interestingly, the two tumours determined as CIMP positive (KR3 and KR10) were the only tumours positive for CDKN2A methylation. In addition, only KR3 tumour was positive for MLH1 methylation and KR10, even though the tumour was not

positive for MLH1 methylation, had the next largest PMR value of 4.13. Moreover, KR3 had been previously determined as fully methylated in the *MLH1* promoter region by bisulphite sequencing, further establishing the high specificity of this specific CIMP marker. The dissimilarities observed between each published CIMP study are likely a result of differences in size and source of samples and differences in PCR conditions and primer design, which will affect the specificity and sensitivity of a particular marker. CIMP analysis is not absolute; therefore, methylation analysis of the other genes mentioned above, in addition to the ones examined in this thesis would improve the current study providing further insight into the CIMP status of *14-3-3 σ* methylated and unmethylated tumours. Another factor to consider when carrying out CIMP analysis is the cut-off value used to assess the different levels of CIMP. In this chapter, CIMP high was defined when 3 or more markers were methylated and CIMP low was defined when less than 3 markers were methylated. The threshold values for CIMP differ between various reports. A recent population-based study defined three subgroups of methylation in colorectal tumours; No-CIMP (tumours with no methylation), CIMP-Low (tumours with 1 -3 loci methylated) and CIMP-High (tumours with 4 or 5 loci methylated) (Barault et al, 2008). The report found that individuals with CIMP-High and CIMP-Low MSS tumours had a significantly worse outcome than those with no-CIMP MSS tumours, demonstrating that higher levels of methylation were associated with poorer survival. Hence, this emphasised the importance of identifying the CIMP-Low group as well as CIMP-High, which is often not carried out in other studies (Barault et al, 2008). Finally, another limitation of this study was the small number of tumour samples that were examined. Even though there was no observed association between *14-3-3 σ* methylation status and CIMP in the colorectal tumours examined, as only two tumours were determined as CIMP positive, the finding that one tumour was *14-3-3 σ* methylated and one was *14-3-3 σ* unmethylated could be just a coincidence. However, these findings do suggest that CIMP and *14-3-3 σ* methylation status are not tightly related. Analysis of a larger dataset would provide more evidence to determine whether there is an actual relationship between *14-3-3 σ* methylation status and CIMP. In addition, with the analysis of a larger dataset, clinicopathological and genetic studies could be performed to investigate any associations with CIMP.

In summary, the work I have presented in this chapter suggests that *14-3-3 σ* hypomethylation may be specific in colorectal cancer and not a result of the genome-wide demethylation that is often associated with colorectal tumours. In addition, I have demonstrated from the analysis of four CIMP markers, that 2/10 tumours were CIMP-High. One of these tumours was *14-3-3 σ* UPR methylated and the other *14-3-3 σ* UPR unmethylated, suggesting that it is unlikely that *14-3-3 σ* methylation is tightly linked to CIMP. The following chapter (chapter 6), investigates the potential functional consequences of gene specific *14-3-3 σ* hypomethylation in colorectal cancer and examines whether associated overexpression of *14-3-3 σ* can contribute to carcinogenesis or tumour progression.

Chapter 6

Analysis of the functional effects of increased 14-3-3 σ expression

6.1 Introduction

So far, I have shown that 14-3-3 σ is unmethylated in the UPR and 5' CpG island region of 14-3-3 σ in the majority of colorectal cancer cell lines. In contrast to this, bisulphite sequencing showed that fresh colorectal tumours displayed varying degrees of methylation, with a small percentage displaying almost unmethylated UPR and 5' CpG island regions. As all matched normal mucosa samples and normal mucosa from a cancer free individual were found to be almost fully methylated in the 14-3-3 σ UPR, this suggests that there may be tumour-specific loss of 14-3-3 σ methylation in colorectal cancer. Furthermore, I have shown that in the majority of colorectal tumours, loss of 14-3-3 σ methylation is associated with higher expression levels when compared with methylated tumours. The aim of this chapter is to test the hypothesis that an increase in 14-3-3 σ expression will have an effect on downstream events relevant to tumour initiation and/or progression, including apoptosis, proliferation, and cell cycle control. In this chapter, cell lines SW480 (14-3-3 σ methylated) and HCT116 (14-3-3 σ unmethylated) were transfected with a 14-3-3 σ GFP-tagged construct (14-3-3- σ GFP-C1) and the empty control construct (GFP-C1). Annexin V apoptosis assays were performed on DNA damaged 14-3-3 σ overexpressing cells and compared to empty vector control transfected cells to determine whether 14-3-3 σ overexpression results in a delay in the apoptotic signal. Proliferation levels were also measured in methylated cells overexpressing the 14-3-3 σ and empty vector control cells using an MTT-based assay in order to establish whether overexpression of 14-3-3 σ affects proliferation. In addition, cell cycle analysis was carried out on methylated cells overexpressing 14-3-3 σ and control cells to determine whether increased 14-3-3 σ expression has an effect on the cell cycle. Finally, it is hypothesised that 14-3-3 σ methylation and *p53* mutations are

mutually exclusive occurring events in colorectal cancer since both proteins play a pivotal role in maintaining genomic stability. Therefore, previously published data on the *p53* status in colorectal cancer cell lines and *14-3-3* σ methylation data from chapter 3 were used to investigate whether there are any associations between *p53* status and *14-3-3* σ methylation. In addition, to investigate any associations *in vivo*, tumour *p53* status was analysed by immunohistochemistry and Western blot analysis in *14-3-3* σ methylated and *14-3-3* σ unmethylated colorectal carcinomas.

6.2 Methodology

6.2.1 Transfection of colorectal cancer cell lines

Approximately 2×10^5 cells were plated in 2ml media, into 6-well dishes on day 1 for transfections prior to apoptosis assays and FACS analysis. Cells were plated at a density of 5000 in 50 μ l media, into 96-well plates on day 1 for transfections prior to proliferation assays. The initial cell number for the proliferation assays was determined by carrying out titration assays (Appendix C). On day 2, transfections of SW480 or HCT116 (for apoptosis assays only) cells with the *14-3-3* σ GFP-C1 and empty control pEGFP-C1 constructs were carried out as described in section 2.7.2. Transfections of the two constructs were set up in triplicate in 6-well or 96-well plates depending on the subsequent functional assay that was carried out. As transient transfections were performed, overexpression of the constructs were initially verified by Western blot analysis (Figure 6.1). For all transfections, fluorescence microscopy was used to confirm transfection was successful at 24 hours by visualising GFP-positive cells (Appendix C), and to calculate transfection efficiencies prior to proliferation assays. For the proliferation assay experiments, fluorescence microscopy and Western blot analysis were both used to confirm expression of *14-3-3* σ GFP-C1 and GFP-C1 constructs for each day over a 4-day period (Appendix C and Figure 6.1 (C) respectively).

6.2.2 Apoptosis assays

Transfected cells were UV-C exposed or unexposed as a control on day 3 as outlined in section 2.7.3. Cells were harvested for apoptosis assays on day 4. Apoptosis assays

were performed by annexin V staining on the transfected SW480 and HCT116 cells as described in section 2.7.3. Apoptotic cells were calculated as a percentage of 200 randomly selected GFP-positive cells.

6.2.3 Proliferation assays

On day 3, MTT-based proliferation assays were performed on transfected SW480 cells as described in section 2.7.4. Transfection efficiencies were calculated prior to the proliferation assays by counting 200 randomly selected cells in triplicate, in one field of view using fluorescence microscopy. The average transfection efficiency was calculated for each independent experiment conducted, for each construct (Appendix C). Proliferation was measured every 24 hours for 4 days in total and was corrected accordingly depending on the transfection efficiency.

6.2.4 Western blot analysis

Cytoplasmic extracts from *14-3-3 σ* methylated and *14-3-3 σ* unmethylated colorectal tumours were purified as outlined in 2.6.5.2 and examined for the expression of stable mutant p53 by Western blot analysis as described in section 2.6.5.3. Cytoplasmic extracts were purified from colorectal cancer cell line HT29 as described in 2.6.5.1 and used as a control for Western blot analysis of p53. Protein loading was assessed by probing for β -actin levels.

6.2.5 Immunohistochemistry

KR tumour sections were embedded and sectioned as described in 2.9.1. Other tumour samples were obtained directly as sections. *14-3-3 σ* methylated and *14-3-3 σ* unmethylated colorectal tumours were analysed for the expression of stable mutant p53 by immunohistochemistry as described in section 2.9.2.

6.2.6 Statistical analysis

Unpaired T- tests, Two-way ANOVA and Fishers exact tests were used as appropriate (2.10.1). The null hypothesis was rejected at the 5% level ($p < 0.05$).

6.3 Results

6.3.1 Analysis of UV-C induced apoptosis in *14-3-3 σ GFP-C1* overexpressing colorectal cancer cell lines

In line with the report by Samuel et al, which demonstrated that 14-3-3 σ delays the apoptotic signal in cancer cells by sequestering Bax protein, I hypothesised that an increase in *14-3-3 σ* expression will result in a reduced level of apoptosis in colorectal cancer cells. SW480 (*14-3-3 σ* methylated) and HCT116 (*14-3-3 σ* unmethylated) cells were transiently transfected with 14-3-3 σ GFP-C1 construct and empty control GFP-C1 construct. Figure 6.1 shows the expression levels of 14-3-3 σ protein in SW480 and HCT116 transfected cells. Without transfections, SW480 cells do not express any basal levels of *14-3-3 σ* , whereas HCT116 cells express high basal levels. 24 hours following transfections, cells were either left unexposed (control) to assess basal levels of apoptosis following transfections, or UV-C exposed to induce apoptosis. The next day, the cells were harvested and stained for annexin V. From previous work in the laboratory and from a previously published report (Stark & Dunlop, 2005), I decided that a time of 24 hours post UV-C exposure would be optimal for measuring apoptosis. Apoptosis was also measured 48 hours after UV-C treatment and the majority of cells were found to be apoptotic (data not shown), therefore a time of 24 hours was taken for assay of the level of apoptosis. Percentage of GFP-positive cells that stained positive for annexin V in the unexposed and UV-C exposed cells were determined from three independent experiments.

Apoptosis assays firstly demonstrated that in unexposed SW480 cells overexpressing *14-3-3 σ GFP-C1* and *GFP-C1* approximately 11% of cells were apoptotic, indicating this as a basal level of apoptosis for this cell line following transfection (Figure 6.2 (A)). Notably, overexpression of *14-3-3 σ* in itself had no effect on apoptosis. However, in UV-C exposed SW480 cells, apoptosis levels were increased and cells overexpressing *14-3-3 σ GFP-C1* were found to have a significantly lower percentage of apoptotic cells (~14%) compared to cells overexpressing the control construct *GFP-C1* (~28%) ($p=0.001$, unpaired T- test) (Figure 6.2 (A)).

In unexposed HCT116 cells, the levels of apoptosis were approximately 9%. Similar to the unexposed SW480 cells, *14-3-3 σ* overexpression had no effect on apoptosis in the HCT116 cells. However, in UV-C exposed HCT116 cells, the percentage of apoptotic cells increased compared to unexposed HCT116 overexpressing cells. HCT116 cells overexpressing *14-3-3 σ GFP-C1* did show a lower level of apoptosis (~21%) compared to HCT116 cells expressing the control construct (~28%). Although, this just failed to reach significance ($p = 0.06$, unpaired T- test) (Figure 6.2 (B)). It seems likely that this finding in HCT116 cells overexpressing *14-3-3 σ GFP-C1* and control *GFP-C1* is different compared to the significant changes observed in SW480 overexpressing cells because of the high levels of endogenous *14-3-3 σ* expression in the HCT116 cells. SW480 *14-3-3 σ* expression levels as demonstrated in chapter 4 are very low. Overall, these results demonstrate that increasing the levels of *14-3-3 σ* in the SW480 colorectal cancer cell line, results in a lower UV-C induced apoptotic response compared to control transfected cells.

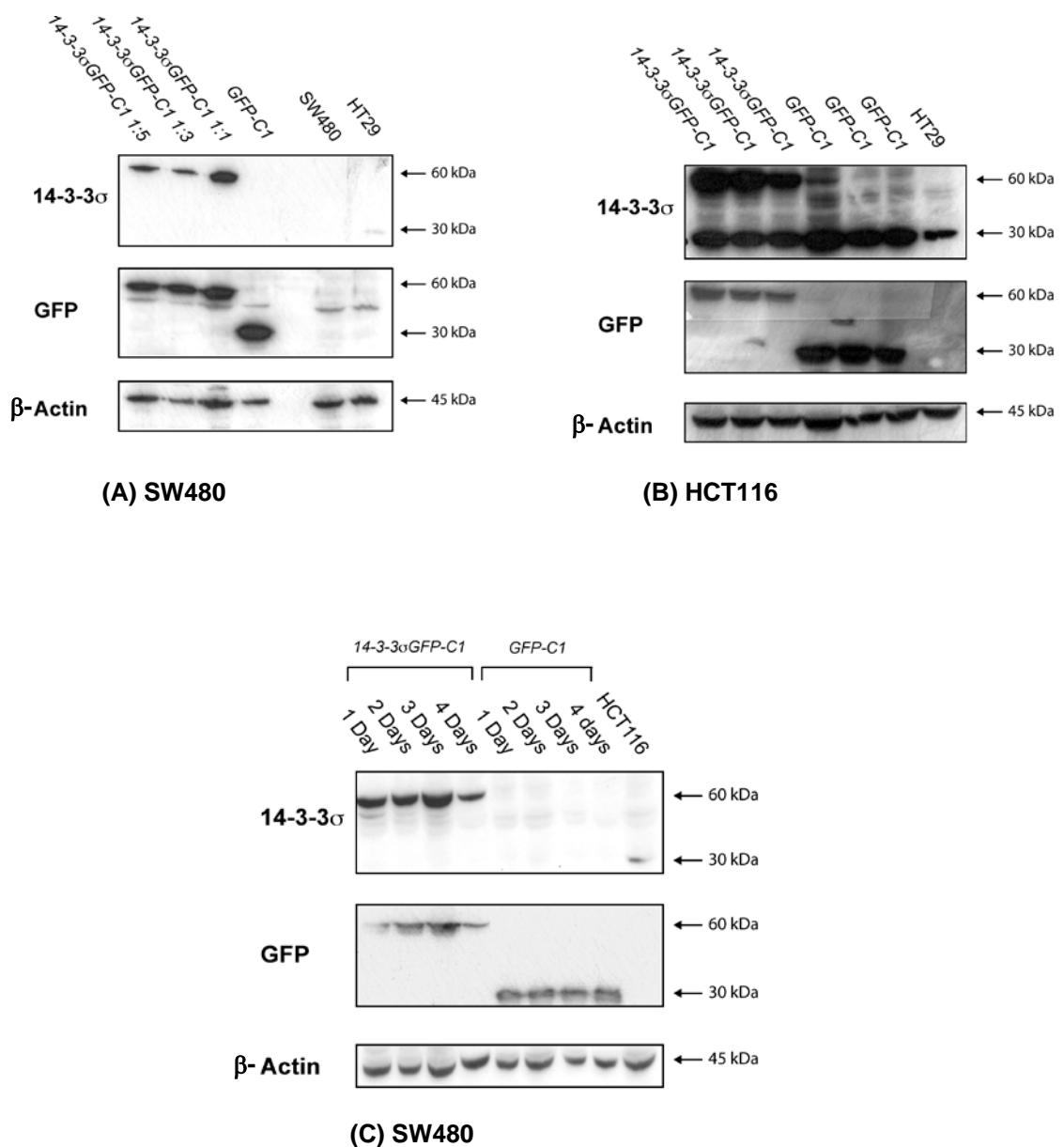


Figure 6.1: Western blot analysis of transient transfections of SW480 (*14-3-3 σ* methylated) cells (A) and HCT116 cells (*14-3-3 σ* unmethylated) 24 hours post transfections (B). SW480 transfected cells showing expression of *14-3-3 σ GFP-C1* over the 4-day period (C). Differing ratios of construct:transfection reagent were initially tested for the SW480 *14-3-3 σ GFP-C1* transfections. A transfection ratio of 1:3 was chosen for all transfections in both cell lines. Arrow indicates endogenous levels of *14-3-3 σ* protein in HCT116 transfected cells. Presence of white line on membrane (B) for GFP is due to a mark from adhesive tape. GFP is shown to demonstrate presence of GFP tag. Rabbit polyclonal anti-GFP was used to probe for GFP in Western blots (A) and (B), mouse monoclonal anti-GFP was used to probe for GFP in Western blot (C) separately from *14-3-3 σ* and actin. HT29 and HCT116 act as positive controls for *14-3-3 σ* expression. β -actin levels were measured to assess protein loading.

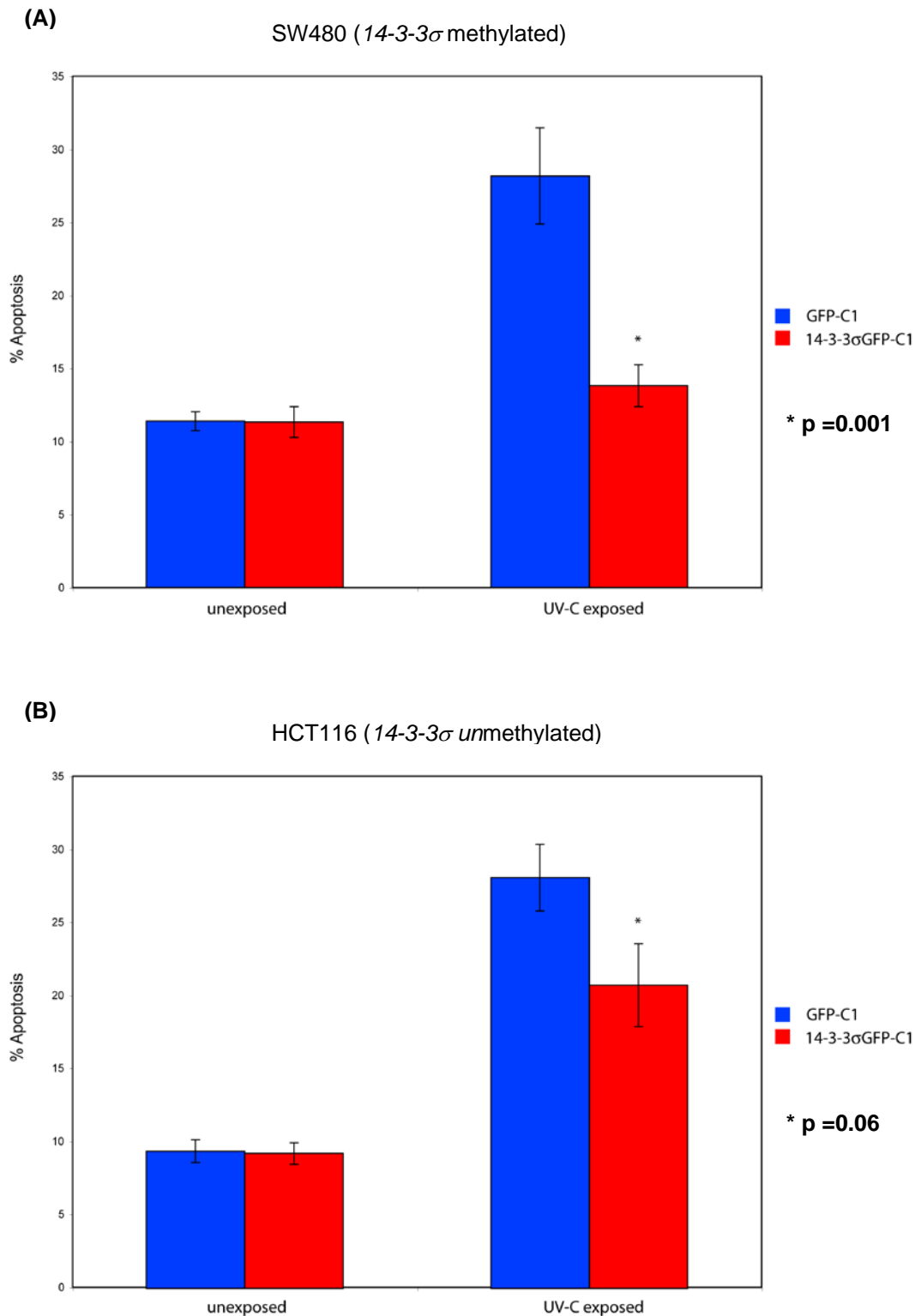


Figure 6.2: Percentage apoptosis in (A) SW480 (*14-3-3 σ* methylated) and (B) HCT116 (*14-3-3 σ* unmethylated) cells transfected with 14-3-3 σ GFP-C1 or control empty construct GFP-C1 after 24 hours without UV-C exposure or with UV-C exposure. Cells were left 24 hours after transfection then unexposed or exposed to UV-C. For unexposed and UV-C exposed cells standard error bars \pm are shown from three separate experiments. p-values are indicated.

6.3.2 Analysis of proliferation in 14-3-3 σ GFP-C1 overexpressing SW480 cell line

Previous *in vivo* data has suggested that 14-3-3 σ expression may be associated with increase proliferation in colorectal tumour cells (Ide et al, 2004). To investigate this further, proliferation assays on SW480 cells overexpressing 14-3-3 σ GFP-C1 and control empty construct GFP-C1 were carried out to determine if increased expression of 14-3-3 σ results in an increase in proliferation. An MTT-based assay was performed to measure the number of viable cells in proliferation. As transient transfections were performed, the transfection efficiency for each construct was calculated using fluorescence microscopy before each proliferation assay was conducted. The 14-3-3 σ GFP-C1 construct tended to have on average a 10% lower transfection efficiency compared to the empty GFP-C1 construct (Appendix C). Proliferation was measured over 4 days and was corrected by the transfection efficiencies for each construct. Fluorescence microscopy (Appendix C) and Western blot analysis (Figure 6.1 (C)) confirmed that both 14-3-3 σ GFP-C1 and control construct GFP-C1 were expressed over the 4-day period.

Figure 6.3 shows that proliferation is higher in SW480 transfected cells on day 1 compared to day 2, which is likely due to the effects of experimental intervention. The standard error bars for both cell types overexpressing 14-3-3 σ GFP-C1 and GFP-C1 at day 1 are very high further suggesting that this may be due technical artefacts. Following 2 days of culture, proliferation does however increase each day in the SW480 transfected cells. Furthermore, the 14-3-3 σ GFP-C1 overexpressing cells show an increased trend for proliferation after days 2, 3 and 4 compared to control GFP-C1 overexpressing cells. This increase is not significantly different at days 2 and 3, although at day 4 there is a significant increase in proliferation in the 14-3-3 σ GFP-C1 overexpressing cells compared to the GFP-C1 control cells ($p < 0.01$, Two-way ANOVA). Overall, the preliminary data demonstrates that there is a trend for an increase in proliferation in 14-3-3 σ overexpressing cells compared to control cells, however, in the 14-3-3 σ overexpressing cells, a significant increase in proliferation is not reached until day 4.

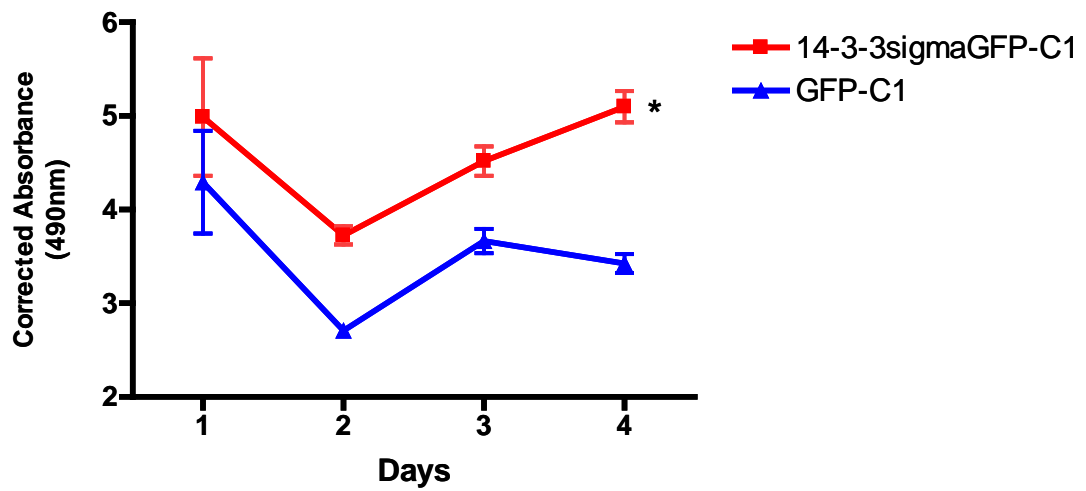


Figure 6.3: Proliferation of SW480 cells transfected with 14-3-3 σ GFP-C1 or control empty construct GFP-C1 over a 4 day period. Cell proliferation was determined by an MTT-based assay. Standard error bars \pm are shown from triplicate results carried out on three separate occasions. At day 4 there was a significant difference in proliferation between 14-3-3 σ GFP-C1 and control GFP-C1 overexpressing cells as indicated * $p < 0.01$.

6.3.3 Analysis of cell cycle in 14-3-3 σ GFP-C1 overexpressing SW480 cell line

As 14-3-3 σ plays a principal role in regulating the cell cycle, I decided next to investigate the effects of 14-3-3 σ overexpression on the cell cycle in the SW480 cell line. The cell cycle was analysed in 14-3-3 σ GFP-C1 overexpressing cells and compared with empty control GFP-C1 overexpressing cells. To ensure only 14-3-3 σ GFP-C1 and GFP-C1 cells were assayed, GFP-positive cells from the 14-3-3 σ GFP-C1 and GFP-C1 transfections were first sorted by FACS analysis. Sorted GFP-positive cells were then stained with propidium iodide and flow cytometry was used for cell cycle analysis on GFP-positive sorted cells from three separate transfections. Using proprietary software, dead cells and doublets were removed from the cell cycle data by plotting FL2-Area against FL2-Width. Cell cycle analysis was then carried out by plotting the number of cells against FL2-Area. To calculate the percentage of cells in each stage of the cell cycle, I used the Watson (Pragmatic) model to fit the data (Watson et al, 1987). The Watson model fits the S-phase exactly by making no assumptions about the shape of the S-Phase distribution. Figure 6.4 shows the cell cycle analysis results from the three transfections of SW480 cells for both the 14-3-3 σ GFP-C1 and GFP-C1 constructs. In all experiments, cells were FACS sorted on GFP expression. The average results, including standard deviations from the cell cycle analysis data from the three separate transfections, are shown in Table 6.1. The cell cycle analysis indicated that 56.78% of GFP-C1 control cells were present in G₀/G₁, 33.94% were in S-phase and 7.04% were present in G₂/M phase. In 14-3-3 σ GFP-C1 cells, the percentage of cells in G₀/G₁ was significantly lower ($40.32 \pm 4.21\%$) ($p = 0.01$, unpaired T- test) and the percentage of cells in the S- phase was significantly higher ($49.10 \pm 3.47\%$) ($p = 0.0079$, unpaired T- test). In the G₂/M phase the percentage of cells was very similar to GFP-C1 control cells ($6.56 \pm 1.05\%$). These results demonstrate that there was a decrease in the number of cells in G₀/G₁ and an accumulation of cells in the S-phase in 14-3-3 σ overexpressing cells compared to control cells. This may additionally indicate the role of 14-3-3 σ expression in cell growth. Alternatively, the increasing trend could indicate an S-phase arrest and therefore increased 14-3-3 σ protein levels in the SW480 cell line

could be causing an induction of the G₁/S DNA damage checkpoint. Further analysis is required to differentiate between these possibilities. This will be discussed in more detail in section 6.4.

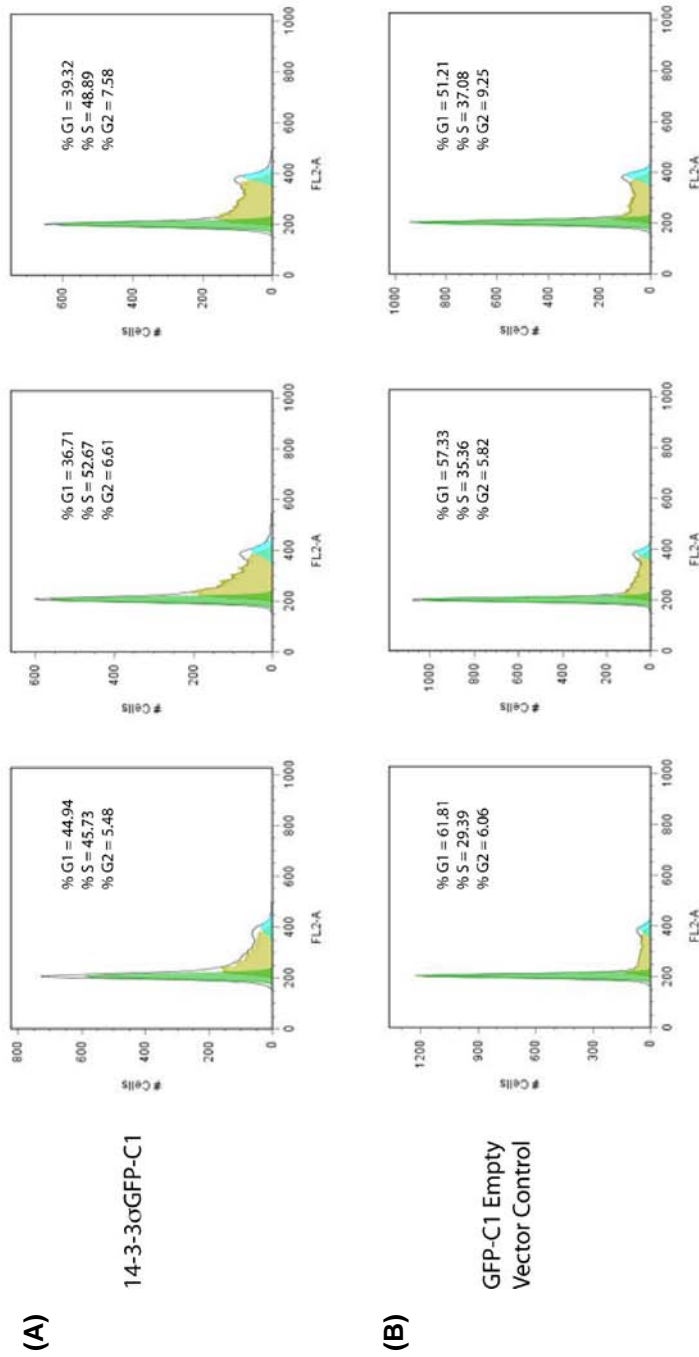


Figure 6.4: Cell cycle analysis of FACS sorted SW480 cells expressing (A) 14-3-3σGFP-C1 and (B) GFP-C1 (control) from three separate transfections. Percentage of cells in each phase were calculated by fitting the Watson Pragmatic model to the cell cycle data. Percentages of cells presented in each phase are indicated. There was a significant decrease in the percentage of cells in the G₀/G₁ phase ($p = 0.01$) and a significant increase in the percentage of cells in the S-phase ($p = 0.0079$) in 14-3-3σGFP-C1 cells compared to control GFP-C1 cells.

	G1%	S%	G2%
14-3-3S1	44.94	45.73	5.48
14-3-3S2	36.71	52.67	6.61
14-3-3S3	39.32	48.89	7.58
Average	40.32	49.10	6.56
St Dev	4.21	3.47	1.05
GFP1	61.81	29.39	6.06
GFP2	57.33	35.36	5.82
GFP3	51.21	37.08	9.25
Average	56.78	33.94	7.04
St Dev	5.32	4.04	1.91

Table 6.1: Summary of cell cycle analysis data of 14-3-3 σ GFP-C1 (14-3-3S) overexpressing cells and GFP-C1 (GFP) overexpressing cells. Average values and standard deviations (St Dev) are shown. There was a significant difference in the percentage of cells in G₀/G₁ (p =0.01) and in the percentage of cells in S-phase (p =0.0079) between 14-3-3 σ GFP-C1 and control GFP-C1 overexpressing cells.

6.3.4 Analysis of *14-3-3* σ methylation and *p53* mutations

The previous sections of this chapter have shown that *14-3-3* σ overexpression may have functional effects on apoptosis and potentially cell growth in colorectal cancer cell lines, although further experimentation is required to determine the exact effect. *p53* is a major player in the response to DNA damage and has been shown to trans-activate *14-3-3* σ expression (Hermeking et al, 1997). *14-3-3* σ methylation and *p53* mutational status in colorectal cancer cell lines and *in vivo* were next investigated to assess whether there is a relationship between *14-3-3* σ methylation and *p53* status.

The association between *14-3-3* σ methylation and *p53* status was first examined in colorectal cancer cell lines. *p53* status was obtained from the International Agency for Research on Cancer (IARC) TP53 mutation database (<http://www-p53.iarc.fr>), unless otherwise stated. Table 6.2 lists the cell lines with corresponding *14-3-3* σ methylation status (as determined in chapter 3 of this thesis) and *p53* status. From the nine cell lines examined there does not appear to be an obvious relationship between *14-3-3* σ methylation and *p53* status. Both *14-3-3* σ methylated cell lines (SW480 and Colo320DM) are *p53* mutated and 4/6 *14-3-3* σ unmethylated cell lines also have *p53* mutation. The number of cell lines is too low to conduct a meaningful statistical analysis. However, this does indicate that *in vitro* *14-3-3* σ methylation and *p53* mutations are not mutually exclusive.

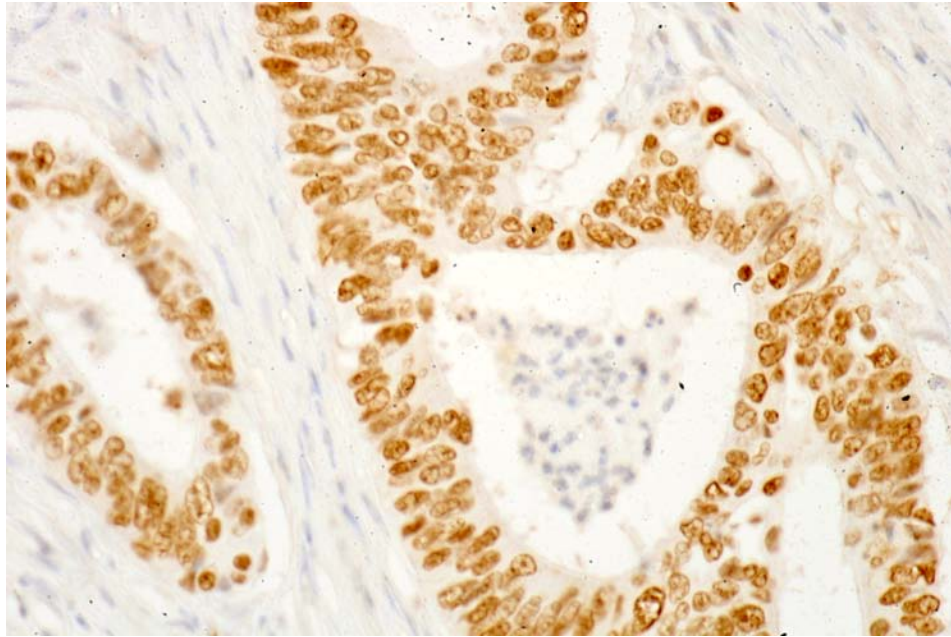
Next, immunohistochemistry and Western blots were utilised to determine *p53* stabilised protein levels in *14-3-3* σ methylated and unmethylated colorectal tumours. The same tumour samples were analysed by each technique apart from tumours 1736, AM27 and AM31, which were not available for immunohistochemistry analysis. Therefore, a total of 16 tumours were examined for *p53* stabilised levels by immunohistochemistry and 19 by Western blot analysis. Immunohistochemistry demonstrated that 6/16 colorectal tumours were likely to have *p53* mutations due to the presence of positive staining in the nuclei of tumour cells (Figure 6.5 (A)). Other tumours displayed heterogeneous *p53* staining with varying intensities and locations (Figure 6.5 (B)), and some tumours were negative for *p53* staining. Detailed scoring of intensity and location of *p53* staining for each tumour section are listed in Table

6.3. Western blot analysis verified that 5/19 colorectal tumours had increased stabilised p53 levels indicating a possible mutation (Figure 6.6). In general, the Western blot data agreed with the immunohistochemistry data apart from two tumours 5123 and 7219 which were positive for p53 stabilised protein by immunohistochemistry analysis and were negative by Western blot analysis.

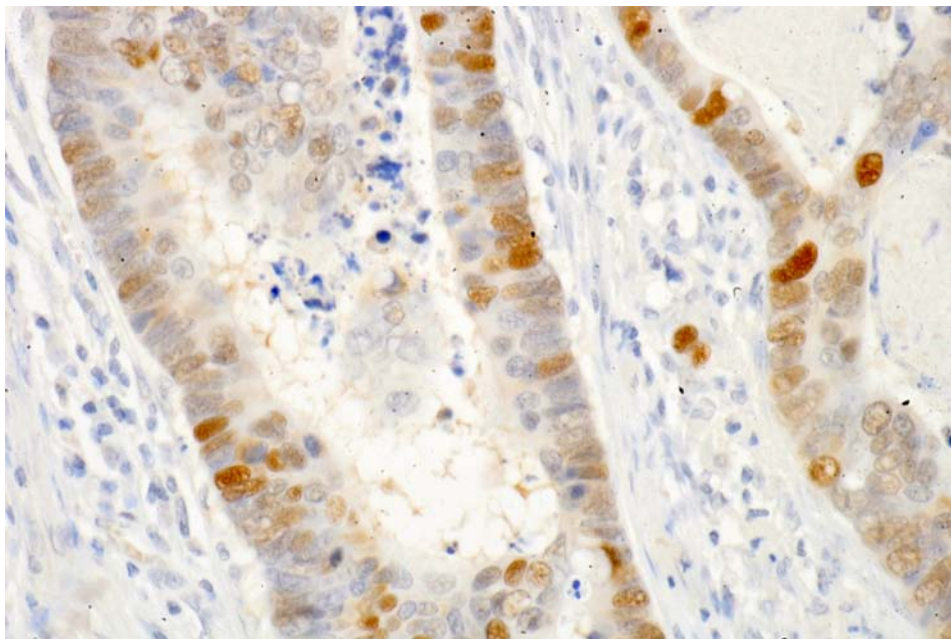
Combining all available results from the immunohistochemistry and Western blot analysis, the data suggests that there is no overall relationship between *14-3-3 σ* methylation and p53 stabilised protein levels (Table 6.4). In the scenario that tumours 5123 and 7219 show increased stabilised p53 levels and are likely to be mutated, then 33% (3/9) *14-3-3 σ* unmethylated colorectal tumours appear to have a *p53* mutation while 50% (5/10) *14-3-3 σ* methylated colorectal tumours have a *p53* mutation ($p=0.6499$, Fishers exact test) (Table 6.5). If tumours 5123 and 7219 are not included, then it is clear there is no relationship between *14-3-3 σ* methylation and *p53* status. These results indicate that similar to the *in vitro* data, *14-3-3 σ* methylation does not occur less frequently in tumours that potentially carry a *p53* mutation. It is accepted that there are small numbers of unmethylated tumours and so statistical power is limited. Nonetheless, my data supports the notion that there is no absolute relationship between *14-3-3 σ* methylation and *p53* status in either colorectal cancer cell lines (where most are unmethylated for *14-3-3 σ*) or in colorectal tumours (where most are *14-3-3 σ* methylated).

Colorectal cancer Cell line	14-3-3σ Methylation Status	14-3-3σ Protein levels	p53 Status
SW480	Methylated	Low	Mut
Colo320DM	Methylated	Low	Mut
HCT116	Unmethylated	High	WT
HRT18	Unmethylated	ND	Mut (Din et al, 2004)
Caco-2	Unmethylated	ND	Mut
SW48	Unmethylated	ND	Unknown
LoVo	Unmethylated	ND	WT
SW620	Unmethylated	ND	Mut
HT29	Unmethylated	High	Mut

Table 6.2: p53 status in relation to 14-3-3 σ methylation status and 14-3-3 σ protein levels in colorectal cancer cell lines. WT = wild-type p53, mut = mutated p53, ND = not determined in this thesis. p53 status was obtained from the International Agency for Research on Cancer (IARC) TP53 mutation database (<http://www-p53.iarc.fr>) unless otherwise stated.



(A)



(B)

Figure 6.5: p53 immunohistochemistry at x40 magnifications. Positive staining in colorectal tumour 7329 (*14-3-3 σ* methylated) (A) and heterogeneous staining in colorectal tumour 7007 (*14-3-3 σ* unmethylated) (B).

Tumour Sample	14-3-3σ methylation Status	Intensity	Percentage of stained epithelial cells (%)	Comments	Suggested p53 mutation
10811	Unmethylated	1	10	Counterstain is very strong so intensity may be >1	NO
10812	Unmethylated	1	10		NO
1924	Unmethylated	1	10	Thick section and counterstain is strong so intensity may be >1	NO
KR2	Unmethylated	2	30	Heterogeneous staining in nuclei	NO
KR3	Unmethylated	2	30	Heterogeneous staining in nuclei	NO
7007	Unmethylated	2-3	100		YES
7645	Unmethylated	1-2	75		YES
2902	Methylated	0	0	Staining may not have worked	NO
5731	Methylated	1	10	Counterstain is very strong, may mask true result	NO
8117	Methylated	1	10	Mostly mucinous tissue	NO
7867	Methylated	2-3	30	Heterogeneous staining	NO
2867	Methylated	0	0	No carcinoma on slide just normal tissue	NO
5123	Methylated	1-2	75		YES
7478	Methylated	2-3	100		YES
7219	Methylated	3	100		YES
7329	Methylated	2-3	75		YES

Table 6.3: p53 immunohistochemistry analysis of 14-3-3 σ unmethylated colorectal tumours and 14-3-3 σ methylated colorectal tumours. Intensity of staining is scored 1-3 depending on strength, 1 = light staining, 3 = strong staining (0 = negative staining). Percentage coverage of positively stained nuclei in epithelial cells within cancerous crypts is scored 0-100%. Tumour sections with strong positive staining in the majority of nuclei across the cancerous crypts were assumed p53 mutated.

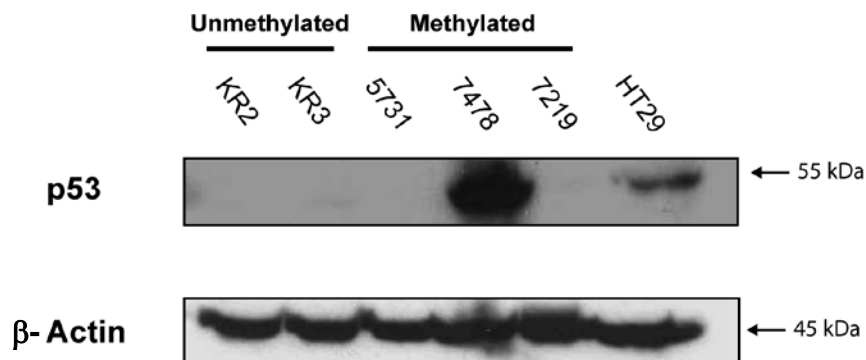
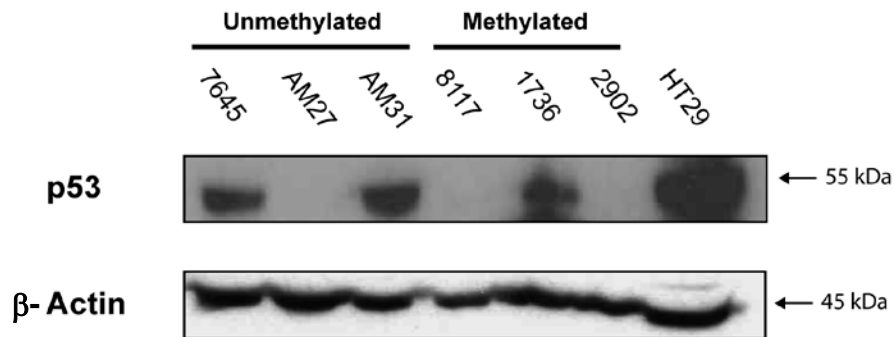
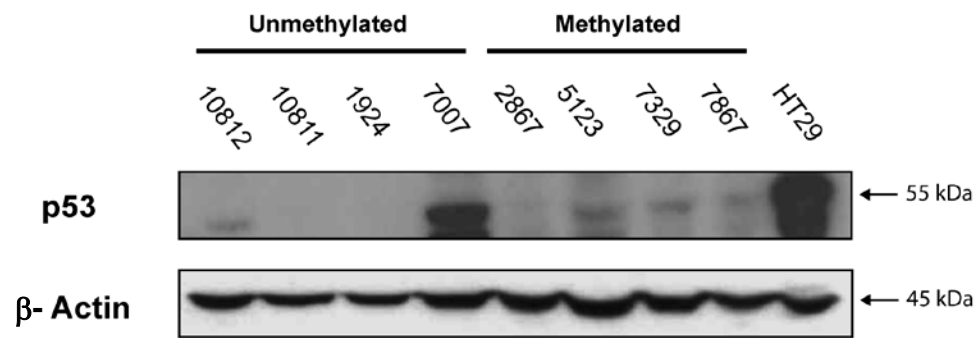


Figure 6.6: p53 Western blot analysis of 14-3-3 σ unmethylated and 14-3-3 σ methylated colorectal tumours as indicated. Tumours overexpressing p53 were assumed *p53* mutated. HT29 is shown as a positive control for *p53* mutation. β - actin levels were analysed to assess protein loading.

Tumour Sample	14-3-3σ Methylation Status	p53 Status from Immunohistochemistry and Western blot analysis
10811	Unmethylated	WT
10812	Unmethylated	WT
1924	Unmethylated	WT
KR2	Unmethylated	WT (heterogeneous staining in section)
KR3	Unmethylated	WT (heterogeneous staining in section)
AM27	Unmethylated	WT (Western blot analysis only carried out)
7007	Unmethylated	Mut
7645	Unmethylated	Mut
AM31	Unmethylated	Mut (Western blot analysis only carried out)
2902	Methylated	WT
5731	Methylated	WT
8117	Methylated	WT
7867	Methylated	WT (heterogeneous staining in section)
2867	Methylated	WT
5123	Methylated	Mut (negative by Western blot analysis)
7478	Methylated	Mut
7219	Methylated	Mut (negative by Western blot analysis)
7329	Methylated	Mut
1736	Methylated	Mut (Western blot analysis only carried out)

Table 6.4: p53 status analysis by indicative increase in stabilised p53 protein levels, using immunohistochemistry and Western blot analysis in 14-3-3 σ unmethylated and methylated colorectal tumours. WT = wild-type p53, mut = mutated p53.

p53 Status	14-3-3σ Methylated	14-3-3σ Unmethylated
Mutated	5	3
Wild-Type	5	6
Total	10	9

Table 6.5: Summary of *p53* status analysis by indicative increase in stabilised *p53* protein levels, and 14-3-3 σ methylation status in colorectal tumours. (p = 0.6499, Fishers exact test).

6.4 Discussion

In this chapter, I set out with the aim to investigate the functional consequences of the tumour-specific overexpression of *14-3-3 σ* . The analysis of effects on apoptosis, proliferation and the cell cycle were undertaken. Functional assays suggest that *14-3-3 σ* overexpression may affect apoptosis, cell growth and the cell cycle of cancer cells *in vitro*. I have demonstrated from carrying out Annexin V apoptosis assays that *14-3-3 σ* overexpression delayed the UV-C induced apoptotic response in the colorectal cancer cell line SW480, but not in the HCT116 colorectal cancer cell line, which is probably due to the different endogenous levels of *14-3-3 σ* in the two cell lines. Overall, these results suggest that *14-3-3 σ* overexpression in colorectal tumours may protect cancer cells from apoptosis. An MTT-based proliferation assay demonstrated an increasing trend in proliferation levels in *14-3-3 σ* overexpressing SW480 cells compared to SW480 control cells, with a significant increase on day 4. This suggests that continued overexpression of *14-3-3 σ* might further result in a significant increase in proliferation in the cancer cells. Thus, together, the apoptosis and proliferation data indicate that increased *14-3-3 σ* levels in cancer cells may contribute to deregulation of the control of cell growth. Cell cycle analysis of SW480 cells overexpressing *14-3-3 σ* showed that there was a decrease in cells presented in G₀/G₁, accompanied with an increase in the number of cells presented in S-phase compared to GFP-C1 control cells. Preliminary data therefore suggests that *14-3-3 σ* overexpression may promote the accumulation of cells in S-phase. However, it must also be considered an accumulation of cells in the S-phase could indicate an S-phase block and thus increased expression of *14-3-3 σ* may in fact result in a DNA damage induced cell cycle response. Further experimental work is required to clarify the relationship between these initial findings.

Analysis of increased levels of stabilised p53 protein was carried out in a number of *14-3-3 σ* methylated and unmethylated colorectal tumours using immunohistochemistry and Western blot. It is generally assumed that an increased level of stabilised p53 protein is indicative of a *p53* mutation. As other changes in p53 related proteins can also have an effect on stabilised p53 levels these results

were only an indication of *p53* mutation status, and sequencing of the gene to screen for mutations would be needed to confirm its actual status. It was hypothesised that *14-3-3* σ methylation and *p53* mutations may be mutually exclusive occurring events in colorectal cancer as both proteins play a pivotal role in maintaining genomic stability. However, my findings showed that there was no relationship between increased expression of stabilised *p53* protein and *14-3-3* σ methylation status in colorectal cancer cell lines or in tumours. These results therefore might suggest that *14-3-3* σ methylation and *p53* mutations occur independently from each other.

A previously published report by Samuel et al demonstrated that a lack of *14-3-3* σ in colorectal cancer cell lines sensitises them to chemotherapy induced apoptosis, therefore suggesting a preventative role of *14-3-3* σ in apoptosis (Samuel et al, 2001). My results agree with this initial finding, with the demonstration that *14-3-3* σ overexpression protected SW480 cells from UV-C induced apoptosis. Samuel et al also found that mechanistically, *14-3-3* σ suppresses apoptosis through binding and sequestering the pro-apoptotic Bax protein. In DNA damaged HCT116 cells, Bax protein was present at high levels in the cytosol fraction. However, in DNA damaged *14-3-3* σ negative HCT116 cells, there was a marked decline of Bax protein in the cytosol (Samuel et al, 2001). It would therefore be interesting to investigate the binding of *14-3-3* σ to Bax and the subcellular localisation of Bax in *14-3-3* σ overexpressing SW480 cells, which could be examined by co-immunoprecipitation analysis and Western blot analysis respectively. It would be expected that in the *14-3-3* σ overexpressing cells, the *14-3-3* σ protein would be bound to the Bax protein and furthermore Bax would be localised mainly in the cytosol compared to other subcellular compartments, and at a higher level compared to Bax levels in the cytosol from control SW480 cells. This would verify whether the overexpression of *14-3-3* σ and associated delay in apoptosis in colorectal tumour cells is functioning through the same mechanism. The apoptosis results presented in this chapter could also be examined using other techniques besides annexin V assays, such as TUNEL immunofluorescence assays. A decrease in pro-caspase-3 levels is characteristic of apoptosis as the protein is cleaved due to the induction of apoptosis. Thus, analysis

of pro-caspase-3 by Western blot could also be used to analyse apoptosis levels in the 14-3-3 σ overexpressing cells.

The proliferation assays demonstrated that 14-3-3 σ overexpression might have a positive effect on SW480 cell growth. A more striking effect may have been observed in 14-3-3 σ GFP-C1 stably transfected cells as the transfections carried out here were only transient, with the efficiency of the 14-3-3 σ GFP-C1 construct being on average less than 50%. Throughout this PhD, I attempted to develop stably transfected 14-3-3 σ GFP-C1 and GFP-C1 cell lines however they were unsuccessful. Nevertheless, these initial findings do suggest that extended 14-3-3 σ overexpression in colorectal tumour cells may induce proliferation. On day 4, the difference in proliferation between the 14-3-3 σ overexpressing cells and control cells increased significantly as proliferation levels began to plateau in the control cells, whereas proliferation in the 14-3-3 σ overexpressing cells continued to increase. It would be interesting to extend the proliferation assay further to see if proliferation continues to increase in the 14-3-3 σ overexpressing cells. The proliferation data agrees with previously published reports in which 14-3-3 σ expression in colorectal and gastric cancers was found to be associated with increased cell proliferation (Ide et al, 2004; Tanaka et al, 2004). In colorectal cancer, it was found from Ki-67 labelling and cyclin B1 staining of colorectal tumour sections that there was a higher proliferative activity at the invasion front in 14-3-3 σ positive carcinomas compared to 14-3-3 σ negative carcinomas (Ide et al, 2004). Ki-67 labelling also demonstrated that there was a significantly positive correlation between 14-3-3 σ overexpression and proliferation ($p=0.001$) in gastric carcinomas but no significant correlation in colorectal cancer (Tanaka et al, 2004). The proliferation results presented in this chapter were obtained from an *in vitro* assay. To investigate whether these results translate *in vivo*, the association between 14-3-3 σ overexpression and proliferation by Ki-67 labelling in colorectal tumour sections or qRT-PCR analysis of proliferating cell nuclear antigen (PCNA) expression could be carried out. The underlying mechanisms which are responsible for the increase in cell proliferation as a result of altered levels of 14-3-3 σ remain to be elucidated. Given 14-3-3 σ 's important

role in cell cycle regulation (Hermeking et al, 1997) and translational control during mitosis (Wilker et al, 2007), it is likely that aberrant expression of 14-3-3 σ directly affects these two processes, which subsequently contributes to altered cell growth. Further investigations *in vitro* using SW480 14-3-3 σ stably overexpressing cells may provide some added insight.

Initial studies carried out on the cell cycle in 14-3-3 σ overexpressing cells appeared to agree with the proliferation data since the cell cycle analysis suggested that there was an accumulation of cells in the S-phase. This could indicate that an increase in DNA synthesis is occurring. To investigate this further, the incorporation of BrdU in the 14-3-3 σ overexpressing cells by immunofluorescent staining could be carried out. Accumulation of cells in the S-phase may also indicate an S-phase arrest. 14-3-3 σ has been previously shown to associate with G₁ specific CDK proteins such as CDK2 and CDK4 (Laronga et al, 2000). Therefore, 14-3-3 σ induced S-phase arrest may function through these or other related CDK proteins. Many studies have reported the impairment of G₂/M arrest following DNA damage in 14-3-3 σ negative cells. Fewer studies have investigated the effects of 14-3-3 σ overexpression on the cell cycle. However, the report by Hermeking et al demonstrated that by infecting HCT116 cells with a 14-3-3 σ expressing adenoviral vector, ectopic expression of 14-3-3 σ in colorectal cancer cells disrupts G₂/M progression and blocks proliferation in colon cancer cells (Hermeking et al, 1997). They showed, using a combination of Fluorescent in situ hybridisation (FISH) and flow cytometry, that exogenous expression of 14-3-3 σ caused an increase in the number of cells with a DNA content of 4N, and hence were arrested at the G₂/M checkpoint (similar to the response observed in DNA damaged HCT116 cells). Further adenoviral transfection caused the cells to re-enter S-phase, where they synthesised DNA without dividing, leading to the production of cells with a DNA content of more than 4N (Hermeking et al, 1997). Interestingly, this block in mitosis is similar to what was observed in the studies by Wilker et al, in which loss of 14-3-3 σ expression in cancer cells resulted in an impaired mitotic exit (Wilker et al, 2007). As with the Wilker et al studies, a block in cytokinesis was observed from the overexpression of 14-3-3 σ . However,

time lapse microscopy showed that following this block, half of the *14-3-3 σ* overexpressing cells re-fused forming one cell with a single nucleus and half of the cells underwent apoptosis (Hermeking et al, 1997). As binucleate cells were generated from the knock-down of *14-3-3 σ* (Wilker et al, 2007), this suggests that *14-3-3 σ* overexpressing cells may undergo an earlier failure in cytokinesis. Nevertheless, in reflection with the data I have presented in this thesis, the study by Hermeking et al suggests that the accumulation of the *14-3-3 σ* overexpressing SW480 cells in the S-phase may in fact be a result of an uncoordinated arrest rather than a change in the replicative state of the cells. Furthermore, the block in proliferation observed in the *14-3-3 σ* overexpressing colon cancer cells (Hermeking et al, 1997) is in contrast to the proliferation data presented in this chapter. Investigative experiments in the SW480 *14-3-3 σ GFP-C1* cells, similar to the ones carried out in the Hermeking et al, would perhaps clarify whether there is a growth arrest at the S-phase or an increase in the replicative state of the cells.

Previous reports, which have investigated the association between *14-3-3 σ* methylation and *p53* status in different cancers have been inconsistent. Some studies have found an association and have suggested that *14-3-3 σ* methylation and *p53* mutations are mutually exclusive occurring events in cancer cells, as loss of genomic stability only requires the inactivation of *p53* or *14-3-3 σ* (Gasco et al, 2002a). Given that the data presented in chapter 3 has indicated that it may be a loss of *14-3-3 σ* methylation rather than gain of methylation which is tumour-specific in colorectal cancer, this hypothesis is perhaps inaccurate. Since *14-3-3 σ* is normally methylated in the colonic epithelium, loss of *14-3-3 σ* methylation and *p53* mutations would perhaps be less likely to occur. Indeed, in this chapter methylation of *14-3-3 σ* was found at a higher frequency in *p53* mutated cancers, although due to the small numbers of colorectal tumours examined the statistical power was limited. It was however concluded that there was no absolute relationship between *14-3-3 σ* methylation and *p53* status in the colorectal cancer cell lines or tumours examined. Similar studies have investigated the association between *p53* status and *14-3-3 σ* expression levels in colorectal cancer. *p53* mutations have been shown to reduce *14-*

3-3 σ expression and affect stable G₂/M arrest in DNA damaged cells (Hermeking et al, 1997). However, the effects of *p53* mutation status on *14-3-3 σ* expression in the absence of DNA damage are not known. Previous studies have demonstrated that there is no association between 14-3-3 σ protein expression and *p53* status in colorectal cancer and gastric cancer (Ide et al, 2004; Tanaka et al, 2004). Furthermore, data in chapter 4 demonstrated that *14-3-3 σ* is expressed at high levels in both wild-type and *p53* mutated *14-3-3 σ* unmethylated colorectal cancer cell lines and fresh tumours. These results therefore suggest that *14-3-3 σ* overexpression occurs irrespective of the *p53* status.

In summary, the work I have presented in this chapter adds to and puts into context previously published data since loss of *14-3-3 σ* methylation may be the key molecular event in colorectal cancer. The data presented demonstrates that overexpression of 14-3-3 σ may contribute to carcinogenesis or tumour progression in colorectal cancer through suppressing apoptosis and affecting cell growth. In addition, I have shown that there was no absolute association between either *14-3-3 σ* expression or methylation status and *p53* mutation status. Further studies are required to fully understand the downstream effects of *14-3-3 σ* overexpression in colorectal cancer and the underlying mechanisms which are involved.

Chapter 7

Discussion

The work I have presented in this thesis has focused on investigating the methylation status of *14-3-3 σ* , its relationship to gene expression and function in colorectal cancer, and the role it may play in initiation or progression of the disease. I studied the methylation status of the *14-3-3 σ* gene in colorectal cancer cell lines and fresh colorectal tumours along with matched normal mucosa samples, as well as normal mucosa and skin from cancer-free individuals. Previous to this work, *14-3-3 σ* methylation analysis had only been carried out in colorectal cancer cell lines and in a very small number of colorectal tumour samples (Ide et al, 2004; Suzuki et al, 2000). Furthermore, the results presented in this thesis are the first to study the methylation status of *14-3-3 σ* in normal colonic mucosa and show the tumour specificity of aberrant *14-3-3 σ* methylation in colorectal cancer. Using bisulphite sequencing of the upstream promoter region and 5' region of the *14-3-3 σ* CpG island, I show that normal colorectal mucosa tissue is essentially fully methylated at CpG sites; whereas colorectal tumours displayed an admixture of both methylated and unmethylated sequences in the upstream and 5' CpG regions. My initial data suggested that the degree of *14-3-3 σ* methylation might vary between individual tumours, since PCR bisulphite sequencing identified approximately 10% of tumours, which appeared to have a low degree of methylation in the upstream promoter region of *14-3-3 σ* . As *14-3-3 σ* is fully methylated in normal colorectal mucosa, these results suggested that loss of methylation is specific to colorectal cancer and that this phenomenon occurs in a minority of tumours, in contrast to previous work which suggested that hypermethylation was rare in the majority of colorectal tumours (Ide et al, 2004).

The remainder of the thesis investigated the specificity of *14-3-3 σ* methylation in colorectal cancer and the functional effects of *14-3-3 σ* hypomethylation, including any associated changes in expression levels. In chapter 4, *14-3-3 σ* expression analysis *in vitro* using cell lines, suggested that there may be an association between

14-3-3 σ methylation status and expression. In fresh human samples however, this association was not so evident. There was no significant difference in expression levels between *14-3-3 σ* unmethylated tumours and corresponding methylated normal tissue; indicating that loss of *14-3-3 σ* methylation in colorectal tumours may not be associated with changes in *14-3-3 σ* expression in colorectal cancer. However, when *14-3-3 σ* protein levels were examined in fully methylated normal colonic tissue and skin tissue, which has lower levels of methylation; there were higher levels of *14-3-3 σ* protein expression in the skin tissue samples compared to normal colonic tissue. In addition, when *14-3-3 σ* expression was analysed in a selection of tumour samples, there was a significant difference in expression between *14-3-3 σ* methylated and unmethylated tumours. As discussed in chapter 3, the effect of *14-3-3 σ* methylation in colorectal cancer may be reduced as a result of tumour heterogeneity. LCM was not carried out; therefore, the colorectal tumours samples which were examined did not exclusively consist of cancer cells. Other cell types such as infiltrating lymphocytes and stromal cells would have also been present, which may have contributed to the observed *14-3-3 σ* methylation and expression data presented in this thesis. Another explanation is that other epigenetic mechanisms may be involved in regulating *14-3-3 σ* expression in colorectal cancer. The 5-Aza-2'-deoxycytidine experiments carried out in cell lines in the final section of chapter 4 added further evidence to support this, since demethylation of *14-3-3 σ* *in vitro* did not result in re-expression of the gene.

In chapter 5, using Nearest Neighbor analysis (Ramsahoye, 2002) and MethyLight (Eads et al, 2000), loss of *14-3-3 σ* methylation in colorectal cancer appeared to not be an epiphenomenon as part of a more general methylation defect. I recognise however, that the small sample numbers limited these studies and analysis of a larger sample is required before any firm conclusions can be drawn. In addition, with regards to the CIMP analysis that was carried out, a panel consisting of only four CIMP markers were selected to determine whether colorectal tumours were CIMP positive or negative. As discussed, there is no consensus definition for the CIMP panel, therefore I decided to use four of the five classical CIMP markers (*hMLH1*,

CDKN2A, *MINT1*, *MINT2* and *MINT31*) defined by Jean Pierre Issa (Issa, 2004). The analysis of other additional CIMP markers, which have more recently been tested for their validity (Ogino et al, 2007; Weisenberger et al, 2006), would improve the analyses carried out and perhaps further support the conclusions drawn from this data. Nevertheless, the studies that I undertook suggest that it is unlikely that there is a strong relationship between *14-3-3σ* methylation status and either a generalised methylation phenotype or the CIMP phenotype.

In chapter 6, I presented data demonstrating that overexpression of *14-3-3σ* *in vitro* results in a delay in the apoptotic signal, an increase in cell proliferation and a change in cell cycle progression. The functional studies suggested that *14-3-3σ* overexpression might contribute to carcinogenesis or tumour progression through altering cell growth. Clearly, these are preliminary observations and future studies are required to investigate the underlying mechanisms involved in these processes, and to clarify whether *14-3-3σ* overexpression due to tumour-specific methylation changes plays a significant role in colorectal cancer development.

In comparison with previously published data, the work presented in this thesis suggests another cancer-type in which overexpression of *14-3-3σ* is associated with *14-3-3σ* CpG demethylation (Iacobuzio-Donahue et al, 2003; Sato et al, 2003). Normal pancreatic tissue was previously found to be largely or completely methylated, while the majority of pancreatic cell lines, and a high proportion of pancreatic carcinomas were completely unmethylated (Sato et al, 2003). Due to the reasons discussed in chapter 3, the proportion of colorectal tumours with low levels of *14-3-3σ* CpG methylation identified in this thesis may be underrepresented; namely, the percentage of colorectal tumours with completely unmethylated upstream and 5' CpG island regions might be higher than the 10% which was found in this current study. Therefore, it could be that *14-3-3σ* demethylation in colorectal cancer is more frequent than was suggested by my work. This would in some way agree with the report from Ide et al, in which the majority of colorectal tumours (9/10) displayed a low percentage of *14-3-3σ* methylation (<15% methylated CpG sites) (Ide et al, 2004). Furthermore, previous reports examining *14-3-3σ* expression

in colorectal cancer have shown that 14-3-3 σ is overexpressed in a high percentage of colorectal carcinomas (23/30; 76.7%) (Tanaka et al, 2004) and (6/8; 75%) (Perathoner et al, 2005) respectively, compared to matched normal tissue. Thus, given that 14-3-3 σ CpG methylation has been shown to be associated with expression, both in normal cell types (Oshiro et al, 2005) and in different cancers (Ferguson et al, 2000; Lodygin et al, 2004); this would add further evidence to suggest that the frequency of 14-3-3 σ demethylation in colorectal cancer may indeed be higher than was observed in this thesis. In contrast to this, a recent study examined 14-3-3 σ promoter methylation in human melanocytes and melanoma (Liu et al, 2009). The study demonstrated that 14-3-3 σ was heavily methylated both in normal melanocyte cells and in 100% (20/20) melanoma tumour samples, which resulted in silencing of 14-3-3 σ gene expression. Therefore, in this case, demethylation and associated changes in expression of 14-3-3 σ were found to be a rare event in melanoma (Liu et al, 2009). As mentioned previously, in order to accurately assess the degree of 14-3-3 σ methylation in colorectal carcinomas in comparison with normal tissue, further work examining 14-3-3 σ methylation status in a series of microdissected colorectal tumours, matched normal tissues, and normal colonic tissue from cancer-free individuals would be helpful.

If I were given the opportunity to continue this research, I would further examine the relationship between 14-3-3 σ CpG island methylation and tissue-specific expression. *In silico* analysis of human 14-3-3 σ expression, using online Affymetrix datasets: GNF SymAtlas V 1.2.4 (<http://symatlas.gnf.org>) (Su et al, 2002) demonstrates that 14-3-3 σ has a tissue-specific expression profile (Appendix D). Tissues expressing high levels of 14-3-3 σ expression (at least 10-fold above the median) are bronchial epithelial cells, prostate, lung, tongue, skin and tonsil. Whole blood, uterus, pancreas, thymus, thyroid and trachea all express medium levels of 14-3-3 σ (3-fold above the median). Whether 14-3-3 σ CpG methylation is involved in regulating normal tissue-specific expression of 14-3-3 σ in vivo remains an unanswered question, despite the work I present here. However, the preliminary studies presented in chapter 4, which compared protein expression of 14-3-3 σ in the normal colon and skin tissue, at least

provide a suggestion that there might be an association between methylation in the upstream promoter region and 5' region of the *14-3-3 σ* CpG island and tissue-specific expression. Furthermore, a previously published paper has demonstrated that cell type-specific expression of *14-3-3 σ* is associated with epigenetic modifications including *14-3-3 σ* CpG island methylation (Oshiro et al, 2005). The authors concluded that *14-3-3 σ* CpG island methylation does partly play a role in its tissue-specific regulation. Similar studies to those carried out in the Oshiro et al report, in a number of microdissected normal tissues (including the analysis of other epigenetic mechanisms such as, histone acetylation/methylation and chromatin structure), would perhaps provide further support to the previously drawn conclusions. In addition to examining the regulatory features within the *14-3-3 σ* promoter region, it would also be interesting to whether there were any other regulatory regions associated with *14-3-3 σ* . These might include miRNA target sequences; enhancer sequences; or CCCTC-binding factor (CTCF) binding sites, which could indicate any insulator elements that are associated with *14-3-3 σ* . The analysis of other regulatory regions would require a huge undertaking, however, they may play a significant role in regulating *14-3-3 σ* tissue-specific expression and perhaps even be involved in *14-3-3 σ* dysregulation associated with carcinogenesis (Ferguson et al, 2000; Lodygin et al, 2004).

Following on from this, one of my other aims would be to establish whether *14-3-3 σ* methylation is causally involved in downregulating *14-3-3 σ* expression. The analysis of *14-3-3 σ* re-expression following 5-Aza-2'-deoxycytidine treatment is one approach which can be used to investigate whether there is any causal relationship. This was carried out in chapter 4, however, due to a number of possible factors, which were discussed, *14-3-3 σ* re-expression was not achieved. Another approach would be to subclone the *14-3-3 σ* promoter region into a luciferase reporter plasmid and carry out *in vitro* expression assays. The *14-3-3 σ* promoter region could be methylated *in vitro* using *SssI* methylase and the suppressive effect of the methylated promoter region determined by comparing its activity, once transfected into a colorectal cancer cell line, with that of an unmethylated *14-3-3 σ* promoter construct.

If there were a reduced promoter activity in cells transfected with the methylated construct, then this would strongly suggest that CpG methylation at the promoter region of *14-3-3 σ* could act as a repressor of *14-3-3 σ* expression in colorectal cancer.

Lastly, another of my aims would be to focus on investigating the complexity of *14-3-3 σ* tissue-specific function. It is not fully understood why in some cancers *14-3-3 σ* is silenced suggesting that *14-3-3 σ* is acting as a tumour suppressor, and overexpressed in others, which would imply that *14-3-3 σ* is tumour promoting. Indeed, the observation that most colorectal cancer cell lines are unmethylated and express high levels of *14-3-3 σ* protein product, whilst most fresh tumour tissues appear not to is interesting. One explanation is that the loss of methylation *in vitro* is a consequence of the generation of cell lines, in which there is selection pressure for particular clones. However, the data presented in this thesis and previously published studies have indicated that increased levels of *14-3-3 σ* (Hermeking et al, 1997; Samuel et al, 2001), in addition to the inactivation of *14-3-3 σ* (Ferguson et al, 2000; Wilker et al, 2007) results in changes in apoptosis and cell cycle progression, both of which may contribute to cancer development. From these findings, a model could be proposed in which ‘too much’ or ‘too little’ of *14-3-3 σ* is detrimental to normal cellular function. It remains unclear however, why *14-3-3 σ* appears to have different functions in different tumour types. As discussed in the introduction of this thesis, *14-3-3 σ* acts as a ‘chaperone molecule’, functioning through modifying the actions of other proteins, and has no activity of its own (Mhawech, 2005). Various screening approaches have identified a number of potential *14-3-3* interacting proteins, demonstrating that via its binding partners, *14-3-3 σ* could perhaps modify the function of many different biological pathways (Meek et al, 2004; Pozuelo Rubio et al, 2004). Therefore, one might speculate that it may be that the role of *14-3-3 σ* in cancer is actually determined by the binding partners that are available for interaction. The availability of these binding partners could vary in different tissues and at different times, or even between normal and neoplastic cells. Hence, this may be why *14-3-3 σ* appears to have such a diverse function in different tumour types. It would be interesting to identify and compare *14-3-3 σ* s binding partners in different

cancers and perhaps during different stages of the cell cycle. Techniques such as, co-immunoprecipitation, yeast two-hybrid assays or tandem affinity purification (TAP) tagging (which would allow *in vivo* capture) could be used to carry out these studies. Candidate 14-3-3 σ binding proteins, such as the proteins involved in cell-cycle control (p53, CDC2-cyclinB1, Cdk2) (Chan et al, 1999; Hermeking et al, 1997; Laronga et al, 2000) or apoptosis (Bax) (Samuel et al, 2001) could be analysed. Alternatively, a library-based approach could be performed, which may coincidentally identify novel 14-3-3 σ binding partners. These studies could be valuable in elucidating 14-3-3 σ s exact role in cancer and the underlying mechanisms which are involved.

In conclusion, the work presented in this thesis provides further insight into the complexities of 14-3-3 σ methylation and its relevance to colorectal cancer. Previously published data and the results presented in this thesis suggest that aberrant methylation and associated changes in expression of 14-3-3 σ may contribute to colorectal carcinogenesis. However, extensive studies to follow up the observations that I have made here, such as those outlined above, would be required to fully determine the clinical relevance of 14-3-3 σ methylation in colorectal cancer. With this further understanding, 14-3-3 σ methylation could perhaps be considered a therapeutic drug target or as a marker for cancer detection or prognosis, at least in a subset of cases.

References

- Adorjan P, Distler J, Lipscher E, Model F, Muller J, Pelet C, Braun A, Florl AR, Gutig D, Grabs G, Howe A, Kursar M, Lesche R, Leu E, Lewin A, Maier S, Muller V, Otto T, Scholz C, Schulz WA, Seifert HH, Schwoppe I, Ziebarth H, Berlin K, Piepenbrock C, Olek A (2002) Tumour class prediction and discovery by microarray-based DNA methylation analysis. *Nucleic Acids Res* **30**(5): e21
- Agrelo R, Cheng WH, Setien F, Ropero S, Espada J, Fraga MF, Herranz M, Paz MF, Sanchez-Cespedes M, Artiga MJ, Guerrero D, Castells A, von Kobbe C, Bohr VA, Esteller M (2006) Epigenetic inactivation of the premature aging Werner syndrome gene in human cancer. *Proc Natl Acad Sci U S A* **103**(23): 8822-8827
- Ahuja N, Li Q, Mohan AL, Baylin SB, Issa JP (1998) Aging and DNA methylation in colorectal mucosa and cancer. *Cancer Res* **58**(23): 5489-5494
- Ahuja N, Mohan AL, Li Q, Stolker JM, Herman JG, Hamilton SR, Baylin SB, Issa JP (1997) Association between CpG island methylation and microsatellite instability in colorectal cancer. *Cancer Research* **57**(16): 3370-3374
- Aitken A, Collinge DB, van Heusden BP, Isobe T, Roseboom PH, Rosenfeld G, Soll J (1992) 14-3-3 proteins: a highly conserved, widespread family of eukaryotic proteins. *Trends Biochem Sci* **17**(12): 498-501
- Akahira J, Sugihashi Y, Suzuki T, Ito K, Niikura H, Moriya T, Nitta M, Okamura H, Inoue S, Sasano H, Okamura K, Yaegashi N (2004) Decreased expression of 14-3-3 sigma is associated with advanced disease in human epithelial ovarian cancer: its correlation with aberrant DNA methylation. *Clin Cancer Res* **10**(8): 2687-2693
- Akiyama Y, Maesawa C, Ogasawara S, Terashima M, Masuda T (2003) Cell-type-specific repression of the maspin gene is disrupted frequently by demethylation at the promoter region in gastric intestinal metaplasia and cancer cells. *Am J Pathol* **163**(5): 1911-1919
- Alaminos M, Davalos V, Ropero S, Setien F, Paz MF, Herranz M, Fraga MF, Mora J, Cheung NK, Gerald WL, Esteller M (2005) EMP3, a myelin-related gene located in the critical 19q13.3 region, is epigenetically silenced and exhibits features of a candidate tumor suppressor in glioma and neuroblastoma. *Cancer Res* **65**(7): 2565-2571
- Aprelikova O, Pace AJ, Fang B, Koller BH, Liu ET (2001) BRCA1 is a selective co-activator of 14-3-3 sigma gene transcription in mouse embryonic stem cells. *J Biol Chem* **276**(28): 25647-25650
- Bachman KE, Park BH, Rhee I, Rajagopalan H, Herman JG, Baylin SB, Kinzler KW, Vogelstein B (2003) Histone modifications and silencing prior to DNA methylation of a tumor suppressor gene. *Cancer Cell* **3**(1): 89-95

- Badal V, Chuang LS, Tan EH, Badal S, Villa LL, Wheeler CM, Li BF, Bernard HU (2003) CpG methylation of human papillomavirus type 16 DNA in cervical cancer cell lines and in clinical specimens: genomic hypomethylation correlates with carcinogenic progression. *J Virol* **77**(11): 6227-6234
- Bailey JA, Carrel L, Chakravarti A, Eichler EE (2000) Molecular evidence for a relationship between LINE-1 elements and X chromosome inactivation: the Lyon repeat hypothesis. *Proc Natl Acad Sci U S A* **97**(12): 6634-6639
- Ballestar E, Esteller M (2002) The impact of chromatin in human cancer: linking DNA methylation to gene silencing. *Carcinogenesis* **23**(7): 1103-1109
- Barault L, Charon-Barra C, Jooste V, de la Vega MF, Martin L, Roignot P, Rat P, Bouvier AM, Laurent-Puig P, Faivre J, Chapusot C, Piard F (2008) Hypermethylator phenotype in sporadic colon cancer: study on a population-based series of 582 cases. *Cancer Res* **68**(20): 8541-8546
- Barski A, Cuddapah S, Cui K, Roh TY, Schones DE, Wang Z, Wei G, Chepelev I, Zhao K (2007) High-resolution profiling of histone methylations in the human genome. *Cell* **129**(4): 823-837
- Bartlett MH, Adra CN, Park J, Chapman VM, McBurney MW (1991) DNA methylation of two X chromosome genes in female somatic and embryonal carcinoma cells. *Somat Cell Mol Genet* **17**(1): 35-47
- Baxter CS, Byvoet P (1975) Intercalating agents as probes of the spatial relationship between chromatin components. *Biochem Biophys Res Commun* **63**(1): 286-291
- Baylin SB, Herman JG, Graff JR, Vertino PM, Issa JP (1998) Alterations in DNA methylation: a fundamental aspect of neoplasia. *Adv Cancer Res* **72**: 141-196
- Baylin SB, Hoppener JW, de Bustros A, Steenbergh PH, Lips CJ, Nelkin BD (1986) DNA methylation patterns of the calcitonin gene in human lung cancers and lymphomas. *Cancer Res* **46**(6): 2917-2922
- Bedford MT, van Helden PD (1987) Hypomethylation of DNA in pathological conditions of the human prostate. *Cancer Res* **47**(20): 5274-5276
- Bell AC, Felsenfeld G (2000) Methylation of a CTCF-dependent boundary controls imprinted expression of the Igf2 gene. *Nature* **405**(6785): 482-485
- Belshaw NJ, Elliott GO, Foxall RJ, Dainty JR, Pal N, Coupe A, Garg D, Bradburn DM, Mathers JC, Johnson IT (2008) Profiling CpG island field methylation in both morphologically normal and neoplastic human colonic mucosa. *Br J Cancer* **99**(1): 136-142
- Benzinger A, Popowicz GM, Joy JK, Majumdar S, Holak TA, Hermeking H (2005) The crystal structure of the non-liganded 14-3-3sigma protein: insights into

determinants of isoform specific ligand binding and dimerization. *Cell Res* **15**(4): 219-227

Bestor T, Laudano A, Mattaliano R, Ingram V (1988) Cloning and sequencing of a cDNA encoding DNA methyltransferase of mouse cells. The carboxyl-terminal domain of the mammalian enzymes is related to bacterial restriction methyltransferases. *J Mol Biol* **203**(4): 971-983

Bhatia K, Siraj AK, Hussain A, Bu R, Gutierrez MI (2003) The tumor suppressor gene 14-3-3 sigma is commonly methylated in normal and malignant lymphoid cells. *Cancer Epidemiol Biomarkers Prev* **12**(2): 165-169

Bird A, Taggart M, Frommer M, Miller OJ, Macleod D (1985) A fraction of the mouse genome that is derived from islands of nonmethylated, CpG-rich DNA. *Cell* **40**(1): 91-99

Bird AP (1986) CpG-rich islands and the function of DNA methylation. *Nature* **321**(6067): 209-213

Bird AP (1995) Gene number, noise reduction and biological complexity. *Trends Genet* **11**(3): 94-100

Bird AP, Wolffe AP (1999) Methylation-induced repression--belts, braces, and chromatin. *Cell* **99**(5): 451-454

Birger Y, Shemer R, Perk J, Razin A (1999) The imprinting box of the mouse Igf2r gene. *Nature* **397**(6714): 84-88

Bocker T, Diermann J, Friedl W, Gebert J, Holinski-Feder E, Karner-Hanusch J, von Knebel-Doeberitz M, Koelble K, Moeslein G, Schackert HK, Wirtz HC, Fishel R, Ruschoff J (1997) Microsatellite instability analysis: a multicenter study for reliability and quality control. *Cancer Res* **57**(21): 4739-4743

Bohr VA, Anson RM (1995) DNA damage, mutation and fine structure DNA repair in aging. *Mutat Res* **338**(1-6): 25-34

Boland CR, Thibodeau SN, Hamilton SR, Sidransky D, Eshleman JR, Burt RW, Meltzer SJ, Rodriguez-Bigas MA, Fodde R, Ranzani, GN, Srivastava S (1998) A National Cancer Institute Workshop on Microsatellite Instability for cancer detection and familial predisposition: development of international criteria for the determination of microsatellite instability in colorectal cancer. *Cancer Research* **58**(22): 5248-5257

Boyer LA, Plath K, Zeitlinger J, Brambrink T, Medeiros LA, Lee TI, Levine SS, Wernig M, Tajonar A, Ray MK, Bell GW, Otte AP, Vidal M, Gifford DK, Young RA, Jaenisch R (2006) Polycomb complexes repress developmental regulators in murine embryonic stem cells. *Nature* **441**(7091): 349-353

- Brakensiek K, Wingen LU, Langer F, Kreipe H, Lehmann U (2007) Quantitative high-resolution CpG island mapping with Pyrosequencing reveals disease-specific methylation patterns of the CDKN2B gene in myelodysplastic syndrome and myeloid leukemia. *Clin Chem* **53**(1): 17-23
- Brenner C, Fuks F (2006) DNA methyltransferases: facts, clues, mysteries. *Curr Top Microbiol Immunol* **301**: 45-66
- Brown CJ, Lafreniere RG, Powers VE, Sebastio G, Ballabio A, Pettigrew AL, Ledbetter DH, Levy E, Craig IW, Willard HF (1991) Localization of the X inactivation centre on the human X chromosome in Xq13. *Nature* **349**(6304): 82-84
- Brown KW, Gardner A, Williams JC, Mott MG, McDermott A, Maitland NJ (1992) Paternal origin of 11p15 duplications in the Beckwith-Wiedemann syndrome. A new case and review of the literature. *Cancer Genet Cytogenet* **58**(1): 66-70
- Caldwell GM, Jones C, Gensberg K, Jan S, Hardy RG, Byrd P, Chughtai S, Wallis Y, Matthews GM, Morton DG (2004) The Wnt antagonist sFRP1 in colorectal tumorigenesis. *Cancer Res* **64**(3): 883-888
- Cameron EE, Bachman KE, Myohanen S, Herman JG, Baylin SB (1999) Synergy of demethylation and histone deacetylase inhibition in the re-expression of genes silenced in cancer. *Nat Genet* **21**(1): 103-107
- Catteau A, Harris WH, Xu CF, Solomon E (1999) Methylation of the BRCA1 promoter region in sporadic breast and ovarian cancer: correlation with disease characteristics. *Oncogene* **18**(11): 1957-1965
- Chan AO, Broaddus RR, Houlihan PS, Issa JP, Hamilton SR, Rashid A (2002) CpG island methylation in aberrant crypt foci of the colorectum. *Am J Pathol* **160**(5): 1823-1830
- Chan TA, Hermeking H, Lengauer C, Kinzler KW, Vogelstein B (1999) 14-3-3Sigma is required to prevent mitotic catastrophe after DNA damage. *Nature* **401**(6753): 616-620
- Chen T, Hevi S, Gay F, Tsujimoto N, He T, Zhang B, Ueda Y, Li E (2007) Complete inactivation of DNMT1 leads to mitotic catastrophe in human cancer cells. *Nat Genet* **39**(3): 391-396
- Chotalia M, Smallwood SA, Ruf N, Dawson C, Lucifero D, Frontera M, James K, Dean W, Kelsey G (2009) Transcription is required for establishment of germline methylation marks at imprinted genes. *Genes Dev* **23**(1): 105-117
- Clark SJ, Harrison J, Paul CL, Frommer M (1994) High sensitivity mapping of methylated cytosines. *Nucleic Acids Res* **22**(15): 2990-2997

Conway KE, McConnell BB, Bowring CE, Donald CD, Warren ST, Vertino PM (2000) TMS1, a novel proapoptotic caspase recruitment domain protein, is a target of methylation-induced gene silencing in human breast cancers. *Cancer Res* **60**(22): 6236-6242

Cooper DN, Taggart MH, Bird AP (1983) Unmethylated domains in vertebrate DNA. *Nucleic Acids Res* **11**(3): 647-658

Corn PG, Kuerbitz SJ, van Noesel MM, Esteller M, Compitello N, Baylin SB, Herman JG (1999) Transcriptional silencing of the p73 gene in acute lymphoblastic leukemia and Burkitt's lymphoma is associated with 5' CpG island methylation. *Cancer Res* **59**(14): 3352-3356

Costello JF, Fruhwald MC, Smiraglia DJ, Rush LJ, Robertson GP, Gao X, Wright FA, Feramisco JD, Peltomaki P, Lang JC, Schuller DE, Yu L, Bloomfield CD, Caligiuri MA, Yates A, Nishikawa R, Su Huang H, Petrelli NJ, Zhang X, O'Dorisio MS, Held WA, Cavenee WK, Plass C (2000) Aberrant CpG-island methylation has non-random and tumour-type-specific patterns. *Nat Genet* **24**(2): 132-138

Costello JF, Futscher BW, Tano K, Graunke DM, Pieper RO (1994) Graded methylation in the promoter and body of the O6-methylguanine DNA methyltransferase (MGMT) gene correlates with MGMT expression in human glioma cells. *J Biol Chem* **269**(25): 17228-17237

Coulondre C, Miller JH, Farabaugh PJ, Gilbert W (1978) Molecular basis of base substitution hotspots in Escherichia coli. *Nature* **274**(5673): 775-780

Cross SH, Charlton JA, Nan X, Bird AP (1994) Purification of CpG islands using a methylated DNA binding column. *Nat Genet* **6**(3): 236-244

Cross SH, Meehan RR, Nan X, Bird A (1997) A component of the transcriptional repressor MeCP1 shares a motif with DNA methyltransferase and HRX proteins. *Nat Genet* **16**(3): 256-259

Damelin M, Bestor TH (2007) Biological functions of DNA methyltransferase 1 require its methyltransferase activity. *Mol Cell Biol* **27**(11): 3891-3899

Dammann R, Li C, Yoon JH, Chin PL, Bates S, Pfeifer GP (2000) Epigenetic inactivation of a RAS association domain family protein from the lung tumour suppressor locus 3p21.3. *Nat Genet* **25**(3): 315-319

de Capoa A, Musolino A, Della Rosa S, Caiafa P, Mariani L, Del Nonno F, Vocaturo A, Donnorso RP, Niveleau A, Grappelli C (2003) DNA demethylation is directly related to tumour progression: evidence in normal, pre-malignant and malignant cells from uterine cervix samples. *Oncol Rep* **10**(3): 545-549

- De Smet C, De Backer O, Faraoni I, Lurquin C, Brasseur F, Boon T (1996) The activation of human gene MAGE-1 in tumor cells is correlated with genome-wide demethylation. *Proc Natl Acad Sci U S A* **93**(14): 7149-7153
- Dellambra E, Golisano O, Bondanza S, Siviero E, Lacal P, Molinari M, D'Atri S, De Luca M (2000) Downregulation of 14-3-3sigma prevents clonal evolution and leads to immortalization of primary human keratinocytes. *J Cell Biol* **149**(5): 1117-1130
- Dennis K, Fan T, Geiman T, Yan Q, Muegge K (2001) Lsh, a member of the SNF2 family, is required for genome-wide methylation. *Genes Dev* **15**(22): 2940-2944
- DePinho RA (2000) The age of cancer. *Nature* **408**(6809): 248-254
- Dhar S, Squire JA, Hande MP, Wellinger RJ, Pandita TK (2000) Inactivation of 14-3-3sigma influences telomere behavior and ionizing radiation-induced chromosomal instability. *Mol Cell Biol* **20**(20): 7764-7772
- Dickson MA, Hahn WC, Ino Y, Ronfard V, Wu JY, Weinberg RA, Louis DN, Li FP, Rheinwald JG (2000) Human keratinocytes that express hTERT and also bypass a p16(INK4a)-enforced mechanism that limits life span become immortal yet retain normal growth and differentiation characteristics. *Mol Cell Biol* **20**(4): 1436-1447
- Dietmaier W, Wallinger S, Bocker T, Kullmann F, Fishel R, Ruschoff J (1997) Diagnostic microsatellite instability: definition and correlation with mismatch repair protein expression. *Cancer Res* **57**(21): 4749-4756
- Din FV, Dunlop MG, Stark LA (2004) Evidence for colorectal cancer cell specificity of aspirin effects on NF kappa B signalling and apoptosis. *Br J Cancer* **91**(2): 381-388
- Dobrovic A, Simpfendorfer D (1997) Methylation of the BRCA1 gene in sporadic breast cancer. *Cancer Res* **57**(16): 3347-3350
- Down TA, Rakyan VK, Turner DJ, Flicek P, Li H, Kulesha E, Graf S, Johnson N, Herrero J, Tomazou EM, Thorne NP, Backdahl L, Herberth M, Howe KL, Jackson DK, Miretti MM, Marioni JC, Birney E, Hubbard TJ, Durbin R, Tavare S, Beck S (2008) A Bayesian deconvolution strategy for immunoprecipitation-based DNA methylome analysis. *Nat Biotechnol* **26**(7): 779-785
- Driscoll DJ, Waters MF, Williams CA, Zori RT, Glenn CC, Avidano KM, Nicholls RD (1992) A DNA methylation imprint, determined by the sex of the parent, distinguishes the Angelman and Prader-Willi syndromes. *Genomics* **13**(4): 917-924
- Eads CA, Danenberg KD, Kawakami K, Saltz LB, Blake C, Shibata D, Danenberg PV, Laird PW (2000) MethyLight: a high-throughput assay to measure DNA methylation. *Nucleic Acids Res* **28**(8): E32

Eads CA, Danenberg KD, Kawakami K, Saltz LB, Danenberg PV, Laird PW (1999) CpG island hypermethylation in human colorectal tumors is not associated with DNA methyltransferase overexpression. *Cancer Res* **59**(10): 2302-2306

Eckhardt F, Lewin J, Cortese R, Rakyan VK, Attwood J, Burger M, Burton J, Cox TV, Davies R, Down TA, Haefliger C, Horton R, Howe K, Jackson DK, Kunde J, Koenig C, Liddle J, Niblett D, Otto T, Pettett R, Seemann S, Thompson C, West T, Rogers J, Olek A, Berlin K, Beck S (2006) DNA methylation profiling of human chromosomes 6, 20 and 22. *Nat Genet* **38**(12): 1378-1385

Ehrlich M, Woods CB, Yu MC, Dubeau L, Yang F, Campan M, Weisenberger DJ, Long T, Youn B, Fiala ES, Laird PW (2006) Quantitative analysis of associations between DNA hypermethylation, hypomethylation, and DNMT RNA levels in ovarian tumors. *Oncogene* **25**(18): 2636-2645

Eis PS, Tam W, Sun L, Chadburn A, Li Z, Gomez MF, Lund E, Dahlberg JE (2005) Accumulation of miR-155 and BIC RNA in human B cell lymphomas. *Proc Natl Acad Sci U S A* **102**(10): 3627-3632

el-Deiry WS, Nelkin BD, Celano P, Yen RW, Falco JP, Hamilton SR, Baylin SB (1991) High expression of the DNA methyltransferase gene characterizes human neoplastic cells and progression stages of colon cancer. *Proc Natl Acad Sci U S A* **88**(8): 3470-3474

el-Deiry WS, Tokino T, Velculescu VE, Levy DB, Parsons R, Trent JM, Lin D, Mercer WE, Kinzler KW, Vogelstein B (1993) WAF1, a potential mediator of p53 tumor suppression. *Cell* **75**(4): 817-825

Estecio MR, Gharibyan V, Shen L, Ibrahim AE, Doshi K, He R, Jelinek J, Yang AS, Yan PS, Huang TH, Tajara EH, Issa JP (2007) LINE-1 hypomethylation in cancer is highly variable and inversely correlated with microsatellite instability. *PLoS ONE* **2**(5): e399

Esteller M (2008) Epigenetics in cancer. *N Engl J Med* **358**(11): 1148-1159

Esteller M, Catusus L, Matias-Guiu X, Mutter GL, Prat J, Baylin SB, Herman JG (1999a) hMLH1 promoter hypermethylation is an early event in human endometrial tumorigenesis. *Am J Pathol* **155**(5): 1767-1772

Esteller M, Corn PG, Baylin SB, Herman JG (2001a) A gene hypermethylation profile of human cancer. *Cancer Res* **61**(8): 3225-3229

Esteller M, Fraga MF, Guo M, Garcia-Foncillas J, Hedenfalk I, Godwin AK, Trojan J, Vaurs-Barriere C, Bignon YJ, Ramus S, Benitez J, Caldes T, Akiyama Y, Yuasa Y, Launonen V, Canal MJ, Rodriguez R, Capella G, Peinado MA, Borg A, Aaltonen LA, Ponder BA, Baylin SB, Herman JG (2001b) DNA methylation patterns in hereditary human cancers mimic sporadic tumorigenesis. *Hum Mol Genet* **10**(26): 3001-3007

Esteller M, Hamilton SR, Burger PC, Baylin SB, Herman JG (1999b) Inactivation of the DNA repair gene O6-methylguanine-DNA methyltransferase by promoter hypermethylation is a common event in primary human neoplasia. *Cancer Res* **59**(4): 793-797

Fabbri M, Garzon R, Cimmino A, Liu Z, Zanesi N, Callegari E, Liu S, Alder H, Costinean S, Fernandez-Cymering C, Volinia S, Guler G, Morrison CD, Chan KK, Marcucci G, Calin GA, Huebner K, Croce CM (2007) MicroRNA-29 family reverts aberrant methylation in lung cancer by targeting DNA methyltransferases 3A and 3B. *Proc Natl Acad Sci U S A* **104**(40): 15805-15810

Fan T, Yan Q, Huang J, Austin S, Cho E, Ferris D, Muegge K (2003) Lsh-deficient murine embryonal fibroblasts show reduced proliferation with signs of abnormal mitosis. *Cancer Res* **63**(15): 4677-4683

Fatemi M, Hermann A, Gowher H, Jeltsch A (2002) Dnmt3a and Dnmt1 functionally cooperate during de novo methylation of DNA. *Eur J Biochem* **269**(20): 4981-4984

Fearon ER, Vogelstein B (1990) A genetic model for colorectal tumorigenesis. *Cell* **61**(5): 759-767

Feinberg AP, Vogelstein B (1983a) Hypomethylation distinguishes genes of some human cancers from their normal counterparts. *Nature* **301**(5895): 89-92

Feinberg AP, Vogelstein B (1983b) Hypomethylation of ras oncogenes in primary human cancers. *Biochem Biophys Res Commun* **111**(1): 47-54

Feldman N, Gerson A, Fang J, Li E, Zhang Y, Shinkai Y, Cedar H, Bergman Y (2006) G9a-mediated irreversible epigenetic inactivation of Oct-3/4 during early embryogenesis. *Nat Cell Biol* **8**(2): 188-194

Ferguson AT, Evron E, Umbricht CB, Pandita TK, Chan TA, Hermeking H, Marks JR, Lambers AR, Futreal PA, Stampfer MR, Sukumar S (2000) High frequency of hypermethylation at the 14-3-3 sigma locus leads to gene silencing in breast cancer. *Proc Natl Acad Sci U S A* **97**(11): 6049-6054

Ferl RJ, Manak MS, Reyes MF (2002) The 14-3-3s. *Genome Biol* **3**(7): REVIEWS3010

Franceschini P, Martino S, Ciocchini M, Ciuti E, Vardeu MP, Guala A, Signorile F, Camerano P, Franceschini D, Tovo PA (1995) Variability of clinical and immunological phenotype in immunodeficiency-centromeric instability-facial anomalies syndrome. Report of two new patients and review of the literature. *Eur J Pediatr* **154**(10): 840-846

Friedrich MG, Weisenberger DJ, Cheng JC, Chandrasoma S, Siegmund KD, Gonzalgo ML, Toma MI, Huland H, Yoo C, Tsai YC, Nichols PW, Bochner BH,

- Jones PA, Liang G (2004) Detection of methylated apoptosis-associated genes in urine sediments of bladder cancer patients. *Clin Cancer Res* **10**(22): 7457-7465
- Frommer M, McDonald LE, Millar DS, Collis CM, Watt F, Grigg GW, Molloy PL, Paul CL (1992) A genomic sequencing protocol that yields a positive display of 5-methylcytosine residues in individual DNA strands. *Proc Natl Acad Sci U S A* **89**(5): 1827-1831
- Fujiwara T, Bandi M, Nitta M, Ivanova EV, Bronson RT, Pellman D (2005) Cytokinesis failure generating tetraploids promotes tumorigenesis in p53-null cells. *Nature* **437**(7061): 1043-1047
- Fuks F, Burgers WA, Godin N, Kasai M, Kouzarides T (2001) Dnmt3a binds deacetylases and is recruited by a sequence-specific repressor to silence transcription. *Embo J* **20**(10): 2536-2544
- Fuks F, Hurd PJ, Deplus R, Kouzarides T (2003) The DNA methyltransferases associate with HP1 and the SUV39H1 histone methyltransferase. *Nucleic Acids Res* **31**(9): 2305-2312
- Gama-Sosa MA, Slagel VA, Trewyn RW, Oxenhandler R, Kuo KC, Gehrke CW, Ehrlich M (1983) The 5-methylcytosine content of DNA from human tumors. *Nucleic Acids Res* **11**(19): 6883-6894
- Gardiner-Garden M, Frommer M (1987) CpG islands in vertebrate genomes. *J Mol Biol* **196**(2): 261-282
- Gasco M, Bell AK, Heath V, Sullivan A, Smith P, Hiller L, Yulug I, Numico G, Merlano M, Farrell PJ, Tavassoli M, Gusterson B, Crook T (2002a) Epigenetic inactivation of 14-3-3 sigma in oral carcinoma: association with p16(INK4a) silencing and human papillomavirus negativity. *Cancer Res* **62**(7): 2072-2076
- Gasco M, Sullivan A, Repellin C, Brooks L, Farrell PJ, Tidy JA, Dunne B, Gusterson B, Evans DJ, Crook T (2002b) Coincident inactivation of 14-3-3sigma and p16INK4a is an early event in vulval squamous neoplasia. *Oncogene* **21**(12): 1876-1881
- Gaudet F, Hodgson JG, Eden A, Jackson-Grusby L, Dausman J, Gray JW, Leonhardt H, Jaenisch R (2003) Induction of tumors in mice by genomic hypomethylation. *Science* **300**(5618): 489-492
- Ghahary A, Marcoux Y, Karimi-Busheri F, Li Y, Tredget EE, Kilani RT, Lam E, Weinfeld M (2005) Differentiated keratinocyte-releasable stratifin (14-3-3 sigma) stimulates MMP-1 expression in dermal fibroblasts. *J Invest Dermatol* **124**(1): 170-177

- Gilbert N, Boyle S, Fiegler H, Woodfine K, Carter NP, Bickmore WA (2004) Chromatin architecture of the human genome: gene-rich domains are enriched in open chromatin fibers. *Cell* **118**(5): 555-566
- Gilbert N, Thomson I, Boyle S, Allan J, Ramsahoye B, Bickmore WA (2007) DNA methylation affects nuclear organization, histone modifications, and linker histone binding but not chromatin compaction. *J Cell Biol* **177**(3): 401-411
- Gius D, Cui H, Bradbury CM, Cook J, Smart DK, Zhao S, Young L, Brandenburg SA, Hu Y, Bisht KS, Ho AS, Mattson D, Sun L, Munson PJ, Chuang EY, Mitchell JB, Feinberg AP (2004) Distinct effects on gene expression of chemical and genetic manipulation of the cancer epigenome revealed by a multimodality approach. *Cancer Cell* **6**(4): 361-371
- Goel A, Nagasaka T, Arnold CN, Inoue T, Hamilton C, Niedzwiecki D, Compton C, Mayer RJ, Goldberg R, Bertagnolli MM, Boland CR (2007) The CpG island methylator phenotype and chromosomal instability are inversely correlated in sporadic colorectal cancer. *Gastroenterology* **132**(1): 127-138
- Goll MG, Kirpekar F, Maggert KA, Yoder JA, Hsieh CL, Zhang X, Golic KG, Jacobsen SE, Bestor TH (2006) Methylation of tRNA^{Asp} by the DNA methyltransferase homolog Dnmt2. *Science* **311**(5759): 395-398
- Gonzalez-Zulueta M, Bender CM, Yang AS, Nguyen T, Beart RW, Van Tornout JM, Jones PA (1995) Methylation of the 5' CpG island of the p16/CDKN2 tumor suppressor gene in normal and transformed human tissues correlates with gene silencing. *Cancer Res* **55**(20): 4531-4535
- Graff JR, Herman JG, Lapidus RG, Chopra H, Xu R, Jarrard DF, Isaacs WB, Pitha PM, Davidson NE, Baylin SB (1995) E-cadherin expression is silenced by DNA hypermethylation in human breast and prostate carcinomas. *Cancer Res* **55**(22): 5195-5199
- Greger V, Passarge E, Hopping W, Messmer E, Horsthemke B (1989) Epigenetic changes may contribute to the formation and spontaneous regression of retinoblastoma. *Hum Genet* **83**(2): 155-158
- Gruenbaum Y, Stein R, Cedar H, Razin A (1981) Methylation of CpG sequences in eukaryotic DNA. *FEBS Lett* **124**(1): 67-71
- Guy J, Hendrich B, Holmes M, Martin JE, Bird A (2001) A mouse Mecp2-null mutation causes neurological symptoms that mimic Rett syndrome. *Nat Genet* **27**(3): 322-326
- Hajkova P, Erhardt S, Lane N, Haaf T, El-Maarri O, Reik W, Walter J, Surani MA (2002) Epigenetic reprogramming in mouse primordial germ cells. *Mech Dev* **117**(1-2): 15-23

- Hansen RS, Wijmenga C, Luo P, Stanek AM, Canfield TK, Weemaes CM, Gartler SM (1999) The DNMT3B DNA methyltransferase gene is mutated in the ICF immunodeficiency syndrome. *Proc Natl Acad Sci U S A* **96**(25): 14412-14417
- Hatada I, Hayashizaki Y, Hirotsune S, Komatsubara H, Mukai T (1991) A genomic scanning method for higher organisms using restriction sites as landmarks. *Proc Natl Acad Sci U S A* **88**(21): 9523-9527
- Hawkins N, Norrie M, Cheong K, Mokany E, Ku SL, Meagher A, O'Connor T, Ward R (2002) CpG island methylation in sporadic colorectal cancers and its relationship to microsatellite instability. *Gastroenterology* **122**(5): 1376-1387
- Heard E, Rougeulle C, Arnaud D, Avner P, Allis CD, Spector DL (2001) Methylation of histone H3 at Lys-9 is an early mark on the X chromosome during X inactivation. *Cell* **107**(6): 727-738
- Hellman A, Chess A (2007) Gene body-specific methylation on the active X chromosome. *Science* **315**(5815): 1141-1143
- Hendrich B, Guy J, Ramsahoye B, Wilson VA, Bird A (2001) Closely related proteins MBD2 and MBD3 play distinctive but interacting roles in mouse development. *Genes Dev* **15**(6): 710-723
- Herman JG, Civin CI, Issa JP, Collector MI, Sharkis SJ, Baylin SB (1997) Distinct patterns of inactivation of p15INK4B and p16INK4A characterize the major types of hematological malignancies. *Cancer Res* **57**(5): 837-841
- Herman JG, Graff JR, Myohanen S, Nelkin BD, Baylin SB (1996a) Methylation-specific PCR: a novel PCR assay for methylation status of CpG islands. *Proc Natl Acad Sci U S A* **93**(18): 9821-9826
- Herman JG, Jen J, Merlo A, Baylin SB (1996b) Hypermethylation-associated inactivation indicates a tumor suppressor role for p15INK4B. *Cancer Res* **56**(4): 722-727
- Herman JG, Latif F, Weng Y, Lerman MI, Zbar B, Liu S, Samid D, Duan DS, Gnarr JR, Linehan WM, et al. (1994) Silencing of the VHL tumor-suppressor gene by DNA methylation in renal carcinoma. *Proc Natl Acad Sci U S A* **91**(21): 9700-9704
- Herman JG, Merlo A, Mao L, Lapidus RG, Issa JP, Davidson NE, Sidransky D, Baylin SB (1995) Inactivation of the CDKN2/p16/MTS1 gene is frequently associated with aberrant DNA methylation in all common human cancers. *Cancer Res* **55**(20): 4525-4530
- Herman JG, Umar A, Polyak K, Graff JR, Ahuja N, Issa JPJ, Markowitz S, Willson JKV, Hamilton SR, Kinzler KW, Kane MF, Kolodner RD, Vogelstein B, Kunkel TA, Baylin SB (1998) Incidence and functional consequences of hMLH1 promoter

hypermethylation in colorectal carcinoma. *Proceedings of the National Academy of Sciences of the United States of America* **95**(12): 6870-6875

Hermeking H (2003) The 14-3-3 cancer connection. *Nat Rev Cancer* **3**(12): 931-943

Hermeking H, Lengauer C, Polyak K, He TC, Zhang L, Thiagalingam S, Kinzler KW, Vogelstein B (1997) 14-3-3 sigma is a p53-regulated inhibitor of G2/M progression. *Mol Cell* **1**(1): 3-11

Holliday R, Pugh JE (1975) DNA modification mechanisms and gene activity during development. *Science* **187**(4173): 226-232

Horii J, Hiraoka S, Kato J, Harada K, Kuwaki K, Fujita H, Toyooka S, Yamamoto K (2008) Age-related methylation in normal colon mucosa differs between the proximal and distal colon in patients who underwent colonoscopy. *Clin Biochem* **41**(18): 1440-1448

Hsiao WL, Gattoni-Celli S, Kirschmeier P, Weinstein IB (1984) Effects of 5-azacytidine on methylation and expression of specific DNA sequences in C3H 10T1/2 cells. *Mol Cell Biol* **4**(4): 634-641

Iacobuzio-Donahue CA, Maitra A, Olsen M, Lowe AW, van Heek NT, Rosty C, Walter K, Sato N, Parker A, Ashfaq R, Jaffee E, Ryu B, Jones J, Eshleman JR, Yeo CJ, Cameron JL, Kern SE, Hruban RH, Brown PO, Goggins M (2003) Exploration of global gene expression patterns in pancreatic adenocarcinoma using cDNA microarrays. *Am J Pathol* **162**(4): 1151-1162

Ide M, Nakajima T, Asao T, Kuwano H (2004) Inactivation of 14-3-3sigma by hypermethylation is a rare event in colorectal cancers and its expression may correlate with cell cycle maintenance at the invasion front. *Cancer Lett* **207**(2): 241-249

Iida S, Akiyama Y, Nakajima T, Ichikawa W, Nihei Z, Sugihara K, Yuasa Y (2000) Alterations and hypermethylation of the p14(ARF) gene in gastric cancer. *Int J Cancer* **87**(5): 654-658

Illingworth R, Kerr A, Desousa D, Jorgensen H, Ellis P, Stalker J, Jackson D, Clee C, Plumb R, Rogers J, Humphray S, Cox T, Langford C, Bird A (2008) A novel CpG island set identifies tissue-specific methylation at developmental gene loci. *PLoS Biol* **6**(1): e22

Irizarry RA, Ladd-Acosta C, Wen B, Wu Z, Montano C, Onyango P, Cui H, Gabo K, Rongione M, Webster M, Ji H, Potash JB, Sabunciyan S, Feinberg AP (2009) The human colon cancer methylome shows similar hypo- and hypermethylation at conserved tissue-specific CpG island shores. *Nat Genet* **41**(2): 178-186

Issa JP (1999) Aging, DNA methylation and cancer. *Crit Rev Oncol Hematol* **32**(1): 31-43

- Issa JP (2000) The epigenetics of colorectal cancer. *Ann N Y Acad Sci* **910**: 140-153; discussion 153-145
- Issa JP (2004) CpG island methylator phenotype in cancer. *Nat Rev Cancer* **4**(12): 988-993
- Issa JP, Ottaviano YL, Celano P, Hamilton SR, Davidson NE, Baylin SB (1994) Methylation of the oestrogen receptor CpG island links ageing and neoplasia in human colon. *Nat Genet* **7**(4): 536-540
- Issa JP, Shen L, Toyota M (2005) CIMP, at last. *Gastroenterology* **129**(3): 1121-1124
- Issa JP, Vertino PM, Boehm CD, Newsham IF, Baylin SB (1996) Switch from monoallelic to biallelic human IGF2 promoter methylation during aging and carcinogenesis. *Proc Natl Acad Sci U S A* **93**(21): 11757-11762
- Iwata N, Yamamoto H, Sasaki S, Itoh F, Suzuki H, Kikuchi T, Kaneto H, Iku S, Ozeki I, Karino Y, Satoh T, Toyota J, Satoh M, Endo T, Imai K (2000) Frequent hypermethylation of CpG islands and loss of expression of the 14-3-3 sigma gene in human hepatocellular carcinoma. *Oncogene* **19**(46): 5298-5302
- Jackson M, Krassowska A, Gilbert N, Chevassut T, Forrester L, Ansell J, Ramsahoye B (2004) Severe global DNA hypomethylation blocks differentiation and induces histone hyperacetylation in embryonic stem cells. *Mol Cell Biol* **24**(20): 8862-8871
- Jones PA (1999) The DNA methylation paradox. *Trends Genet* **15**(1): 34-37
- Jones PA, Baylin SB (2002) The fundamental role of epigenetic events in cancer. *Nat Rev Genet* **3**(6): 415-428
- Jones PA, Laird PW (1999) Cancer epigenetics comes of age. *Nat Genet* **21**(2): 163-167
- Jones PA, Taylor SM (1980) Cellular differentiation, cytidine analogs and DNA methylation. *Cell* **20**(1): 85-93
- Jones PL, Veenstra GJ, Wade PA, Vermaak D, Kass SU, Landsberger N, Strouboulis J, Wolffe AP (1998) Methylated DNA and MeCP2 recruit histone deacetylase to repress transcription. *Nat Genet* **19**(2): 187-191
- Jones PL, Wolffe AP (1999) Relationships between chromatin organization and DNA methylation in determining gene expression. *Semin Cancer Biol* **9**(5): 339-347
- Jost CA, Marin MC, Kaelin WG, Jr. (1997) p73 is a simian [correction of human] p53-related protein that can induce apoptosis. *Nature* **389**(6647): 191-194

- Juttermann R, Li E, Jaenisch R (1994) Toxicity of 5-aza-2'-deoxycytidine to mammalian cells is mediated primarily by covalent trapping of DNA methyltransferase rather than DNA demethylation. *Proc Natl Acad Sci U S A* **91**(25): 11797-11801
- Kambara T, Simms LA, Whitehall VL, Spring KJ, Wynter CV, Walsh MD, Barker MA, Arnold S, McGivern A, Matsubara N, Tanaka N, Higuchi T, Young J, Jass JR, Leggett BA (2004) BRAF mutation is associated with DNA methylation in serrated polyps and cancers of the colorectum. *Gut* **53**(8): 1137-1144
- Kanai Y, Ushijima S, Nakanishi Y, Sakamoto M, Hirohashi S (2003) Mutation of the DNA methyltransferase (DNMT) 1 gene in human colorectal cancers. *Cancer Lett* **192**(1): 75-82
- Kane MF, Loda M, Gaida GM, Lipman J, Mishra R, Goldman H, Jessup JM, Kolodner R (1997) Methylation of the hmlh1 promoter correlates with lack of expression of hmlh1 in sporadic colon tumors and mismatch repair-defective human tumor cell lines. *Cancer Research* **57**(5): 808-811
- Kaneuchi M, Sasaki M, Tanaka Y, Shiina H, Verma M, Ebina Y, Nomura E, Yamamoto R, Sakuragi N, Dahiya R (2004) Expression and methylation status of 14-3-3 sigma gene can characterize the different histological features of ovarian cancer. *Biochem Biophys Res Commun* **316**(4): 1156-1162
- Kawakami K, Ruszkiewicz A, Bennett G, Moore J, Griew F, Watanabe G, Iacopetta B (2006) DNA hypermethylation in the normal colonic mucosa of patients with colorectal cancer. *Br J Cancer* **94**(4): 593-598
- Keshet I, Schlesinger Y, Farkash S, Rand E, Hecht M, Segal E, Pikarski E, Young RA, Niveleau A, Cedar H, Simon I (2006) Evidence for an instructive mechanism of de novo methylation in cancer cells. *Nat Genet* **38**(2): 149-153
- Kiyono T, Foster SA, Koop JJ, McDougall JK, Galloway DA, Klingelhutz AJ (1998) Both Rb/p16INK4a inactivation and telomerase activity are required to immortalize human epithelial cells. *Nature* **396**(6706): 84-88
- Knudson AG (2000) Chasing the cancer demon. *Annu Rev Genet* **34**: 1-19
- Kochanek S, Renz D, Doerfler W (1993) DNA methylation in the Alu sequences of diploid and haploid primary human cells. *Embo J* **12**(3): 1141-1151
- Kohlmaier A, Savarese F, Lachner M, Martens J, Jenuwein T, Wutz A (2004) A chromosomal memory triggered by Xist regulates histone methylation in X inactivation. *PLoS Biol* **2**(7): E171

- Kondo E, Gu Z, Horii A, Fukushima S (2005) The thymine DNA glycosylase MBD4 represses transcription and is associated with methylated p16(INK4a) and hMLH1 genes. *Mol Cell Biol* **25**(11): 4388-4396
- Kouzarides T (2007) Chromatin modifications and their function. *Cell* **128**(4): 693-705
- Kwabi-Addo B, Chung W, Shen L, Ittmann M, Wheeler T, Jelinek J, Issa JP (2007) Age-related DNA methylation changes in normal human prostate tissues. *Clin Cancer Res* **13**(13): 3796-3802
- Lachner M, O'Carroll D, Rea S, Mechtler K, Jenuwein T (2001) Methylation of histone H3 lysine 9 creates a binding site for HP1 proteins. *Nature* **410**(6824): 116-120
- Laronga C, Yang HY, Neal C, Lee MH (2000) Association of the cyclin-dependent kinases and 14-3-3 sigma negatively regulates cell cycle progression. *J Biol Chem* **275**(30): 23106-23112
- Larsen F, Gundersen G, Lopez R, Prydz H (1992) CpG islands as gene markers in the human genome. *Genomics* **13**(4): 1095-1107
- Lee DY, Hayes JJ, Pruss D, Wolffe AP (1993) A positive role for histone acetylation in transcription factor access to nucleosomal DNA. *Cell* **72**(1): 73-84
- Lee JT, Davidow LS, Warshawsky D (1999) Tsix, a gene antisense to Xist at the X-inactivation centre. *Nat Genet* **21**(4): 400-404
- Lee PJ, Washer LL, Law DJ, Boland CR, Horon IL, Feinberg AP (1996) Limited up-regulation of DNA methyltransferase in human colon cancer reflecting increased cell proliferation. *Proc Natl Acad Sci U S A* **93**(19): 10366-10370
- Lee S, Kim WH, Jung HY, Yang MH, Kang GH (2002) Aberrant CpG island methylation of multiple genes in intrahepatic cholangiocarcinoma. *Am J Pathol* **161**(3): 1015-1022
- Lee WH, Morton RA, Epstein JI, Brooks JD, Campbell PA, Bova GS, Hsieh WS, Isaacs WB, Nelson WG (1994) Cytidine methylation of regulatory sequences near the pi-class glutathione S-transferase gene accompanies human prostatic carcinogenesis. *Proc Natl Acad Sci U S A* **91**(24): 11733-11737
- Leffers H, Madsen P, Rasmussen HH, Honore B, Andersen AH, Walbum E, Vandekerckhove J, Celis JE (1993) Molecular cloning and expression of the transformation sensitive epithelial marker stratifin. A member of a protein family that has been involved in the protein kinase C signalling pathway. *J Mol Biol* **231**(4): 982-998

- Lei H, Oh SP, Okano M, Juttermann R, Goss KA, Jaenisch R, Li E (1996) De novo DNA cytosine methyltransferase activities in mouse embryonic stem cells. *Development* **122**(10): 3195-3205
- Lengauer C, Kinzler KW, Vogelstein B (1997) Genetic instability in colorectal cancers. *Nature* **386**(6625): 623-627
- Leonhardt H, Page AW, Weier HU, Bestor TH (1992) A targeting sequence directs DNA methyltransferase to sites of DNA replication in mammalian nuclei. *Cell* **71**(5): 865-873
- Leung SY, Yuen ST, Chung LP, Chu KM, Chan AS, Ho JC (1999) hMLH1 promoter methylation and lack of hMLH1 expression in sporadic gastric carcinomas with high-frequency microsatellite instability. *Cancer Res* **59**(1): 159-164
- Lewis JD, Meehan RR, Henzel WJ, Maurer-Fogy I, Jeppesen P, Klein F, Bird A (1992) Purification, sequence, and cellular localization of a novel chromosomal protein that binds to methylated DNA. *Cell* **69**(6): 905-914
- Li E, Bestor TH, Jaenisch R (1992) Targeted mutation of the DNA methyltransferase gene results in embryonic lethality. *Cell* **69**(6): 915-926
- Li LC, Dahiya R (2002) MethPrimer: designing primers for methylation PCRs. *Bioinformatics* **18**(11): 1427-1431
- Liang G, Chan MF, Tomigahara Y, Tsai YC, Gonzales FA, Li E, Laird PW, Jones PA (2002) Cooperativity between DNA methyltransferases in the maintenance methylation of repetitive elements. *Mol Cell Biol* **22**(2): 480-491
- Liu B, Farrington SM, Petersen GM, Hamilton SR, Parsons R, Papadopoulos N, Fujiwara T, Jen J, Kinzler KW, Wyllie AH, et al. (1995a) Genetic instability occurs in the majority of young patients with colorectal cancer. *Nat Med* **1**(4): 348-352
- Liu B, Nicolaides NC, Markowitz S, Willson JK, Parsons RE, Jen J, Papadopoulos N, Peltomaki P, de la Chapelle A, Hamilton SR, et al. (1995b) Mismatch repair gene defects in sporadic colorectal cancers with microsatellite instability. *Nat Genet* **9**(1): 48-55
- Liu B, Parsons R, Papadopoulos N, Nicolaides NC, Lynch HT, Watson P, Jass JR, Dunlop M, Wyllie A, Peltomaki P, de la Chapelle A, Hamilton SR, Vogelstein B, Kinzler KW (1996) Analysis of mismatch repair genes in hereditary non-polyposis colorectal cancer patients. *Nat Med* **2**(2): 169-174
- Liu S, Howell P, Ren S, Fodstad O, Riker AI (2009) The 14-3-3sigma gene promoter is methylated in both human melanocytes and melanoma. *BMC Cancer* **9**: 162
- Lodygin D, Diebold J, Hermeking H (2004) Prostate cancer is characterized by epigenetic silencing of 14-3-3sigma expression. *Oncogene* **23**(56): 9034-9041

- Lodygin D, Yazdi AS, Sander CA, Herzinger T, Hermeking H (2003) Analysis of 14-3-3sigma expression in hyperproliferative skin diseases reveals selective loss associated with CpG-methylation in basal cell carcinoma. *Oncogene* **22**(35): 5519-5524
- Lopes EC, Valls E, Figueroa ME, Mazur A, Meng FG, Chiosis G, Laird PW, Schreiber-Agus N, Grealley JM, Prokhortchouk E, Melnick A (2008) Kaiso contributes to DNA methylation-dependent silencing of tumor suppressor genes in colon cancer cell lines. *Cancer Res* **68**(18): 7258-7263
- Lothe RA, Andersen SN, Hofstad B, Meling GI, Peltomaki P, Heim S, Brogger A, Vatn M, Rognum TO, Borresen AL (1995) Deletion of 1p loci and microsatellite instability in colorectal polyps. *Genes Chromosomes Cancer* **14**(3): 182-188
- Luedi PP, Dietrich FS, Weidman JR, Bosko JM, Jirtle RL, Hartemink AJ (2007) Computational and experimental identification of novel human imprinted genes. *Genome Res* **17**(12): 1723-1730
- Lyon MF (1998) X-chromosome inactivation: a repeat hypothesis. *Cytogenet Cell Genet* **80**(1-4): 133-137
- Maatouk DM, Kellam LD, Mann MR, Lei H, Li E, Bartolomei MS, Resnick JL (2006) DNA methylation is a primary mechanism for silencing postmigratory primordial germ cell genes in both germ cell and somatic cell lineages. *Development* **133**(17): 3411-3418
- Maesawa C, Tamura G, Nishizuka S, Ogasawara S, Ishida K, Terashima M, Sakata K, Sato N, Saito K, Satodate R (1996) Inactivation of the CDKN2 gene by homozygous deletion and de novo methylation is associated with advanced stage esophageal squamous cell carcinoma. *Cancer Res* **56**(17): 3875-3878
- Magdinier F, Wolffe AP (2001) Selective association of the methyl-CpG binding protein MBD2 with the silent p14/p16 locus in human neoplasia. *Proc Natl Acad Sci U S A* **98**(9): 4990-4995
- Margueron R, Trojer P, Reinberg D (2005) The key to development: interpreting the histone code? *Curr Opin Genet Dev* **15**(2): 163-176
- Meek SE, Lane WS, Piwnicka-Worms H (2004) Comprehensive proteomic analysis of interphase and mitotic 14-3-3-binding proteins. *J Biol Chem* **279**(31): 32046-32054
- Meissner A, Gnirke A, Bell GW, Ramsahoye B, Lander ES, Jaenisch R (2005) Reduced representation bisulfite sequencing for comparative high-resolution DNA methylation analysis. *Nucleic Acids Res* **33**(18): 5868-5877
- Merlo A, Herman JG, Mao L, Lee DJ, Gabrielson E, Burger PC, Baylin SB, Sidransky D (1995) 5' CpG island methylation is associated with transcriptional

silencing of the tumour suppressor p16/CDKN2/MTS1 in human cancers. *Nat Med* **1**(7): 686-692

Mhawech P (2005) 14-3-3 proteins--an update. *Cell Res* **15**(4): 228-236

Mhawech P, Benz A, Cerato C, Greloz V, Assaly M, Desmond JC, Koeffler HP, Lodygin D, Hermeking H, Herrmann F, Schwaller J (2005) Downregulation of 14-3-3sigma in ovary, prostate and endometrial carcinomas is associated with CpG island methylation. *Mod Pathol* **18**(3): 340-348

Motokura T, Nakamura Y, Sato H (2007) Aberrant overexpression of an epithelial marker, 14-3-3sigma, in a subset of hematological malignancies. *BMC Cancer* **7**: 217

Muslin AJ, Tanner JW, Allen PM, Shaw AS (1996) Interaction of 14-3-3 with signaling proteins is mediated by the recognition of phosphoserine. *Cell* **84**(6): 889-897

Nakajima T, Shimooka H, Weixa P, Segawa A, Motegi A, Jian Z, Masuda N, Ide M, Sano T, Oyama T, Tsukagoshi H, Hamanaka K, Maeda M (2003) Immunohistochemical demonstration of 14-3-3 sigma protein in normal human tissues and lung cancers, and the preponderance of its strong expression in epithelial cells of squamous cell lineage. *Pathol Int* **53**(6): 353-360

Nakamura N, Takenaga K (1998) Hypomethylation of the metastasis-associated S100A4 gene correlates with gene activation in human colon adenocarcinoma cell lines. *Clin Exp Metastasis* **16**(5): 471-479

Nakayama H, Sano T, Motegi A, Oyama T, Nakajima T (2005) Increasing 14-3-3 sigma expression with declining estrogen receptor alpha and estrogen-responsive finger protein expression defines malignant progression of endometrial carcinoma. *Pathol Int* **55**(11): 707-715

Nan X, Campoy FJ, Bird A (1997) MeCP2 is a transcriptional repressor with abundant binding sites in genomic chromatin. *Cell* **88**(4): 471-481

Nan X, Meehan RR, Bird A (1993) Dissection of the methyl-CpG binding domain from the chromosomal protein MeCP2. *Nucleic Acids Res* **21**(21): 4886-4892

Nan X, Ng HH, Johnson CA, Laherty CD, Turner BM, Eisenman RN, Bird A (1998) Transcriptional repression by the methyl-CpG-binding protein MeCP2 involves a histone deacetylase complex. *Nature* **393**(6683): 386-389

Ng HH, Zhang Y, Hendrich B, Johnson CA, Turner BM, Erdjument-Bromage H, Tempst P, Reinberg D, Bird A (1999) MBD2 is a transcriptional repressor belonging to the MeCP1 histone deacetylase complex. *Nat Genet* **23**(1): 58-61

- Nie Y, Liao J, Zhao X, Song Y, Yang GY, Wang LD, Yang CS (2002) Detection of multiple gene hypermethylation in the development of esophageal squamous cell carcinoma. *Carcinogenesis* **23**(10): 1713-1720
- Ogino S, Kawasaki T, Kirkner GJ, Kraft P, Loda M, Fuchs CS (2007) Evaluation of markers for CpG island methylator phenotype (CIMP) in colorectal cancer by a large population-based sample. *J Mol Diagn* **9**(3): 305-314
- Okano M, Bell DW, Haber DA, Li E (1999) DNA methyltransferases Dnmt3a and Dnmt3b are essential for de novo methylation and mammalian development. *Cell* **99**(3): 247-257
- Okano M, Xie S, Li E (1998) Cloning and characterization of a family of novel mammalian DNA (cytosine-5) methyltransferases. *Nat Genet* **19**(3): 219-220
- Ordway JM, Williams K, Curran T (2004) Transcription repression in oncogenic transformation: common targets of epigenetic repression in cells transformed by Fos, Ras or Dnmt1. *Oncogene* **23**(21): 3737-3748
- Osada H, Tatematsu Y, Yatabe Y, Nakagawa T, Konishi H, Harano T, Tezel E, Takada M, Takahashi T (2002) Frequent and histological type-specific inactivation of 14-3-3sigma in human lung cancers. *Oncogene* **21**(15): 2418-2424
- Oshiro MM, Futscher BW, Lisberg A, Wozniak RJ, Klimecki WT, Domann FE, Cress AE (2005) Epigenetic regulation of the cell type-specific gene 14-3-3sigma. *Neoplasia* **7**(9): 799-808
- Panning B, Jaenisch R (1996) DNA hypomethylation can activate Xist expression and silence X-linked genes. *Genes Dev* **10**(16): 1991-2002
- Paz MF, Fraga MF, Avila S, Guo M, Pollan M, Herman JG, Esteller M (2003) A systematic profile of DNA methylation in human cancer cell lines. *Cancer Res* **63**(5): 1114-1121
- Pellegrini G, Dellambra E, Golisano O, Martinelli E, Fantozzi I, Bondanza S, Ponzin D, McKeon F, De Luca M (2001) p63 identifies keratinocyte stem cells. *Proc Natl Acad Sci U S A* **98**(6): 3156-3161
- Peng CY, Graves PR, Thoma RS, Wu Z, Shaw AS, Piwnicka-Worms H (1997) Mitotic and G2 checkpoint control: regulation of 14-3-3 protein binding by phosphorylation of Cdc25C on serine-216. *Science* **277**(5331): 1501-1505
- Perathoner A, Pirkebner D, Brandacher G, Spizzo G, Stadlmann S, Obrist P, Margreiter R, Amberger A (2005) 14-3-3sigma expression is an independent prognostic parameter for poor survival in colorectal carcinoma patients. *Clin Cancer Res* **11**(9): 3274-3279

- Petrovich M, Veprintsev DB (2008) Effects of CpG Methylation on Recognition of DNA by the Tumour Suppressor p53. *J Mol Biol*
- Pomraning KR, Smith KM, Freitag M (2009) Genome-wide high throughput analysis of DNA methylation in eukaryotes. *Methods* **47**(3): 142-150
- Pozuelo Rubio M, Geraghty KM, Wong BH, Wood NT, Campbell DG, Morrice N, Mackintosh C (2004) 14-3-3-affinity purification of over 200 human phosphoproteins reveals new links to regulation of cellular metabolism, proliferation and trafficking. *Biochem J* **379**(Pt 2): 395-408
- Prasad GL, Valverius EM, McDuffie E, Cooper HL (1992) Complementary DNA cloning of a novel epithelial cell marker protein, HME1, that may be down-regulated in neoplastic mammary cells. *Cell Growth Differ* **3**(8): 507-513
- Prendergast GC, Lawe D, Ziff EB (1991) Association of Myn, the murine homolog of max, with c-Myc stimulates methylation-sensitive DNA binding and ras cotransformation. *Cell* **65**(3): 395-407
- Prokhortchouk A, Hendrich B, Jorgensen H, Ruzov A, Wilm M, Georgiev G, Bird A, Prokhortchouk E (2001) The p120 catenin partner Kaiso is a DNA methylation-dependent transcriptional repressor. *Genes Dev* **15**(13): 1613-1618
- Prokhortchouk A, Sansom O, Selfridge J, Caballero IM, Salozhin S, Aithozhina D, Cerchietti L, Meng FG, Augenlicht LH, Mariadason JM, Hendrich B, Melnick A, Prokhortchouk E, Clarke A, Bird A (2006) Kaiso-deficient mice show resistance to intestinal cancer. *Mol Cell Biol* **26**(1): 199-208
- Pyronnet S, Dostie J, Sonenberg N (2001) Suppression of cap-dependent translation in mitosis. *Genes Dev* **15**(16): 2083-2093
- Pyronnet S, Pradayrol L, Sonenberg N (2000) A cell cycle-dependent internal ribosome entry site. *Mol Cell* **5**(4): 607-616
- Qi W, Liu X, Qiao D, Martinez JD (2005) Isoform-specific expression of 14-3-3 proteins in human lung cancer tissues. *Int J Cancer* **113**(3): 359-363
- Qu GZ, Grundy PE, Narayan A, Ehrlich M (1999) Frequent hypomethylation in Wilms tumors of pericentromeric DNA in chromosomes 1 and 16. *Cancer Genet Cytogenet* **109**(1): 34-39
- Quirke P (1997) Molecular pathology of colorectal cancer. *Ann Pathol* **17 Suppl 5**: 22
- Rakyan VK, Down TA, Thorne NP, Flicek P, Kulesha E, Graf S, Tomazou EM, Backdahl L, Johnson N, Herberth M, Howe KL, Jackson DK, Miretti MM, Fiegler H, Marioni JC, Birney E, Hubbard TJ, Carter NP, Tavare S, Beck S (2008) An

integrated resource for genome-wide identification and analysis of human tissue-specific differentially methylated regions (tDMRs). *Genome Res* **18**(9): 1518-1529

Ramsahoye BH (2002) Nearest-neighbor analysis. *Methods Mol Biol* **200**: 9-15

Ramsahoye BH, Biniszkiwicz D, Lyko F, Clark V, Bird AP, Jaenisch R (2000) Non-CpG methylation is prevalent in embryonic stem cells and may be mediated by DNA methyltransferase 3a. *Proc Natl Acad Sci U S A* **97**(10): 5237-5242

Rauch TA, Zhong X, Wu X, Wang M, Kernstine KH, Wang Z, Riggs AD, Pfeifer GP (2008) High-resolution mapping of DNA hypermethylation and hypomethylation in lung cancer. *Proc Natl Acad Sci U S A* **105**(1): 252-257

Reik W (2007) Stability and flexibility of epigenetic gene regulation in mammalian development. *Nature* **447**(7143): 425-432

Rhee I, Bachman KE, Park BH, Jair KW, Yen RW, Schuebel KE, Cui H, Feinberg AP, Lengauer C, Kinzler KW, Baylin SB, Vogelstein B (2002) DNMT1 and DNMT3b cooperate to silence genes in human cancer cells. *Nature* **416**(6880): 552-556

Rhee I, Jair KW, Yen RW, Lengauer C, Herman JG, Kinzler KW, Vogelstein B, Baylin SB, Schuebel KE (2000) CpG methylation is maintained in human cancer cells lacking DNMT1. *Nature* **404**(6781): 1003-1007

Rice JC, Allis CD (2001) Histone methylation versus histone acetylation: new insights into epigenetic regulation. *Curr Opin Cell Biol* **13**(3): 263-273

Riggs AD (1975) X inactivation, differentiation, and DNA methylation. *Cytogenet Cell Genet* **14**(1): 9-25

Robertson KD (2001) DNA methylation, methyltransferases, and cancer. *Oncogene* **20**(24): 3139-3155

Robertson KD (2005) DNA methylation and human disease. *Nat Rev Genet* **6**(8): 597-610

Robertson KD, Jones PA (1998) The human ARF cell cycle regulatory gene promoter is a CpG island which can be silenced by DNA methylation and down-regulated by wild-type p53. *Mol Cell Biol* **18**(11): 6457-6473

Robertson KD, Keyomarsi K, Gonzales FA, Velicescu M, Jones PA (2000) Differential mRNA expression of the human DNA methyltransferases (DNMTs) 1, 3a and 3b during the G(0)/G(1) to S phase transition in normal and tumor cells. *Nucleic Acids Res* **28**(10): 2108-2113

Robertson KD, Uzvolgyi E, Liang G, Talmadge C, Sumegi J, Gonzales FA, Jones PA (1999) The human DNA methyltransferases (DNMTs) 1, 3a and 3b: coordinate

mRNA expression in normal tissues and overexpression in tumors. *Nucleic Acids Res* **27**(11): 2291-2298

Rollins RA, Haghighi F, Edwards JR, Das R, Zhang MQ, Ju J, Bestor TH (2006) Large-scale structure of genomic methylation patterns. *Genome Res* **16**(2): 157-163

Ropero S, Setien F, Espada J, Fraga MF, Herranz M, Asp J, Benassi MS, Franchi A, Patino A, Ward LS, Bovee J, Cigudosa JC, Wim W, Esteller M (2004) Epigenetic loss of the familial tumor-suppressor gene exostosin-1 (EXT1) disrupts heparan sulfate synthesis in cancer cells. *Hum Mol Genet* **13**(22): 2753-2765

Rush LJ, Plass C (2002) Restriction landmark genomic scanning for DNA methylation in cancer: past, present, and future applications. *Anal Biochem* **307**(2): 191-201

Ruzov A, Dunican DS, Prokhortchouk A, Pennings S, Stancheva I, Prokhortchouk E, Meehan RR (2004) Kaiso is a genome-wide repressor of transcription that is essential for amphibian development. *Development* **131**(24): 6185-6194

Sado T, Fenner MH, Tan SS, Tam P, Shioda T, Li E (2000) X inactivation in the mouse embryo deficient for Dnmt1: distinct effect of hypomethylation on imprinted and random X inactivation. *Dev Biol* **225**(2): 294-303

Saito Y, Kanai Y, Sakamoto M, Saito H, Ishii H, Hirohashi S (2002) Overexpression of a splice variant of DNA methyltransferase 3b, DNMT3b4, associated with DNA hypomethylation on pericentromeric satellite regions during human hepatocarcinogenesis. *Proc Natl Acad Sci U S A* **99**(15): 10060-10065

Samowitz WS, Albertsen H, Herrick J, Levin TR, Sweeney C, Murtaugh MA, Wolff RK, Slattery ML (2005) Evaluation of a large, population-based sample supports a CpG island methylator phenotype in colon cancer. *Gastroenterology* **129**(3): 837-845

Samuel T, Weber HO, Rauch P, Verdoodt B, Eppel JT, McShea A, Hermeking H, Funk JO (2001) The G2/M regulator 14-3-3sigma prevents apoptosis through sequestration of Bax. *J Biol Chem* **276**(48): 45201-45206

Sato N, Maitra A, Fukushima N, van Heek NT, Matsubayashi H, Iacobuzio-Donahue CA, Rosty C, Goggins M (2003) Frequent hypomethylation of multiple genes overexpressed in pancreatic ductal adenocarcinoma. *Cancer Res* **63**(14): 4158-4166

Schlesinger Y, Straussman R, Keshet I, Farkash S, Hecht M, Zimmerman J, Eden E, Yakhini Z, Ben-Shushan E, Reubinoff BE, Bergman Y, Simon I, Cedar H (2007) Polycomb-mediated methylation on Lys27 of histone H3 pre-marks genes for de novo methylation in cancer. *Nat Genet* **39**(2): 232-236

Schmid CW (1998) Does SINE evolution preclude Alu function? *Nucleic Acids Res* **26**(20): 4541-4550

- Schumacher A, Kapranov P, Kaminsky Z, Flanagan J, Assadzadeh A, Yau P, Virtanen C, Winegarden N, Cheng J, Gingeras T, Petronis A (2006) Microarray-based DNA methylation profiling: technology and applications. *Nucleic Acids Res* **34**(2): 528-542
- Seimiya H, Sawada H, Muramatsu Y, Shimizu M, Ohko K, Yamane K, Tsuruo T (2000) Involvement of 14-3-3 proteins in nuclear localization of telomerase. *Embo J* **19**(11): 2652-2661
- Shames DS, Minna JD, Gazdar AF (2007) Methods for detecting DNA methylation in tumors: from bench to bedside. *Cancer Lett* **251**(2): 187-198
- Shen L, Kondo Y, Guo Y, Zhang J, Zhang L, Ahmed S, Shu J, Chen X, Waterland RA, Issa JP (2007) Genome-wide profiling of DNA methylation reveals a class of normally methylated CpG island promoters. *PLoS Genet* **3**(10): 2023-2036
- Shen L, Kondo Y, Rosner GL, Xiao L, Hernandez NS, Vilaythong J, Houlihan PS, Krouse RS, Prasad AR, Einspahr JG, Buckmeier J, Alberts DS, Hamilton SR, Issa JP (2005) MGMT promoter methylation and field defect in sporadic colorectal cancer. *J Natl Cancer Inst* **97**(18): 1330-1338
- Siedlecki P, Zielenkiewicz P (2006) Mammalian DNA methyltransferases. *Acta Biochim Pol* **53**(2): 245-256
- Siegmund KD, Laird PW (2002) Analysis of complex methylation data. *Methods* **27**(2): 170-178
- Spada F, Haemmer A, Kuch D, Rothbauer U, Schermelleh L, Kremmer E, Carell T, Langst G, Leonhardt H (2007) DNMT1 but not its interaction with the replication machinery is required for maintenance of DNA methylation in human cells. *J Cell Biol* **176**(5): 565-571
- Spotswood HT, Turner BM (2002) An increasingly complex code. *J Clin Invest* **110**(5): 577-582
- Stark LA, Dunlop MG (2005) Nucleolar sequestration of RelA (p65) regulates NF-kappaB-driven transcription and apoptosis. *Mol Cell Biol* **25**(14): 5985-6004
- Strahl BD, Allis CD (2000) The language of covalent histone modifications. *Nature* **403**(6765): 41-45
- Su AI, Cooke MP, Ching KA, Hakak Y, Walker JR, Wiltshire T, Orth AP, Vega RG, Sapinoso LM, Moqrich A, Patapoutian A, Hampton GM, Schultz PG, Hogenesch JB (2002) Large-scale analysis of the human and mouse transcriptomes. *Proc Natl Acad Sci U S A* **99**(7): 4465-4470

- Sullivan MJ, Taniguchi T, Jhee A, Kerr N, Reeve AE (1999) Relaxation of IGF2 imprinting in Wilms tumours associated with specific changes in IGF2 methylation. *Oncogene* **18**(52): 7527-7534
- Suter CM, Norrie M, Ku SL, Cheong KF, Tomlinson I, Ward RL (2003) CpG island methylation is a common finding in colorectal cancer cell lines. *Br J Cancer* **88**(3): 413-419
- Suzuki H, Gabrielson E, Chen W, Anbazhagan R, van Engeland M, Weijenberg MP, Herman JG, Baylin SB (2002) A genomic screen for genes upregulated by demethylation and histone deacetylase inhibition in human colorectal cancer. *Nat Genet* **31**(2): 141-149
- Suzuki H, Itoh F, Toyota M, Kikuchi T, Kakiuchi H, Imai K (2000) Inactivation of the 14-3-3 sigma gene is associated with 5' CpG island hypermethylation in human cancers. *Cancer Res* **60**(16): 4353-4357
- Suzuki M, Shigematsu H, Shames DS, Sunaga N, Takahashi T, Shivapurkar N, Iizasa T, Frenkel EP, Minna JD, Fujisawa T, Gazdar AF (2005) DNA methylation-associated inactivation of TGFbeta-related genes DRM/Gremlin, RUNX3, and HPP1 in human cancers. *Br J Cancer* **93**(9): 1029-1037
- Szyf M, Bozovic V, Tanigawa G (1991) Growth regulation of mouse DNA methyltransferase gene expression. *J Biol Chem* **266**(16): 10027-10030
- Takahashi T, Shigematsu H, Shivapurkar N, Reddy J, Zheng Y, Feng Z, Suzuki M, Nomura M, Augustus M, Yin J, Meltzer SJ, Gazdar AF (2006) Aberrant promoter methylation of multiple genes during multistep pathogenesis of colorectal cancers. *Int J Cancer* **118**(4): 924-931
- Takai D, Jones PA (2002) Comprehensive analysis of CpG islands in human chromosomes 21 and 22. *Proc Natl Acad Sci U S A* **99**(6): 3740-3745
- Tanaka K, Hatada T, Kobayashi M, Mohri Y, Tonouchi H, Miki C, Nobori T, Kusunoki M (2004) The clinical implication of 14-3-3 sigma expression in primary gastrointestinal malignancy. *Int J Oncol* **25**(6): 1591-1597
- Tatematsu KI, Yamazaki T, Ishikawa F (2000) MBD2-MBD3 complex binds to hemi-methylated DNA and forms a complex containing DNMT1 at the replication foci in late S phase. *Genes Cells* **5**(8): 677-688
- Tazi J, Bird A (1990) Alternative chromatin structure at CpG islands. *Cell* **60**(6): 909-920
- Tchou JC, Lin X, Freije D, Isaacs WB, Brooks JD, Rashid A, De Marzo AM, Kanai Y, Hirohashi S, Nelson WG (2000) GSTP1 CpG island DNA hypermethylation in hepatocellular carcinomas. *Int J Oncol* **16**(4): 663-676

- Tollefsbol TO, Hutchison CA, 3rd (1998) Analysis in *Escherichia coli* of the effects of in vivo CpG methylation catalyzed by the cloned murine maintenance methyltransferase. *Biochem Biophys Res Commun* **245**(3): 670-678
- Toyota M, Ahuja N, Toyota MO, Herman JG, Baylin SB, Issa JP (1999a) CpG Island methylator phenotype in colorectal cancer. *Proceedings of the National Academy of Sciences of the United States of America* **96**: 8681-8686
- Toyota M, Ho C, Ahuja N, Jair KW, Li Q, Ohe-Toyota M, Baylin SB, Issa JP (1999b) Identification of differentially methylated sequences in colorectal cancer by methylated CpG island amplification. *Cancer Res* **59**(10): 2307-2312
- Toyota M, Issa JP (1999) CpG island methylator phenotypes in aging and cancer. *Semin Cancer Biol* **9**(5): 349-357
- Toyota M, Ohe-Toyota M, Ahuja N, Issa JP (2000) Distinct genetic profiles in colorectal tumors with or without the CpG island methylator phenotype. *Proc Natl Acad Sci U S A* **97**(2): 710-715
- Tuck-Muller CM, Narayan A, Tsien F, Smeets DF, Sawyer J, Fiala ES, Sohn OS, Ehrlich M (2000) DNA hypomethylation and unusual chromosome instability in cell lines from ICF syndrome patients. *Cytogenet Cell Genet* **89**(1-2): 121-128
- Uhlmann K, Brinckmann A, Toliat MR, Ritter H, Nurnberg P (2002) Evaluation of a potential epigenetic biomarker by quantitative methyl-single nucleotide polymorphism analysis. *Electrophoresis* **23**(24): 4072-4079
- Umbricht CB, Evron E, Gabrielson E, Ferguson A, Marks J, Sukumar S (2001) Hypermethylation of 14-3-3 sigma (stratifin) is an early event in breast cancer. *Oncogene* **20**(26): 3348-3353
- Urano T, Saito T, Tsukui T, Fujita M, Hosoi T, Muramatsu M, Ouchi Y, Inoue S (2002) Efp targets 14-3-3 sigma for proteolysis and promotes breast tumour growth. *Nature* **417**(6891): 871-875
- Urano T, Takahashi S, Suzuki T, Fujimura T, Fujita M, Kumagai J, Horie-Inoue K, Sasano H, Kitamura T, Ouchi Y, Inoue S (2004) 14-3-3sigma is down-regulated in human prostate cancer. *Biochem Biophys Res Commun* **319**(3): 795-800
- van Rijnsoever M, Grieu F, Elsaleh H, Joseph D, Iacopetta B (2002) Characterisation of colorectal cancers showing hypermethylation at multiple CpG islands. *Gut* **51**(6): 797-802
- Varley KE, Mutch DG, Edmonston TB, Goodfellow PJ, Mitra RD (2009) Intra-tumor heterogeneity of MLH1 promoter methylation revealed by deep single molecule bisulfite sequencing. *Nucleic Acids Res* **37**(14): 4603-4612

- Villaret DB, Wang T, Dillon D, Xu J, Sivam D, Cheever MA, Reed SG (2000) Identification of genes overexpressed in head and neck squamous cell carcinoma using a combination of complementary DNA subtraction and microarray analysis. *Laryngoscope* **110**(3 Pt 1): 374-381
- Vogelstein B, Fearon ER, Hamilton SR, Kern SE, Preisinger AC, Leppert M, Nakamura Y, White R, Smits AM, Bos JL (1988) Genetic alterations during colorectal-tumor development. *N Engl J Med* **319**(9): 525-532
- Volinia S, Calin GA, Liu CG, Ambs S, Cimmino A, Petrocca F, Visone R, Iorio M, Roldo C, Ferracin M, Prueitt RL, Yanaihara N, Lanza G, Scarpa A, Vecchione A, Negrini M, Harris CC, Croce CM (2006) A microRNA expression signature of human solid tumors defines cancer gene targets. *Proc Natl Acad Sci U S A* **103**(7): 2257-2261
- Walsh CP, Bestor TH (1999) Cytosine methylation and mammalian development. *Genes Dev* **13**(1): 26-34
- Wang W, Shakes DC (1996) Molecular evolution of the 14-3-3 protein family. *J Mol Evol* **43**(4): 384-398
- Ward RL, Cheong K, Ku SL, Meagher A, O'Connor T, Hawkins NJ (2003) Adverse prognostic effect of methylation in colorectal cancer is reversed by microsatellite instability. *J Clin Oncol* **21**(20): 3729-3736
- Watson JV, Chambers SH, Smith PJ (1987) A pragmatic approach to the analysis of DNA histograms with a definable G1 peak. *Cytometry* **8**(1): 1-8
- Weber M, Davies JJ, Wittig D, Oakeley EJ, Haase M, Lam WL, Schubeler D (2005) Chromosome-wide and promoter-specific analyses identify sites of differential DNA methylation in normal and transformed human cells. *Nat Genet* **37**(8): 853-862
- Weisenberger DJ, Campan M, Long TI, Kim M, Woods C, Fiala E, Ehrlich M, Laird PW (2005) Analysis of repetitive element DNA methylation by MethyLight. *Nucleic Acids Res* **33**(21): 6823-6836
- Weisenberger DJ, Siegmund KD, Campan M, Young J, Long TI, Faasse MA, Kang GH, Widschwendter M, Weener D, Buchanan D, Koh H, Simms L, Barker M, Leggett B, Levine J, Kim M, French AJ, Thibodeau SN, Jass J, Haile R, Laird PW (2006) CpG island methylator phenotype underlies sporadic microsatellite instability and is tightly associated with BRAF mutation in colorectal cancer. *Nat Genet* **38**(7): 787-793
- Weisenberger DJ, Velicescu M, Cheng JC, Gonzales FA, Liang G, Jones PA (2004) Role of the DNA methyltransferase variant DNMT3b3 in DNA methylation. *Mol Cancer Res* **2**(1): 62-72

- Widschwendter M, Jiang G, Woods C, Muller HM, Fiegl H, Goebel G, Marth C, Muller-Holzner E, Zeimet AG, Laird PW, Ehrlich M (2004) DNA hypomethylation and ovarian cancer biology. *Cancer Res* **64**(13): 4472-4480
- Wilker EW, Grant RA, Artim SC, Yaffe MB (2005) A structural basis for 14-3-3sigma functional specificity. *J Biol Chem* **280**(19): 18891-18898
- Wilker EW, van Vugt MA, Artim SA, Huang PH, Petersen CP, Reinhardt HC, Feng Y, Sharp PA, Sonenberg N, White FM, Yaffe MB (2007) 14-3-3sigma controls mitotic translation to facilitate cytokinesis. *Nature* **446**(7133): 329-332
- Wynshaw-Boris A (2007) Cell biology: lost in mitotic translation. *Nature* **446**(7133): 274-275
- Xiong Y, Dowdy SC, Eberhardt NL, Podratz KC, Jiang SW (2006) hMLH1 promoter methylation and silencing in primary endometrial cancers are associated with specific alterations in MBDs occupancy and histone modifications. *Gynecol Oncol*
- Xiong Y, Hannon GJ, Zhang H, Casso D, Kobayashi R, Beach D (1993) p21 is a universal inhibitor of cyclin kinases. *Nature* **366**(6456): 701-704
- Xu GL, Bestor TH, Bourc'his D, Hsieh CL, Tommerup N, Bugge M, Hulten M, Qu X, Russo JJ, Viegas-Pequignot E (1999) Chromosome instability and immunodeficiency syndrome caused by mutations in a DNA methyltransferase gene. *Nature* **402**(6758): 187-191
- Yamashita K, Dai T, Dai Y, Yamamoto F, Perucho M (2003) Genetics supersedes epigenetics in colon cancer phenotype. *Cancer Cell* **4**(2): 121-131
- Yang A, Kaghad M, Wang Y, Gillett E, Fleming MD, Dotsch V, Andrews NC, Caput D, McKeon F (1998) p63, a p53 homolog at 3q27-29, encodes multiple products with transactivating, death-inducing, and dominant-negative activities. *Mol Cell* **2**(3): 305-316
- Yang AS, Estecio MR, Doshi K, Kondo Y, Tajara EH, Issa JP (2004) A simple method for estimating global DNA methylation using bisulfite PCR of repetitive DNA elements. *Nucleic Acids Res* **32**(3): e38
- Yang HY, Wen YY, Chen CH, Lozano G, Lee MH (2003) 14-3-3 sigma positively regulates p53 and suppresses tumor growth. *Mol Cell Biol* **23**(20): 7096-7107
- Yarden RI, Pardo-Reoyo S, Sgagias M, Cowan KH, Brody LC (2002) BRCA1 regulates the G2/M checkpoint by activating Chk1 kinase upon DNA damage. *Nat Genet* **30**(3): 285-289
- Yegnasubramanian S, Haffner MC, Zhang Y, Gurel B, Cornish TC, Wu Z, Irizarry RA, Morgan J, Hicks J, DeWeese TL, Isaacs WB, Bova GS, De Marzo AM, Nelson

WG (2008) DNA hypomethylation arises later in prostate cancer progression than CpG island hypermethylation and contributes to metastatic tumor heterogeneity. *Cancer Res* **68**(21): 8954-8967

Yoder JA, Soman NS, Verdine GL, Bestor TH (1997a) DNA (cytosine-5)-methyltransferases in mouse cells and tissues. Studies with a mechanism-based probe. *J Mol Biol* **270**(3): 385-395

Yoder JA, Walsh CP, Bestor TH (1997b) Cytosine methylation and the ecology of intragenomic parasites. *Trends Genet* **13**(8): 335-340

Yoshikawa H, Matsubara K, Qian GS, Jackson P, Groopman JD, Manning JE, Harris CC, Herman JG (2001) SOCS-1, a negative regulator of the JAK/STAT pathway, is silenced by methylation in human hepatocellular carcinoma and shows growth-suppression activity. *Nat Genet* **28**(1): 29-35

Yu L, Liu C, Vandeusen J, Becknell B, Dai Z, Wu YZ, Raval A, Liu TH, Ding W, Mao C, Liu S, Smith LT, Lee S, Rassenti L, Marcucci G, Byrd J, Caligiuri MA, Plass C (2005) Global assessment of promoter methylation in a mouse model of cancer identifies ID4 as a putative tumor-suppressor gene in human leukemia. *Nat Genet* **37**(3): 265-274

Zhang X, Yazaki J, Sundaresan A, Cokus S, Chan SW, Chen H, Henderson IR, Shinn P, Pellegrini M, Jacobsen SE, Ecker JR (2006) Genome-wide high-resolution mapping and functional analysis of DNA methylation in arabidopsis. *Cell* **126**(6): 1189-1201

Zhao X, Ueba T, Christie BR, Barkho B, McConnell MJ, Nakashima K, Lein ES, Eadie BD, Willhoite AR, Muotri AR, Summers RG, Chun J, Lee KF, Gage FH (2003) Mice lacking methyl-CpG binding protein 1 have deficits in adult neurogenesis and hippocampal function. *Proc Natl Acad Sci U S A* **100**(11): 6777-6782

Zhu J, Jiang J, Zhou W, Chen X (1998) The potential tumor suppressor p73 differentially regulates cellular p53 target genes. *Cancer Res* **58**(22): 5061-5065

Zochbauer-Muller S, Fong KM, Virmani AK, Geradts J, Gazdar AF, Minna JD (2001) Aberrant promoter methylation of multiple genes in non-small cell lung cancers. *Cancer Res* **61**(1): 249-255